Identification of novel proto-oncogenes in murine myeloid leukemias by retroviral insertional mutagenesis

The peripheral cannabinoid receptor

Petrus Jacobus Maria Valk

Identification of novel proto-oncogenes in murine myeloid leukemias by retroviral insertional mutagenesis

The peripheral cannabinoid receptor

Identificatie van nieuwe proto-oncogenen in myeloide muizenleukemieën
door middel van retrovirale insertionele mutagenese –
De perifere cannabinoide receptor

PROEFSCHRIFT

Ter verkrijging van de graad van doctor aan de Erasmus Universiteit Rotterdam
op gezag van de Rector Magnificus Prof. Dr. P.W.C. Akkermans, M.A.
en volgens het besluit van het College voor Promoties.

De openbare verdediging zal plaatsvinden op
woensdag 19 mei 1999 om 11:45 uur

door

Petrus Jacobus Maria Valk

geboren te Delft

Promotiecommissie

Promotor	Prof. dr. B. Löwenberg
Overige leden	Prof. dr. A.J.M. Berns Prof. dr. J.A. Grootegoed Prof. dr. A.D.M.E. Osterhaus
Co-promotor	Dr. R. Delwel

The work described in this thesis was performed at the Institute of Hematology, Erasmus University Rotterdam, The Netherlands. This work was supported by grants from the Dutch Cancer Society (KWF), the Netherlands Organization for Scientific Research (NWO) and the Royal Dutch Academy of Sciences (KNAW). Printing of this thesis was financially supported by the Dutch Cancer Society (KWF).

Printed by Haveka B.V., Alblasserdam, The Netherlands.

in liefdevolle herinnering aan *mijn moeder*
voor *mijn vader*

voor *Barbara en*
Menno

Contents

List of abbreviations

ALL	-	acute lymphoblastic leukemia
AML	-	acute myeloid leukemia
Cb1	-	central cannabinoid receptor
Cb2	-	peripheral cannabinoid receptor
cDNA	-	complementary DNA
CHO-cells	-	Chinese hamster ovary cells
CLL	-	chronic lymphocytic leukemia
CML	-	chronic myeloid leukemia
CSL	-	Cas-Br-M MuLV Swiss Leukemias
THC	-	tetrahydrocannabinol
EPO	-	erythropoietin
ERK	-	extracellular signal-regulated protein kinase
Evi	-	ecotropic virus integration site
G-CSF	-	granulocyte colony-stimulating factor
GM-CSF	-	granulocyte-macrophage colony-stimulating factor
GPCR	-	G protein-coupled receptor
G protein	-	guanine-nucleotide-binding protein
HGF	-	hematopoietic growth factor
HSC	-	hematopoietic stem cell
IAP	-	intracisternal type A particle
IL	-	interleukin
JCML	-	juvenile chronic myeloid leukemia
LTR	-	long terminal repeat
MAPK	-	mitogen-activated protein kinase
M-CSF	-	macrophage colony-stimulating factor
MDS	-	myelodysplastic syndrome
MuLV	-	murine leukemia virus
NCBI	-	National Center for Biotechnology Information
Nf1	-	neurofibromatosis type 1
7TM	-	seven-transmembrane
PCR	-	polymerase chain reaction
UTR	-	untranslated region
VIS	-	virus integration site

CHAPTER 1

INTRODUCTION

Part of this introduction has been published in:

Valk PJM and Delwel R
The peripheral cannabinoid receptor, Cb2, in leukemic transformation and hematopoiesis
Leukemia and Lymphoma 32(1-2), 29-44, 1998

1.1 *General introduction*

Dynamic and complex processes of cell proliferation, differentiation, maturation, apoptosis, and survival maintain homeostasis in bone marrow and peripheral blood. In steady state, the turnover of blood cells is approximately 1 x 10^{12} cells per day. During stress conditions, such as infections or bleeding, blood cell formation is properly adjusted by the production of terminally differentiated functional cells. Leukemia is a progressive neoplastic disease of the blood cell forming system, in which non-functional blood cells accumulate in the bone marrow, thereby interfering with normal blood cell formation.

The main objectives of the experimental work described in this thesis were the identification of novel proto-oncogenes or tumor suppressor genes involved in myeloid leukemia development by using retroviral insertional mutagenesis (Chapters 2, 3, 4 and 5), and the characterization of these novel genes (Chapters 6 and 7).

1.2 *Hematopoiesis*

Blood cell formation or hematopoiesis in adult vertebrates occurs mainly in the bone marrow. All different blood cells are derived from one common precursor, the bone marrow hematopoietic stem cell (HSC). The HSC has self-renewal capacity and at the same time produces progenitor cells, which finally mature towards the different blood cell types, e.g., neutrophils, eosinophils, basophils, macrophages, mast cells, natural killer cells, dendritic cells, erythrocytes, megakaryocytes, and B- and T-lymphocytes (Figure 1). Transplantation of purified HSCs into lethally irradiated recipients results in the full reconstitution of the hematopoietic system (220).

Embryonic primitive blood cell formation starts in the yolk sac (in the mouse at embryonic day 7.5 post coitus (E7.5)) with the production of primitive erythrocytes, which form the blood islands. Another site of early hematopoiesis is the aorta-gonad-mesonephros (AGM) region (92). Actually, the first pluripotent HSCs from the mouse embryo that can be visualized by using *in vivo* and *in vitro* functional assays are derived from the AGM region (E10). Around E11 blood cell formation is extended from yolk sac and AGM region to the fetal liver, in which definitive hematopoiesis is initiated. After birth, definitive hematopoiesis mainly occurs in the bone marrow (in mice also in the spleen).

Homeostasis of hematopoiesis is tightly regulated by hematopoietic growth factors (HGFs) (Figure 1). HGFs produced by fibroblasts, endothelial cells, monocytes, T-cells and macrophages stimulate proliferation, differentiation, maturation, survival, and function of hematopoietic cells. HGFs that act on early progenitors are, e.g., stem cell factor (SCF), interleukin-1 (IL-1), IL-3, IL-4, IL-6, IL-11, IL-12, and

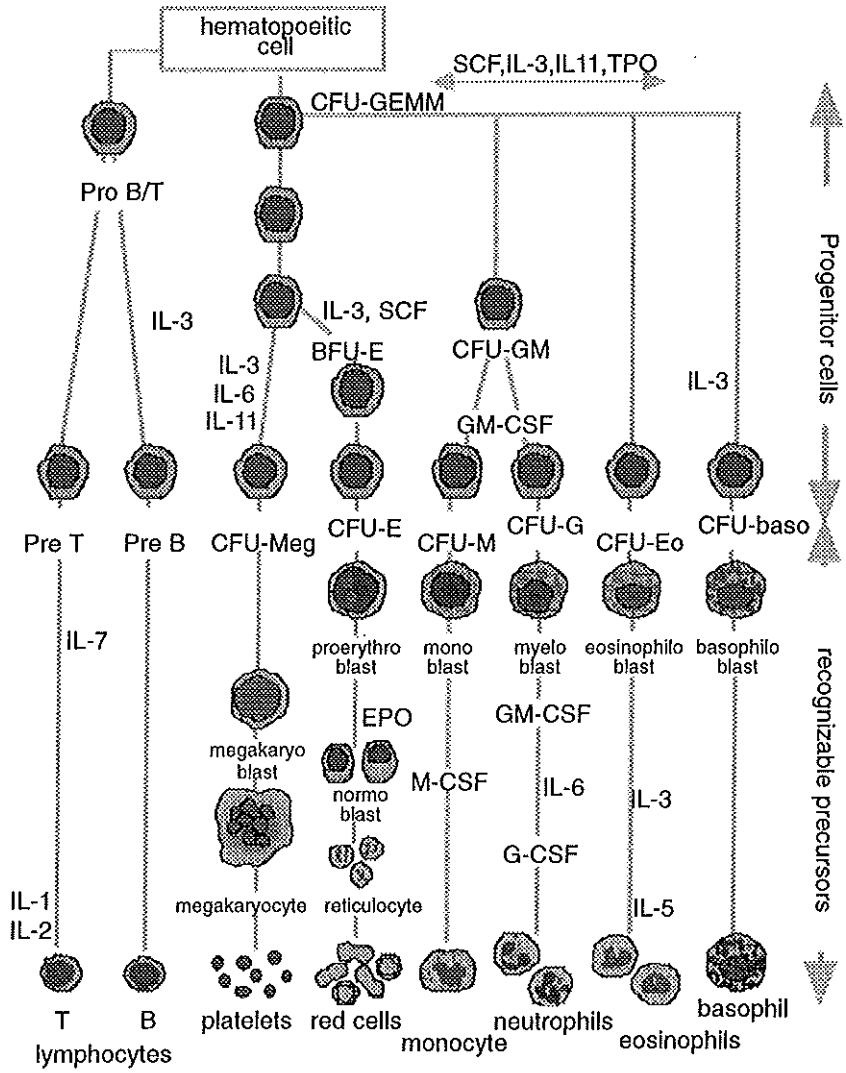

Figure 1: Schematic representation of the hematopoietic system
Blood cell formation originates from the self-renewing hematopoietic stem cell (HSC). Subsequently, all hematopoietic lineages arise following activation by different hematopoietic growth factors (IL: interleukin; G-CSF: granulocyte colony-stimulating factor; GM-CSF: granulocyte-macrophage colony-stimulating factor; EPO: erythropoietin; TPO: thrombopoietin; M-CSF: macrophage colony-stimulating factor; SCF: stem cell factor). The different distinct stages in hematopoietic development are visualized by *in vitro* colony assays. The lineage-specific burst- and colony-forming units (BFUs and CFUs) are indicated (GEMM: granulocyte-erythroid-monocyte-megakaryocyte; GM: granulocyte-monocyte; G: granulocyte; Meg: megakaryocyte; Eo: eosinophil; M; monocyte; baso: basophil).

granulocyte-macrophage colony-stimulating factor (GM-CSF). Examples of late-acting lineage-specific HGFs are, e.g., erythropoietin (EPO) (erythrocytes), IL-5 (eosinophils), macrophage colony-stimulating factor (M-CSF) (macrophages), granulocyte colony-stimulating factor (G-CSF) (granulocytes), and thrombopoietin (TPO) (megakaryocytes). All these stimuli act through HGF receptors on the surface of hematopoietic cells, which, upon activation by the proper HGF, initiate specific intracellular signals that will lead to specific gene expression and finally to hematopoietic development. Most of the cytokine/HGF receptors belong to the superfamily of cytokine/hematopoietin receptors, based on structural homologies (61, 211).
The major signal transduction pathways by which these cytokine/HGF receptors transmit signals towards the nucleus are the Ras/MAPK (36, 274) and the Jak/STAT (66, 132) routes. However, the involvement of additional signaling pathways in cytokine signaling, e.g., the Rho, PI3kinase, protein kinase A, or protein kinase C routes, as well as crosstalk between the different pathways, have been demonstrated (48, 332).
HGF signaling results in transcriptional activation of specific genes, which are essential during hematopoiesis. Transcriptional control, by lineage-restricted as well as generally expressed transcription factors and co-activators, during blood cell formation is therefore a central theme in developmental biology (287).

1.3 *Leukemogenesis*

The balances between hematopoietic cell proliferation, differentiation, maturation, apoptosis and survival are crucial to maintain homeostasis. Disruption of these critical balances, e.g., unregulated proliferation, prolonged cell survival or blocked differentiation of hematopoietic progenitor cells, may cause leukemia. Leukemia is a neoplastic disease in which immature hematopoietic progenitors accumulate in the bone marrow, thereby dislocating the normal hematopoietic progenitors. The neoplastic cells finally enter the peripheral blood and other tissues.
Broadly, the disease is divided into the aggressive acute leukemias and the chronic less aggressive forms of leukemia. The acute leukemias are a heterogeneous group of blood cell diseases characterized by accumulation of immature malignant cells in the bone marrow, whereas the chronic leukemias are characterized by accumulation of more differentiated cells. Further classification is based on the cell lineage of the malignant stem cell, i.e., myeloid or lymphoid, and the maturation status of the blood cell, i.e., FAB-classification (26, 27). This introduction will further concentrate on acute myeloid leukemias, since the research described in this thesis is focused on these types of blood cell diseases.

1.4 *Proto-oncogenes and tumor suppressor genes in human acute myeloid leukemia*

It has generally been accepted that the development of leukemia, like other cancers, is a multistep process involving inappropriate activation of proto-oncogenes or inactivation of tumor suppressor genes (1, 129, 327). The class of proto-oncogenes consists of genes encoding growth factors, growth factor receptors, signaling molecules, transcription factors and molecules necessary for RNA and DNA synthesis (129, 130). Inappropriate activation of these proto-oncogenes as a result of critical mutations (39), chromosomal translocations (188, 232, 253) or viral infections (101) may cause cellular transformation. Mutant oncoproteins affect proliferation, differentiation, maturation or survival of hematopoietic cells by interfering in the HGF receptor signaling cascades or the transcriptional regulation in the nucleus.
Much knowledge about the involvement of proto-oncogenes in acute leukemias is accomplished by careful cloning of breakpoints at chromosomal translocations (188, 232, 253). Chromosomal translocations result in overexpression of full-length oncoprotein, or aberrant expression of fusion oncoproteins. Since aberrant expression of a proto-oncogene can confer a growth advantage to the hematopoietic progenitor cell, the consequence is clonal outgrowth of transformed cells containing the chromosomal translocation. Numerous recurrent clonal chromosomal abnormalities have been discovered in chronic and acute lymphoblastic and myeloid leukemias (253). The genes located at chromosomal breakpoints in acute myeloid or acute lymphoblastic leukemia (AML and ALL, respectively) most often encode for nuclear transcription factors (188), including the hematopoietic transcription factors *SCL*, *AML1*, and *CBFβ* (287). The involvement of improper expression of transcription factor proteins in leukemia development demonstrates that the complex transcriptional regulation of hematopoiesis is critical for maintaining homeostasis (287). Most of the proto-oncogenes in AML, which have been identified by cloning chromosomal breakpoints, encode transcription factors (Table 1) (188). However, several examples of signal transducers and nuclear proteins other than transcription factors have also been implicated in chromosomal breakpoints in AML (Table 1). The first identified reoccurring chromosomal translocation involved in myeloid leukemia was the Philadelphia translocation, which was discovered in 1984 in CML patients with t(9,22)(q34;q11) (115, 162). The t(9;22) translocation results in the production of a chimeric malignant protein BCR/ABL (328).

In 15 years time the number of proto-oncogenes in AML, identified by cloning chromosomal breakpoints, has remained relatively small (Table 1) and the diversity in translocation partners is limited, since several genes are involved in different chromosomal aberrations, i.e., RARα, EVI1, CBFβ, TEL, AML1, and MLL (Table 1). Moreover, 36% percent of all AMLs contains random chromosomal translocations

Breakpoints	Affected gene(s)	Disease	Gene type
t(3;3), ins(3), t(3;5), t(2;3)	*EVI1*	AML, CML, MDS	TF
t(6;11), t(9;11), t(11;19)	*MLL* and *AF6, AF9* or *ENL*	AML	TF
t(5;17), t(11;17), t(15;17)	*RARα* and *NPM, PLZF* or *PML*	APL	TF
inv(16), t(16;16)	*CBFβ* and *MYH11*	AML	TF
t(3;21), t(8;21)	*AML1* and *EAP, MDS, EVI1* or *ETO*	CML, MDS, AML	TF
t(16;21)	*TLS* and *ERG*	AML, CML, MDS	TF
t(12;22)	*MN1* and *TEL*	AML	TF
t(5;12), t(9;12)	*TEL* and *PDGFβ, JAK2* or *ABL*	MDS, AML, AUL	ST
t(9;22)	*BCR* and *ABL*	CML	ST
t(6;9)	*DEK* and *NUP214*	AML	NP
t(3;5)	*NPM* and *MLF1*	AML, MDS	NP
t(7;11)	*NUP98* and *HOXA9*	AML	NP/TF

Table 1: Recurrent chromosomal abnormalities in human myeloid leukemias.
(AML: acute myeloid leukemia; CML: chronic myeloid leukemias; MDS: myelodysplastic syndrome; APL: acute promyelocytic leukemia; AUL: acute undifferentiated leukemia; TF: transcription factor; ST: signal transducer; NP: nuclear protein)

and 19% displays a normal karyotype (188). In these AMLs, the isolation and characterization of novel oncoproteins is hampered by the absence of reoccurring chromosomal breaks. Other strategies, like retroviral insertional mutagenesis in mice, are required to identify and study the genes responsible for transformation in these cases of AML.

The induction of neoplasias can also be initiated following inactivation of tumor suppressor genes, which generally encode for negative regulators of cell proliferation (333). Cellular transformation by these genes is caused by loss-of-function of the tumor suppressor protein and requires inactivation of the gene on both alleles. The identification of tumor suppressor genes is therefore based on loss of heterozygosity of parts of a chromosome, since these regions often harbor tumor suppressor genes. Although numerous germline mutations in different hereditary cancer syndromes have now been defined (95), the tumor suppressor genes which appear to be involved in AML are those encoding neurofibromatosis type 1 (*NF1*), the cyclin-dependent kinase inhibitors *p15* and *p16*, and the regulator of apoptosis *p53*. The product of *NF1*, neurofibromin, is a GTPase activating protein capable of accelerating the GTPase activity of RAS proteins, and is therefore a negative regulator of RAS (13,

342). Loss of heterozygosity of *NF1* has been found in malignant myeloid disorders of children with neurofibromatosis type 1 (277), and recently also in juvenile myelomonocytic leukemias from children without a clinical diagnosis of neurofibromatosis type 1 (288). Deletions in the genes encoding the cyclin-dependent kinase inhibitors of the INK4 family, p15 and p16, have been demonstrated in cases of AML and MDS (84), and p53 mutations have been found in numerous cases of CML, AML, and pre-leukemic myelodysplastic syndromes (MDSs) (110, 235, 340).

Since the number of tumor suppressors in AML characterized by linkage studies is small (95) and the isolation of these genes by loss of heterozygosity is time-consuming and limited to hereditary cancer syndromes, other methods to define novel tumor suppressors are required. Retroviral insertional mutagenesis has been shown to be a good alternative method to isolate novel tumor suppressor genes involved in myeloid leukemogenesis (46, 175).

1.5 *Retroviral insertional mutagenesis*

1.5.1 *Mutagenesis by retroviruses*

Retroviruses have been demonstrated to be able to induce cancer in various species, and have consequently been valuable in cancer research. The oncogenic retroviruses are generally classified into two groups based on their pathogenic characteristics. In the acute-transforming retroviruses, which induce polyclonal tumors within a couple of weeks, viral genes have been replaced by cellular proto-oncogenes via recombination events. These proto-oncogenes, e.g., viral (v)-*Myc*, v-*Myb*, and v-*Src* with their counterparts cellular (c)-*Myc*, c-*Myb*, and c-*Src*, respectively, are responsible for the oncogenic capacity of the acute-transforming retroviruses. The second group of oncogenic retroviruses is the group of slow-transforming retroviruses, which induce mono- or oligo-clonal tumors within several months. The slow-transforming retroviruses do not contain proto-oncogenes, and their oncogenicity is the result of insertion of the provirus into the host genome during the retroviral life cycle (Figure 2), thereby interfering with the expression of host genes. In mice, proto-oncogenes are therefore effectively identified in leukemias and lymphomas by retroviral insertional mutagenesis (135, 148, 340).
The retrovirus-infected murine hematopoietic cells are transformed due to proviral integrations into the host genome (Figure 2), which results in the juxtaposition of regulatory sequences of the proviral long terminal repeats (LTR) and cellular genes. These regulatory promoter, enhancer, and polyadenylation signal sequences can subsequently cause aberrant expression of neighboring cellular proto-oncogenes (Figure 3) (148, 340). Whether cellular genes are activated (promoter or enhancer) or

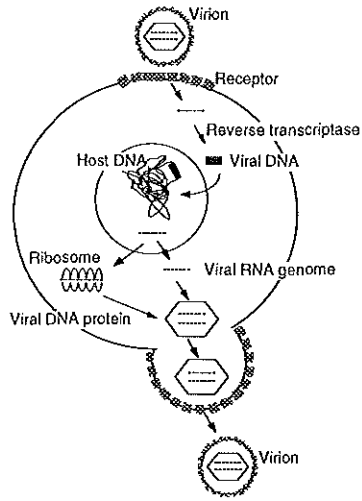

Figure 2: Retroviral life cycle.
Retroviruses contain two identical single-stranded genomic RNA molecules and two essential enzymes, i.e., the viral reverse transcriptase and integrase. The retrovirus enters the host cell by binding to specific cell surface receptors. The RNA is subsequently reverse transcribed in the retroviral particle into a double-stranded DNA molecule. The 3' and 5' ends of the produced DNA molecules are identical long terminal repeats (LTRs) (Figure 3). The DNA molecule integrates into the host genome by using the viral integrase. After insertion of the provirus, new virus particles are formed. The 5'LTR contains the regulatory sequences necessary for proper transcription of the viral genes. However, the 5' and 3' LTRs of the provirus are able to activate proto-oncogenes located on the host genome.

whether transcription is prematurely terminated (polyadenylation signal) depends on the site of integration and the orientation of the provirus. Promoter insertion and enhancement are the most frequently found modes of activation of proto-oncogenes in murine leukemias and lymphomas (148). The aberrant expression of the target proto-oncogene gives the hematopoietic progenitor cell a growth advantage and the ability to expand. The clonal or oligo-clonal population of leukemic cells that arises after retroviral infection contains multiple provirus integrations. Insertion in an identical genomic locus in various independent tumors marks the position of a potential proto-oncogene. Such genomic loci are called common virus integration sites (VISs). VISs are tagged by the proviral genome and can easily be visualized and cloned by molecular techniques (Figure 4). Various genes encoding signaling molecules functioning from cell surface to the nucleus have been shown to be targets for retroviral insertion in myeloid as well as lymphoid malignancies (135, 148, 340).
A prerequisite for the proper usage of retroviral insertional mutagenesis is a random distribution of proviral insertions into the genome. Several studies *in vitro* as well as

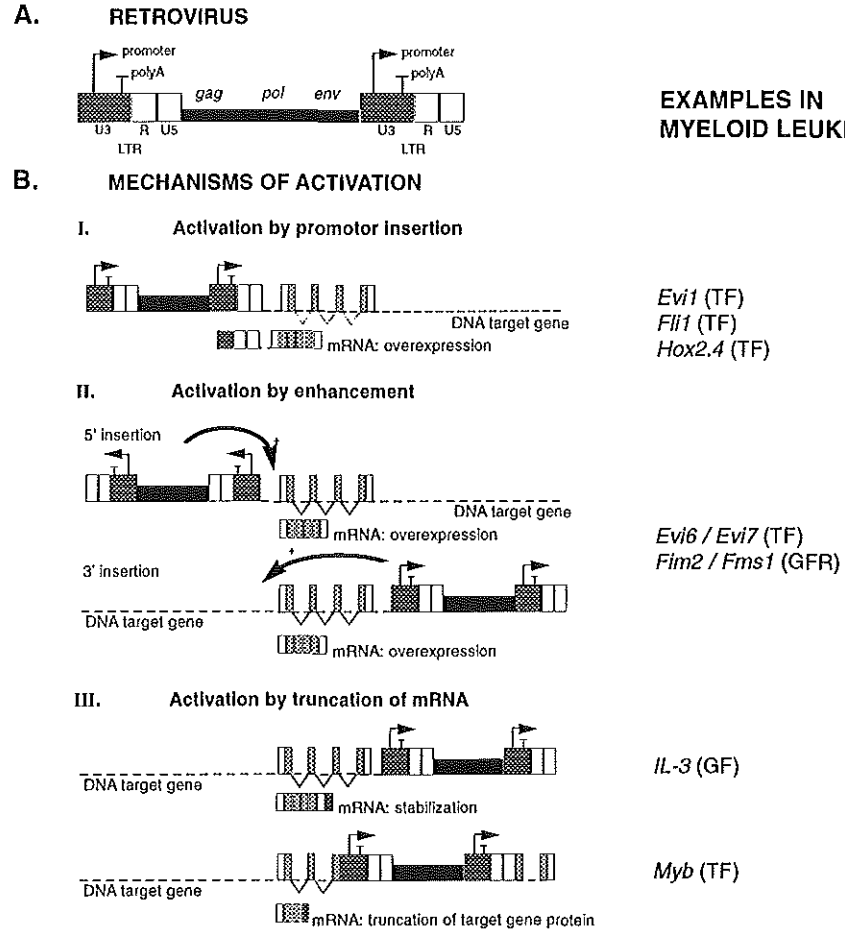

Figure 3: Mechanisms of activation of proto-oncogenes by retroviral insertion and examples of common VISs in retrovirally-induced myeloid mouse leukemias

A. The proviral genome. The inserted retrovirus contains viral genes, encoding structural proteins (*gag* and *env*) and different enzymes (*pol*). These genes are flanked by the long terminal repeats (LTRs), which contain the different regulatory sequences, i.e., promoter (arrow), enhancer and polyadenylation signal (polyA). Each LTR consists of an U_3, R and U_5 region.

B. Modes of activation by retroviral insertion: (I) Overexpression of the target gene by the viral promoter resulting in mRNA fusions between LTR sequences and the target gene (*Evi1* (217), *Fli1* (30), *Hox2.4* (35, 161)). (II) Insertion upstream or downstream of the target gene resulting in an elevated expression of normal full-length mRNAs by the enhancer sequences within the LTR (*Evi6/Evi7* (228), *Fim2/c-Fms* (109)). (III) Truncation of the mRNA of the target gene producing either stabilized mRNAs by removing destabilizing sequences in the 3' untranslated region (*IL-3* (3, 200)) or truncated target gene proteins with transforming potential (c-*Myb* (278)). Examples in myeloid leukemias are depicted for each mechanism of activation. TF:transcription factor; GFR: growth factor receptor; GF: growth factor.

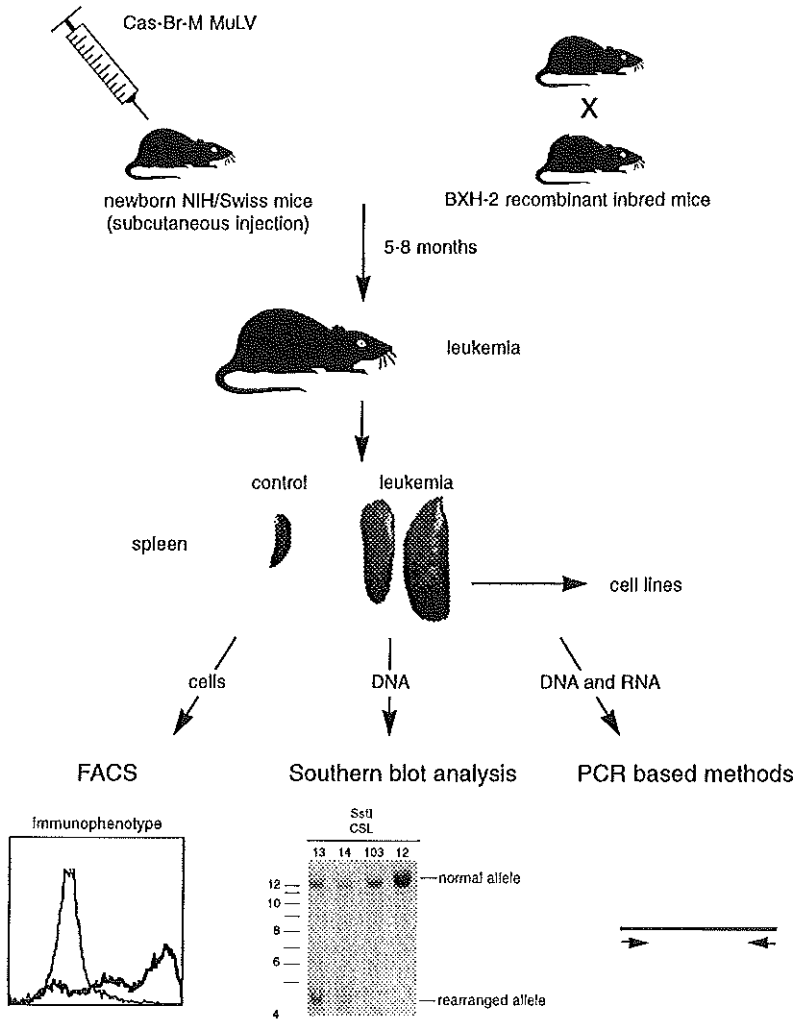

Figure 4: Induction of leukemias in mice with MuLV
Newborns of susceptible mice subcutaneously-injected with Cas-Br-M MuLV, or the highly leukemogenic BXH-2 recombinant inbred mice develop leukemia within 5 to 8 months. This results in the development of enlarged spleens (and sometimes thymomas) in the leukemic mice. The leukemias are characterized by morphology, immunophenotype and determination of known common VISs. To maintain the leukemias, cell lines are made of the primary tumors. The clonal outgrowth of retrovirally-transformed leukemic cells is visualized by Southern blot analysis of genomic DNA from primary leukemias or cell lines with probes flanking the VIS. These probes are isolated by means of genomic cloning or other PCR-based methods. In this figure, the rearranged allele demonstrated by Southern blot analysis is the result of retroviral insertion in CSL13 and CSL14, and represents the leukemic cell population. No rearranged allele is detected in the control tumors CSL103 and CSL12.

in vivo have been carried out showing that retroviruses indeed integrate in a random fashion (93, 321, 338). However, other studies show a mild preference for provirus to insert in transcriptionally active regions (271), bent DNA (208), CpG methylated regions (157), DNase hypersensitive sites (262, 326) or other preferred sites (282). Although there might be a bias to certain areas in the genome, the selective proliferative advantage conferred by the provirus insertion is anticipated to be much higher than selection for preferred insertion sites.
Erythroid, myeloid, and lymphoid malignancies can be induced by injection of inbred mice with ecotropic (restricted to murine cells) slow-transforming retroviruses (24, 29, 31, 219) or by using recombinant inbred strains, like BXH-2 (46, 218, 228) (Figure 4). The mouse inbred strain used, e.g., BALB/c (24) or NFS (219), as well as the injected retrovirus, e.g., Cas-Br-E MuLV (29, 31) or Friends-MuLV (24), determine the type of leukemia or lymphoma that will develop. For example, inoculation of newborn BALB/c or NIH/Swiss mice with Friend murine leukemia virus predominantly results in erythroid leukemias (24), whereas myeloblastic leukemias develop following infection of BALB/c or NFS mice with Graffi virus (265). One mouse strain that has been particularly useful for identifying proto-oncogenes in myeloid disease is BXH-2 (46, 218, 228). BXH-2 is a recombinant inbred strain derived from a cross between C57BL/6J and C3H/HeJ mice (23). The BXH-2 strain spontaneously produces B-ecotropic MuLV throughout their life (23). More than 95% of BXH-2 mice die of granulocytic leukemia before 1 year of age (22). Depending on the hematopoietic malignancy to be studied, the best suited combination of mouse strain and type of leukemia virus should be determined.

The studies described in this thesis are focused on myeloid leukemias induced by Cas-Br-M MuLV (122). Cas-Br-M MuLV is known to induce myeloid leukemias as well as erythroid, B- and T-cell neoplasms in NFS mice (126), or predominantly myeloid leukemias in NIH/Swiss mice (29-31).

1.5.2 *Common virus integration sites in retrovirally-induced murine myeloid leukemias*

Examples of (common) VISs identified in murine myeloid leukemias are shown in Table 2. In this section some important features of the known VISs in retrovirally-induced myeloid leukemias will be discussed.

Locus	Gene involved	Gene type	Mouse Chr.	Common VIS	Human AML	Reference
M-CSF	*M-CSF*	GF	3	-	+	(18)
IL-3	*IL-3*	GF	11	+	+	(3, 344)
GM-CSF	*GM-CSF*	GF	11	+	+	(183)
Fim1	unknown		13	+		(295)
Fim2	c-*fms*	GFR	18	+	+	(109, 295)
Evi2	*Nf1*	ST	11	+	+	(46)
Fis1	*CyclinD1*	CCR	7	+		(290)
Evi1	*Evi1*	TF	3	+	+	(219)
Cb1	*Evi1*	TF	3	+	+	(16)
Evi6	*Hoxa9*	TF	6	+	+	(228)
Evi7	*Hoxa7*	TF	6	+		(228)
Evi9	unknown		11	+		(228)
Meis1/ Evi8/ Evi10	*Meis1*	TF	11	+		(218, 228)
Fli1	*Fli1*	TF	9	+		(31)
Scl	*Scl*	TF	1	-		(304)
Mml1	unknown		10	+		(160)
N-*myc*	N-*myc*	TF	12	+	+	(275)
Hox2.4	*Hoxb8*	TF	11	-		(35)
p53	p53	TF	11	+	+	(29)
c-*Myb*	*c-Myb*	TF	10	+		(278)
His1	uRNA		2	+		(6)
His2	unknown		19	+		(6)

Table 2: Virus integration sites in murine myeloid leukemias.
(GF: growth factor; GFR: growth factor receptor; ST: signal transducer; CCR: cell cycle regulator; TF: transcription factor; uRNA: untranslated RNA)

Growth factors and growth factor receptors

GM-CSF

Rearrangement and overexpression of the GM-CSF gene, as the result of insertion of an intracisternal A-type element, was shown in an *in vivo*-passaged myelomonocytic leukemia, i.e., WEHI-274 (183). Intracisternal A-type particles (IAPs) (170) belong to a family of endogenous defective retrovirus-like elements, which like true retroviruses, contain two LTRs and are also capable of interfering with normal gene expression. Splicing from the IAP promoter resulted in *gag*-to-*GM-CSF* fusion transcripts in WEHI-247 cells (183). Besides the IAP insertion in the *GM-CSF* gene

these WEHI-274 cells also contained rearrangements in the c-*Myb* gene (183). *In vivo*-injection of IL-3 and GM-CSF-dependent FDC-P1 cells into irradiated DBA/2 mice resulted in a leukemic subpopulation that produced IL-3 and GM-CSF caused by IAP insertion upstream of both genes (89). Mice transplanted with hematopoietic cells constitutively expressing the multipotent HGF GM-CSF develop a myeloproliferative syndrome, but not an acute myeloid leukemia (145). Genetic mutations secondary to constitutive GM-CSF expression are apparently required for full transformation of the hematopoietic progenitors.

IL-3

A second selected class of *in vivo*-passaged WEHI-274 myelomonocytic leukemia cells with rearrangements in c-*Myb* contained IAP integrations upstream of the *IL-3* gene leading to *gag*-to-*IL-3* fusion transcripts (183), and out of the FDC-P1 cells injected into irradiated DBA/2 mice clones developed that also contained an IAP in the *IL-3* gene (see *GM-CSF*) (89). Another example of IL-3 autocrine growth of an IL-3 dependent cell line was caused by an IAP insertion in the 3' untranslated region of the *IL-3* gene (3), resulting in truncation and stabilization of the *IL-3* mRNA (200). The myelomonocytic cell line WEHI-3B contains an IAP in the *IL-3* gene resulting in constitutive expression of IL-3 (344). In this cell line an IAP simultaneously inserted in *Hoxb8* (35, 161). Transplantation of hematopoietic cells overexpressing *IL-3* by retroviral gene transfer results in a myeloid disorder (341), showing that IL-3 by itself, like GM-CSF, is not sufficient to induce acute myeloid leukemia. However, infection of bone marrow cells with retrovirus overexpressing both *IL-3* and *Hoxb8* resulted in retarded differentiation *in vitro* and a rapid, transplantable myeloid leukemia (239).

M-CSF

Retroviral insertion of an ecotropic BALB/c virus in the gene encoding M-CSF was demonstrated in a monocyte-macrophage tumor induced by a c-*Myc* containing retrovirus (18). The provirus inserted in the opposite transcriptional orientation 3 kb upstream of the *M-CSF* promoter resulting in high levels of growth factor and autocrine growth. Transcription of *M-CSF* mRNA in this tumor is presumably elevated by the enhancer sequences in the LTR of the provirus.

c-Fms

The expression of the c-*Fms* gene, which encodes the receptor for M-CSF, is highly elevated in Friend MuLV-induced myeloblastic cells containing insertions upstream of c-*Fms* in the common VIS *Fim2* (295). Mutations in the intrinsic tyrosine kinase domain of c-Fms have been implicated in murine leukemogenesis (280).

Signal transducers

Evi2/Nf1

The common VIS *Evi2* has been identified in 15% of all leukemias in the BXH2 model (see 1.5.1) (46). Proviruses integrated in *Evi2*, in a large intron of the neurofibromatosis type 1 gene (*Nf1*), cause expression of truncated unstable Nf1 proteins (175). Reconstitution of the hematopoietic system with hematopoietic stem cells from Nf1 deficient mice results in a disease with myeloproliferative symptoms, also found in human juvenile CML, probably induced by Ras-dependent GM-CSF hypersensitivity (174). Furthermore, mice with a heterozygous mutation of *Nf1* are predisposed to get AML among other forms of cancer (140). As mentioned earlier the tumor suppressor gene *NF1* has also been implicated in human AMLs (see 1.4).

Cyclins

Fis1/CyclinD1

Retroviral insertions in *Fis1* (290) in Friend MuLV-induced myeloid leukemias elevate expression of *CyclinD1* (171). *Fis1* insertions are thought to be functionally equivalent with *BCL1* translocations in B-cell malignancies, in which *CyclinD1* is activated as well (69).

Transcription factors

Evi1 and *Cb1*

Evi1, which is normally not, or at very low levels, expressed in hematopoietic cells, has been shown to be activated in many leukemia models (30, 126, 136, 217, 219). An alternative site for proviral insertion and subsequent *Evi1* activation is the *Fim3/Cb1* locus, which is located 90 kb upstream of the *Evi1* gene (15, 16). Evi1 is a transcription factor containing two zinc finger domains conferring DNA binding activity to the protein (217). *Evi1* overexpression results in a block of granulocytic differentiation in 32Dcl3 cells (215). Interestingly, the DNA recognition sequence of Evi1 contains putative GATA1 binding sites (74, 199), and Evi1 has therefore also been implicated in defective erythroid differentiation (166).

Evi6 and *Evi7*

The common VISs *Evi6* and *Evi7* were identified in respectively 2.9% and 7.2% of spontaneous retrovirally-mediated myeloid leukemias in BXH-2 mice (228). *Evi6* and *Evi7* activate the homeobox genes *Hoxa9* and *Hoxa7*, respectively (228). The family of homeobox (*Hox*) genes is involved in pattern formation during development (169). Interestingly, tumors that contained a proviral insertion near one of the *Hox*-genes,

Hoxa9 or *Hoxa7*, also had provirus in another common VIS, i.e., the gene encoding the Pbx-related protein Meis1 (218). *Pbx1* is involved in t(1;19), found in 5% of all ALL cases (188), and Pbx-related proteins bind DNA cooperatively with Hox proteins (52). Recently, it was shown that Hoxa9 transforms primary bone marrow cells through specific collaboration with Meis1 and not Pbx1 (168).

Meis, Evi8* and *Evi10

Retroviral insertions in *Meis*, *Evi8* and *Evi10* all enhance full-length or truncated mRNA expression of the *Pbx*-related gene, *Meis1* (218, 228). As mentioned in the former paragraph, Meis1 in combination with Hoxa9 (*Evi6* (228)) is able to transform primary bone marrow cells (168). *Meis1* and *Hoxa9* apparently cooperate in transformation of hematopoietic cells to AML.

Hoxb8

The first identified *Hox*-family member activated by an IAP insertion upstream was *Hox-2.4* (*Hoxb8*) in the promyelocytic cell line WEHI-3B (35, 161) (see 1.5.2.1 *IL-3*).

Scl

Scl or *Tal1* is a basic helix-loop-helix protein and is critical for the establishment of the hematopoietic system (250, 286). *SCL* expression is activated in 40% of all T cell leukemias (109). In the parental G-CSF-responsive promyelomonocytic WEHI-3B, cell line IAPs inserted in the *IL-3* gene (344) and the gene encoding the homeobox protein *Hoxb8* (35, 161) (see 1.5.2.1 IL-3). In addition, Tanigawa *et al.* (304) showed in a G-CSF unresponsive subline of the WEHI-3B cell line an IAP in the 3' untranslated region of the *Scl* gene, which was not apparent in the parental cell line. This suggests that the IAP insertion, which leads to constitutive *Scl* expression, interferes with normal G-CSF-induced differentiation. The constitutive activation of *IL-3*, *Hoxb8*, and *SCL* in WEHI3B cells by IAPs (35, 304, 344), may indicate that these proto-oncogenes collaborate in myeloid tumor formation and progression.

Fli1

Fli1, which is a member of the Ets-family of transcription factors (25), was originally identified in 75% of Friend MuLV-induced erythroleukemias in BALB/c or NIH/Swiss mice (24). However, recently, *Fli1* insertions in 72% of Cas-Br-E MuLV-induced non-T-, non-B-cell leukemias, which consist of immature blast-like cells that lack differentiation markers, have been demonstrated (29-31). *Fli1* expression in myeloid or erythroid leukemias is increased as a result of LTR promoter insertion (30) or by activation through enhancement (25), respectively.

N-*Myc*

The proto-oncogenes c-*Myc* and N-*Myc* encode sequence-specific transcription factors (5). The encoded proteins contain helix-loop-helix and leucine zipper

domains. The *Myc* proteins become transcriptionally active by binding to their heterodimeric partners, and are involved in cellular proliferation and programmed cell death (5). Although aberrant expression of c-*Myc* and N-*Myc* are more frequently found in retrovirally-induced T-cell lymphomas (148), there is one case of insertion of an endogenous Moloney-MuLV-like element in the N-*Myc* gene in a macrophage-derived cell line (275). Transformation of the monocyte-macrophage lineage by *Myc* is shown *in vivo* and *in vitro*, by infection with retrovirus carrying the *Myc* gene (19).

c-*Myb*
The gene encoding the transcription factor c-Myb is one of the best-studied oncogenes in myeloid disease (138), and has shown to be a frequent target for retroviral integration in mouse myeloid leukemias (340). All proviral insertions in the c-*Myb* gene result in C- or N-terminal truncation of the protein (278). c-*Myb* has been implicated in hematopoietic cell proliferation and differentiation (138). All leukemias that arise as a result of proviral insertion in c-*Myb* are committed to the monocyte lineage and are partially differentiated (138).

p53
The tumor suppressor gene *p53* has been implicated in proliferation, cell cycling, apoptosis, and neoplasia (110). Rearrangements have been mainly observed in erythroleukemias induced by Friend helper MuLV or spleen focus-forming virus (86, 213). However, recently, *p53* rearrangements were found in 23% of Cas-Br-E MuLV-induced immature non-T-, non-B-cell leukemias in NIH/Swiss mice (29).

Other common virus integration sites

There are several common VIS which have been identified in myeloid leukemias from which the target proto-oncogenes are currently unknown, i.e., *Fim1* (295), *Mml1* (close to c-*Myb*) (160), *Evi9* (close to *Rel* oncogene), (228) and *His2* (6). Interestingly, *His1* represents a common VIS in which mRNAs without extensive open reading frames are activated (8).

From all these examples it is evident that retroviral insertional mutagenesis is an effective method to identify proto-oncogenes representing HGFs, HGF receptors, signaling molecules, transcription factors and cell cycling molecules important in myeloid cell transformation. However, most of these known common VISs are relatively rare. The aim of the research described in this thesis is the identification of more frequent novel common VISs in retrovirally-induced myeloid mouse leukemias (Chapters 2 and 5). The determination of the frequency and coincidence of known as well as novel common VISs in Cas-Br-M MuLV-induced myeloid leukemias (Chapter

5) may result in the definition of complementation groups of proto-oncogenes or tumor suppressor genes that are essential for the complete transformation of myeloid progenitor cells.

1.5.3 *Cooperation of proto-oncogenes*

Leukemia development, like oncogenesis in general, is thought to be the resultant of sequential activation of proto-oncogenes or disruption of tumor suppressor genes (1, 129, 327). For instance, the transition of CML from the chronic phase to the acute phase is thought to be the resultant of accumulating mutations, secondary to the *BCR/ABL* translocation, in the proto-oncogenes *Myc* or *Ras*, the tumor suppressor genes encoding p53, the retinoblatoma protein, p16, or the fusion protein AML1/EVI1 (203).
The relatively long latency period between slow-transforming MuLV-infection and the manifestation of the leukemia suggests that retroviral transformation is a multistep process involving various genes as well (148). Thus, retroviral insertional mutagenesis apparently resembles the multistep process of tumor formation (1, 129, 327). Because the probability of two concurrent insertions near two proto-oncogenes in various independent tumors is negligible, these provirus integrations must be functional in tumor formation or progression. There are many examples of retrovirally-induced myeloid neoplasms that acquired *in vivo* or *in vitro* provirus or IAPs near potential proto-oncogenes simultaneously. For instance, *Hox*- and *Pbx1*-related genes in myeloid leukemias (228), c-*Myc* and *M-CSF* in a monocyte tumor (18), *IL-3*, *SCL* and *Hoxb8* in WEHI-3B cells (35, 161, 304, 344), *IL-3* or *GM-CSF* and c-*Myb* in WEHI-274 cells (183), *IL-3* and *GM-CSF* in *in vivo*-passaged FDC-P1 cells (89), *Fim2*/c-*Fms* and *Fim3*/*Cb1* in transformed myeloblasts (102), and *Fli1* or *p53* in non-T-, non-B-cell leukemias (29). Cooperation of transforming genes has also been demonstrated in retrovirally-induced erythroid, B- and T-cell leukemias (44, 64, 213, 313).
The cooperation of proto-oncogenes in B- and T-cell lymphomagenesis has been further studied in proto-oncogene bearing transgenic mice by infection with slow-transforming retroviruses, thereby accelerating leukemia formation (1, 32). For instance, retroviral infection of Eμ-*Myc* or Eμ-*Pim1* transgenic mice resulted in the characterization of several collaborating proto-oncogenes, such as *Pim1*, *Pal1*, and *Bmi1* (Eμ-*Myc*) (323) or *Myc* and N-*Myc* (Eμ-*Pim1*) (322). These results nicely correspond with the collaboration of c-*Myc* and *Pim1*, demonstrated by Cuypers *et al.* (64) in retrovirally-infected non-transgenic mice. Recently, a related *in vivo* model to identify genes involved in tumor progression has been employed (149). The retransplantation of MuLV-induced Eμ-*Pim1* T-cell lymphomas in syngenic hosts led to the identification of the tumor progression gene *Frat1* (149). These examples

demonstrate that retroviral insertional mutagenesis in proto-oncogene bearing transgenic mice is valuable for the identification of new collaborating cancer genes.

The coexistence of common VISs in multiple retrovirally-induced tumors or tumor cell lines apparently represents two proto-oncogenes that collaborate in tumor formation. The identification of cooperating proto-oncogenes in Cas-Br-M MuLV-induced myeloid leukemias in NIH/Swiss mice (Chapters 4 and 5) may result in the description of the different oncogenic pathways that act together in full transformation of myeloid progenitor cells.

1.5.4 *Identification of virus integration sites*

The isolation of the actual VIS by genomic cloning and subsequent identification of the target gene that is aberrantly expressed due to viral interference, is laborious and time-consuming. A common VIS is characterized by retroviral insertions within corresponding genomic loci of various independent tumors, and marks the position of a possible proto-oncogene. These common proviral integration sites are visualized by Southern blot analysis with probes flanking the actual VIS (Figure 4). Unknown flanking DNA sequences have been determined by genomic cloning (6, 46, 218, 219), inversed PCR (291, 312), biotinylated DNA labeling followed by PCR (296, 297), and other PCR based methods (147, 187, 209, 337). However, these methods carry certain disadvantages. Isolation of flanking DNA fragments by genomic cloning requires the establishment of genomic libraries, which is time-consuming and restricted to one tumor or cell line. The quick PCR based methods consist of critical ligation (147, 291, 312), tailing (187), or biotinylating steps (296, 297). In addition, many of the PCR methods select for adjacent genomic DNA fragments (147, 209, 291, 296, 297, 312, 337). Selection for genomic fragments when investigating retrovirally-activated genes, may be a disadvantage because after isolation of the VIS flanking cellular DNA fragment and identification of the common VIS, the identity of the affected gene is not yet known. Therefore, larger fragments of that particular locus have to be isolated and coding sequences have to be extracted by Northern analysis with genomic DNA fragments or other approaches (237).

Since the methods of cloning genomic fragments and identifying mRNA coding sequences are major rate-limiting steps in positional cloning, many techniques have been simplified and improved. To further facilitate the identification of VISs, an RT-PCR based method was established for the rapid extraction of VIS-flanking sequences from Cas-Br-M MuLV-induced primary tumors or cell lines (Chapter 3).

1.5.5 *Chromosomal breakpoints and common virus integration sites*

The power of the retroviral mutagenesis approach for obtaining putative proto-oncogenes is best exemplified by the co-incidence of common VISs with mutations in human genetic malignancies. For example, Evi1 is a transcription factor, which was initially identified as a common ecotropic virus integration site in myeloid leukemias (217, 219). Interestingly, 3% of human acute myeloid leukemias contain recurrent translocations involving *Evi1* (188). Similarly, the common VIS *Evi6* in mouse leukemias (228) and the chromosomal translocation t(7;11) in 1% of human AMLs (38, 227), both involve the *Hoxa9* gene. Another example is the common VIS *Evi2* identified in highly-leukemogenic BXH-2 mice, which is located within the *Nf1* tumor suppressor gene (46). As mentioned earlier, *NF1* has been found to be mutated in multiple cases of human AML as well (277, 288). Recently we have identified a retroviral integration in the *Erg* gene (317), which is involved in t(16;21) (283) and present in 1% of human AMLs (188). Rearrangements in the *p53* gene, which is implicated in AML among many other forms of cancer (110), have been found in retrovirally-induced myeloid as well as erythroid leukemias (29, 86, 213). Furthermore, the identification of common VISs in genes encoding HGFs (18, 183, 344) or HGF receptors (109) demonstrates the presence of autocrine loops inducing autonomous growth in retrovirally-induced leukemias. Although autocrine growth stimulation by itself is not sufficient to induce leukemia, autonomous growth is also found in human AMLs (189).

All these examples clearly illustrate that the identification of proto-oncogenes in murine myeloid leukemias by using retroviral insertional mutagenesis may contribute to the explanation of oncogenic transformation mechanisms in human AMLs.

1.6 *Outline of this thesis*

The main objectives of the experimental work described in this thesis were the identification of novel common VISs and the target proto-oncogenes in retrovirally-induced myeloid mouse leukemias. In ***Chapter 2*** the characterization of a novel common VIS *Evi11* is described. This novel common VIS was identified in two Cas-Br-M MuLV-induced myeloid cell lines (NFS mice), NFS78 and NFS107, and five Cas-Br-M MuLV-induced primary tumors (NIH/Swiss mice). *Evi11* was shown to be located near the genes encoding the peripheral cannabinoid receptor (*Cb2*) and α-L-fucosidase on mouse chromosome 4. Retroviral insertion in *Evi11* occurred in the *Cb2* gene and resulted in aberrant mRNA expression of *Cb2*. *Cb2* was therefore indicated as the candidate target proto-oncogene in *Evi11*. To facilitate and accelerate the isolation of novel common VISs as well as the identification of target proto-oncogenes, a novel RT-PCR based method was established, which is described in

Chapter 3. With this technique, cDNA fragments flanking retrovirus integration sites are easily isolated. The power of the technique was confirmed by the isolation of cDNA fragments from the known common integration site *Evi1* (16, 217) and the murine homologue of human *ERG* (90). *EVI1* is frequently activated in human AMLs due to translocation of chromosome 3q26 (216) and ERG is involved in AML t(16;21) (283). The identification of additional primary tumors containing insertions in *Evi1* is described in ***Chapter 4***. In addition, experiments concerning the identification of *Evi1/Cb2*-cooperating genes resulted in the isolation of a novel common VIS, *Evi12*, which is located near the gene encoding tumor rejection antigen *Tra1* (201). *Evi12* showed a high coincidence with retroviral insertions in *Evi1* suggesting a cooperative role between the target proto-oncogenes in these two common VISs. The experiments in ***Chapter 5*** were performed to establish a novel panel of Cas-Br-M MuLV-induced primary leukemias suitable for the isolation of novel common VISs and identification of new proto-oncogenes. All primary tumors were characterized morphologically, phenotypically, and genotypically. In this study we demonstrate that *Evi1/Cb2*- and *Evi12*-rearrangements occurred in myeloid as well as T-lymphoid Cas-Br-M MuLV-induced leukemias, suggesting that insertions in these two loci represent early events in leukemogenesis. The experiments in ***Chapter 6*** are concerned with a possible role for the Cb2 receptor in hematopoietic cells. RNase protection analysis of murine tissues and many different hematopoietic murine hematopoietic cell lines representing multiple hematopoietic lineages, i.e., macrophage, eyrthroid, myeloid, mast, B- and T-lymphoid, demonstrated that the peripheral cannabinoid receptor Cb2, and not the brain type cannabinoid Cb1 receptor, is an hematopoietic receptor. Furthermore, serum-free cell cultures revealed that the fatty-acid derivative anandamide, a natural ligand for the peripheral cannabinoid receptor Cb2, acts as a novel synergistic growth factor for hematopoietic cells. In ***Chapter 7*** experiments are described to explain the mechanisms of synergistic proliferation following HGF and anandamide stimulation.

CHAPTER 2

THE GENES ENCODING THE PERIPHERAL CANNABINOID RECEPTOR AND α-L-FUCOSIDASE ARE LOCATED NEAR A NEWLY IDENTIFIED COMMON VIRUS INTEGRATION SITE, *Evi11*.

Peter J.M. Valk, Samantha Hol, Yolanda Vankan, James N. Ihle, David Askew, Nancy A. Jenkins, Debra J. Gilbert, Neal G. Copeland, Nico J. de Both, Bob Löwenberg, and Ruud Delwel.

Journal of Virology 71 (9): 6796 - 6804, 1997.

Abstract

A new common region of virus integration, *Evi11*, has been identified in two retrovirally induced murine myeloid leukemia cell lines, i.e. NFS107 and NFS78. By interspecific backcross analysis it was shown that *Evi11* is located at the distal end of mouse chromosome 4, in a region that shares homology with human 1p36. The genes encoding the peripheral cannabinoid receptor (*Cb2*) and α-L-fucosidase (*Fuca1*) were identified near the integration site by using a novel exon trapping system. *Cb2* is suggested to be the target gene for viral interference in *Evi11*, since proviruses are integrated in the first intron of *Cb2* and retroviral integrations alter mRNA expression of *Cb2* in NFS107 and NFS78. In addition, proviral integrations were demonstrated within the 3' untranslated region of *Cb2* in five independent newly derived Cas-Br-M MuLV (mouse murine leukemia virus) tumors, i.e. CSL13, CSL14, CSL16, CSL27 and CSL97. The *Cb2* gene encodes a seven-transmembrane G-protein-coupled receptor that is normally expressed in hematopoietic tissues. Our data suggest that the peripheral cannabinoid receptor gene might be involved in leukemogenesis as a result of aberrant expression of *Cb2* due to retroviral integration in *Evi11*.

Introduction

The identification of common virus integration sites (VISs) in retrovirally induced murine cancers has been proved successful for isolating transforming genes from hematopoietic malignancies and solid tumors (7, 148, 321). Cellular genes may become aberrantly expressed following proviral integration, through activation by viral promoter or enhancer sequences. Alternatively, proviral integration within the protein-coding region of a gene may result in the expression of an altered product (321). Abnormal expression of a proto-oncogene may provide the target cell with a growth abnormality and contribute to malignant transformation. A number of common VISs have been identified in murine retrovirally induced hematopoietic malignancies. These VIS are frequently designated ecotropic VIS (*Evi1* to *Evi10*), although other names have been used as well (6, 46, 148, 152, 185, 219, 228). Leukemia development in retrovirally induced leukemias is a multistep process which usually takes more then three months (7, 148, 321). Thus, in a retrovirally induced leukemia one can predict more than one common VIS, resulting in aberrant expression of multiple genes. The frequency of a particular common VIS is usually low, i.e., below 5%, indicating that a large number of different genes may be responsible for retrovirus mediated leukemogenesis in mice (7, 148, 321).
From a number of primary hematopoietic tumors, induced by Moloney murine leukemia virus (MoMuLV) or the wild mouse ecotropic retrovirus Cas-Br-M MuLV, in vitro cell lines have been established (126, 136). In these interleukin-3 (IL-3)-dependent cell lines, several common VISs and potential oncogenes, including *Evi1*

(217), *Evi2* (46), *His1* and *His2* (6), have been found. In the present study we describe the identification of a new common VIS, designated *Evi11*, in two myeloid leukemia cell lines and five newly isolated Cas-Br-M MuLV-induced primary tumors.
Exon trapping has been used as an effective method for deducing mRNA-coding sequences from genomic DNA fragments (9, 47, 91, 120). We used a new exon trap vector, pEVRF0-ET, based on the rabbit-β-globin (RβG) gene, which, in contrast to pSPL1 with an artificial intron (47), contains the natural intervening sequence 2 of the RβG gene (IVS2-β). This exon trap system was applied to the *Evi11* locus, and two genes, the peripheral cannabinoid receptor (*Cb2*) gene and the α-L-fucosidase (*Fuca1*) gene, were identified. The results of the studies presented here suggest that the hematopoietic receptor gene, *Cb2*, is the candidate gene for viral interference in *Evi11*.

Materials and Methods

Cell lines - Nine leukemic cell lines established in vitro from Cas-Br-M MuLV-initiated primary tumors (NFS22, -36, -56, -58, -60, -61, -78, -107 and -124) (126) and 13 cell lines derived from MoMuLV induced tumors (DA1, -2, -3, -7, -8, -13, -24, -25, -28, -29, -31, -33 and -34) (136) were cultured in RPMI1640 medium supplemented with penicillin (100 IU/ml), streptomycin (100 ng/ml), 10% fetal calf serum (FCS) and 10% WEHI-3B cell conditioned medium (134). COS-1 cells were cultured in Dulbecco's modified Eagles medium (DMEM) containing 10% FCS, penicillin and streptomycin.

Primary tumors - Newborn NIH-Swiss mice were injected subcutaneous with cell culture supernatant of Cas-Br-M MuLV-producing NIH-3T3 cells (obtained from H. Morse III, NCI, Frederick, Md.). Between 150 and 220 days after injection the mice developed leukemias. All leukemic mice had enlarged (5- to 10-fold) spleens and some had thymomas. Sixty Cas-Br-M MuLV-induced leukemias (CSL: Cas-Br-M MuLV Swiss Leukemias) were cryopreserved in liquid nitrogen. From these tumors high molecular DNA was isolated (267) for Southern blot analysis.

Genomic cloning - From NFS107 cells high-molecular-weight DNA was isolated as described previously (267). The DNA was partially digested with *Sau*3A and separated on 0.4% agarose. DNA fragments of 9 to 23 kb were isolated by electroelution and purified on NACS columns (Bethesda Research Laboratories, Bethesda, Md.). These fragments were then ligated into BamHI EMBL3 phage arms and packaged (Stratagene, La Jolla, Calif.). DNA from $1x10^6$ plaques was transferred to nitrocellulose filters and screened (267) with a [^{32}P]-dATP-labelled 270-bp *Sma*I-*Pvu*II fragment isolated from the U_3 long terminal repeat (LTR) of MoMuLV (63). Probes were labelled by random priming (96). Filters were hybridized in 50%

[vol/vol] formamide, 5% dextran sulphate sodium salt, 5xSSPE (0.9M NaCl, 0.05M $NaH_2PO_4.H_20$, 0.005M EDTA pH7.7), 10xDenhardt's solution (0.2%[wt/vol] bovine serum albumin (BSA), 0.2%[wt/vol] Ficoll 400, 0.2%[wt/vol] polyvinylpyrrolidone), 0.1% [wt/vol] sodium dodecyl sulfate (SDS) and 0.1 mg of sonicated salm sperm DNA per ml. The blots were hybridized at 42°C overnight and washed for 15 min at 65°C in 2xSSPE/0.5% SDS and for 15 min at 65°C 0.5xSSPE and analyzed by autoradiography. Phage DNA was isolated (267) and restriction maps of the different clones were prepared. DNA fragments adjacent to the VIS were isolated, subcloned in pBluescript II SK+ (Stratagene) and used for Southern blot analysis using DNA of the different DA and NFS cell lines. Cosmid clones were isolated from a female (4-8 weeks) mouse liver genomic library (Stratagene catalog no. 946305) and a murine embryonic stem cell genomic library in cosmid pTBE using standard techniques (267).

Southern and Northern blot analysis - Genomic DNA was isolated as described (68), digested with the appropriate restriction enzymes, and electrophoresed on a 0.6% agarose gel. Fragments were transferred to Hybond-N^+ (Amersham) nylon membranes with 0.25M NaOH/1.5M NaCl. Total RNA from cell lines was extracted with guanidinium isothiocyanate as described (267). 10µg total RNA was separated on a 1% agarose, 6% formaldehyde gel and blotted with 20x SSC onto Hybond-N^+ nylon membranes (Amersham). Hybridization and washing procedures of Northern and Southern blots were identical to those described in the former paragraph. mRNA hybridization signals were quantitated by scanning of the Northern blots with a Vilber Lourmat camera and Bio-Profil V 4.6 software.

RNase protection - RNase protection was performed as described previously (267). Fragments were cloned into pBluescript II SK+ and linearized using the proper enzymes, and RNA probes were synthesized using T_3 or T_7 polymerase. For each incubation 10 µg of RNA and radiolabelled RNA probe (15.000 cpm) were suspended in 30 µl hybridization buffer (80% deionized formamid, 40mM piperazine-N,N'-bis(2-ethanesulfonic acid) (PIPES; pH 6.4), 0.4M sodium acetate, 1mM EDTA). The samples were heated to 85°C for 5 minutes and then incubated for 16 hours at an annealing temperature of 50°C. To these mixtures, 300 µl RNase digestion buffer (10 mM Tris-HCl (pH7.5), 5mM EDTA, 200 mM sodium acetate and 1 Unit RNase One (Promega, Leiden, The Netherlands) were added. After 1 hour at 37°C, the reaction was stopped by the addition of 3.3 µl 10% SDS and 20 µg carrier tRNA. The reaction products were precipitated with ethanol, fractionated by electrophoresis in a 6% polyacrylamide/7M urea gel, and analyzed by autoradiography. A radiolabeled *GAPDH* RNA fragment was used as a control (142).

Interspecific backcross mapping - Interspecific backcross progeny were generated by mating (C57BL/6J x *Mus spretus*)F_1 females and C57BL/6J males as described

previously (59). A total of 205 backcross mice were used to map the λ6.2 locus (see Results for details). DNA isolation, restriction enzyme digestion, agarose gel electrophoresis, Southern blot transfer, and hybridization were performed essentially as described elsewhere (143). All blots were prepared with Hybond-N^+ nylon membrane (Amersham). The probe, a 1.2-kb *SalI/SstI* fragment of mouse genomic DNA, was labeled with [α^{32}P]dCTP using a random prime labeling kit (Amersham); washing was done to a final stringency of 0.8X SSCP, 0.1% SDS at 65°C. A 10.5-kb fragment was detected in *Hin*cII-digested C57BL/6J DNA, while 6.2- and 4.0-kb fragments were detected in M. spretus DNA. The presence or absence of the 6.2- and 4.0-kb *M. spretus*-specific *Hin*cII fragments, which cosegregated, were followed in backcross mice. A description of the probes and RFLPs for the loci linked to the *Evi11* locus, including Gardner-Rasheed feline sarcoma viral oncogene homolog (*Fgr*) and natriuretic peptide precursor type A gene (*Nppa*) have been described previously (51). Recombination distances were calculated as described by Green (113), using the computer program SPRETUS MADNESS. Gene order was determined by minimizing the number of double and multiple recombination events across the chromosome.

Exon trapping - The exon trap vector was based on an eukaryotic expression vector pEVRF0, which had been designed for the analysis of mutant proteins (221). The vector contains pSP65 bacterial plasmid sequences, the human cytomegalovirus enhancer/promoter, the translation initiation region from the herpes simplex virus thymidine kinase gene, splicing and polyadenylation signals from the RβG gene and the simian virus 40 origin of replication (276) (see Figure 4A). The RβG fragment includes map position 905 (*Bam*HI) to 2080 of the RβG gene. This fragment consists of the IVS2-β flanked by thymidine kinase-RßG exon 2 and RβG exon 3. A 39-bp *SmaI/Hin*cII fragment from the polylinker of pBluescript II SK+ was cloned into the *Hin*cII site of the IVS2-β to introduce multiple cloning sites. Genomic DNA from cosmids #5 and #10 (see Figure 2A) were partially digested with *Hpa*II and separated on a 1% agarose gel, and fragments between 2 and 5 kb were isolated. These *Hpa*II fragments were ligated in the newly created ClaI site. COS cells were grown to ±50% confluency. DEAE-dextran (100 µg/ml) and 10 µg DNA in DMEM were added; and after two hours, this solution was replaced by 0.1 mM chloroquine in DMEM. Cells were incubated with this mixture for three hours, and then the medium was refreshed by DMEM with 10% FCS. The cells were cultured for 2 to 3 days, and total RNA was isolated. RT-PCR was carried out with primer set 1A (5'-GGGGGATCTTGGT-GGCGTG-3') and 1B (5'-AGATCTCAGTGGTATTTGTGAGC-3'). Subsequently, a nested PCR was performed with primers 2A (5'-CGTCTAGAGGAGT-GAATTCTTTGC-3') and 2B (5'-ATCCATGGATCCTGAGAACTTCAG-3'). The PCR cycling conditions were as follows: for primer set 1A/1B, 1 min at 94°C, 1 min at 64°C and 1 min at 72°C (30 cycles); primer set 2A/2B, 1 min at 94°C, 1 min at 52°C and 1 min at 72°C (30 cycles). Amplified fragments were visualized on a 2%

agarose gel by ethidium bromide staining. Potential exons were subcloned into pBluescript II SK+ by digestion with BamHI/EcoRI (see Figure 4A). Border sequences of RβG exon 2 and RβG exon 3 were thereby included in the cloned product.

Sequence analysis - Nucleotide sequencing was performed by the method of Sanger and Coulsen (268). Fragments were cloned into pBluescript II SK+ and sequenced with T_3, T_7, or sequence specific primers. Deduced sequences were analyzed using the BLAST network service of the National Centre for Biotechnology Information. The accession number of the murine peripheral cannabinoid receptor-2 is X93168.

RT-PCR - Reversed transcriptase reactions were performed 1.5 hour at 37°C with 3μg total RNA in 50mM Tris-HCl (pH 8.3), 75mM KCl, 3mM $MgCl_2$, 1mM dithiothreitol, 40mM oligo$(dT)_{16}$, 0.5mM deoxynucleoside triphosphates ($dNTP^s$), 1 unit RNAguard (Pharmacia) and 100 units of SuperScript RT (Gibco, Breda, The Netherlands). The PCR reaction mixture contained 10mM Tris-HCl (pH 8.3), 50mM KCl, 1.5mM $MgCl_2$, 150μM $dNTP^s$ and 2.5 units of Taq polymerase. PCR cycling started with 10 min at 94°C and ended with 10 min extension at 72°C.

cDNA cloning by PCR - All RT-reactions of the RACE experiments were done with 2 μg poly$(A)^+$ RNA. Poly$(A)^+$ RNA was purified by affinity chromatography using oligo(dT)-cellulose columns (Pharmacia). 3' RACE experiments were performed by using an oligo(dT)-adapter primer (5'-GTCGCGAATTCGTCGACGCG$(dT)_{15}$-3') for first strand synthesis. Subsequently, PCR was carried out using the adapter primer (5'-GTCGCGAATTCGTCGACGCG-3') in combination with gene specific primers (CBR15: 5'-CACGCTTAGTGATTTAGACT-3' (bp 2634 to 2653), CBR16: 5'-GTATTTCAACATCAACTTGG-3' (bp 2654 to 2673)). Cycling parameters were 1 min at 94°C, 2 min at 57°C and 3 min at 72°C (25 cycles). Products were cloned into pBluescript II SK+ and sequenced. The 5'-AmpliFINDER™ RACE Kit (Clontech, Palo Alto, Calif.) was used to isolate additional 5' cDNA sequences. The strategy for the 5' RACE was as follows. A gene-specific primer (CBR3: 5'-GTGAAGGTCATGGTCACACT-3' (bp 517 to 536)) was used for first-strand synthesis and then an anchor primer was ligated to the cDNA 3'-end. Subsequently, the anchor primer and nested primers (CBR9: 5'-CCGTTGGTCACTTCTGTCTC-3' (bp 199 to 218), CBR10: 5'-GAGCTGTCCAGAAGACTGGG-3' (bp 138 to 158)) were used to amplify additional 5' cDNA fragments. Cycling parameters for both primersets were 1 min at 94°C, 1 min at 57°C and 3 min at 72°C (25 cycles). The products that were obtained by 5' RACE, were cloned into pBluescript II SK+ and sequenced.

Results

Identification of a common integration site (*Evi11*) in cell lines NFS107 and NFS78 - A *Sau*3A partial genomic library from NFS107 was prepared in EMBL3. The library was screened with a specific U_3 LTR probe from MoMuLV (63) and 8 different LTR-positive clones were obtained (data not shown). The restriction map of one clone, λ6.2, is shown in Figure 1A. From this phage clone a nonviral, nonrepetitive 1.2 kb-*Sst*I/*Sal*I probe F (Figure 1A) was isolated and used for further analysis. With this probe, DNAs from 13 MoMuLV and 9 Cas-Br-M MuLV-induced leukemic cell lines were screened by Southern analysis using the restriction enzymes *Pvu*II, *Sst*I, *Xba*I, *Kpn*I, *Pst*I and *Hin*dIII. As shown in Figure 1B, rearrangements

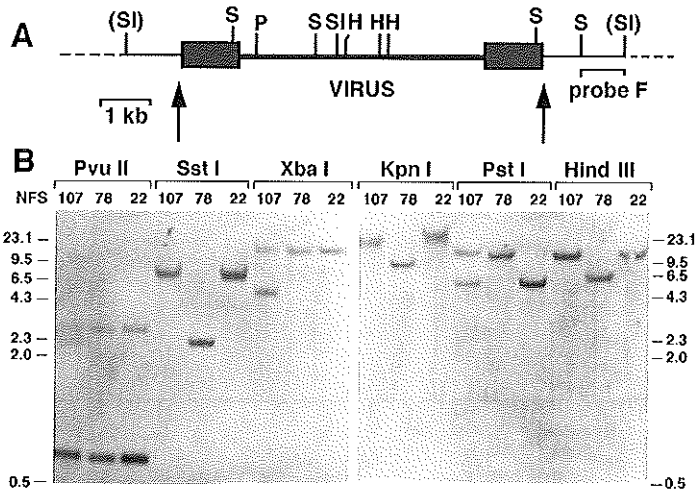

Figure 1: Identification of common integration site *Evi11*.
A. Restriction enzyme map of virus integration site λ6.2 (Sl: *Sal*I; S: *Sst*I; H: *Hin*dIII; P: *Pst*I; (Sl): *Sal*I from EMBL3 phage arms).
B. Rearrangement of the *Evi11* locus by Southern blot analysis of genomic DNA from retrovirus- induced murine leukemia cell lines NFS22, NFS78 and NFS107. Filters were hybridized to a 1.2 kb fragment (probe F) from the λ6.2 integration site. Sizes are indicated as kilobases.

were identified in NFS107 and in the leukemic cell line, NFS78. Southern analysis also revealed that NFS78 had lost its normal allele (Figure 1B, *Sst*I/*Kpn*I/*Pst*I/*Hin*dIII). NFS107 and NFS78 are both IL-3 dependent, and do not respond to granulocyte and granulocyte-macrophage colony-stimulatory factors (G-CSF and GM-CSF), stem cell factor, and IL-7 (data not shown). NFS107 cells express the myeloid markers, myeloperoxidase, Mac-1 and Mac-2 (133). NFS78 is a leukemic

cell line with myeloblastic characteristics (126) and expresses the myeloid marker Mac-1 (133). Immunoglobulin heavy chain genes of both cell lines are in germline configuration. Southern blotting and genetic back cross analysis with a fragment derived from another integration site in NFS107 demonstrated that this integration had occurred in the recently identified common VIS, *Evi3* (data not shown and 31). NFS78 expresses another common VIS, *Evi1* (217). NFS22 (Figure 1B) and 19 other cell lines did not show rearrangements in the *Evi11* locus after hybridization with probe E, F or C (Figure 2B). To obtain genomic DNA of the normal *Evi11* locus, two genomic cosmid libraries were screened with probe F (Figure 1A and 2B). We isolated three cosmid clones, #32B, #5, and #10, covering a region of approximately 70-kb of the locus that we designated *Evi11*. A limited restriction map of *Evi11* is shown in Figure 2A. The orientation of the viral DNA in NFS107 and NFS78 was deduced from restriction enzyme analysis of the normal genomic organization

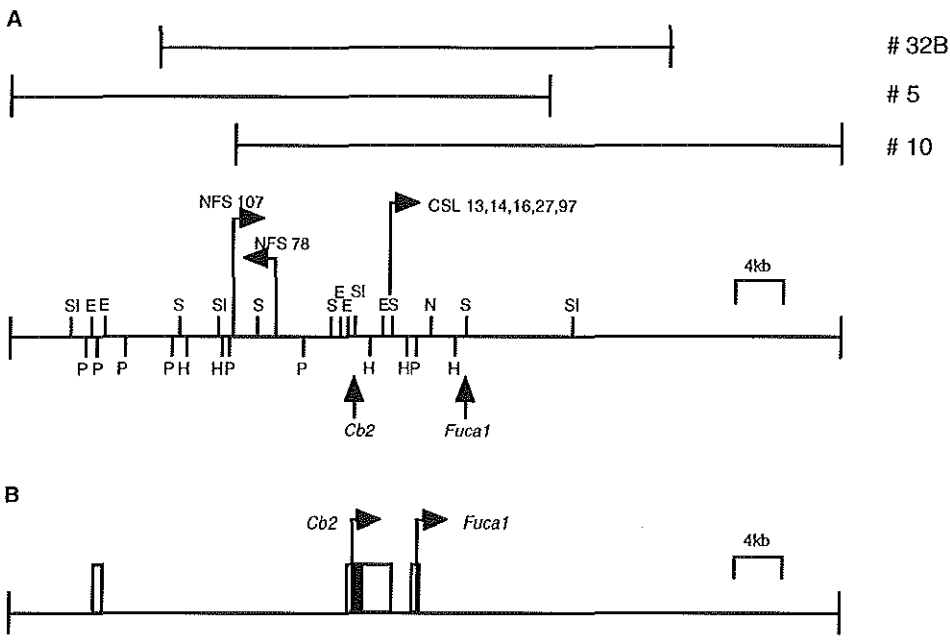

Figure 2: Restriction enzyme map and genomic structure of *Evi11*.
A. Restriction pattern *Evi11* based on Southern blot analysis with cosmid clones #5,#10 and #32B (N: *Not*I; SI: *Sal*I; E: *Eco*RI, S: *Sst*I; H: *Hin*dIII and P: *Pst*I). The location of the trapped *Cb2* fragment (*Cb2*) and exon 3 of Fuca1 (*Fuca1*) are indicated. Arrows indicate the locations and orientations of provirus in NFS78 and NFS107 as well as CSL13, CSL14, CSL16, CSL27, and CSL97.
B. Genomic structure of the *Evi11* locus. The location of the 5' noncoding exon 1 and protein-coding exon 2 of *Cb2*, the 5' exon of α-L-fucosidase and probes E, F and C are depicted diagrammatically, with notation corresponding to that in panel A.

(cosmid #5 and #32B) and Figure 1B, in combination with the restriction map of Cas-Br-M MuLV (accession no. X57540). In NFS78, retroviral DNA is oriented opposite the integrated viral DNA within the same locus in NFS107 (Figure 2A). The distance between the two integrations is approximately 3 kb.

Chromosomal localisation of *Evi11* - The chromosomal localisation of *Evi11* was initially determined to be on murine chromosome 4 by fluorescence in situ hybridization (FISH) analysis (data not shown). A more exact positioning of *Evi11* was obtained by interspecific backcross analysis using progeny derived from matings of [(C57BL/6J x *M. spretus*)F_1 x C57BL/6J] mice. This interspecific backcross mapping panel has been typed for over 2,100 loci that are well distributed among all mouse autosomes and the X chromosome (59, 60). C57BL/6J and *M. spretus* DNAs

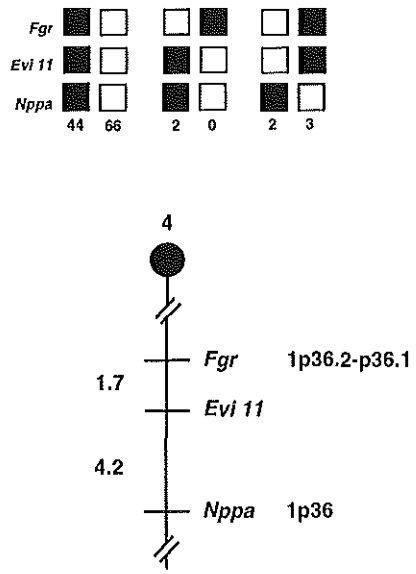

Figure 3: *Evi11* maps in the distal region of mouse chromosome 4.
Evi11 was mapped to mouse chromosome 4 by interspecific backcross analysis. The segregation patterns of *Evi11* and flanking genes in 117 backcross animals are shown at the top. For some of the individual pairs of loci, more than 117 animals were typed (see text). Each column represents the chromosome identified in the backcross progeny that was inherited from the (C57BL/6J x *M. spretus*)F1 parent. The shaded boxes represent the presence of a *M. spretus* allele. The number of offspring inheriting each type of chromosome is listed below each column. A partial chromosome 4 linkage map showing the location of *Evi11* in relation to linked genes is shown at the bottom. Recombination distances between loci in centimorgans (cM) are shown to the left of the chromosome, and the positions of loci in human chromosomes are shown to the right. References for human map positions can be obtained from GDB (Genome Data Base), a computerized database of human linkage information maintained by The William H. Welch Medical Library of The Johns Hopkins University (Baltimore, Md.).

were digested with several restriction enzymes and analyzed by Southern blot hybridization for informative restriction fragment length polymorphisms (RFLPs) using the mouse 1.2 kb-*SstI*/*SalI* probe F (Figure 1A). Cosegregating 6.2- and 4.0-kb *M. spretus*-specific *Hin*cII fragments were used to follow the segregation of the *Evi11* locus in backcross DNAs. The mapping results indicated that *Evi11* is located in the distal region of mouse chromosome 4 (Figure 3). Although 117 mice were analyzed for all three markers shown in the haplotype analysis (Figure 3), up to 121 mice could be typed for one pair of markers. Each locus was analyzed in pairwise combinations for recombination frequencies, using the additional data. The ratios of the total number of mice exhibiting recombinant chromosomes to the total number of mice analyzed for each pair of loci and the most likely gene order are: centromere - *Fgr* - 2/121 - *Evi11* - 5/119 - *Nppa*. The recombination frequencies (expressed as genetic distances in centimorgans (cM) ± the standard error) are: centromere - *Fgr* - 1.7±1.2 - *Evi11* - 4.2±1.8 - *Nppa*. No recombinations were observed between *Evi11* and the α-L-fucosidase gene. The distal half of mouse chromosome 4 shares a region of homology with human chromosome 1 (Figure 3).

Identification of transcribed sequences in the *Evi11* locus by using exon trapping - To isolate coding sequences from the *Evi11* locus, an exon trapping system was designed (Figure 4A) and applied to cosmid clones #5 and #10 (Figure 2A). *Hpa*II-partially-digested fragments of cosmids #5 and #10, between 2 and 5 kb, were cloned into the *Cla*I site of the exon trap vector. These constructs were pooled in groups of 6 clones per COS-cell transfection. Thirty transfections were performed. RT-PCR was carried out on RNA isolated from the transfected COS-cells. Potential exons with sizes ranging from 50 to 300 bp were amplified from the different pools, using primers 1A/1B followed by 2A/2B, and visualized by ethidium bromide staining. Eight examples of COS cell transfections are shown in Figure 4B (lanes 1 to 8). Transfection of the exon trap vector without insert resulted in the isolation of a 97-bp fragment representing the fusion of exon 2 and 3 of the RβG gene (Figure 4B, lane V). Potential exons were subcloned into *Bam*HI/*Eco*RI-digested (Figure 4A) pBluescript II SK+ and sequenced. The DNA sequences were compared to those in the National Center for Biotechnology Information database. Among 16 clones analyzed, one exon was the mouse homolog of exon 3 of human α-L-fucosidase (*FUCA1*) (167), a gene which by interspecific backcrossing had been shown to be located in the proximity of *Evi11* (Figure 3). Seven clones contained sequences that were homologous to part of the coding region of the *CB2* gene (222). However, the *Cb2* fragments were trapped in between the two RβG-exons in the reversed transcriptional orientation. Sequence analysis of these trapped fragments and of the human cDNA of *CB2* demonstrated the presence of cryptic splice sites at the proper positions in the reversed orientation (see Figure 6A). Eight clones contained cosmid vector sequences. The trapped fragments were radiolabeled and used for Northern analysis to examine the expression of the representing genes in the different cell lines.

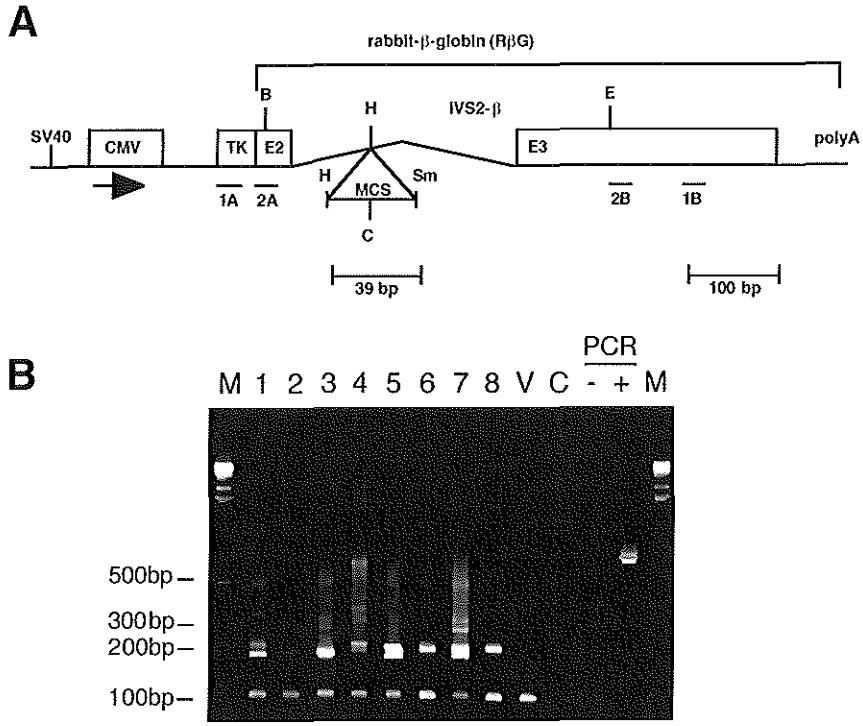

Figure 4: Isolation of transcribed sequences from *Evi11* by exon trapping.
A. Exon trap vector pERVF0. Abbreviations: SV40, simian virus 40 origin of replication; CMV, human cytomegalovirus enhancer/promoter region; TK, thymidine kinase translation initiation region; E2 and E3, exon 2 and exon 3 of RβB gene; IVS2-β, intervening sequence-2 of the RβG gene; MCS, multiple cloning site (B: *Bam*HI; C: *Cla*I; E: *Eco*RI; H: *Hin*cII; Sm: *Sma*I; primers 1A, 1B, 2A and 2B).
B. Agarose gel electrophoresis of RT-PCR fragments (primerset 2A and 2B) obtained from COS-1 cells transfected with the exon trap vector pERVF0. Lanes 1-8: EtBr stainings of RT-PCR fragments obtained from transfections with pERVF0 containing *Evi11* genomic inserts. Lane V: RT-PCR fragment from a transfection with empty vector. Lane C: RT-PCR using RNA from non-transfected COS cells. M: 1-kb ladder (Boehringer).

Two different mRNAs of ±1.6 kb and ±4.0 kb were identified (Figure 5). Analysis using separate probes revealed that the ±1.6 kb signal represented α-L-fucosidase and the *Cb2* fragment detected the ±4.0 kb mRNA. In NFS78, NFS107 and control cell lines, NFS22 and NFS36, variable levels of *Cb2* mRNA were apparent (Figure 5). In NFS78, *Cb2* mRNA levels were higher than in control cell lines, whereas in NFS107 no *Cb2* mRNA could be identified (Figure 5 and Table 1). In fact, Northern analysis using RNAs from a panel of cell lines demonstrated variable levels of *Cb2* mRNA expression in all DA and NFS lines (data not shown). Levels of *Fuca1* transcripts in

	Level (% of *GAPDH* control)			
mRNA*	NFS22	NFS36	NFS78	NFS107
Fuca1	15%	12%	18%	7%
Cb2	10%	4%	36%	0%

Table 1: *Cb2* and *Fuca1* mRNA levels in NFS cell lines
*Identified by Northern blot analysis (Figure 5).

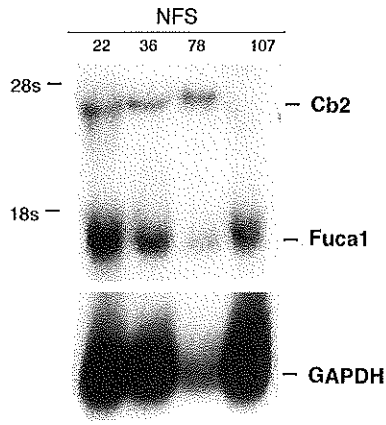

Figure 5: Expression of *Cb2* and *Fuca1* in retrovirally induced leukemias.
Northern analysis of NFS22, NFS36, NFS78 and NFS107. Total RNA was hybridized to a ^{32}P-labelled *Fuca1* exon 3 probe and a ^{32}P-labelled *Cb2* fragment that had been obtained by exon trapping. The filter was subsequently hybridized with a radiolabeled *GAPDH* probe (142).

the different cell lines were comparable (Figure 5, Table 1 and data not shown). Although the levels of *Fuca1* mRNA in the different leukemic cell lines (Table 1 and data not shown) were less variable versus the *Cb2* mRNA levels, the Northern analysis was not conclusive with respect to altered gene expression caused by virus integration.

The *Cb2* nucleotide sequence and exon structure - Southern blot analysis was carried out on the three *Evi11* cosmid clones to determine the positions of the amplified fragments (Figure 2A). The trapped *Cb2* fragment was mapped on a 3 kb *Eco*RI/*Eco*RI fragment (Figure 2). The localization was confirmed by the presence of a relatively rare *Sal*I site in this fragment. Exon 3 of α-L-fucosidase is situated approximately 12 kb from the provirus in NFS78. Since *Cb2* is located nearer the VIS than the α-L-fucosidase gene, and the gene encodes a hematopoietic receptor (222),

which may be involved in monocyte/macrophage differentiation (223), we decided to determine the nucleotide sequence and the genomic structure of the *Cb2* gene. Southern analysis with a 5'- and 3'- cDNA probe of the human *CB2* gene suggested that the entire protein-coding sequence was located within the 3-kb *Eco*RI/*Eco*RI fragment (Figure 2). *Hpa*II and *Sau*3A fragments of the 3-kb *Eco*RI/*Eco*RI fragment were subcloned into, respectively, the *Cla*I and *Bam*HI sites of pBluescript II SK+ and sequenced (Figure 6A). The merged nucleotide sequences of the 3-kb *Eco*RI/*Eco*RI showed that the complete protein-coding sequence of the murine *Cb2* receptor is present within this 3-kb fragment. The aminoacid sequence of the murine *Cb2* gene product is 82% homologous to that of the human *CB2* gene product. The C-terminal end of the murine homolog lacks 9 aminoacids. An aminoacid sequence comparison of murine *Cb2*, human *CB2* (222) and murine (accession no. U22948) and human CB1 (106) brain cannabinoid receptor gene products, is shown in Figure 6B. Nucleotide sequencing of the *Cb2* protein-coding region from NFS107 and NFS78 cDNA did not show any mutations. The 3' non-coding sequence was isolated by 3' RACE on poly(A)$^+$ from control cell line NFS22 by using two gene-specific primers (CBR15 and CBR16). Two fragments which terminated at 2,951bp and 3,756bp were isolated. The 3' untranslated regions appeared to be, respectively, 1,724bp and 2,528bp long, with putative polyadenylation signals (AAUAAA) at bp 2928 and 3743. This variability in 3' UTR lengths has also been shown for the rat brain cannabinoid receptor (197). The complete *Cb2* sequence identified so far is located in one exon. Upstream of the ATG start site of mouse *Cb2* on the 3-kb *Eco*RI/*Eco*RI fragment, a potential 3' splice acceptor site was identified (Figure 7B). To investigate whether 5' exons, which could splice to this potential acceptor site, existed, 5' RACE was carried out using poly(A)$^+$ RNA from the control cell line NFS22. Amplification with the anchor primer and CBR9, followed by a nested PCR with the anchor primer and CBR10, resulted in the isolation of a fragment of 179 bp (Figure 6A). This fragment was cloned into pBluescript II SK+ and sequence analysis revealed that an exon of at least 121 bp was spliced to the predicted splice acceptor site. Since this exon introduces a stop codon in frame with the ATG start site, this exon is noncoding (Figure 6A). Interestingly, Southern blot analysis demonstrated that exon 1 of *Cb2* is located approximately 20 kb upstream of protein-coding exon 2. Thus, virus integrations in NFS107 and NFS78 have occurred in an intron of *Cb2* (Figure 7A).

***Cb2* expression studies in leukemic cell lines** - Northern analysis demonstrated variable levels of *Cb2* mRNA expression in the distinct cell lines studied (Figure 5, Table 1, and data not shown) but was not conclusive with respect to the viral integrations. Since in NFS78 and NFS107, proviral DNA is integrated in the *Cb2* intron we verified with RNase protection whether the levels of expression of the two exons had been altered. A 195-bp *Eco*RI (anchor 5'RACE)/*Nco*I fragment

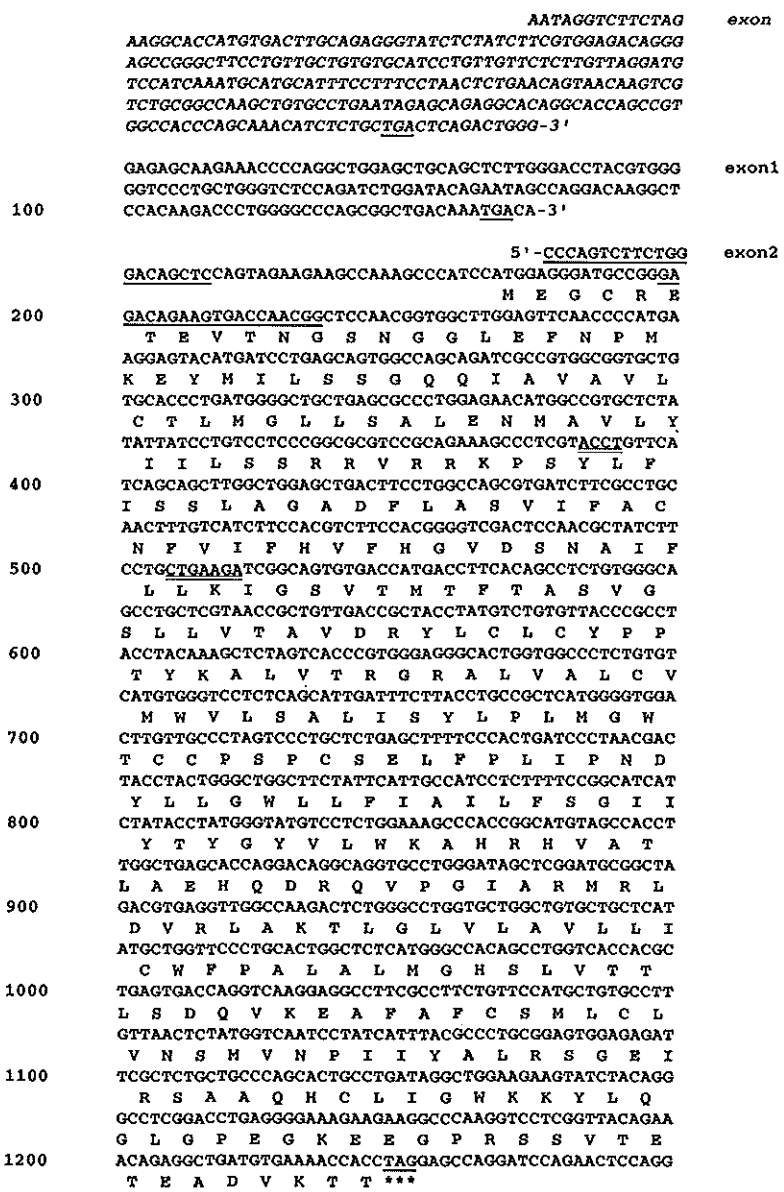

Figure 6A: Partial nucleotide and complete protein sequence of the mouse peripheral cannabinoid receptor *Cb2*.
The nucleotide and deduced protein sequence of mouse *Cb2*. In-frame stop codons in the 5' and 3' UTRs and 5'RACE primers CBR9 (bp 199 to 218) and CBR10 (bp 138 to 158) are underlined. Exon 1 of NFS78 is italicized. The cryptic splice sites located on the non-coding strand are double underlined.

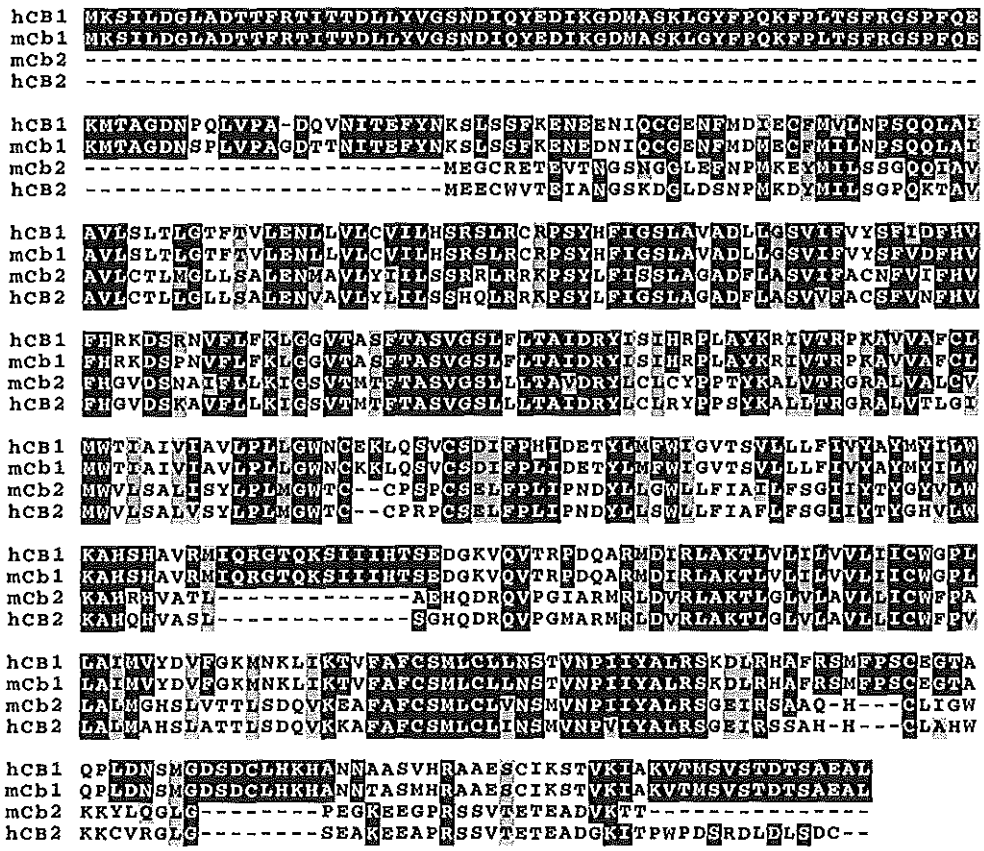

Figure 6B: Nucleotide and protein sequences of the mouse and human cannabinoid receptors.
Amino acid comparison of the human CB1 (hCB1), mouse Cb1 (mCb1), mouse Cb2 (mCb2), and human CB2 (hCB2). Identities are on a black background and similarities are on a gray background.

overlapping *Cb2* exons 1 and 2 (Figure 7A) was generated to protect both exons with RNase protection. RNase protection analysis revealed variable levels of full-length *Cb2* mRNA in the control cell lines (NFS36, NFS56, NFS58, NFS61, and NFS124) (Figure 7B, 187 bp (exon 1+2)). In NFS107, full-length *Cb2* as well as 137 bp transcripts, representing exon 1, were detected. Thus, although no *Cb2* transcripts could be detected in NFS107 by Northern blot analysis, *Cb2* mRNA was demonstrated using the more sensitive RNase protection technique. In NFS78 full-length *Cb2* mRNA could not be demonstrated; however, a 50-bp fragment which corresponds to exon 2 mRNA was protected. This is in agreement with the Southern

blot analysis (Figure 1B), showing a normal and rearranged allele in NFS107 and only an abnormal allele in NFS78. 5'RACE carried out on poly(A)$^+$ RNA of NFS78 resulted in fragments of different sizes. Sequencing (Figure 6A) showed that in this cell line, another noncoding exon located downstream of provirus DNA was fused to the splice acceptor site of exon 2 of *Cb2* (Figure 7A). In an assay using a 680-bp probe specific for exon 1' + 2 (Figure 7A) two large fragments (600 and 430 bp) were protected in NFS 78 only (Figure 7C). The 600-bp band represents the complete exon 1'-plus-2 transcript, whereas the smaller band corresponds with a part of exon 1' fused to exon 2. In the other cell lines a band of 350 bp which represents exon 2 only is protected. Thus, the RNase protection analyses demonstrate altered aberrant *Cb2* mRNA expression in both NFS107 and NFS78.

***Evi11* in Cas-Br-M MuLV-induced primary tumors** - To determine the frequency of *Evi11/Cb2* retroviral insertions Southern blot analysis was carried out using probe E, F or C (Figure 2B) and different restriction enzymes on high-molecular-weight DNA isolated from Cas-Br-M MuLV-induced splenic tumors. Interestingly, DNA rearrangements were observed within the *Evi11* locus in 5 cases, i.e., CSL13, CSL14, CSL16, CSL27, and CSL97, using probe C (Figure 8), which corresponds to the protein-coding region of *Cb2* (Figure 2B). No rearrangements were detected in control primary tumors, e.g., CSL103 and CSL12. From the Southern blot analysis of DNA digested with multiple enzymes (*Sst*I, *Pst*I, and *Bam*HI) it was concluded that retroviral integrations in *Evi11* had occurred within the 3' UTR of *Cb2* in the same transcriptional orientation (Figure 2B). The location and orientation of the proviruses was confirmed by PCR analysis using *Cb2* and MuLV LTR-specific primers (data not shown)..

Discussion

Neoplasias induced by retroviruses that lack dominant-acting oncogenes, have been shown to depend on proviral integrations into particular loci of the cellular genome (7, 148, 321). Integration of viral DNA independently in the same locus in different tumors might indicate loci that have a functional role in the multistep process of malignant transformation. In two murine IL-3-dependent myeloid leukemia cell lines (126), i.e., NFS107 and NFS78, and five primary tumors, i.e., CSL13, CSL14, CSL16, CSL27, and CSL97, induced in Cas-Br-M MuLV-infected NFS/N mice, a new common virus integration site, *Evi11*, was identified and cloned. NFS107 was initially chosen for this study because of the absence of rearrangements in loci of several known proto-oncogenes (133). Interestingly, however, among eight integration sites that we isolated from NFS107, one represented the recently identified common VIS Evi3 (data not shown and (152)). This might suggest that alterations in

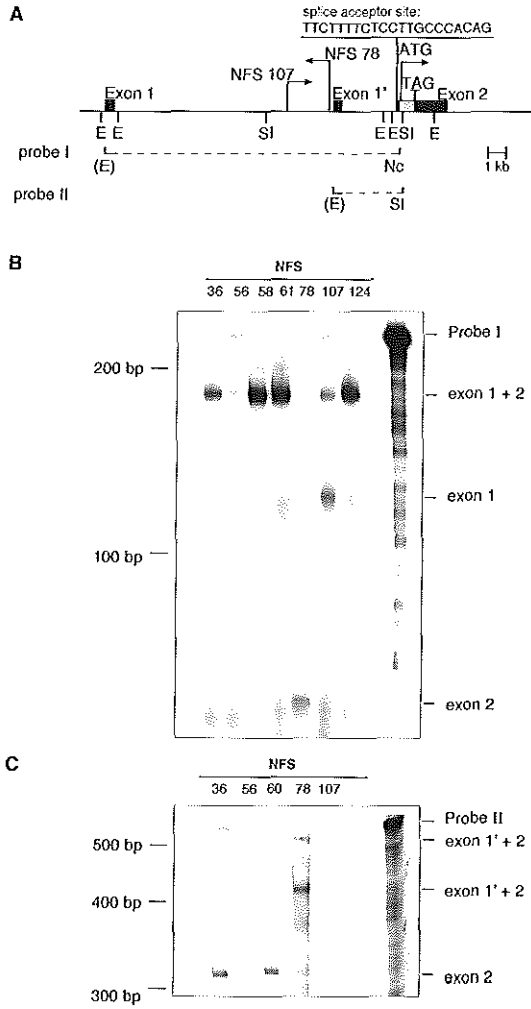

Figure 7: *Cb2* is aberrantly expressed in the murine myeloid leukemia cell lines NFS78 and NFS107.

A. Genomic organisation of mouse *Cb2*. The shaded box represents the open reading frame. The sites of proviral integrations as well as the orientations are shown by arrows. Exon 1' is the alternative exon, which is fused to exon 2 in NFS78. The fragments and the restriction sites that were used to generate RNA probes for RNase protection experiments are indicated (E: *Eco*RI; N: *Not*I; Nc: *Nco*I; Sl: *Sal*I; (R): *Eco*RI site in anchor primer 5' RACE).

B. RNase protection on 10 µg total RNA of a series leukemic cell lines using an exon 1 and 2 specific probe (see figure 7A). The full-length *Cb2* protected fragment was 187 bp (exon 1 [137 bp] and exon 2 [50 bp]).

C. RNase protection on 10 µg total RNA of a series leukemic cell lines using an exon 1' and 2 specific probe (A). The full-length protected fragment was 600 bp (exon 1' [250 bp] and exon 2 [350 bp]). Another fragment of approximately 430 bp represents part of exon 1' plus exon 2.

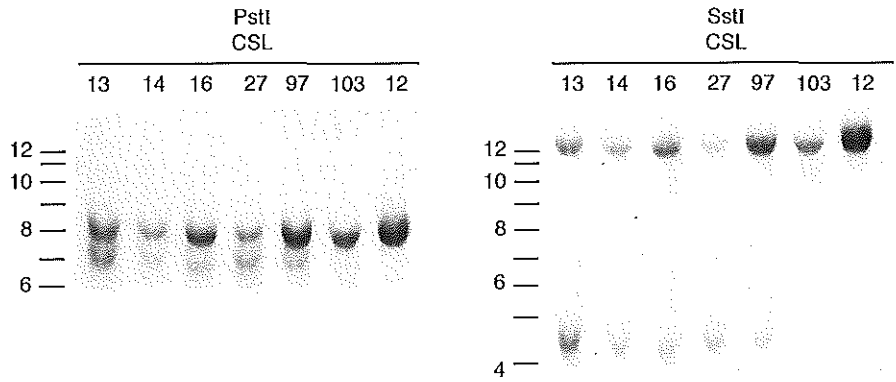

Figure 8: Proviral integrations within the 3'UTR of the *Cb2* gene.
Southern blot analysis with probe C (Figure 2B) on *Pst*I- and *Sst*I-digested genomic DNA from Cas-Br-M MuLV-induced primary tumors. The location and orientation of the retroviruses in *Evi11* are depicted in Figure 2B.

the expression of the *Evi11* and an *Evi3* proto-oncogene synergise to generate a malignantly transformed myeloid cell. Likewise, in NFS78 leukemia cells, provirus is integrated in the *Evi1* locus (217), which may suggest that aberrant expression of an *Evi11* proto-oncogene and Evi1 cooperated in the development of the latter myeloid leukemia. Cooperation of genes involved in the initiation and/or progression of hematopoietic tumors has been shown by others (148, 228).
To isolate genes located near the VIS, we established an exon trapping/amplification system based on the expression vector pEVRF0 (221). This exon trap vector is related to the pSPL1-vector (47), that also uses the RβG gene exons 2 and 3. The main difference between pEVRF0 and pSPL1 is that the natural intervening sequence, IVS2-β, is used in pERVF0, whereas in pSPL1, IVS2-β is replaced by the HIV-tat intron. Thus, by using pERVF0, we wished to avoid the possibility of isolating false positives caused by a cryptic splice site present within the HIV-*tat* intron sequence (56, 234). With the novel exon trapping system, we identified two genes in *Evi11*. The α-L-fucosidase exon that was trapped is the mouse homolog of exon 3 of human *FUCA1* (103). The second fragment that was isolated from the *Evi11* locus encodes part of the murine cannabinoid receptor 2, based on a strong homology to human *CB2* (222) and identity to the recently cloned mouse *Cb2* (284). The isolated fragment of *Cb2* was trapped in the incorrect transcriptional orientation because of the presence of cryptic 5' and 3' splice sites on the noncoding strand (Figure 6A). Thus, although apparently exons can be isolated efficiently using pERVF0, it is also clear that false positives may be isolated by using exon trapping procedures. Since sequences derived

from the cosmid vector were also trapped, it appears useful to eliminate vector DNA before cloning genomic DNA into the pERVF0 vector.

Two genes, *Fuca1* and *Cb2*, were identified in the *Evi11* locus. The data suggest that *Cb2* is the candidate target gene, since provirus is integrated in the *Cb2* intron in NFS78 and NFS107, and although the mechanism needs further study, virus integrations in this locus lead to aberrant *Cb2* mRNA expression in NFS78 and NFS107. In addition, all proviral integrations identified in the Cas-Br-M MuLV-induced primary tumors reside within the 3' UTR of *Cb2*. These integrations resemble classical proviral integrations, which generally enhance expression of the target gene (7, 148, 321). However, the possibility remains that another gene within the *Evi11* locus is affected due to retroviral insertion.

Cb2 encodes a hematopoietic receptor that belongs to the class of seven-transmembrane G-protein-coupled receptors. *Cb2* consists of a small 5' noncoding exon 1 and a large exon 2 that contains the complete protein-coding region. Interestingly, small 5' non-coding exons have been identified in a series of genes that encode for G-protein-coupled receptors, e.g., the Burkitt's lymphoma receptor-1 (*BLR1*) (82), the *mas* oncogene-related rat thoracic aorta receptor (*RTA*) (263), and recently also *CB1* (285). This could suggest that the small 5' exons are important in regulation of gene expression. In NFS78 and NFS107 cells, proviruses are integrated in the intron that separates exon 1 from exon 2. Our data indicate abnormal expression of *Cb2* exon 1 in NFS107 and NFS78. The RNase protection data are indicative of an mRNA in NFS107 that contains exon 1 only. This deleted transcript is probably the result of the polyadenylation signal introduced by the LTR of the provirus that is integrated in the proper orientation downstream of exon 1 (Figure 7A). In NFS78, exon 1 is absent and an alternative exon is fused to the protein-coding exon 2 (Figures 6A and 7A). If aberrant mRNA expression of exon 1 as the result of proviral integration leads to abnormal levels of *Cb2* receptors and contributes to leukemic transformation, this would suggest that exon 1 contains important regulatory sequences. We are currently raising antibodies to examine the levels of *Cb2* receptors on NFS78 and NFS107 versus control cell lines.

Interestingly, RNase protection experiments have demonstrated that *Cb2* may be expressed in most hematopoietic lineages and that the ligand for cannabinoid receptors, anandamide, synergistically stimulates proliferation of hematopoietic progenitor cell lines with cytokines, e.g., IL3, GM-CSF, erythropoietin, and G-CSF (314). Thus, *Cb2* appears to encode an important hematopoietic receptor which following activation enhances the response to hematopoietic growth factors. These findings adds further support to the hypothesis that this receptor, when aberrantly expressed, may alter the proliferative response of hematopoietic cells and contribute to the development of leukemia. Several other genes that encode G-protein-coupled receptors have been implicated in oncogenic transformation (4, 302, 335, 346).

FISH analysis and interspecific backcrossing demonstrated that *Evi11* is located on the distal end of murine chromosome 4. This locus is distinct from known proto-

oncogenes and common viral integration loci previously identified in the mouse. This particular region on murine chromosome 4 is homologous to a region on human chromosome 1p, i.e., 1p36. *Evi11* was found to localize between two genes, Fgr and Nppa. These comparative mapping results suggest that *FUCA1* and *CB2* map to human 1p36 as well. In fact, it had already been shown that human *FUCA1* resides on chromosome 1p36 (103). FISH analysis using a human *CB2* cDNA probe indeed demonstrated that this gene is also located on 1p36 in humans (data not shown). 1p36 is involved in breakpoints in certain cases of acute myeloid leukemia and myelodysplastic syndrome (37, 325) but also in other malignancies, e.g., neuroblastomas (33, 55, 177). This raises the question as to whether the human *EVI11* locus and possibly *CB2* is mutated and aberrantly expressed in certain human diseases with 1p36 abnormalities.

CHAPTER 3

A RAPID RT-PCR BASED METHOD TO ISOLATE COMPLEMENTARY DNA FRAGMENTS FLANKING RETROVIRUS INTEGRATION SITES.

Peter J.M. Valk, Marieke Joosten, Yolanda Vankan, Bob Löwenberg, and Ruud Delwel.

Nucleic Acids Research 25 (21): 4419-4421, 1997.

Abstract

Proto-oncogenes in retrovirally induced myeloid mouse leukemias are frequently activated following retroviral insertion. The identification of common virus integration sites (VISs) and isolation of the transforming oncogene is laborious and time-consuming. We established a rapid and simple PCR based procedure which facilitates the identification of VISs and novel proto-oncogenes. Complementary DNA fragments adjacent to retrovirus integration sites were selectively isolated by applying a reverse transcriptase reaction (RT) using an oligo(dT)-adapter primer, followed by PCR using the adapter sequence and a retrovirus long terminal repeat (LTR) specific primer. Multiple chimeric cDNA fragments suitable for Southern and northern blot analysis were isolated.

Results and Discussion

Retroviral insertional mutagenesis is a powerful method to isolate proto-oncogenes from retrovirally induced leukemias and lymphomas (reviewed in (148)). A common VIS, which marks the position of a possible proto-oncogene, is characterized by retroviral insertions within corresponding genomic loci of various independent tumors and visualized by Southern blot analysis with probes flanking the actual VIS. Unknown flanking DNA sequences have been determined by genomic cloning (6), inversed PCR (291), biotinylated DNA labelling followed by PCR (297) and other PCR based methods (187, 209). However, these methods carry certain disadvantages. Isolation of VIS flanking cellular DNA fragments by genomic cloning requires the establishment of DNA libraries, which is time-consuming and the libraries have to be made for every individual tumor or cell line. The PCR based methods consist of critical ligation (291), tailing (187) or biotinylating steps (297).
Several mechanisms are known by which retroviral sequences affect normal gene expression (148). Promoter activation as well as enhancement by proviral integration within the 3' untranslated region require that the viral LTR and the cellular gene are in the same transcriptional orientation (148). As a result of these integrations transcription may be initiated from the retroviral LTR promoters and terminated by poly(A) signals of cellular genes (Figure 1A). Consequently, retrovirally initiated chimeric mRNA transcripts consist of a 5' leader derived from the viral LTR (6, 217) and a 3' poly(A) tail of a cellular gene. The overall RT-PCR based method to isolate these chimeric cDNAs is schematically shown in Figure 1A. Poly(A)$^+$ RNA was purified using oligo(dT) cellulose columns (Pharmacia) from a panel of Cas-Br-M MuLV-induced murine myeloid leukemia cell lines (NFS22, NFS56, NFS58, NFS60 and NFS78) (126). First-strand cDNA was obtained by reverse transcriptase (RT) reactions at 37°C with 3µg poly(A)$^+$ RNA, 1 unit RNAguard (Pharmacia) and 100 units of SuperScript RT (Gibco) in 50mM Tris-HCl (pH 8.3), 75mM KCl, 3mM $MgCl_2$,1mM DTT, 0.5mM dNTP^s and 40mM oligo(dT)-adapter primer (5'-

GTCGCGAATTCGTCGACGCG($dT)_{15}$-3'). The integrity of the poly(A)$^+$ RNA and first-strand cDNA synthesis was verified by PCR (10mM Tris-HCl (pH 8.3), 50mM KCl, 1.5mM $MgCl_2$, 150µM dNTP^s and 2.5 units of Taq-polymerase (Pharmacia), 1 min at 94°C, 1 min at 50°C and 3 min at 72°C (25 cycles)) with human β-actin specific primers, highly homologous to murine β-actin and located in two separate exons (MB6: 5'-CTGGACTTCGAGCAAGAGAT-3' and MB7: 5'-TCGTCATACTCCTGCTTGCT-3'). Fragments of 433 bp were amplified with the β-actin primers solely in the presence of reverse transcriptase (Figure 1B). Subsequently, PCRs (1 min at 94°C, 1 min at 58°C and 3 min at 72°C (30 cycles)) were performed on the RT-reactions of the NFS cell lines by using the LTR-specific primer (pLTR1: 5'-GGGTCTCCTCAGAGTGATTG-3') and the adapter primer (adapter: 5'-GTCGCGAATTCGTCGACGCG-3'). Fragments of different size, 0.1 to 2.5 kb, were detected in all cell lines tested (Figure 1B). No DNA fragments were amplified if PCR was not preceded by cDNA synthesis, indicating that only transcribed fragments were amplified. Fragments were cloned into the *Eco*RV site of pBluescript SK$^+$ (Statagene, La Jolla, CA) and the viral origin of the cDNAs was confirmed by sequence analysis (Figure 1C). No cDNAs were detected entirely consisting of viral sequences but, as expected, 100% of the cDNAs contained LTR sequences at the 5' end. The cDNA sequences were compared with the database of the National Center for Biotechnology Information (NCBI) to identify possible homologous sequences. VISs were detected within the murine homolog of the h*ERG* gene (90), which encodes a transcription factor, involved in AML t(16;21) (283) and within the promoter region of the mouse T-cell receptor γ chain near the Vg6 gene (139).

The basis of insertional mutagenesis to identify proto-oncogenes is the isolation of common VISs in independent tumors or tumor cell lines. Southern blot analysis of one fragment, derived from NFS22, is shown in Figure 2A. Rearrangements in various independent cell lines, i.e., NFS22, NFS58, NFS60 and NFS78, were detected. A partial restriction map and the orientations of the proviruses were established (Figure 2B) using the Southern blot data. The orientation and location of the proviral DNAs in NFS58, NFS60 and NFS78 implicated that fragment 1 was localized in the commonly rearranged *Evi1* locus (16, 217), within intron 2 of the *Evi1* gene. Northern blot analysis showed that this intron due to proviral integration is highly expressed in NFS22 and NFS78 (Figure 2C), which could be expected from the orientation of virus integrations in NFS22 and NFS78 (Figure 2B). In myeloid leukemias the *Evi1* gene is frequently activated due to viral integration within the murine gene (217) and in human AMLs due to translocation involving chromosome 3q26 (216).

Transcripts initiated from the retroviral promoter were selectively amplified. The existence of a poly(A) signal (AATAAA) (70%) and more than 15 adenine residues (55%) at the 3' end of all cDNA fragments (data not shown) may suggest that cDNA synthesis regularly initiated at mRNA poly(A) tails. It is however possible that cDNA

synthesis initiates at A-rich sequences. In fact, the isolated *Evi1* cDNA represents a sequence located 5' within a cellular gene. Nevertheless, the isolation of cDNA fragments will eventually facilitate the identification of target genes in the leukemias (Figure 2C). cDNA fragments which did not show homology with known genes will be used for Southern blot screening purposes to search for new common VISs. The fact that three out of thirteen cDNAs represent known genes of which two (*Evi1* and *Erg*) have been demonstrated to be involved in myeloid leukemia (216, 283) suggests that the described method is powerful for the rapid identification of novel common VISs and proto-oncogenes.

Figure 1: RT-PCR based method to isolate cDNA fragments flanking VISs.
A. Schematic representation of the strategy to rapidly amplify cDNA fragments adjacent to virus integration sites. Viral insertions in a cellular gene may generate aberrant mRNAs initiated through transcription from the viral promoter located on the long terminal repeat (LTR). The aberrant mRNA is polyadenylated downstream of the cellular polyadenylation signal (AATAAA). cDNA is synthesized by reverse transcription using an oligo(dT)-adapter primer which primes on the poly(A) tails or A rich sequences (3'RACE: 3' rapid amplification of cDNA ends). Using the adapter primer and an LTR specific primer (pLTR1) the cellular DNA fragments flanking the VIS are amplified by PCR.
B. RT-PCR (adapter/pLTR1) on poly(A)$^+$ RNA isolated from Cas-Br-M MuLV-induced myeloid leukemia cell lines NFS22, NFS56, NFS58, NFS60 and NFS78 (+RT). As a control PCR was carried out on poly(A)$^+$ RNA samples without the addition of reverse transcriptase (-RT). The integrity of the isolated poly(A)$^+$ RNA and the first-strand cDNA was confirmed by RT-PCR with β-actin primers (M:marker).
C. Sequence analysis of downstream of the LTR primer located MuLV LTR-specific sequences. The arrows (5'-TTTCA^NN-3') indicate the general fusion site of viral and cellular cDNA in both A and C. The cDNA sequence depicted in this figure is identical to the murine EST (DDBJ/EMBL/GenBank accession no. W97251).

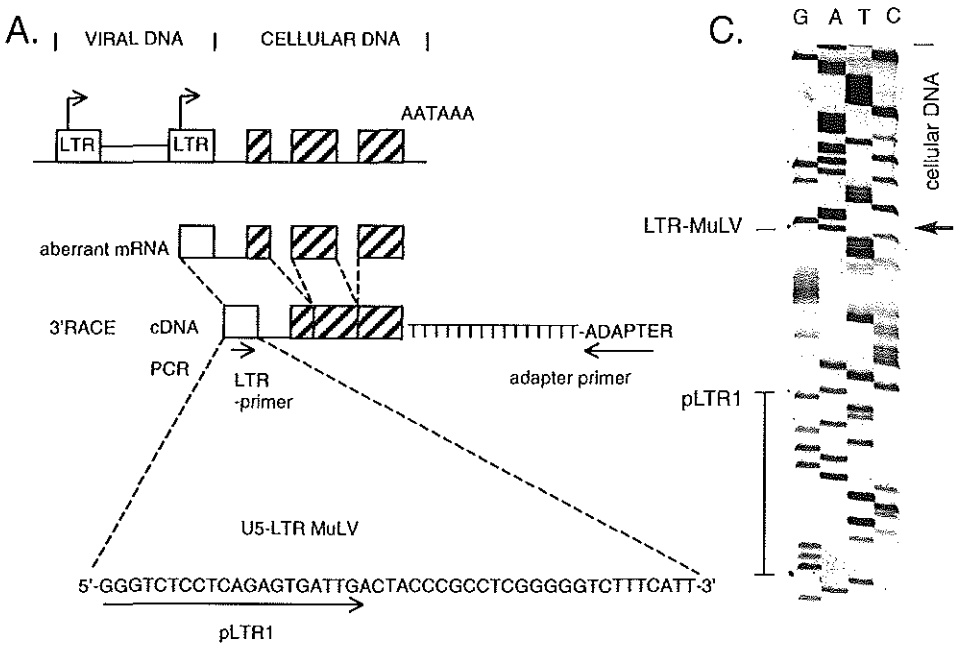
A.
VIRAL DNA
CELLULAR DNA
AATAAA
LTR
LTR
aberrant mRNA
3'RACE
cDNA
TTTTTTTTTTTTTT-ADAPTER
PCR
LTR
-primer
adapter primer
U5-LTR MuLV
5'-GGGTCTCCTCAGAGTGATTGACTACCCGCCTCGGGGGTCTTTCATT-3'
pLTR1
C.
G A T C
cellular DNA
LTR-MuLV
pLTR1

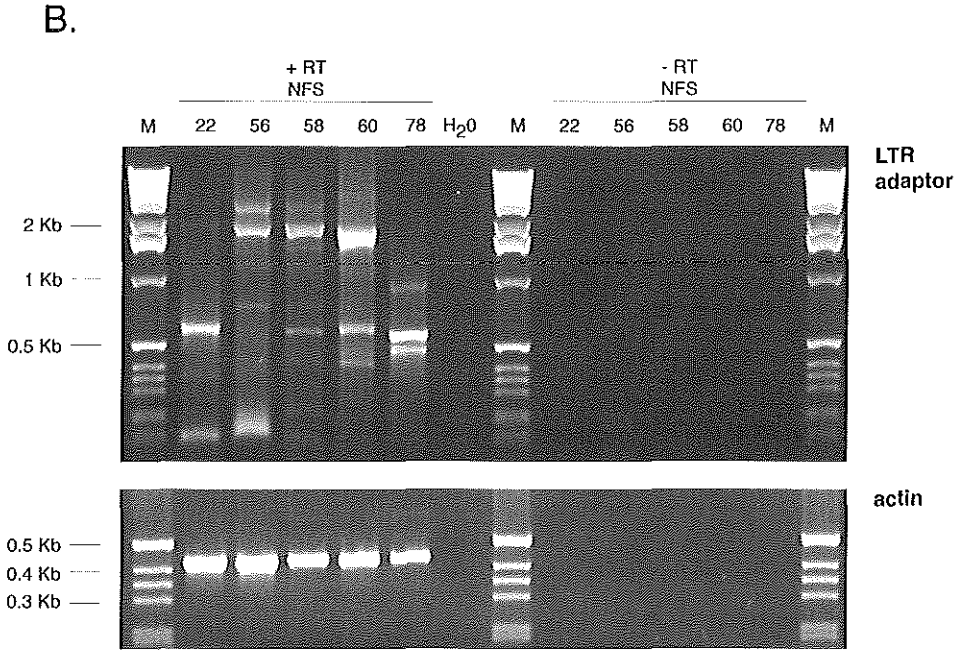
B.
+ RT
NFS
- RT
NFS
M 22 56 58 60 78 H2O M 22 56 58 60 78 M
2 Kb
1 Kb
0.5 Kb
LTR
adaptor
0.5 Kb
0.4 Kb
0.3 Kb
actin

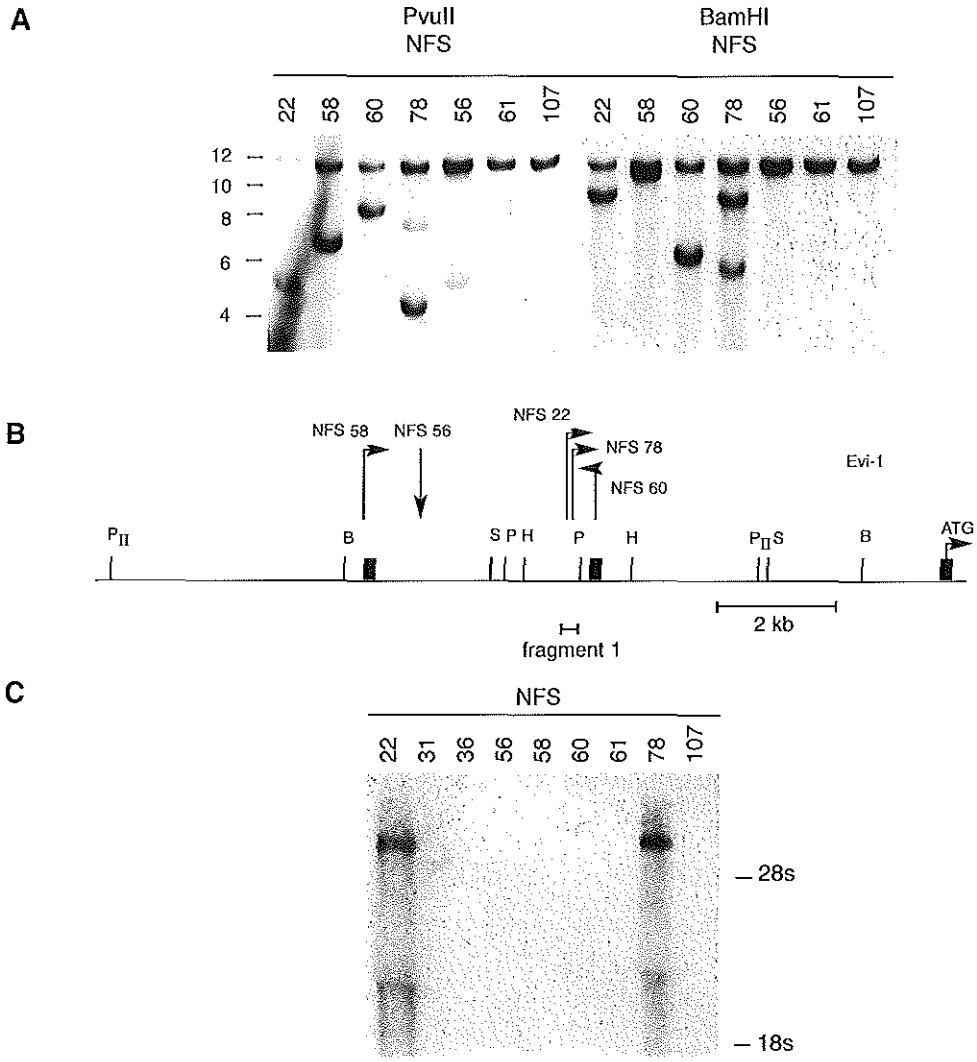

Figure 2: Fragment 1 is located in the known common VIS *Evi1*.
A. Southern blot analysis (*Pvu*II and *Bam*HI digest) of a panel of retrovirally induced leukemic cell lines NFS22, NFS58, NFS60, NFS78, NFS61 and NFS107 hybridized with fragment 1.
B. Limited restriction map of the *Evi1* locus with the site and orientation of viral integrations, indicated by arrows, in the leukemic cell lines NFS22, NFS58, NFS60 and NFS78 (PII:*Pvu*II; B:*Bam*HI, S:*Sst*I; P:*Pst*I; H:*Hin*dIII). The black boxes indicate the 5' end exon structure of the *Evi1* gene (7,12).
C. Northern analysis of the cell lines NFS22, NFS31, NFS36, NFS56, NFS58, NFS60, NFS61, NFS78 and NFS107 probed with fragment 1.

CHAPTER 4

RETROVIRAL INSERTIONS IN *Evi12*, A NOVEL COMMON VIRUS INTEGRATION SITE UPSTREAM OF *Tra1/Grp94*, FREQUENTLY COINCIDE WITH INSERTIONS IN THE GENE ENCODING THE PERIPHERAL CANNABINOID RECEPTOR *Cb2*.

Peter J.M. Valk, Yolanda Vankan, Marieke Joosten, Nancy A. Jenkins, Neal G. Copeland, Bob Löwenberg and Ruud Delwel

Journal of Virology 73(5), 1999 (in press)

Abstract

The common virus integration site (VIS) *Evi11* was recently identified within the gene encoding the hematopoietic G protein-coupled peripheral cannabinoid receptor *Cb2* (also referred to as *Cnr2*). Here we show that *Cb2* is a frequent target (12%) for insertion of Cas-Br-M murine leukemia virus (MuLV) in primary tumors in NIH/Swiss mice. Multiple provirus insertions in *Evi11* were cloned and shown to be located within the 3' untranslated region of the candidate proto-oncogene *Cb2*. These results suggest that proviral insertion in the *Cb2* gene is an important step in Cas-Br-M MuLV-induced leukemogenesis in NIH/Swiss mice. To isolate *Evi11/Cb2* collaborating proto-oncogenes, we searched for novel common VISs in the Cas-Br-M MuLV-induced primary tumors and identified a novel frequent common VIS, *Evi12* (14%). Interestingly, 54% of the *Evi11/Cb2*-rearranged primary tumors contained insertions in *Evi12* as well, which suggests cooperative action of the target genes in these two common VISs in leukemogenesis. By interspecific backcross analysis it was shown that *Evi12* resides on mouse chromosome 10 in a region that shares homology with human chromosomes 12q and 19p. Sequence analysis demonstrated that *Evi12* is located upstream of the gene encoding the molecular chaperone *Tra1/Grp94*, which was previously mapped to mouse chromosome 10 and human chromosome 12q22-24. Thus, *Tra1/Grp94* is a candidate target gene for retroviral activation or inactivation in *Evi12*. However, Northern and Western blot analysis did not provide evidence that proviral insertion had altered the expression of *Tra1/Grp94*. Additional studies are required to determine whether *Tra1/Grp94* or another candidate proto-oncogene in *Evi12* is involved in leukemogenesis.

Introduction

During leukemogenesis hematopoietic progenitor cells acquire growth advantages, expand, and accumulate in bone marrow, blood, and other hematopoietic tissues. In this process the expression patterns of multiple critical genes involved in hematopoietic cell proliferation and differentiation change. Human leukemias frequently contain chromosomal translocations (232) and, as a consequence, proto-oncogenes located near these translocations become aberrantly expressed, resulting in the clonal outgrowth of leukemic cells. Retroviral insertional mutagenesis represents an elegant way to study genes involved in hematopoietic tumor formation in mice (148, 340). Retroviral insertion results in activation of proto-oncogenes (25, 149, 217, 218, 228) or inactivation of tumor suppressor genes (46). Multiple human proto-oncogenes and tumor suppressors, e.g., *EVI1* (216), *NF1* (277), and *HOXA9* (227) have been shown to be involved in murine hematopoietic transformation (46, 217, 228) as well, which shows that retroviral insertional mutagenesis in mice clearly shares common features with tumorigenesis in humans. It has generally been accepted

that tumor initiation and progression is a multistep process (1, 129, 327). The latency period of several months between retroviral infection and manifestation of the disease suggests that multiple integrations representing mutations in various critical genes may be necessary for complete transformation (148). The cooperation of tumor-inducing genes in leukemia progression has convincingly been demonstrated in proto-oncogene bearing transgenic mice, which develop tumors more rapidly after retroviral infection than do virus-infected control littermates (1, 32). Thus, the collaboration of various mutated genes can be explored in mouse models by using retroviral insertional mutagenesis. The coexistence of two common virus integration sites (VISs) in multiple tumors may provide an indication for the cooperation of the target genes in malignant transformation (64, 148).

Recently, we identified a novel common VIS, *Evi11*, which is located on mouse chromosome 4 in a region that shares homology with human chromosome 1p36 (315). The common VIS *Evi11* was initially identified in two retrovirally induced myeloid cell lines, NFS107 and NFS78. Subsequently, retroviral insertions in *Evi11* were also demonstrated in multiple primary tumors (315). The cell lines as well as the primary tumors originated from NIH/Swiss mice after inoculation with Cas-Br-M murine leukemia virus (MuLV) (126, 315). The candidate proto-oncogene in this locus is *Cb2*, the gene encoding the peripheral cannabinoid receptor (315). We and others have shown that murine *Cb2* is specifically expressed in spleen, thymus, blood cells, and hematopoietic cell lines (105, 222, 314). An endogenous ligand for Cnr2, anandamide, enhances hematopoietic cell proliferation induced by various growth factors, such as interleukin-3 (IL-3), erythropoietin, and granulocyte and granulocyte-macrophage colony stimulatory factors, in serum-free medium (314). Together, these results suggest a role for aberrantly expressed Cnr2 receptors in leukemia development.

In this study we investigated the exact location and the frequency of retroviral insertions in *Evi11/Cb2* in a new panel of 91 Cas-Br-M MuLV-induced primary tumors in NIH/Swiss mice and 20 previously established cell lines (126, 136). Retroviral insertion in *Evi11* occurred frequently, i.e., in 13 of 111 cases studied. These proviral integrations in *Evi11* were mainly located in the 3' untranslated region (UTR) of *Cb2*. To search for new common VISs and to isolate oncogenes cooperating with *Evi11/Cb2*, new provirus flanking cDNA fragments were isolated from the *Evi11/Cb2* rearranged myeloid cell line NFS107. We identified a novel frequent common VIS, *Evi12*, which was found in 16 of our panel of 111 primary tumors and cell lines. Proviruses in *Evi12* inserted upstream of the gene encoding the molecular chaperone *Tra1/Grp94*. Interestingly, in 54% of the *Evi11/Cb2* rearranged tumors insertions were also observed in *Evi12*, suggesting that the target proto-oncogenes in *Evi11/Cb2* and *Evi12* collaborate in leukemic transformation.

Materials and Methods

Cell lines - The myeloid cell line NFS107 was established *in vitro* from Cas-Br-M MuLV-initiated primary tumors (126). The NFS (126) and DA (136) cell lines were cultured in RPMI1640 medium supplemented with penicillin (100 IU/ml), streptomycin (100 ng/ml), 10% fetal calf serum and murine IL-3 (1 µg/ml).

Primary tumors - Newborn NIH/Swiss mice were injected subcutaneously with cell culture supernatant of Cas-Br-M MuLV producing NIH3T3 cells (obtained from H. Morse III and J. W. Hartley). Between 150 and 220 days after injection the mice developed leukemias. Ninety-one leukemic mice were sacrificed when moribund. Forty-seven leukemic mice had 5- to 10-fold-enlarged spleens, and 17 mice had slightly enlarged spleens (up to 2-fold). Lymph nodes and thymus were isolated when they were enlarged. Cells from spleen, thymus, or lymph nodes from 91 Cas-Br-M MuLV-infected mice (CSL [Cas-Br-M MuLV Swiss Leukemia]) were cryopreserved in liquid nitrogen. From these cells, high-molecular-weight DNA was isolated (267) for Southern blot analysis. To analyze the morphology of the primary tumor cells, cells were examined after May-Grünwald-Giemsa staining.

PCRs - To determine the exact locations and orientations of Cas-Br-M provirus in the *Evi11* and *Evi12* loci, PCR was carried out on 1 µg of genomic DNA from the primary tumors with VIS-specific primers in combination with Cas-Br-M MuLV long terminal repeat (LTR)-specific primers (Figure 1A [*Evi11*] and 4A [*Evi12*]). Insertions in *Evi11* were amplified with primer CBR16 (5'-GTATTTCAACAT-CAACTTGG-3') and primer pLTR-A (5'-CCGAAACTGCTTACCAC-3') (cycling conditions were 1 min at 94°C, 1 min at 48°C, and 3 min at 72°C [30 cycles]), followed by nested PCRs with CBR22 (5'-CCTCTCATTGCTCTAACATG-3') and pLTR-B (5'-CTGTTTGGCCCAACTTCAGCTG-3') (cycling conditions were 1 min at 94°C, 1 min at 58°C, and 3 min at 72°C [30 cycles]). To determine virus integrations in *Evi12*, PCR was carried out with primer p503-1 (5'-GTGTGAAAACCCTAATTCCGG-3') and pLTR1 (5'-GGGTCTCCTCAGAGTGA-TTG-3') (cycling conditions were 1 min at 94°C, 1 min at 57°C, and 3 min at 72°C [30 cycles]), followed by PCR with p503-1 and pLTR2 (5'-TAAGTCGAC-TACCCGCCTCG-3') (cycling conditions were 1 min at 94°C, 1 min at 48°C, and 3 min at 72°C [30 cycles]). A reverse transcription-PCR (RT-PCR) strategy was carried out to isolate cDNA fragments from NFS107 flanking VISs as described previously (317). Poly(A)$^+$ RNA was purified from NFS107 by affinity chromatography with oligo(dT) cellulose columns (Pharmacia). Reverse transcriptase reactions were performed for 1.5 hr at 37°C with 3 µg of poly(A)$^+$ RNA in 50 mM Tris-HCl (pH 8.3), 75 mM KCl, 3 mM $MgCl_2$,1 mM dithiothreitol, 0.5 mM desoxynucleoside triphosphates (dNTP^s), 1 U of RNAguard (Pharmacia), and 100 U of SuperScript RT (Gibco, Breda, The Netherlands). For first-strand synthesis 40 mM oligo(dT)-adapter

(5'-GTCGCGAATTCGTCGACGCG(dT)$_{15}$-3') was used. Subsequently, PCR was carried out by using the adapter primer (5'-GTCGCGAATTCGTCGACGCG-3') in combination with the LTR-specific primer pLTR1 (5'-GGGTCTCCTCAGAGTGA-TTG-3') to isolate the cDNA fragments adjacent to the VISs. The PCR reaction mixture contained 10 mM Tris-HCl (pH 8.3), 50 mM KCl, 1.5 mM $MgCl_2$, 150 µM dNTPs and 2.5 U of *Taq*-polymerase (Pharmacia, Uppsala, Sweden). Reactions started with 10 min at 94°C and ended with 10 min at 72°C. Products were cloned into pBluescript II SK(+) (*Eco*RV) (Statagene, Westburg, Leusden, The Netherlands) and sequenced.

Sequence analysis - Nucleotide sequencing was performed on the ABI310 sequencer (Perkin Elmer, Nieuwerkerk a/d IJsel, The Netherlands). Fragments were cloned into pBluescript II SK(+) and sequenced with T_3, T_7, or sequence-specific primers. Deduced sequences were analyzed by using the BLAST network service of the National Center for Biotechnology Information (NCBI). The accession number for the 1.7-kb fragment containing the Cas-Br-M MuLV insertion sites is AF091114.

Southern and Northern blot analysis – Southern and Northern blot analysis were performed as described previously (315).

Interspecific backcross mapping - Interspecific backcross progeny were generated by mating (C57BL/6J x *Mus spretus*)F_1 females and C57BL/6J males as described previously (59). A total of 205 N_2 backcross mice were used to map the *Evi12* locus (see Results for details). DNA isolation, restriction enzyme digestion, agarose gel electrophoresis, Southern blot transfer, and hybridization were performed essentially as described earlier (143). All blots were prepared with Hybond-N^+ nylon membrane (Amersham). The 503 probe, a 233-bp cDNA fragment flanking a VIS in NFS107, was labeled with [α-^{32}P]dCTP by using a random prime labeling kit (Stratagene); washing was done to a final stringency of 1.0X SSCP (1XSSCP is 0.12 M NaCl plus 15 mM $Na_3C_6H_5O_7$ and 20 mM $NaPO_4$), 0.1% sodium dodecyl sulfate at 65 °C. A 5.5-kb fragment was detected in *Hin*dIII-digested C57BL/6J DNA and a fragment of 4.3 kb was detected in *Hin*dIII digested *M. spretus* DNA. The presence or absence of the 4.3-kb *Hin*dIII *M. spretus*-specific fragment was monitored in backcross mice.
A description of the probes and the restriction fragment length polymorphisms (RFLPs) for the loci linked to the *Evi12* locus, including *Gna15*, *Pah* and *Tmpo*, have been reported previously (28, 336). Recombination distances were calculated by using Map Manager, version 2.6.5. The gene order was determined by minimizing the number of recombination events required to explain the allele distribution patterns.

Western blot analysis - NFS cells were washed with ice-cold phosphate-buffered saline with 10 mM Na_3VO_4. Subsequently, cells were spun down and lysed by incubation for 10 min at 4°C in lysis buffer (50 mM Tris-HCl pH 8.0, 100 mM NaCl,

1% Triton X-100, 0.1 mM Na_3VO_4, 1% Pefabloc SC, 50 µg of aprotinin, 50 µg of leupeptin, 50 µg of bacitracin, 50 µg of iodoacetamide per ml and 1 mM dithiothreitol). Insoluble material was removed by centrifugation for 30 min at 10,000xg at 4°C. Following sodium dodecyl sulfate-polyacrylamide gel electrophoresis, proteins were electroblotted onto nitrocellulose (0.2 µm; Schleicher & Schuell, Dassel, Germany). Filters were blocked by incubation in 0.3% Tween-20 in Tris-buffered saline (TBS; 10 mM Tris-HCl pH 7.4, 150 mM NaCl) for 1 h at 37°C, washed in TBST (0.05% Tween-20 in TBS), and incubated with antibodies diluted in TBST. The Grp94 antibody used for Western blotting was goat polyclonal anti-Grp94 (Santa Cruz Biotechnology, Inc., Santa Cruz, Calif.). After being washed with TBST, immune complexes were detected with horseradish peroxidase-conjugated anti-goat immunoglobulin G specific antiserum (Santa Cruz Biotechnology), followed by an enhanced chemiluminescence reaction (DuPont, Boston, Mass.).

Results

Frequent retroviral insertions in the *Cb2* gene in *Evi11* - Recently, we demonstrated that retroviral insertions in the *Evi11* locus in two Cas-Br-M MuLV-induced cell lines, NFS78 and NFS107, and in five Cas-Br-M MuLV-induced primary tumors occurred in the *Cb2* gene (315). To determine the frequency of retroviral insertions in *Evi11* we screened DNA from a panel of 111 leukemias, i.e., 91 Cas-Br-M MuLV-induced tumors and 20 cell lines (126, 136) by Southern blot analysis with a probe complementary to the protein-coding region of *Cb2* (probe C, Figure 1A) (reference 51 and data not shown). Rearrangements in *Evi11/Cb2* were found in 13 of 111 cases (12%; Table 1). Based on the restriction enzyme map of Cas-Br-M MuLV (accession number X57540) and the restriction sites within the *Evi11 /Cb2* locus (315), the orientations of the retroviruses were determined (Figure 1A). In all primary tumors provirus integrations occurred in the same orientation, i.e., in the direction of transcription of the *Cb2* gene. After PCR (Figure 1A) with the LTR-specific primers pLTR-A and pLTR-B in combination with the *Cb2*-specific primers CBR16 and CBR22, respectively, the exact sites of proviral insertion in a number of primary tumors were determined (Figure 1B). As shown in Figure 1B, all proviruses, except CSL75, were located in the 3' UTR of the *Cb2* gene. Based on Southern blot analysis, it was concluded that as a result of recombination the genomic structure of the *Evi11* locus in CSL63 was altered (data not shown). How retroviral insertion affects expression of Cnr2 receptors in the *Cb2*-mutated leukemias is the subject of current investigations. In this study we focus on the identification of novel common VISs representing transforming genes cooperating with *Cb2* in leukemogenesis.

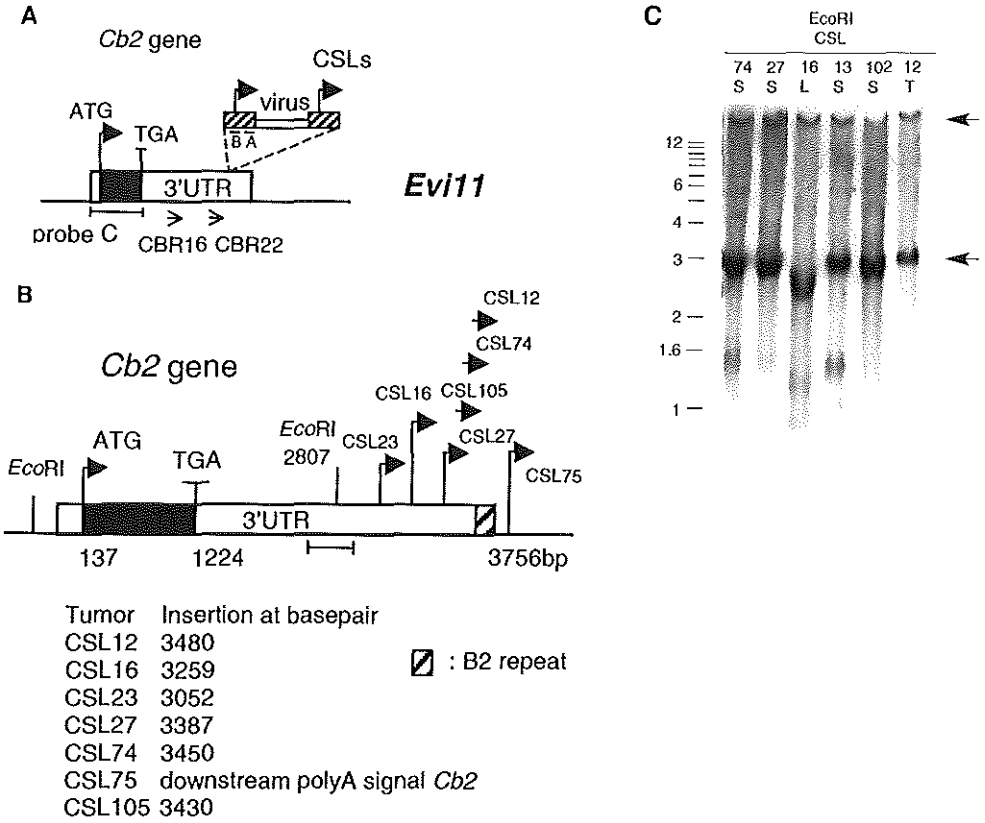

Figure 1: Isolation of Cas-Br-M MuLV proviral insertions in *Evi1 1/Cb2*.
A. Schematic representation of the *Cb2* gene in the *Evi1 1* locus and the orientation and site of integration of proviral DNA within the 3' UTR of *Cb2* in the primary tumors (CSLs). The locations of the primers used for PCR amplification on genomic DNA, i.e., primers set CBR16 and pLTR-A followed by CBR22 and pLTR-B are indicated by small arrows. Probe C used for Southern blot analysis of the primary tumors (reference 51 and data not shown) is indicated. The protein-coding region of the *Cb2* gene is indicated by the black box. **B.** Exact locations of the proviral integrations in various independent Cas-Br-M MuLV-induced primary tumors in the 3' UTR of the *Cb2* gene. An arrow with a CSL number indicates the insertion site in this particular tumor. Probe D was used for Southern blot analysis (Figure 1C). The protein-coding region of the *Cb2* gene is indicated by the black box. **C.** Southern blot analysis of high-molecular-weight DNA of Cas-Br-M MuLV-induced primary tumors digested with *Eco*RI to detect MCF viruses. Hybridizations were performed with probe D (*Hin*dIII/*Nco*I fragment (at 2,474 and 2,974 bp of the *Cb2* cDNA, respectively)) (Figure 1B) (315). Since this probe contains an *Eco*RI site, two bands representing a normal allele appear indicated by arrows. Rearranged fragments of approximately 1.6 kb were detected in CSL13, CSL16, CSL27, and CSL74 but not in the control tumors CSL102 and CSL12 without rearrangements in *Evi1 1/Cb2* (S, spleen; T, thymus; L, lymph nodes). The rearranged fragments represent the leukemic cell population containing provirus in *Evi1 1/Cb2*.

Tumor number	Tissue type	Phenotype	Latency period (days)	*Evi11*	*Evi12*
CSL11	Spleen	ND	137		M
CSL12	Spleen and Thymus	ND	148	PCR	M
CSL13	Spleen	ND†	166	M	M
CSL14	Thymus and Spleen	ND	167	M	M
CSL15	Spleen	ND†	170		M
CSL16	Lymph node	lymphoid	196	M	M
CSL17	Thymus	lymphoid	175		M
CSL23	Spleen	ND	203	PCR	
CSL27	Thymus and Spleen	immature blasts	191	M	M
CSL29	Spleen	ND†	208		M
CSL35	Spleen	immature blasts	196		M
CSL60	Spleen	immature blasts	224		M
CSL63	Thymus	lymphoid	209	M [R]	
CSL74	Spleen	ND	216	M	
CSL75	Spleen	ND	216	M	
CSL85	Spleen	immature blasts	210		M
CSL89	Lymph node and Spleen	immature blasts	229		M
CSL93	Spleen	ND†	229		M
CSL97	Spleen	ND†	253	M	M
CSL105	Spleen	immature blasts	294	M	
NFS78	Cell line	myeloid		E	
NFS107	Cell line	myeloid		M	E

Table 1: *Evi11* and *Evi12* insertions in Cas-Br-M MuLV-induced CSL primary tumors in NIH/Swiss mice. Abbreviations (phenotypes were determined by morphology after May-Grünwald staining): M, MCF MuLV; E, ecotropic MuLV; [R], unable to determine exact MuLV insertion in the *Cb2* gene because of recombination of the *Evi11/Cb2* locus; ND, not determined; PCR, rearrangement undetectable by Southern blot analysis, proviral insertion determined by PCR (Figure 1B). A dagger indicates the mice were dead.

Identification of a novel common virus integration site, *Evi12* - To isolate *Evi11/Cb2* cooperating transforming genes we applied a novel RT-PCR technique (317) on RNA from NFS107, a retrovirally induced myeloid tumor cell line with a provirus insertion in *Evi11/Cb2* (315). Multiple novel cDNA fragments flanking provirus were isolated from NFS107 (data not shown). A cDNA fragment of 233 bp, designated 503, was cloned into pBluescript SK(+) and sequenced (see Figure 4B). No homologous sequences were found by searching the database of the NCBI. RT-PCR analysis with primer set 503-2 (see Figure 4B) and pLTR1 demonstrated high mRNA expression of cDNA fragment 503 in NFS107 compared to control cell lines. It is at present uncertain whether cDNA fragment 503 represents a transcript of a cellular gene (317), since no mRNA was detected in RNA from various murine tissues by using Northern blot analysis or RNase protection analysis (data not shown). However, Southern blot analysis with 503 on high-molecular-weight DNA from all

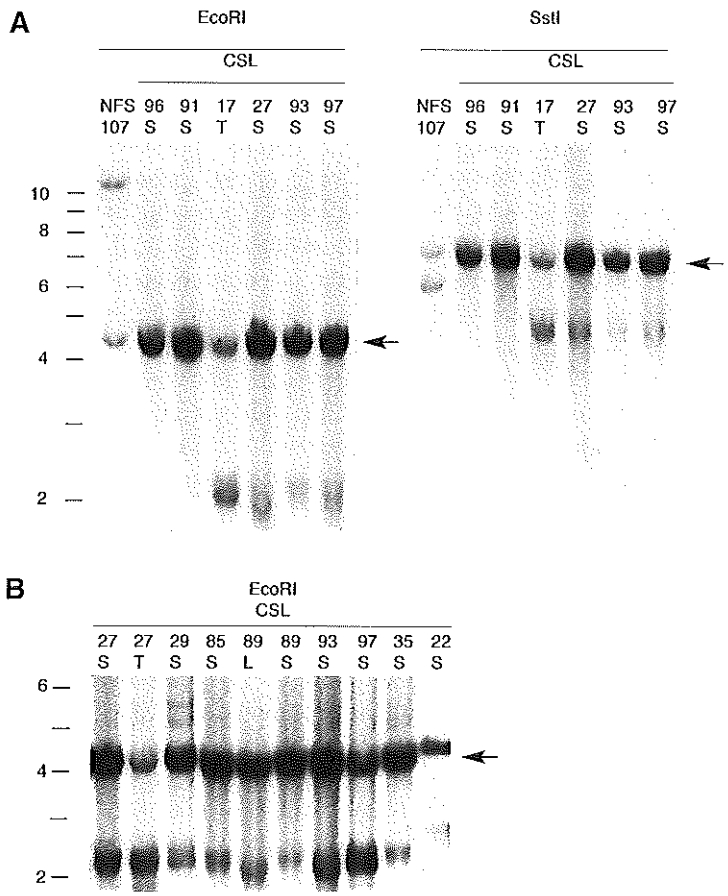

Figure 2: Identification of common virus integration site Evi12.
Southern blot analysis of high- molecular-weight DNA of NFS107 and a number of Cas-Br-M MuLV-induced primary tumors (CSL) digested with *Eco*RI or *Sst*I. Filters were hybridized with fragment 503 (Figure 6). Rearrangements (2.0 kb) were detected in CSL17, CSL27, CSL29, CSL85, CSL89, CSL93, and CSL97 but not in with the control tumors CSL22, CSL91, and CSL96 (S, spleen; T, thymus; L, lymph nodes). Arrows indicate the normal nonrearranged alleles.

91 Cas-Br-M MuLV-induced primary tumors demonstrated rearranged alleles in a number of independent tumors, e.g., CSL17, CSL27, CSL29, CSL85, CSL89, CSL93, and CSL97 (Figure 2). From Southern blot analyses of the primary tumors digested with multiple enzymes and the restriction enzyme map of Cas-Br-M MuLV (accession number X57540), it was concluded that the DNA rearrangements were indeed the result of proviral integration (data not shown). To date, we have identified rearrangements in this locus in 15 of 91 primary tumors, and we have designated this

ecotropic virus integration site 12, *Evi12*. From the 20 cell lines studied sofar, an *Evi12* rearrangement was shown in one cell line, i.e., NFS107.

Insertion of mink cell focus-forming (MCF) viruses in *Evi11/Cb2* and *Evi12* – The primary tumors were isolated from the outbred NIH/Swiss mice that were infected with ecotropic Cas-Br-M MuLV (122, 172). Inoculation of NFS/N and NIH/Swiss mice with Cas-Br-M MuLV results in the production of both ecotropic and MCF recombinant MuLVs (125, 172). Most of the MCF MuLVs are identified by a unique *Eco*RI site within the *env* gene in the proviral genome (252). Interestingly, based on the size of the rearranged alleles after *Eco*RI digestion in *Evi11/Cb2*-rearranged tumors (ca. 1.6 kb; Figure 1C), an *Eco*RI site must be located just downstream of the 5' LTR. The size of the rearranged alleles after *Eco*RI digestion in *Evi12*-rearranged tumors (ca. 2.0 kb; Figure 2) is indicative for the MCF virus unique *Eco*RI site at 6.9 kb of the proviral genome (252). Southern blot analysis demonstrated that in the Cas-Br-M MuLV-induced primary tumors, all proviruses in either *Evi11/Cb2* or *Evi12* are of the MCF-type (Table 1).

***Evi12* is located on the central region of mouse chromosome 10** - The mouse chromosomal location of *Evi12* was determined by interspecific backcross analysis using progeny derived from matings of ([C57BL/6J x *Mus spretus*] F_1 females X C57BL/6J) mice. This interspecific backcross mapping panel has been typed for over 2500 loci that are well distributed among all autosomes as well as the X chromosome (59). C57BL/6J and *M. spretus* DNAs were digested with several enzymes and analyzed by Southern blot hybridization for informative RFLPs by using the 233 bp mouse 503 cDNA probe. The 4.3 kb *Hin*dIII *Mus spretus* RFLP (see Materials and Methods) was used to monitor the segregation of the *Evi12* locus in backcross mice. The mapping results indicated that *Evi12* is located in the central region of mouse chromosome 10 linked to *Gna15*, *Pah*, and *Tmpo*. Although 126 mice were analyzed for every marker and are shown in the segregation analysis (Figure 3), up to 177 mice were typed for some pairs of markers. Each locus was analyzed in pairwise combinations for recombination frequencies with the additional data. The ratios of the total number of mice exhibiting recombinant chromosomes to the total number of mice analyzed for each pair of loci and the most likely gene order are as follows: centromere - *Gna15* - 7/139 - *Evi12* - 1/137 - *Pah* - 5/177 - *Tmpo*. The recombination frequencies (expressed as genetic distances in centiMorgans [cM] ± the standard error) are as follows: *Gna15* - 5.0 ± 1.9 - *Evi12* - 0.7 ± 0.7 - *Pah* - 2.8 ± 1.3 - *Tmpo*.
We have compared our interspecific backcross map of chromosome 10 with a composite mouse linkage map that reports the map location of many uncloned mouse mutations (provided from the Mouse Genome Database, a computerized database maintained at The Jackson Laboratory, Bar Harbor, Maine). *Evi12* mapped in a region of the composite map that lacks mouse mutations with a phenotype that might be expected for an alteration in this locus (data not shown). The central region of

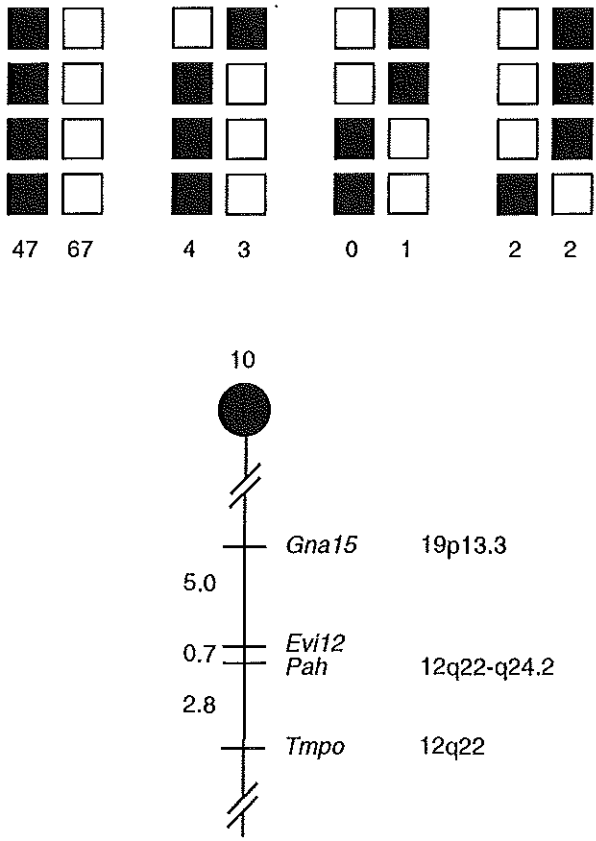

Figure 3: *Evi12* maps in the central region of mouse chromosome 10.
Evi12 was placed on mouse chromosome 10 by interspecific backcross analysis. The segregation patterns of *Evi12* and flanking genes in 126 backcross animals that were typed for all loci are shown at the top of the figure. For individual pairs of loci, more than 126 animals were typed (see text). Each column represents the chromosome identified in the backcross progeny that was inherited from the (C57BL/6J x *M. spretus*) F_1 parent. The shaded boxes represent the presence of a C57BL/6J allele, and the white boxes represent the presence of a *M. spretus* allele. The number of offspring inheriting each type of chromosome is listed at the bottom of each column. A partial chromosome 10 linkage map showing the location of *Evi12* in relation to linked genes is shown at the bottom of the figure. Recombination distances between loci in centiMorgans (cM) are shown to the left of the chromosome and the positions of loci in human chromosomes are shown to the right. References for human map positions can be obtained from the GDB (Genome Data Base), a computerized database of human linkage information maintained by The William H. Welch Medical Library of The Johns Hopkins University (Baltimore, M.).

mouse chromosome 10 shares regions of homology with human chromosomes 19p and 12q (summarized in Figure 3), suggesting that the human homolog of *Evi12* will map to 19p or 12q.

***Evi12* is located near the promoter region of the *Tra1/Grp94* gene** - Following a PCR approach (Figure 4A), we have cloned the MuLV integration sites in *Evi12* from 13 primary tumors (Figure 4B). These *Evi12* proviral insertions were located within a region of approximately 1.7-kb and had been inserted opposite to the proviral integration in NFS107 (Figure 4B and 5). The nucleotide sequence of the 1.7 kb PCR fragment from CSL16 was compared with sequences in the NCBI database and demonstrated high homology with the promoter region of the *Sus scrofa Ppk98* gene (X90848) (Figure 4B) (71, 72). The murine homolog of porcine *Ppk98* is *Tra1/Grp94* (also referred to as *Erp99*, endoplasmin, and *Gp96* in other studies). The gene encoding *Tra1/Grp94* is located on mouse chromosome 10 (300) in a region that shares homology with human chromosome 12q (191, 258). This suggested that the retroviral integrations in *Evi12* were located upstream of the murine *Tra1/Grp94* gene. The 233-bp fragment 503 was, subsequently, used to screen an embryonic stem cell (E14) mouse genomic library to isolate genomic DNA fragments representing the *Evi12* locus. One phage clone (λ503) was isolated and used to generate a restriction enzyme map (Figure 5). This map showed identity with the 5' region of the mouse *Tra1/Grp94* gene (299), which confirmed that *Evi12* is indeed located upstream of the gene encoding the molecular chaperone, *Tra1/Grp94* (Figure 5). Moreover, sequence analysis demonstrated coding sequences of *Tra1/Grp94* on a 1.6 kb *Eco*RI fragment isolated from λ503 (Figure 5). Although *Tra1/Grp94* is constitutively expressed in the endoplasmic reticulum (ER) of all eukaryotic cells (201), we investigated whether expression of this gene was altered in the myeloid cell line NFS107 and the primary tumors CSL11 and CSL17, which contain provirus in *Evi12*. Northern blot analysis demonstrated comparable levels of *Tra1/Grp94* mRNA in NFS107 and in cell lines without retroviral insertions in *Evi12*, i.e., DA3, NFS22, NFS60, NFS61, and NFS70 (Figure 6A). Likewise, no changes in *Tra1/Grp94* mRNA expression were observed in CSL11 and CSL17 (Figure 6A). Moreover, no fusion or readthrough mRNA transcripts of retroviral sequences and *Tra1/Grp94* were apparent by Northern blot analysis. Western blot analysis showed comparable *Tra1/Grp94* protein levels in NFS107 and control cell lines without *Evi12* insertions, i.e., NFS22, NFS61, NFS70 and NFS78 (Figure 6B). Recent studies showed that expression of *Tra1/Grp94* and

Figure 4: Locations of proviral insertions in the *Evi12* locus.
A. Representation of the proviral integration in *Evi12* in the myeloid cell line NFS107. Fragment 503 flanking provirus in NFS107 and the orientation and site of insertion of the proviruses in the primary tumors (CSLs) are shown. VISs were amplified with primer set p503-1 and pLTR1 followed by p503-1 and pLTR2. **B.** DNA sequence of the 1.7-kb region and the locations and orientations of the retroviral integrations in *Evi12* identified in the myeloid cell line NFS107 and the Cas-Br-M MuLV-induced primary tumors (CSL). The first 233 bp represent fragment 503. Both 503-specific primers, p503-1 and p503-2, are indicated by an arrow. cDNA synthesis of fragment 503 was primed on the poly(A) stretch from 234 to 276 bp. The region homologous to the promoter of the *S. scrofa ppk98* gene (NCBI, E value 1.10^{-6}) is double underlined.

A

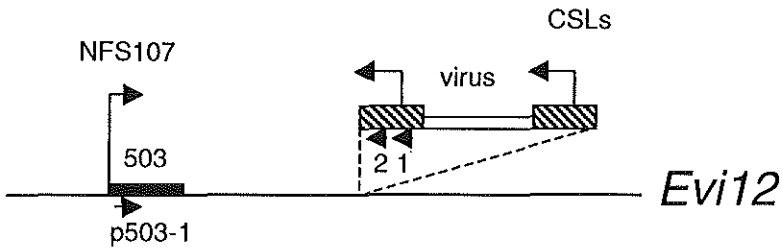

B

```
      >NFS107
1     ATGTGAGTGT GAAAACCCTA ATTCCGGTTA TAGTTCAAGT GGGGCAATCA TTTTATCCAC
      p503-1 ------------------------>
61    TAAGCCATCT CTCCTCAGCT GAAAGCATGT ATTTTCCAGG AGCTTGGCCA GCAAGTCAAG

121   ATAAGGACTG ACCATCTTCT GCCAGCCTGG AAGTAGATTC TCTCTCTCTG ATTCTCTCTC
      <CSL15
181   TCTCTCCTTT CTATCTGGGG ACCATCATCT GCAGAAACTT CTACCCCCCC CCCAAAAAAA
                <------------------------ p503-2
241   AAAAAAAAAA AGAACAAAAC CAAAAACCCA CCAGCTTTAT TTTGGAGGAC AAATCTCATT
                     <CSL29
                   <CSL85
301   CTCAGTTCCT CCCAGGTGCA GCCCGATCTA CCTCCCACTG GCCAGTTAAG ATGCAGTCAC

361   AGTTTCACAA TACTTGCTTA CTTGCTCGAT AAAAAAAAAA AGAAAGGAAG AAAGAAAGAA
                   <CSL17                  <CSL14
421   AGAAAGAAAG AAAGAAAGAA AGAAAGAGAG TAAGAAAGAA AGAAAGTGGA TGATGGGCTG
            <CSL97
      <CSL89                                                        <
481   TCATACGCAG AAATGGCCAT CTTTTTCCAA AAGCACAAAT AAATAAGATC CTGGTATGCT
      CSL12S
541   CTAAACAACA AACACAAGCA CAGAGGCATA AGGCCTTCGT CTTACATTTC TGTATGCTTT
                                        <CSL60
                                  <CSL11          <CSL35
601   GGCAAATGTA GGTAAATCAG ACAGATGTAA ATAAGCCATC ACCACATTAT GTAAACACCA

661   AACCACAGAT TCAAGTTCTA CAAGTCTAAA TTCTTGAAGT GTCAAAGGGA CTATGACATT
                                              <CSL13
721   GTCACTGAAA AGCTTGCCTT CGAGAACCTG GATTGCCTAA AAAAAAACAT CTCGAATTTT
            <CSL12T
781   CTTGGAGAAA GCGGTGATGG AATGGATGTG TTGAGGGCAG GCAAGCGTGC TGGTGGAAAA
841   TTGGTTAAAA TGAGGCTAAA GAGCCTAGAA AACATTTCGG AACGTACAAG CTGGCCCTAG
901   GGACTTCCCT CACCAGAAAG AGCCTCTTTT GCTATCTTTC GGAAGGCGGA AAGGTGTTTC
961   TATGAAGTTA CAAAGCCACA ATCCAGGCTG TTTTGCAAGC TCTGCGGCTT TTGCTTTCAA
1021  GTATCTGCAT AAGTTCTTTC CTGTTCTATG CTAGCCTGGA CTTCACCACC GCGCTCTCTG
1081  GCTGATTCAC AAAAGAGGCT CTAGATTGCC CAGTCATTCT TTGATATTTA TGGGGATGTC
1141  AAAGGAACTT GGGTCCTTGT TTCCTTCGGG GTTGGAGAGC CCCTACATCC TCAACTGCAA
1201  ACCAAACCAG AGAGGACAGG AAATGCGAGC AGCGCAACGC CAAGTGTAAC CGAAGGCTCT
1261  AGGGACCCTG AGTGACGCGC AAGAAAGCGG ACGTGGAAAC CCGGGTGCTA CCACCAGCCC
1321  AGAATCCAGG GCTGACCCTC TGACACGGTG AGACTAGGGC TACGCGGGGC TGCTTTTCAG
1381  GTCCGCCTCT GAAAACTGTG TGCATTAGAG TCCTAGAACA AGCACAGATC TATTCTGCAA
1441  TCTGAATGAG GTGGNAATCC TATAATCACT CAGAGACATT TCCCGCGGAC ACAAGATTGG
1501  AGTAAGCAAG GGCCAAGTAC GCAACTGGCC TAGACGCCAG AGACTACAAT TCCCAGCATT
1561  CATGAGATTA GTGCGTTGCA TGCCGGAAAC TGTAGTTTCT CACCACCATC CAAACGCATT

1621  CCGGATATTC AACCCCTCAC AAATTTCTCT TTTGCGAAAA GAAACGCCCA AAAGAAAGGT
1681  GACGGCGAAC GTAGCGCTGA AAGGACTCGT AACGTGACCC GCGTCGTAGA CGAGAAAAGG
      <CSL16
1741  GT
```

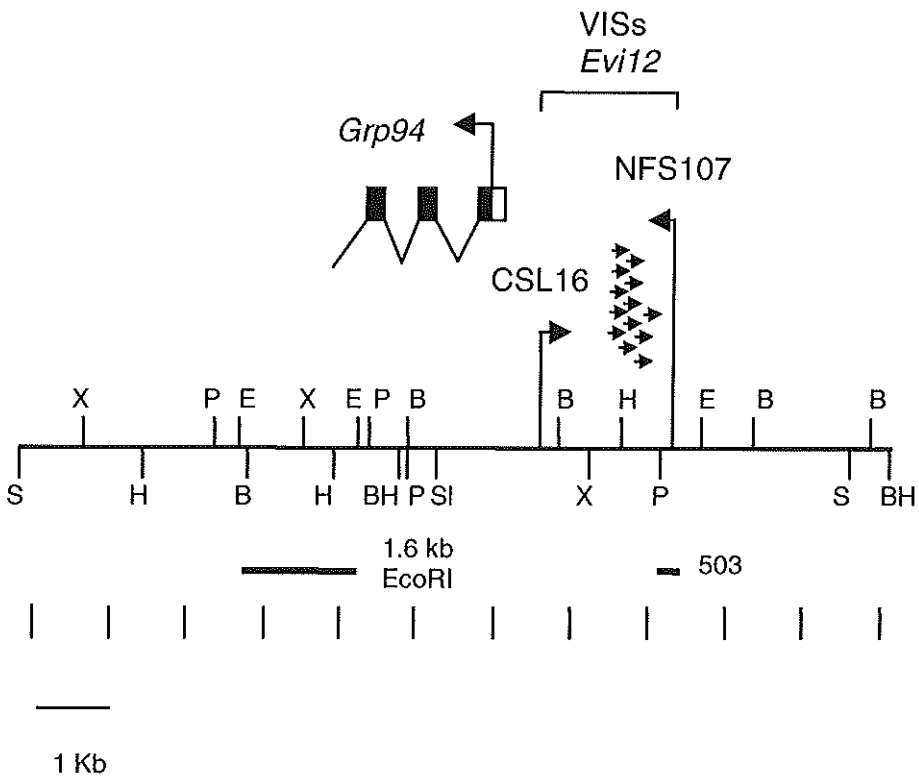

Figure 5: Restriction enzyme map of the *Evi12* locus.
Restriction map of the genomic phage λ503 representing the *Evi12* locus (Sl, *Sal*I; S, *Sst*I; BH, *Bam*HI; P, *Pst*I; B, *Bgl*II; H, *Hin*dIII; X, *Xba*I; E, *Eco*RI). The proviral insertion region of 1.7 kb is flanked by the virus integration sites in NFS107 and CSL16. Arrows indicate the viral insertions in the other CSL tumors. The locations of the first three exons of the *Tra1/Grp94* gene are depicted as boxes with the protein-coding region in black. The 1.6-kb *Eco*RI fragment used for sequence analysis and the cDNA fragment 503 flanking the *Evi12* VIS in NFS107 are indicated below the restriction map.

the ER molecular chaperone *Grp78* is tightly regulated by hematopoietic growth factors (45). Although we were able to reproduce the results of Brewer and coworkers, i.e., induction of *Tra1/Grp94* mRNA expression by IL-3 in growth-factor-deprived cell lines, no differences were observed between NFS107 (*Evi12* provirus insertion) and DA3 (no *Evi12* provirus insertion) (data not shown). Together, these results indicated that *Grp94* is located near the common VIS *Evi12* but that expression of the *Tra1/Grp94* gene is not affected as a result of proviral insertion in *Evi12*.

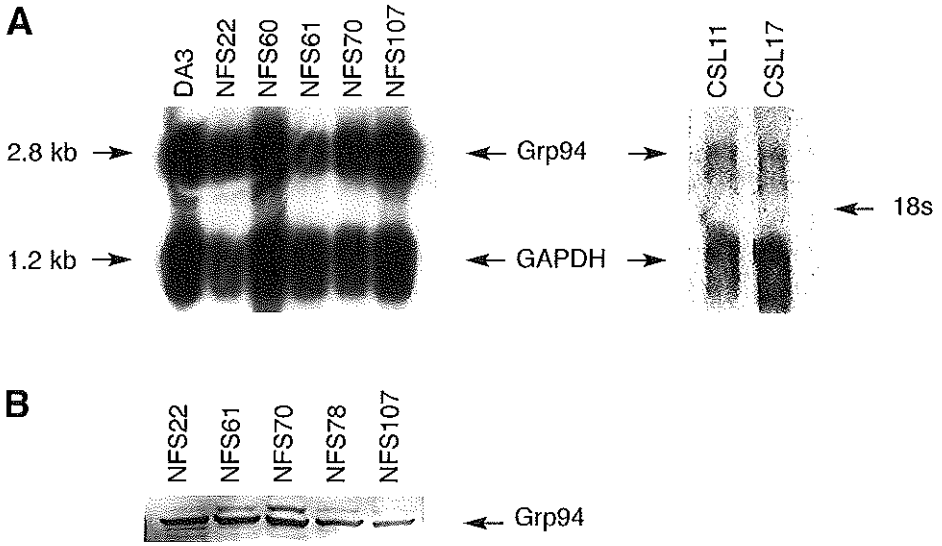

Figure 6: Expression of *Tra1/Grp94* mRNA in NFS cell lines and primary tumors.
A. Northern blot analysis of MuLV-induced cell lines DA3, NFS22, NFS60, NFS61, NFS70, and NFS107 (*Evi12*) and primary tumors CSL11 (*Evi12*) and CSL17 (*Evi12*). Filters were hybridized with full-length cDNA of *Tra1/Grp94* (201) cloned from NFS22. **B.** Western blot analysis of MuLV-induced cell lines NFS22, NFS61, NFS70, NFS78, and NFS107 (*Evi12*) with an anti-Grp94 antibody.

High coincidence of retroviral insertion in *Evi11* and *Evi12* in Cas-Br-M MuLV-induced primary tumors – The *Evi12* flanking cDNA 503, was isolated from the IL-3-dependent myeloid cell line NFS107 that also contains an insertion in *Evi11/Cb2*. In fact, 54% of the tumors, i.e., 7 of 13, bearing provirus within *Evi11/Cb2* contained insertions in the novel common VIS *Evi12* as well (Table 1). The equal intensities of the rearrangements in *Evi11* or *Evi12* in each tumor containing insertions in both these loci shown by Southern blot analysis suggest a clonal outgrowth of leukemic cells (data not shown). The high percentage of coincidence between *Evi11* and *Evi12* demonstrated in this study provides evidence for cooperative transforming activity between the target proto-oncogenes in *Evi11* and *Evi12*.

Discussion

Tumor initiation and progression is a multistep process (1, 129, 327). Therefore, proviral insertion in *Evi11/Cb2* is probably one of multiple genetic alterations required before a hematopoietic progenitor cell becomes fully malignant. Interestingly, in outbred NIH/Swiss mice, *Evi11/Cb2* is a frequent target for Cas-Br-

M MuLV (12%). In an attempt to isolate *Evi11/Cb2* cooperating genes, novel provirus flanking cDNA fragments were isolated (317). Clone 503 represented a novel common VIS *Evi12*, which was found in 14% of the Cas-Br-M MuLV-induced NIH/Swiss leukemias. More interestingly, 54% of the tumors containing proviruses in the gene encoding the peripheral cannabinoid receptor *Cb2* also have insertions in *Evi12*. Retroviral infection of *Cb2* transgenic mice (1, 32), with the *Cb2* gene controlled by the *Sca1* promoter (207), is currently being performed to determine whether transgenic mice develop leukemia earlier after Cas-Br-M MuLV injection than control nontransgenic littermates. It is anticipated that retroviral infection of *Cb2* transgenics will add to our insight into the cooperation between *Evi11/Cb2*, the target gene in *Evi12*, and other proto-oncogenes. Nevertheless, the frequent coincidence of *Evi11/Cb2* and *Evi12* in the Cas-Br-M MuLV-induced primary tumors suggests that the target genes in these two loci cooperate in leukemogenesis.

Evi12 is located upstream of the gene encoding the molecular chaperone *Tra1/Grp94*. The glucose-regulated stress protein Tra1/Grp94 is involved in protein processing and stimulates strong antitumor responses (231). *Tra1/Grp94* is ubiquitously expressed and the most abundant glycoprotein in the ER of eukaryotic cells (201). Tra1/Grp94 and another ER chaperone Grp78 are upregulated severalfold during differentiation of the macrophage cell line M1 after IL-6 stimulation (226) and *Grp94/Grp78* also induce resistance to apoptosis (184, 186, 202). These examples suggest that changes in *Tra1/Grp94* expression may affect normal differentiation or apoptosis of hematopoietic cells. Furthermore, expression of *TRA1/GRP94* is elevated in human breast cancer cells (unpublished results A. Lee) and increased expression of *Tra1/Grp94* in a model of rat colon adenocarcinoma has been associated with greater tumorigenicity (204). This would imply that provirus in Evi12 should increase the expression of *Tra1/Grp94*. However, retroviral insertion in *Evi12* occurred outside the conserved regulatory elements that are responsible for basal expression as well as the inducibility of the *Tra1/Grp94* promoter (53, 192), and we could not demonstrate any significant changes in levels of *Tra1/Grp94* expression in cells containing proviral insertions in *Evi12*. Moreover, although it has recently been shown that *Tra1/Grp94* is tightly regulated by hematopoietic growth factors (45), no differences in the regulation of *Tra1/Grp94* expression after IL-3 starvation and IL-3 stimulation were observed in NFS107 compared to DA3 cells (data not shown). Thus, our results do not provide evidence to support the hypothesis that *Tra1/Grp94* represents the proto-oncogene affected by proviral insertion in the myeloid cell line NFS107 or the Cas-Br-M MuLV-induced primary tumors.

The proviruses in the Cas-Br-M MuLV-induced primary leukemias integrated in the opposite orientation compared to the direction of transcription of *Tra1/Grp94* (Figure 6). This might suggest that not *Tra1/Grp94* but another gene downstream of the provirus insertions is the proviral target in *Evi12*. The transcriptional activation of this potential target gene may be by promoter insertion since proviruses integrated in a relatively small region of 1.7 kb (148, 340). To identify other potential proto-

oncogenes in *Evi12*, an exon trapping system that we recently developed (315) is currently being applied to several bacterial artificial chromosomes (BAC) clones covering approximately 250 kb of the *Evi12* locus.
Since leukemic spleen and thymus contain normal tissue as well and the amount of normal tissue depends on the degree of tumor progression, frequent low intensity of the rearranged *Evi11* and *Evi12* alleles in relation to the normal as well as variation between the primary tumors was shown by Southern blot analysis. Underrepresentation of the rearranged allele may be caused by polymorphism. However, since most of the proviral insertions have been cloned and sequenced and since Southern blot analysis of all tumors has been carried out with multiple restriction enzymes, the possibility of rearrangements as a result of polymorphism in outbred NIH/Swiss mice is excluded.
In the cases of *Evi11* and *Evi12*, there is a strong selective advantage for integrations of MCF viruses. MCF viruses originate from recombination events between ecotropic MuLVs with endogenous proviruses involving the retroviral *env* gene and part of the LTR. Recombination results in the release of leukemogenic MCF viruses with an altered host range and the capability of superinfecting target cells. In a number of virus-induced hematologic diseases, particularly T-cell lymphomas, activation of the target proto-oncogene is regulated by insertion of viruses of the MCF type (30, 54). Provirus in *Evi11* contains a unique *Eco*RI site downstream of the 5' LTR and is therefore distinct from the highly lymphomagenic NS-6(186) MCF virus, which has been cloned from a thymic T-cell lymphoma in NFS mice inoculated with Cas-Br-M MuLV (54). In *Evi12* the proviral genomes contain an altered *env* region characteristic for MCF viruses (252). Although the exact role of MCF viruses is still unclear, the invariable insertion of MCF type proviruses and not Cas-Br-M MuLVs in *Evi11/Cb2* and *Evi12* suggests an important role for MCF viruses in the activation of the target proto-oncogenes.
Evi11/Cb2 and *Evi12* retroviral insertions have been found in myeloid as well as in lymphocytic leukemias. Thus, there is no apparent correlation between morphology of the leukemia and proviral insertion in *Evi11*, *Evi12*, or both (Table 1). To define the phenotypes of *Evi11/Cb2* and *Evi12* rearranged as well as nonrearranged leukemias more exactly, all primary tumors are currently being analyzed by fluorescence-activated cell sorter analysis with lymphoid- and myeloid-specific antibodies. The fact that *Evi11/Cb2* and *Evi12* were identified in myeloid as well as in lymphoid lineages suggests that those insertions are early transforming events of immature multipotent progenitor cells. Other genetic defects may ultimately determine whether immature myeloid or lymphoid cells accumulate in the hematopoietic system.
Evi12 was mapped on mouse chromosome 10 by interspecific backcross analysis and this mapping result was confirmed by the cytogenetic location of *Tra1/Grp94* (191). No putative proto-oncogenes have been identified in the mouse locus yet. *Evi12* is distinct from the known MuLV common integration sites *Mml1* (160) and *Mis2* (249), which both map close to *c-Myb* on mouse chromosome 10. *TRA1/GRP94* was

cytogenetically mapped to human 12q24.2→24.3 (300). Subsequently, human *TRA1/GRP94* was placed on a yeast artificial chromosome contig representing 12q22-q23 (258). Thus, *EVI12* is located on human 12q22-24 as well. Although, no recurrent chromosomal breakpoints in human acute myeloid leukemia (AML) have been assigned to the human chromosomal region 12q22-24, an individual AML patient with a translocation between 3q21 and 12q24 has been described (343). Interestingly, 12q22 and 12q24 breakpoints have been associated with chronic lymphocytic leukemia (151) and B-cell non-Hodgkin lymphoma (348), respectively. Thus, the chromosomal region 12q22-24 may be involved in AML, chronic lymphocytic leukemia or B-cell non-Hodgkin lymphoma. It will be of interest to investigate whether the *Evi12* locus also represents a nonrandom chromosomal breakpoint region of human malignancies.

CHAPTER 5

GENERATION OF A PANEL OF Cas-Br-M MuLV-INDUCED HEMATOPOIETIC MALIGNANCIES: IMMUNOPHENOTYPES OF *Evi1*-, *Evi11/Cb2*-, AND *Evi12*-TRANSFORMED LEUKEMIAS.

Marieke Joosten, Peter J.M. Valk, Yolanda Vankan, Nico de Both, Bob Löwenberg and Ruud Delwel.

Submitted

Abstract

The slow-transforming retrovirus Cas-Br-M murine leukemia virus (MuLV) is a potent agent to induce leukemias in mice and useful for retroviral insertional mutagenesis. We used Cas-Br-M MuLV with the objective to establish a new panel of mainly myeloid leukemias in NIH/Swiss mice. All tumors were classified by gross pathology, morphology, immunophenotype and the incidence of known common virus integration sites (VISs) in MuLV-induced myeloid malignancies, i.e., *Evi1*, *Evi11/Cb2*, *Evi12*, *Fli1* and c-*Myb*. Interestingly, male NIH/Swiss mice were more susceptible than females to the induction of leukemia by Cas-Br-M MuLV. Seventy-four Cas-Br-M MuLV-inoculated mice developed a severe splenomegaly, sometimes in association with a thymoma. Although, most of the immunophenotyped Cas-Br-M MuLV tumors were of myeloid origin (58%), numerous T-cell leukemias (21%) and mixed myeloid/T-cell leukemias (21%) were found. The myeloid leukemias and myeloid compartment of the mixed leukemias were further characterized by immunophenotyping with stem cell-, myeloid- and erythroid-specific antibodies. The known Cas-Br-M MuLV common VISs *Evi1*, *Evi11/Cb2* and *Evi12* were demonstrated in 19%, 12% and 20% of the cases, respectively. *Fli1* and c-*Myb* rearrangements were not found. The *Evi1* provirus integrations were restricted to myeloid leukemias, whereas *Evi11*/Cb2 and *Evi12* were identified in myeloid as well as T-lymphoid leukemias. This panel of well-characterized Cas-Br-M MuLV-induced hematopoietic tumors may be useful for the isolation and characterization of new proto-oncogenes involved in myeloid or T-cell leukemias.

Introduction

Slow-transforming retroviruses that do not contain oncogenes in their genome induce tumors by means of insertional mutagenesis (135, 148, 340). The identification of common virus integration sites in retrovirally-induced tumors provided a powerful strategy to isolate novel transforming genes from leukemias and lymphomas (135, 148, 340). Moreover, genes located on chromosomal breakpoint regions, and aberrantly expressed in human hematopoietic malignancies, have frequently been identified through retroviral insertional mutagenesis in murine leukemias, e.g., *Evi1* (214, 217), *Evi2 (NF1)* (46, 277, 288), *Evi6 (Hoxa9)* (227, 228), *Bcl1 (CyclinD1)* (69, 290), N-*Myc* (124, 275) and *Erg* (283, 317). The basis of retroviral insertional mutagenesis is the activation of proto-oncogenes or inactivation of tumor suppressor genes as a result of retroviral integration into the host genome. Generally, expression of proto-oncogenes located in the vicinity of an inserted provirus is elevated by retroviral promoter or enhancer sequences. However, retroviral integration within the protein-coding region of a cellular target gene results in the expression of truncated products (148, 340).

Cas-Br-M MuLV leukemia virus (also referred to as Cas-Br-E MuLV) is a wild-mouse ecotropic virus that induces a wide variety of hematologic diseases in NFS mice (125) and non-B, non-T-cell leukemias in NIH/Swiss mice (31). To isolate novel common VISs and identify new target proto-oncogenes and cooperating proto-oncogenes (318) involved in myeloid leukemia development, we have generated a novel panel of Cas-Br-M MuLV-induced leukemias in NIH/Swiss mice. We have characterized the hematologic malignancies by gross pathology, cytology and immunophenotyping, using a panel of monoclonal antibodies directed to cell surface antigens of various blood cell lineages. Seventy-four of the 91 cases with a hematopoietic disease represented leukemias, manifested by a splenomegaly or a thymoma. The majority of the leukemias were of myeloid origin (59%), however, a significant number of the leukemias expressed a T-cell phenotype (21%) or a mixed myeloid/T-cell phenotype (21%). We also determined the frequencies of proviral insertion in loci that have previously been shown to be recurrent targets in myeloid malignancies for Cas-Br-M MuLV, i.e., *Evi1* (29, 217, 219), *Evi11/Cb2* (315), *Evi12* (318) and *Fli1* (31) or for Moloney and Friend MuLV, i.e., c-*Myb* (229, 230, 279). *Evi1* encodes a zinc-finger transcription factor (217) and overexpression of *Evi1* has been shown to interfere in granulocytic (215) as well as erythroid differentiation (166). *Evi11* and *Evi12* are two relatively novel common VISs that we recently identified in Cas-Br-M MuLV-induced IL-3 dependent myeloid cell line NFS107 and the Cas-Br-M MuLV-induced primary tumors described in this manuscript (315, 318). *Evi11* is located on mouse chromosome 4 and the target proto-oncogene in this locus is the gene encoding the hematopoietic peripheral cannabinoid receptor Cb2 (315). The candidate proto-oncogene in *Evi12*, which was mapped on mouse chromosome 10 (318), is currently unknown. The ets-transcription factor Fli1 was originally identified by cloning proviral insertions from Friend MuLV-induced erythroid leukemias (24), but proviruses in Fli1 were later also shown in non-B, non-T-cell leukemias (31). The transcription factor c-*Myb* is one of the best-studied proto-oncogenes in myeloid disease (138) and has been shown to be a target for proviral insertions in myeloid leukemias (340). Here we demonstrate frequent retroviral insertion in *Evi1*, *Evi11* and *Evi12*, but not in *Fli1* and c-*Myb*. Retroviral insertion in relation to the immunophenotype of the Cas-Br-M MuLV-induced leukemias has been investigated.

This well characterized panel of retrovirally-induced leukemias provides a powerful source for the isolation of novel transforming proto-oncogenes involved in myeloid and T-cell leukemia development.

Materials and Methods

Mice, viruses and pathology of tumors - NIH/Swiss mice were obtained from Harlan (Horst, The Netherlands). Cas-Br-M MuLV-producing NIH 3T3 cells

(donated by Dr. Janet W. Hartley from the National Institutes of Health, Bethesda, MD) (122) were cultured in Dulbecco's modified Eagle's medium (DMEM) (GIBCO, Gent, Belgium) containing 10% fetal calfs serum (FCS). A 70% sub-confluent culture of Cas-Br-M MuLV-producing NIH 3T3 cells was incubated in 5 ml of culture medium for 18 hours at 37 ^{0}C, in a 75cm^2 culture flask. Newborn NIH/Swiss mice were subcutaneously injected with 100 µl filtered (pore size, 0.22 µm; Nucleopore Corp., Pleasanton, CA) tissue culture medium. Leukemias appeared 5 to 13 months after inoculation. Mice were sacrificed when moribunded. The leukemic mice had enlarged spleens, frequently accompanied with gross thymus enlargements as well. Diagnosis was based on gross pathology, May-Grünwald Giemsa staining and flow-cytometric analysis using monoclonal antibodies directed to membrane surface antigens (Table 1). Leukemias were also characterized for DNA rearrangements within immunoglobulin heavy chain (IgH) genes. Cells were cryopreserved in aliquots of 50 x 10^6 cells in 7.5% DMSO and 20% FCS using a controlled freezing apparatus and storage in liquid nitrogen.

Antibody	Antigen	Specificity	References
ER-MP54	ER-MP54 Ag	myeloid cells	(182)
ER-MP58	ER-MP58 Ag	myeloid cells	(182)
M1/70	Mac1	non-fixed macrophages granulocytes, natural killer cells	(298)
F4/80	F4/80 Ag	macrophages	(10)
RB68C5	Gr1	granulocytes	(123)
ER-MP21	Transferrin receptor	cells in cycle, erythroid cells	(181)
TER119	Glycophorin A	mature erythroid cells	(137)
59-AD2.2	Thy1	T-cells, hematopoietic stem cells, myeloid cells	(178)
KT3	CD3	mature functional T-cells	(309)
RA3 6B2	B220	B-cells, myeloid cells	(58)
E13 161-7	Sca1	hematopoietic precursors, T-cells	(2)

Table 1: Monoclonal antibodies.

Labeling of cells with monoclonal antibodies and flow-cytometry - Cells were labeled with rat monoclonal antibodies (MoAbs) and with a second step reagent GARa (Goat anti Rat)-FITC (Nordic, Tilburg, The Netherlands). All incubations were carried out 30 minutes on ice in phosphate buffered saline supplemented with 1% bovine serum albumin. The specifications of the MoAbs used in this study are

described in Table 1. Cell surface fluorescence was analyzed by flow cytometric analysis using a FACScan flow cytometer (Becton Dickinson, Mountain View, CA). A sample was considered positive for a particular marker when 30% of the cells or more showed positive fluorescence (Figure 2). In case of Thy1 expression a discrimination between intermediate positive ($Thy1^{+}$; not more then 1 log difference in fluorescence intensity between positive and the negative control) and strongly positive ($Thy1^{++}$; 2 log difference or more between positive and negative) (Figure 2) was made.

DNA isolation, Southern blot analysis and probes - Isolation of genomic DNA and Southern blot analysis was carried out exactly as described previously (315). The immunoglobulin heavy chain region was analyzed with a J_h probe *Eco*RI-*Bgl*II (2.5 kb) of clone H24 (127) (a gift from Dr. T.Honjo, Kyoto University, Japan). The T-cell-receptor β-chain gene was analyzed with a 4 kb *Hin*dIII-*Hin*dIII $J_{\beta 1}$ probe (87). To study rearrangements in the *Evi1* locus a 535 bp cDNA fragment was used that we recently described (317). Rearrangements in the *Evi11* locus comprising the *Cb2* gene were studied with a 1.2 kb *Eco*RI-*Bam*HI *Cb2* cDNA fragment (315). *Evi12* rearrangements were studied with the 503 probe obtained with a RT-PCR based strategy to isolate complementary DNA fragments flanking retrovirus integration sites (317). Rearrangements in the c-*Myb* gene were determined with a 450 bp *Nco*I (vector) - *Eco*RI and a 500bp *Pst*I-*Pst*I cDNA probe spanning exons 3,4,5 and 6 of the gene (278). *Fli1* insertions were studied using a 1.7 kb *Eco*RI cDNA probe (25).

Results

Leukemia development and gross pathology.

Tumor incidence, gross pathology and histology - Newborn NIH/Swiss mice were inoculated with Cas-Br-M MuLV-containing culture supernatant. Ninety-one among 116 inoculated mice developed hematologic malignancies (Table 2). Seventy-four of these became severely sick with signs of splenomegaly and/or a thymoma (Table 2). The other 17 mice developed a mild disease, with a moderate increase (two-fold) in

	Number of mice	Number of leukemias	Frequency
Males	54	41	76%
Females	62	33	53%
Total	116	74	64%

Table 2: Frequency of Cas-Br-M MuLV-induced leukemias in NIH/Swiss mice.

spleen size. Eighteen of the 25 mice without evidence of hematological disease died of unknown causes. The remaining 7 mice (females) were sacrificed at the end of the experiment, i.e., after 394 days, without signs of leukemia or any other disease.
Histological analysis of mice with a splenomegaly alone, immature blast cells (46%), myeloblasts with granulocytic features (27%) or lymphocytes (27%) were demonstrated. In 82% of the mice with a thymoma histology revealed the presence of a high percentage of lymphocytes, whereas the remaining (18%) contained immature blast cells without signs of granulocytic differentiation.
Differences between male and female mice - In this study we focused on the 74 cases with severe hematologic malignancies. Interestingly, only 33 out of 62 (53%) female mice developed severe leukemia, whereas tumor formation in male mice was evident in 41 of 54 (76%) cases. Furthermore, male mice developed leukemia more rapidly then female mice (Figure 1). Thus, male NIH/Swiss mice appear more susceptible to leukemia induction by Cas-Br-M MuLV than female animals. Gross pathology revealed that these differences are not the result of differences in the leukemia types found in males or females (Table 3). Thirty-one out of 41 male mice (71%) and 24 out of 33 females (73%) manifested leukemia with a major spleen enlargement. In 10 of 41 males (24%) and 7 of 33 females (21%) the mice also developed a thymoma. Two females developed thymoma without splenomegaly.

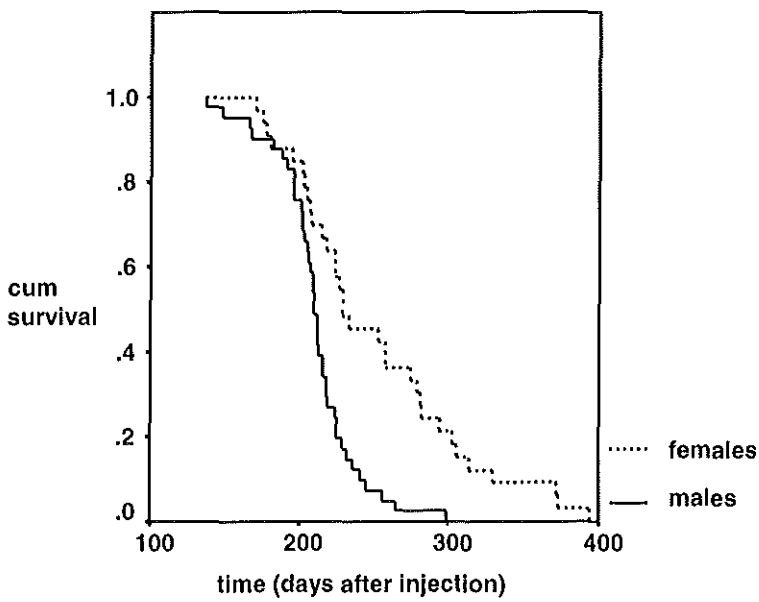

Figure 1: Survival curves of male (—) and female (---) NIH/Swiss mice developing leukemia after inoculation with Cas-Br-M MuLV.

Sex	Gross pathology	Number of mice	(%)	Latency period (days)	(mean)
Males	splenomegaly	31	(76)	166-299	(215)
	thymus enlargement	0	(0)		
	splenomegaly and thymus enlargment	10	(24)	137-236	(197)
	total	41	(100)	137-299	(211)
Females	splenomegaly	24	(73)	170-394	(263)
	thymus enlargement	2	(6)	175, 224	
	splenomegaly and thymus enlargement	7	(21)	177-314	(245)
	total	33	(100)	170-394	(245)

Table 3: Gross pathology of Cas-Br-M MuLV-induced leukemias.

Phenotype of Cas-Br-M MuLV-induced leukemias.

T-cell leukemias - Leukemic cells from spleen, thymus or bone marrow of 63 of the 74 cases with severe disease could be immunophenotyped by flowcytometry using monoclonal antibodies (Table 1). Thirteen cases displayed a T-cell phenotype, i.e., $CD3^{++}$, $Thy1^{++}$ (11 cases), $CD3^{++}$, $Thy1^{-}$ (one case) or $CD3^{-}$, $Thy1^{++}$ (one case). Those leukemias did not express myeloid markers (Figure 2 and Table 4). In ten of those mice the T-cell origin of the leukemia was substantiated by the presence of a thymoma (Table 4). A $CD3^{-}/Thy1^{-}$ or $CD3^{-}/Thy1^{+}$ non-T-cell phenotype (Figure 2 and Table 4) was found in 37 cases. Thirty-six of those 37 cases displayed a major

	Immunophenotype	Splenomegaly	Thymoma*	Total
T-cell leukemias	$CD3^{++}/Thy1^{++}$	3**	10***	13
Non-T-cell leukemias#	$CD3^{-}/Thy1^{-\text{ or }+}$	36	1	37
Mixed leukemias##	$CD3^{++}/Thy1^{++}$ and $CD3^{-}/Thy1^{-\text{ or }+}$	5	8	13
Not evaluable		11	0	11
Total		55	19	74

Table 4: Immunophenotyping of Cas-Br-M MuLV-induced leukemias: T-cell versus non-T-cell leukemias (* Mice with a thymoma include cases with or without a splenomegaly; ** In one case (CSL70) $CD3^{++}/Thy1^{-}$ lymphocytes were found; *** In one case (CSL54) $CD3^{-}/Thy1^{++}$ lymphocytes were observed; # $CD3^{-}$ non-T-cell leukemias Thy^{-} or $Thy1^{+}$ but not $Thy1^{++}$ cells; ## Mixed leukemias contain $CD3^{++}/Thy1^{++}$ T-lymphocytes as well as $CD3^{-}$ leukemia cells).

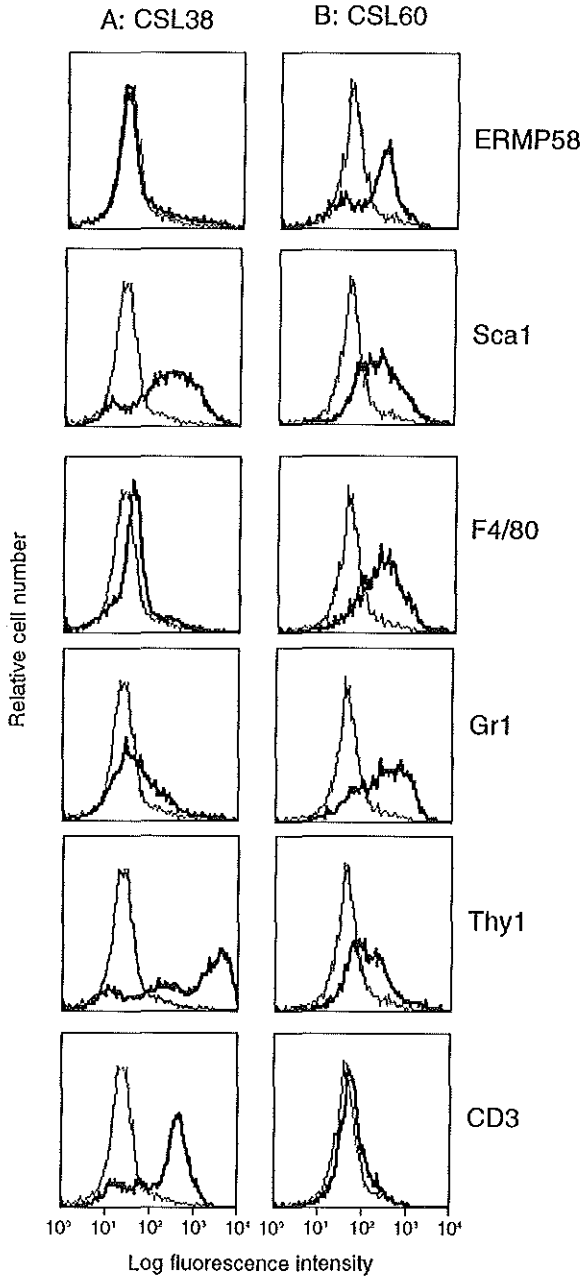

Figure 2: Immunophenotyping of Cas-Br-M MuLV-induced primary CSL tumors. Representatives of leukemias with a T-cell phenotype ($Thy1^{++}$ and $CD3^{++}$) (**A**, CSL38) and with a non-T-cell phenotype ($CD3^{-}$ and $Thy1^{+or-}$) (**B**, CSL60). CSL60 is a typical example of a leukemia type IV (Table 5), i.e., blasts with granulocytic and monocytic differentiation.

spleen enlargement without a thymoma. In 13 cases the leukemic cells expressed T-cell as well as myeloid markers. Eight of those cases displayed a thymus enlargement as well.

Myeloid leukemias - The leukemias were further immunophenotyped using the complete panel of monoclonal antibodies (Table 1). Analysis of the 37 non-T-cell leukemias and the non-lymphoid compartment of the 13 mixed leukemias, containing both $CD3^{++}/Thy1^{++}$ and $CD3^{-}$ cells, revealed heterogeneity among the cases. Six cases (5 non-T-cell and 1 mixed leukemia) revealed an immature myeloid phenotype, i.e., Imm^{+} (Sca^{+}, $Thy1^{+}$, ER-MP58^{+} and/or ER-MP54^{+}), $Gr1^{-}$, $Mac1^{-}$ and $F4/80^{-}$ (Table 5).

Leukemia type	Immunophenotype*	Non-T-cell Leukemias	Mixed leukemias**
I Immature blast cells	$Gr1^{-}$, $F4/80^{-}$, $Mac1^{-}$ and Imm^{+}	5	1
II Blasts with neutrophilic differentiation	$Gr1^{+}$, $F4/80^{-}$, (Mac^{+})*** and Imm^{+}	4	0
III Blasts with monocytic differentiation and	$Gr1^{-}$, $F4/80^{+}$, $Mac1^{+}$ Imm^{+}	11	5
IV Blasts with granulocytic and monocytic differentiation	$Gr1^{+}$, $F4/80^{+}$, $Mac1^{+}$ and Imm^{+}	9	3
V Blasts with myeloid and erythroid differentiation	ER-MP21^{+}, TER119^{+}, Imm^{+},$(Mac1^{+})$, $(F4/80^{+})$ $(F4/80^{+})$ and $(Gr1^{+})$	6	4
VI B-lymphocytic	$B220^{+}$ and other^{-}	2	0
Total		37	13

Table 5: Immunophenotyping of non-T-cell leukemias (Leukemias were immunophenotyped using the monoclonal antibodies indicated in Table 1; *Imm^{+} indicates that cells may express a combination of Sca1, ER-MP58, ER-MP54, and /or Thy1; **Mixed leukemias contain T lymphocytic as well as non T-cell leukemia cells, in this case the non-T-cell compartment is analyzed; ***expression markers between brackets may be positive or negative).

Four cases revealed a myeloid phenotype with neutrophil characteristics, i.e., Imm^{+}, Gr^{+}, $(Mac1^{+})$ but $F4/80^{-}$. Myeloid leukemias expressing monocyte/macrophage differentiation markers, i.e., Imm^{+}, $F4/80^{+}$, $Mac1^{+}$, but $Gr1^{-}$ were identified in 16 (11 plus 5) cases. Twelve (9 plus 3) cases expressed monocytic as well as granulocytic differentiation markers, i.e., Imm^{+}, $F4/80^{+}$, $Mac1^{+}$ and $Gr1^{+}$. In 10 cases myeloid and erythroid differentiation markers (ER-MP21^{+} and Ter119^{+}) were identified. In 2 out of the 37 non-T-cell leukemia cases, mainly $B220^{+}$ lymphocytes were found.

Although these data suggest that these leukemias are of B-lymphocyte origin, no rearrangements in the immunoglobulin heavy chain genes were found using a J_h-probe on *Eco*RI digested genomic DNAs of these cells (data not shown). In fact, no rearrangements in the IgH gene were found in any of the other cases (data not shown).

Retroviral integrations in Cas-Br-M MuLV induced leukemias.
Cas-Br-M MuLV-associated common VISs - Loci shown to be targets for Cas-Br-M provirus are, *Evi1* (29, 30, 217, 219), *Evi11/Cb2* (315), *Evi12* (318) and *Fli1* (31) or for Moloney- and Friend MuLV, c-*Myb* (229, 230, 279). To study the frequencies of rearrangements in these loci, Southern blot analysis was carried out on spleen and/or thymus DNA obtained from the 74 mice with severe disease. Rearrangements in *Evi1*, *Evi11* or *Evi12* were found in 28 cases (Figure 3). No abnormalities in *Fli1* or c-*Myb* were observed. In 48 out of 74 cases no retroviral insertions in any of these regions could be identified.
Evi1 - Rearrangements in the *Evi1* gene were found in 14 out of 74 cases, i.e., CSL13, -23, -29, -30, -41, -46, -57, -78, -93, -94, -95, -99, -117, and -123 (Figure 3 and 4A). Those novel retroviral insertions in the *Evi1* locus are situated in the same region of the *Evi1* locus, as the previously described Cas-Br-M MuLV *Evi1* insertions (Figure 4B) (16, 29, 317). *Evi1* rearrangements were demonstrated in non-T-cell or mixed lineage leukemias, and not in T-cell leukemias only (Table 5). Two leukemias

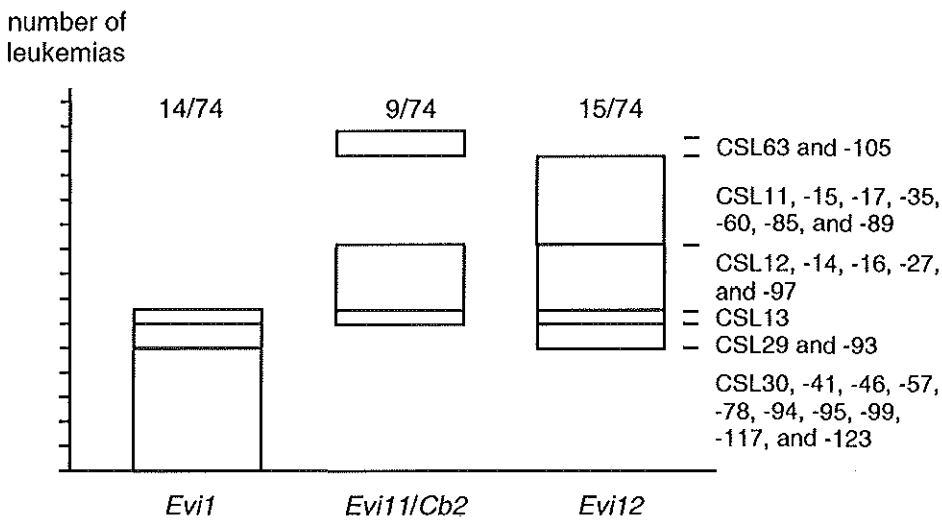

Figure 3: Common virus integration sites *Evi1*, *Evi11/Cb2* and *Evi12* in primary CSL tumors. Diagram representing the different provirus insertions in *Evi1*, *Evi11/Cb2* and *Evi12* in the primary CSL tumors. Overlapping boxes symbolize coincidence of provirus insertions in two or three common VISs, i.e., *Evi1*, *Evi11/Cb2* and/or *Evi12*. The CSL leukemia numbers are depicted (right).

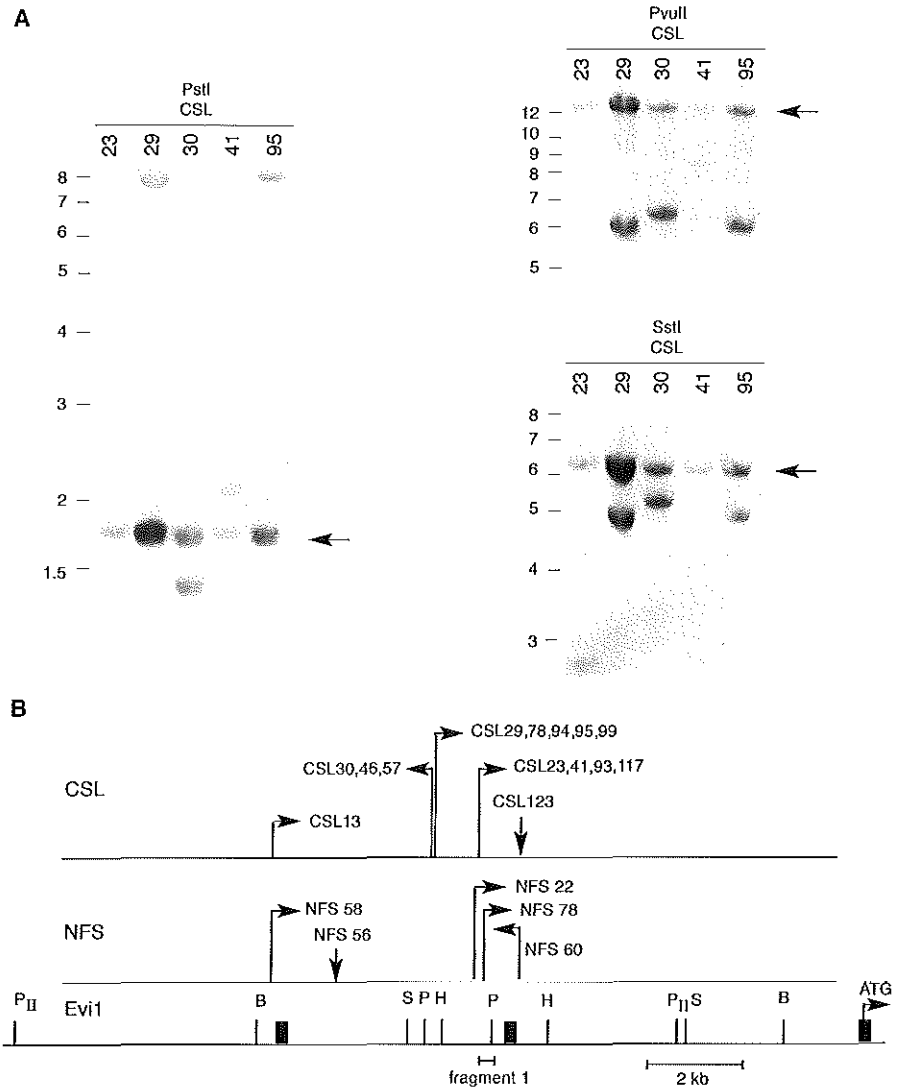

Figure 4: Provirus insertion in the common VIS *Evi1*.
A. Southern blot analysis of *Pst*I-, *Pvu*II- and *Sst*I-digested genomic DNA of primary CSL tumors. Filters were hybridized with fragment 1 (Figure 4B), a cDNA specific for the *Evi1* locus (317). The size marker is depicted in kilobases and an arrow indicates the size of the normal allele. All tumors, i.e., CSL23, -29, -30, -41 and –95 contain rearrangements in the *Evi1* locus, representing the leukemic subpopulation.
B. Schematic representation of the genomic structure of the *Evi1* locus (P:*Pvu*II, B:*Bam*HI, S:*Sst*I, P:*Pst*I, H:*Hin*dIII). The first three exons of the *Evi1* gene are indicated by black boxes. The location and orientation of proviruses in the Cas-Br-M MuLV-induced primary CSL tumors and NFS cell lines (126) are depicted by arrows.

expressed an immature immunophenotype, 1 leukemia showed monocytic differentiation, a fourth leukemia expressed granulocytic markers and 2 other leukemias coexpressed monocytic as well as granulocytic characteristics (Figure 5). Interestingly, 5 leukemias showed an erythroid phenotype, i.e., the cells were ER-MP21 and TER119 positive (Figure 4). Three mice, from which the tumors afterwards were shown to have *Evi1* rearrangements, died before any viable cell could be harvested and examined.

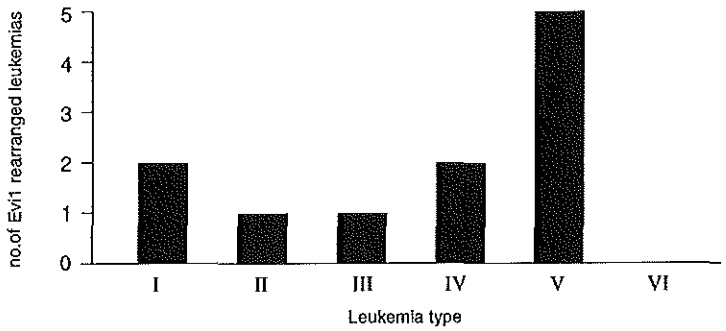

Figure 5: *Evi1* rearrangements and the phenotype of the leukemia.
Distribution of the non-T-cell leukemia phenotypes (Table 5) of the *Evi1*-rearranged Cas-Br-M MuLV-induced primary CSL tumors.

Evi11/Cb2 - The target gene in *Evi11* has been shown to be *Cb2*. Retroviral insertions in *Cb2* occur either 5' or 3' of the protein-coding region (315, 318). Rearrangements in *Evi11/Cb2* were found in 9 of the 74 cases studied, i.e., CSL12, -13, -14, -16, -23, -27, -63, -97, and -105 (Figure 3). The exact positions of these *Evi11* retroviral insertion sites have been documented recently (318). *Evi11* rearrangements were found in T-cell (3 cases), myeloid (1 case) or mixed leukemias (3 cases) (Table 6).

Leukemia type	*Evi1*	*Evi11/Cb2*	*Evi12*
T-cell leukemia	0	2	3
Non-T non-B-cell leukemia	9	1	2
Mixed leukemia*	2	3	4
Dead**	3	3	5
Total	14	9	15

Table 6: Common virus integration sites in Cas-Br-M MuLV-induced tumors: immunologic characterization (* Mixed leukemias contain T lymphocytic as well as non T-cell leukemia cells; **Immunophenotype could not be determined due to the high percentage of dead cells).

Three *Evi11* rearrangements were found in leukemic spleens obtained from mice that died before immunological analysis could be carried out. Interestingly, in addition to the 9 *Evi11/Cb2* rearranged cases, Southern blot analysis revealed rearrangements in the *Evi11/Cb2* locus in spleen DNA from 2, i.e., CSL74 and CSL75, of the 17 cases with a mild disease.

Evi12 - *Evi12* rearrangements occurred in 15 of the 74 cases, i.e., CSL11, -12, -13, -14, -15, -16, -17, -27, -29, -35, -60, -85, -89, -93, and -97 (Figure 3). Those proviral insertions are all present in a relatively small 1600 bp region, located upstream of the *Tra1/Grp94* gene and have been described recently (318). The target gene in *Evi12* is currently unknown. As with *Evi11/Cb2* rearrangements, retroviral insertions in *Evi12* have been found in T-cell (3 cases), non-T-cell (2 cases) and mixed leukemias (4 cases) (Table 6). Out of the 74 mice that developed a severe leukemia, 5 died before any viable cell could be harvested. Interestingly, all five mice carried a retroviral insertion in *Evi12*.

Tumors with multiple rearrangements - Coincidence of *Evi1* with other integrations appeared to be rare: *Evi1* and *Evi11/Cb2* in 1 case (CSL23), *Evi1* and *Evi12* in 2 cases (CSL29 and -93), *Evi1*, *Evi11/Cb2* and *Evi12* in 1 case (CSL13) (Figure 3). Interestingly, six of the *Evi11/Cb2* rearranged cases also harbored *Evi12* virus integrations (CSL12, -13, -14, -16, -27, -97) (Figure 3). These data may suggest cooperation in leukemia development between *Cb2* and an *Evi12*-related target gene. Only three of those cases could be analyzed phenotypically. One leukemia had a T-cell phenotype (CSL14) and 2 mixed leukemias expressed T-cell as well as myeloid markers (CSL12 and -16).

Discussion

Cas-Br-M MuLV-injected newborn NIH/Swiss mice developed leukemias at approximately 150 to 400 days after inoculation. Most of these were myeloid leukemias (59%), however, also T-cell (21%) and mixed T-cell/myeloid (21%) leukemias were found. These results appear to differ somewhat from experimental data from studies by others. Cas-Br-M induces a wide spectrum of hematopoietic neoplasias in NFS/N mice, including T-, pre-B- and B-cell lymphomas and erythroid, myeloid as well as megakaryocytic leukemias (125, 126). Bergeron *et al.* (29-31) reported the development of mainly non-T, non-B-cell lymphomas in NIH/Swiss mice after injection with Cas-Br-E MuLV, whereas we observed T-cell and myeloid leukemias using the same mouse strain. The major difference between the two studies is that Bergeron used a molecular clone, NE-8, described by Jolicoeur *et al.* (146), whereas we inoculated a biologically cloned Cas-Br-M MuLV-stock, obtained by limiting dilution (122). In contrast to our studies, Bergeron *et al.* observed frequent insertions of Cas-Br-E MuLV in *Fli1* (29-31), whereas these investigators neither observe Cas-Br-M provirus insertions in *Evi11/Cb2* nor in *Evi12* loci (personal

communication E. Rassart). In addition, no rearrangements of c-*Myb* were detected in either study, indicating that the c-*Myb* locus is a frequent target for Moloney- and Friend MuLV (229, 230, 279), but not Cas-Br-type viruses. The results from these studies together emphasize once again that different retroviruses or even subclones of a particular retrovirus may result in proviral integration in distinct loci, thereby determining the development of selective types of leukemia or lymphoma (148, 340).
More males then females developed leukemia following Cas-Br-M MuLV-injection. In fact, seven female mice did not develop any hematological malignancy at all and were sacrificed when the experiment was completed, i.e., 394 days after virus inoculation. Moreover, male mice developed leukemia more rapidly than females did. Sex-related sensitivity to tumor inducing agents in rodents has been documented in several tumorigenic conditions before. For instance, female animals have been reported to be more sensitive to certain tumor inducing agents or viruses (289, 301), whereas other studies have demonstrated a higher tumor incidence in males following exposure to radiation (81, 345). Interestingly, the radiation-induced tumors, showing greater susceptibility in male mice, represent cases of acute myeloid leukemia (81, 345). Explanations to clarify these sex-specific differences are mainly based on speculation. These explanations include possible differences in sensitivity of certain tumor cells to sex steroid hormones (289, 345). Although, sex-specific leukemia development is currently not one of the purposes of our investigations, the difference in sensitivity between male and female mice to Cas-Br-M MuLV-induced leukemia progression is intriguing and requires further study.
Retroviral insertions in the *Evi1* locus occurred in myeloid, erythroid or mixed myeloid/cell leukemias (19% (14/74)). These results are in agreement with many reports showing that *Evi1* is a proto-oncogene mainly involved in myeloid leukemia progression (16, 29, 30, 217). In humans, *EVI1* has shown to be mutated in acute myeloid leukemias (214) with chromosome 3q26 abnormalities and in certain cases of myelodysplastic syndrome (85), a preleukemic disease characterized by a severe anemia. Overexpression of *Evi1* in 32Dcl3 cells has shown to interfere with granulocytic differentiation of these cells when stimulated with G-CSF (215). Kreider *et al.* (166) demonstrated a block of erythroid differentiation by *Evi1 in vitro*. Possibly, Evi1 interferes with GATA1, a transcription factor that is indispensable for erythropoiesis (244, 245). Recent studies with *Evi1* transgenic mice underline the results documented by Kreider *et al.* (166), i.e., a defective erythropoiesis as a result of *Evi1* overexpression (Louz *et al.*, manuscript in preparation). In this study, we show that *Evi1* retroviral integrations frequently occur in leukemic blast cells expressing myeloid but also erythroid differentiation markers, i.e., ER-MP21 and TER119. These observations support the hypothesis that one of the major effects of aberrantly expressed *Evi1* in hematopoietic precursors is a block of erythropoiesis.
In contrast to *Evi1* proviral insertions, retroviral integrations in *Evi11/Cb2* (12% (9/74)) and *Evi12* (20% (15/74)) are not lineage-restricted. The observations that *Evi11/Cb2* and *Evi12* mutations occurred in T-cell leukemias as well as in myeloid

leukemias, suggest that retroviral insertions in those loci may have occurred early in hematopoiesis, i.e., in primitive hematopoietic stem cells. Subsequently, additional mutations, e.g., *Evi1* retroviral insertions, may determine whether myeloid or lymphoid leukemias evolve.

Leukemia initiation and progression involves aberrant expression of multiple genes (1). Two or more VISs have frequently been shown to be present in one particular tumor or tumor cell line. For instance, *Hoxa* and *Pbx1*-related genes in myeloid leukemias (228), c-*Myc* and M-CSF in a monocyte tumor (18), *IL-3*, *SCL* and *Hoxb8* in myeloid WEHI-3B(D$^-$) cells (304), *IL-3* or *GM-CSF* and c-*Myb* in WEHI-274 cells (183), *IL-3* and *GM-CSF* in *in vivo*-passaged FDC-P1 cells (89), *p53* and *PU.1* in erythroleukemias (213), *Fli1* and *p53* in non-T-, non-B-cell leukemias (29). These data indicate that leukemogenesis, like oncogenesis in general (129, 327), indeed is a multistep process involving mutation of multiple oncogenes (1). Furthermore, the coincidence of VISs suggests that retroviral insertional mutagenesis with MuLVs apparently resembles this phenomenon in leukemogenesis. *Evi11/Cb2* and *Evi12* insertions frequently coincided in the same leukemias suggesting that *Cb2* in *Evi11* and the currently unknown *Evi12* target oncogene cooperate in leukemia development. Here we demonstrate retroviral integration in *Evi1* and *Evi11/Cb2* in two cases, i.e., CSL13 and -23. In fact, aberrant expression of *Evi1* and *Evi11/Cb2*, as a result of retroviral insertions in both loci has been demonstrated in the myeloid cell line NFS78 (315). These results suggest that in certain cases of myeloid leukemia these two proto-oncogenes collaborated in hematopoietic transformation. This hypothesis may be assessed *in vivo*, by cross-breeding of *Evi1*- and *Cb2*-transgenic mice that we have generated recently (unpublished results). *Evi1* also appears to collaborate with an *Evi12*-related proto-oncogene since three leukemias contain insertions in both these loci, i.e., CSL13, -29 and -93. Two common VISs, which frequently coincide are *Evi11/Cb2* and *Evi12*, i.e., rearrangements were shown in both common VISs in CSL12, -13, -16, -27 and 97. Although the target gene in *Evi12* is currently unknown, the data obtained so far are highly suggestive for collaboration of *Cb2* and an *Evi12*-related proto-oncogene in leukemia progression. In one leukemia, CSL13, three loci, *Evi1*, *Evi11/Cb2* and *Evi12* harbor Cas-Br-M provirus, which may imply that indeed three or maybe more genetic defects are required for full leukemic transformation (327).

Interestingly, in 18 of the 26 cases retroviral insertion in only one locus, i.e., *Evi1, Evi11 or Evi12* was observed and in 48 cases we did not identify any retroviral insertion in the loci that we studied. These results suggest that many unknown candidate target genes for Cas-Br-M provirus are still waiting to be discovered in our panel of leukemias. Large-scale isolation of retroviral flanking sequences is currently being carried out in our series of leukemias using inverse PCR procedures. Nucleotide sequence analysis and differential probing to gritted high density filters from a BAC library will be carried out to identify novel common integration sites and new (collaborating) proto-oncogenes. These studies may result in the definition of

complementation groups of transforming genes which may provide insight into the defects that may occur in different signaling pathways leading to full malignant transformation of hematopoietic cells.

CHAPTER 6

ANANDAMIDE, A NATURAL LIGAND FOR THE PERIPHERAL CANNABINOID RECEPTOR IS A NOVEL SYNERGISTIC GROWTH FACTOR FOR HEMATOPOIETIC CELLS.

Peter J.M. Valk, Sandra Verbakel, Yolanda Vankan, Samantha Hol, Shanta Mancham, Rob Ploemacher, Angelique Mayen, Bob Löwenberg and Ruud Delwel.

Blood 90 (4): 1448-1457, 1997

Abstract

We recently demonstrated that the gene encoding the peripheral cannabinoid receptor (*Cb2*) might be a proto-oncogene involved in murine myeloid leukemias. Here we show that *Cb2* may have a role in hematopoietic development. RNase protection analysis revealed that *Cb2* is normally expressed in spleen and thymus. *Cb2* mRNA is also expressed in 45 of 51 cell lines of distinct hematopoietic lineages, i.e., myeloid, macrophage, mast, B-lymphoid, T-lymphoid and erythroid cells. The effect of the fatty acid anandamide, an endogenous ligand for cannabinoid receptors, on primary murine marrow cells and hematopoietic growth factor (HGF)-dependent cell lines was then investigated. *In vitro* colony cultures of normal mouse bone marrow cells showed anandamide to potentiate interleukin-3 (IL-3)-induced colony growth markedly. While HGFs alone stimulate proliferation of the various cell lines in serum-free culture only weakly, anandamide enhances the proliferative response of the cell lines to HGFs profoundly. This was apparent for responses induced by IL-3, granulocyte-macrophage colony-stimulating factor (GM-CSF), granulocyte colony-stimulating factor (G-CSF), and erythropoietin (Epo). Anandamide was already effective at concentrations as low as 0.1 to 0.3 µM and plateau effects were reached at 0.3 to 3 µM. The addition of anandamide as single growth factor had no effect. The costimulatory effect of anandamide was not evident when cells were cultured with fetal calf serum (FCS), suggesting that FCS contains anandamide or another ligand capable of activating the peripheral cannabinoid receptor. Other cannabinoid ligands did not enhance the proliferative responsiveness of hematopoietic cells to HGFs. Transfection experiments of *Cb2* in myeloid 32D cells revealed that anandamide specifically activates proliferation through activation of the peripheral cannabinoid receptor. Anandamide appears a novel and synergistic growth stimulator for hematopoietic cells.

Introduction

Proliferation and differentiation of hematopoietic precursor cells is regulated by hematopoietic growth factors (57, 205). These cytokines bind and activate receptors that belong to the hematopoietin receptor superfamily (21). Receptors of this superfamily are single transmembrane proteins that, upon binding to their specific ligands, form heterodimeric or homodimeric complexes (21). Ligands that bind hematopoietin receptors are small glycoproteins, e.g. IL-3, GM-CSF, G-CSF, Epo or monocyte colony stimulating factor (M-CSF). Another family of surface membrane receptors are the G-protein-coupled receptors (GPCRs) (116, 269). This superfamily of receptor molecules is characterized by seven hydrophobic stretches of 20 to 25 amino acids that form seven transmembrane-helices connected by alternating extracellular and intracellular loops. Up to now, more than 300 GPCRs have been iden-

tified (116, 269). In contrast to receptors of the hematopoietin family, GPCRs are in most cases not activated by glycoproteins. Ligands of heptahelical GPCRs include amines, amino acids, peptides or proteins, nucleosides or nucleotides, fatty acid derivates, and phospholipid derivates (116, 269). Little is known about the role of GPCRs in hematopoietic growth and development. We recently identified the peripheral cannabinoid receptor (*Cb2*), which encodes a GPCR, in a common ecotropic virus integration site (*Evi11*) (222, 315). *In vitro* transfection studies in 32D cells supported the hypothesis that *Cb2* is a proto-oncogene that is involved in leukemogenesis ((315) and data not shown).
In the present study we investigated by RNase protection analysis the expression pattern of the *Cb2* gene in comparison to the gene that encodes the central cannabinoid receptor (*Cb1*) (106, 198) in different murine tissues and a panel of murine hematopoietic cell lines. We demonstrate that *Cb2* encodes a hematopoietic receptor that is expressed in myeloid, macrophage, erythroid, lymphoid and mast cells. In contrast, *Cb1* is mainly expressed in brain and in testis (106, 198). The effects of the fatty acid N-arachidonylethanolamide or anandamide, an endogenous ligand for cannabinoid receptors, on the proliferative abilities of HGF-dependent hematopoietic cell lines were investigated.
The results of this study demonstrate that anandamide is a ligand which stimulates proliferation of hematopoietic cell lines in synergy with IL3, Epo, GM-CSF and G-CSF under serum-free conditions.

Materials and Methods

Mouse hematopoietic cell lines - A list of murine hematopoietic cell lines used in this study is presented in Table 1. Macrophage cell lines were cultured in Dulbecco's modified Eagles Medium (Gibco, Ghent, Belgium) plus supplements (100 IU/ml penicillin, 100 ng/ml streptomycin, and 10% fetal calf serum (FCS)). The other cell lines were cultured in RPMI1640 medium plus supplements. Myeloid cell lines were cultured with 10 ng murine IL-3 and CTLL cells with 10 IU/ml IL-2 (Cetus, Emmeryville, CA). The pro-B-cell line BAF3 and myeloid 32D cell line both transfected with the human G-CSF receptor gene (BAF-G and 32D(G-CSF-R), respectively) were donated by Dr. I.P. Touw (Erasmus University Rotterdam, The Netherlands, (83)).

RNA isolation - Mouse tissues were homogenized using a Ultratarax T25 shearing device (IKA Labortechnique, Heiterheim, Germany). Total RNA was extracted from murine hematopoietic cell lines with guanidinium thiocyanate followed by phenol extraction (267). Dr. J. Cleveland (St. Judes Children Hospital, Memphis, TN) kindly donated RNA samples of several cell lines.

(A) *Cb2*$^{+}$/*Cb1*$^{-}$

Myeloid	Ref.	Macrophage	Ref.
32D	(114)	RAW 264.7	(256)
32Dcl3	(206)	RAW 309.	(256)
DA-1	(136)	WR19M.1	(256)
DA-3	(136)	Pu5-1.8	(255)
DA-13	(136)	J774	(254)
DA-24	(136)	WEHI 3	(330)
DA-28	(136)		
DA-29	(136)	**Erythroid**	
DA-31	(136)	RED5	(119)
DA-33	(136)	RED8	(119)
NFS-22	(126)	32D-Epo	(206)
NFS-36	(126)		
NFS-56	(126)	**B-Lymphoid**	
NFS-58	(126)	DA-25	(136)
NFS-60	(126)	WEHI 231	(173)
NFS-61	(126)	WEHI 279	(329)
NFS-78	(126)	BAF3	(236)
NFS-107	(126)	DA-8	(136)
NFS-124	(126)		
BXH2-43	(46)	**T-lymphoid**	
BXH2-115	(46)	DA-2	(136)
14-122	(310)	RL12	(73)
C6	(11)	WEHI 22	(121)
RMB1	(70)		
RMB3	(180)	**Mast cells**	
ABPL-4	(88,X)	ABFTL-1	(246)
		ABFTL-2	(246)

(B) *Cb2*$^{-}$/*Cb1*$^{-}$

Myeloid		Macrophage	
M1	(131)	P388-D1	(163)
14-166	(310)		
14-259	(310)	**T-lymphoid**	
		EL4	(281)

(C) *Cb2*$^{-}$/*Cb1*$^{+}$

T-lymphoid	
CTLL	(108)

Table 1: *Cb2* and *Cb1* mRNA expression in hematopoietic cell lines.
Cb2 and *Cb1* mRNA expression was determined by RNase protection (Figure 2) and references are the original reports describing the cell lines.

RNase protection - RNase protection was performed as described previously (267). Fragments were cloned into pBluescript II SK+ and linearized using the proper enzymes, and RNA probes were synthesized using T_3 or T_7 polymerase. For each incubation 10 µg of RNA and radiolabeled RNA probe (15.000 cpm) were suspended in 30 µl hybridization buffer (80% deionized formamid, 40mM piperazine-N,N'-bis(2-ethanesulfonic acid) (PIPES; pH 6.4), 0.4M sodium acetate, 1mM EDTA). The samples were heated to 85°C for 5 minutes and then incubated for 16 hours at an annealing temperature of 50°C. To these mixtures, 300 µl RNase digestion buffer (10 mM Tris-HCl (pH7.5), 5mM EDTA, 200 mM sodium acetate and 1 Unit RNase One (Promega, Leiden, The Netherlands) were added. After 1 hour at 37°C, the reaction was stopped by the addition of 3.3 µl 10% SDS and 20 µg carrier tRNA. The reaction products were precipitated with ethanol, fractionated by electrophoresis in a 6% polyacrylamide/7M urea gel, and analyzed by autoradiography. A radiolabelled *GAPDH* RNA fragment was used as a control (142).

Serum-free culture medium - A serum-free culture medium was used to study responses to HGFs and cannabinoid ligands (247, 248, 266). Iscove's modified Dulbecco's medium (Gibco, Ghent, Belgium) was supplemented with 15mg/ml bovine serum albumin (Cohn fraction V, Sigma, Bornem, Belgium), 10^{-7} M sodium selenite (Merck, Darmstad, Germany), $7.7x10^{-6}$ M iron-saturated human transferrin (Behring Institute, Marburg, Germany), 7.8 µg/ml cholesterol (Sigma), and 2.8 µg/ml linoleic acid (Merck). In normal bone marrow colony cultures 10ng/ml insulin (Sigma), 10^{-4} M β-mercaptoethanol (Merck), and 50 µg/ml of the nucleosides, adenosine, thymidine, guanosine, cytidine, uridine, 2'deoxycytidine, 2'deoxy-adenosine and 2'deoxyguanosine (Sigma) were added to the culture medium.

Hematopoietic growth factors and cannabinoid ligands - IL-3 (10 ng/ml) (donated by Dr. J.N. Ihle (St Jude Children's Research Hospital, Memphis, TN), G-CSF (100 ng/ml) (Amgen, Thousand Oaks, CA), GM-CSF (50 ng/ml) (Genetics Institute, Cambridge, MA) and Epo (2 IU/ml) (Boehringer Mannheim, Mannheim, Germany) were added to the cultures at optimal concentrations, which had been determined with normal bone marrow colony cultures (247, 248). Cannabinoid ligands included anandamide, Δ^8-tetrahydrocannabinol (Δ^8-THC), WIN55212-2, cannabinol and cannabidiol (Sigma, Bornem, Belgium) and CP55,940 (Pfizer, Groton, CT). They were added at final concentrations between 0.1 to 10 µM.

Tritiated thymidine (^{3}H-TdR) incorporation - DNA synthesis was measured essentially as described (266). Five thousand cells from various cell lines were cultured in 100 µl serum-free medium, with or without the addition of HGFs or cannabinoid ligands in 96-well round-bottom microtiter trays (Greiner Nurtingen, Germany) for 90 hours. Four hours before harvesting, 0.1 µCi tritiated thymidine (2 Ci/mmol ^{3}H-TdR; Amersham International, Amersham, UK) was added. Cells were

harvested on nitrocellulose using a filtermate 196 harvester (Packerd Instrument Co, Meriden, CT). Radioactivity was determined with a Topcount, microscintillation counter (Packerd).

Colony formation by normal mouse bone marrow - Normal bone marrow cells isolated from femora and tibiae from BCBA mice were collected in Hank's Balanced Salt Solution. Fifty thousand cells were cultured in 1 ml serum-free medium with 1.2% methylcellulose. Dishes were incubated with or without 10 ng/ml IL-3 in the presence or absence of 10 µM anandamide at 37°C and 100% humidity and 5% CO_2. Colonies containing 50 cells or more were scored at day 14.

Results

***Cb2* and *Cb1* mRNA expression in murine tissues** - The expression of *Cb2* and *Cb1* transcripts in murine tissues was determined by RNase protection (Figure 1B). Using *Cb2* cDNA probe I (Figure 1A), an expected mRNA fragment of 185bp was protected in spleen, thymus and heart (Figure 1B). No *Cb2* transcripts were identified in any of the other tissues examined. RNase protection experiments using a 460-bp *Cb1* probe (Figure 1A), demonstrated *Cb1* transcripts in brain and to a lesser extent in testis (Figure 1B). No detectable levels of *Cb1* mRNA were identified in any of the other organs investigated.

***Cb2* and *Cb1* mRNA expression in murine hematopoietic cell lines** - To examine in which hematopoietic lineages the *Cb2* gene may be expressed, RNase protection experiments were carried out using mRNA samples from a large panel of murine hematopoietic cell lines (see the Materials and Methods). Using a 187-bp *Cb2* cDNA fragment representing exon-1 (137 bp) and exon-2 (50 bp; Figure 1A), *Cb2* transcripts of the correct size were identified in 26 of 29 myeloid, 6 of 7 macrophage, 5 of 5 B-lymphoid, 3 of 5 T-lymphoid, 2 of 2 mast cell lines and, 3 of 3 erythroid cell lines (Table 1). An example of an RNase protection experiment is presented in Figure 2. Interestingly, a 460-bp *Cb1* transcript was demonstrated in a murine CTLL cell line (Figure 2 and Table 1). In the CTLL cell line no *Cb2* transcripts were identified (Figure 2). No detectable *Cb1* mRNA levels were found in any of the other cell lines (Figure 2 and Table 1). No *Cb1* or *Cb2* transcripts were found in 3 myeloid, 1 macrophage, and 1 T-lymphoid cell line. These results demonstrate that the peripheral cannabinoid receptor is a blood cell receptor that may be expressed in all hematopoietic lineages. The central cannabinoid receptor is only incidentally expressed in hematopoietic cell lines.

Anandamide potentiates the proliferative response of myeloid cells to IL-3 - The effect of a natural ligand of cannabinoid receptors, anandamide, on the proliferation

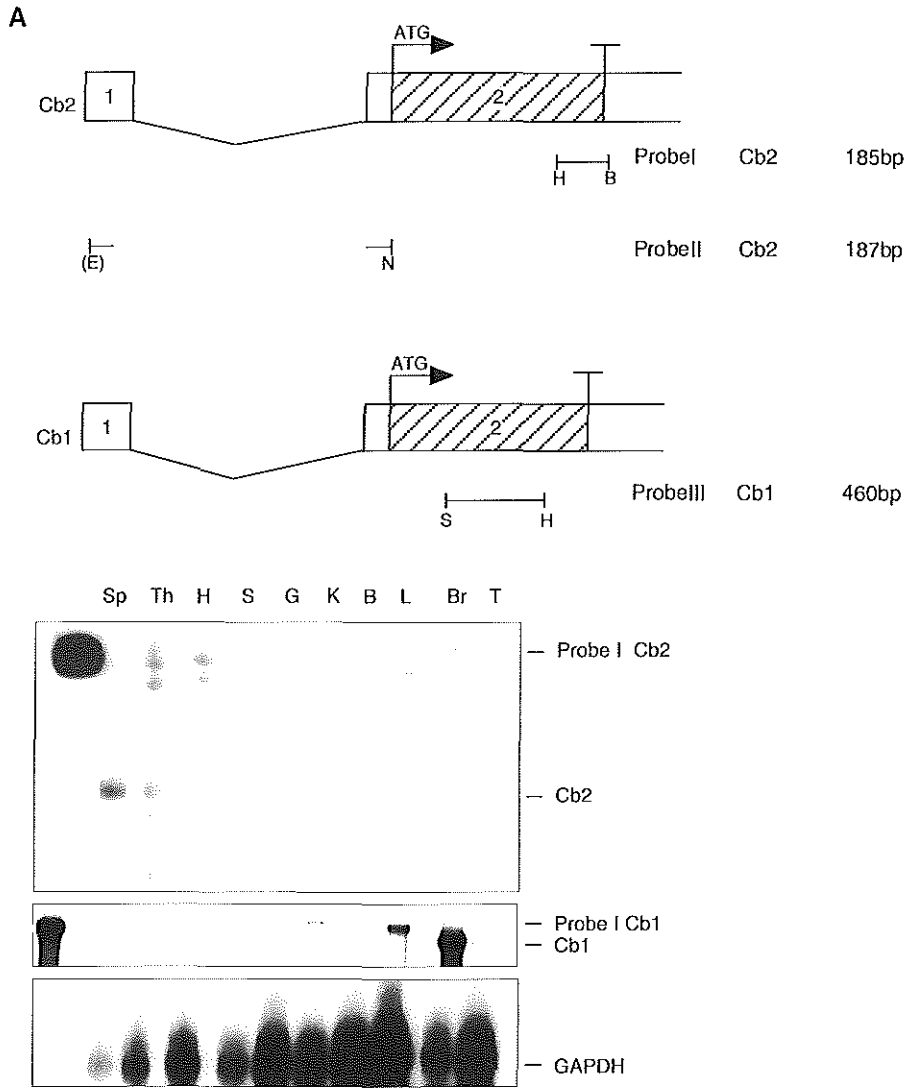

Figure 1: *Cb2* and *Cb1* mRNA expression in murine organ tissues.
A. Schematic representation of murine *Cb2* and *Cb1* mRNA (noncoding exon 1 and protein-coding exon 2) and the cDNA probes used for RNase protection experiments. The shaded boxes represent open reading frames. H: *Hin*cII; B: *Bam*HI; S: *Stu*I; N: *Nco*I; (E): *Eco*RI in vector.
B. RNase protection analysis on 10 µg total RNA of different mouse organs using *Cb2* probe I and *Cb1* probe I (See panel A). The protected fragments were 185 bp (*Cb2*) and 460 bp (*Cb1*). Sp:Spleen; Th:Thymus; H:Heart; S:Stomach; G:Gut; K:Kidney; B:Bladder; L:Liver; Br:Brain; T:Testis.

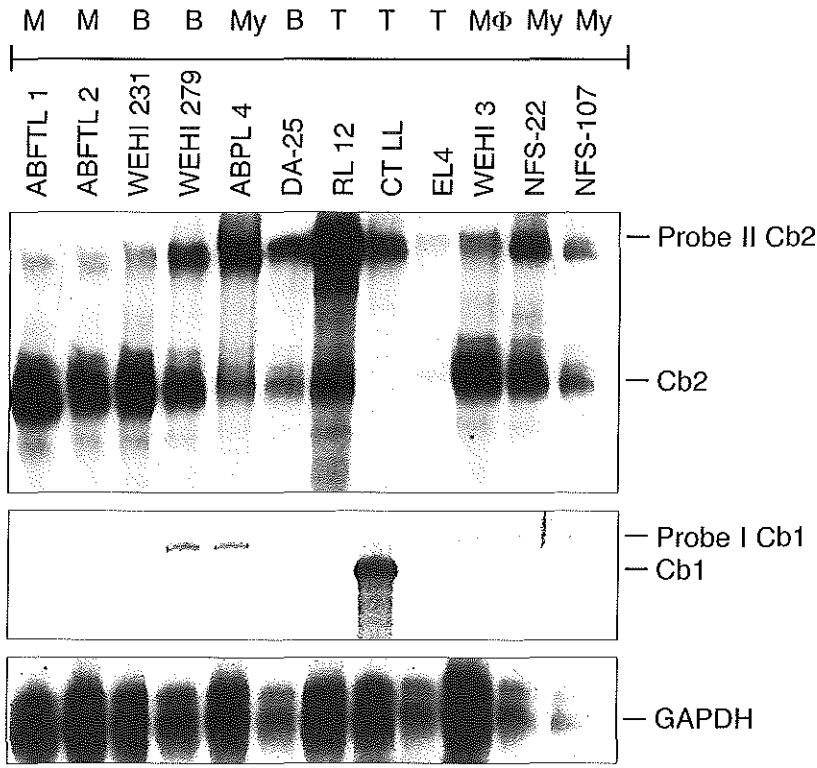

Figure 2: *Cb2* and *Cb1* mRNA expression in murine hematopoietic cell lines.
RNase protection on 10 µg total RNA of different murine hematopoietic cell lines, using *Cb2* probe II and *Cb1* probe I (see Figure 1A). The hematopoietic phenotype of the cell lines is indicated at the top of the figure. M:Mast cell; B:B-lymphoid; My: Myeloid; T:T-lymphoid; MΦ: Macrophage.

of an IL-3-dependent myeloid cell line 32Dcl3 was studied *in vitro*. When cultured with FCS, anandamide did not alter IL-3-induced proliferation of 32D cells (Figure 3A). However, in serum-free medium anandamide significantly enhanced the proliferative response of 32D cells to IL-3 (Figure 3B). Anandamide as a single factor did not induce a measurable proliferative effect in 32Dcl3 cells. Tritiated thymidine incorporation (^{3}H-TdR) demonstrated that as little as 0.1 to 0.3 µM anandamide was sufficient to augment DNA synthesis in synergy with IL-3 in 32Dcl3, NFS-60, and NFS-78 cells (Figure 4). The maximal stimulative effect was reached at concentration 0.3 to 3 µM anandamide. ^{3}H-TdR experiments with other IL-3-dependent myeloid cell lines, i.e., DA-13, DA-28, DA-29, DA-31, NFS-36, NFS-56, and NFS-107, showed similar synergistic dose-response relationships between IL-3 and anandamide (data not shown).

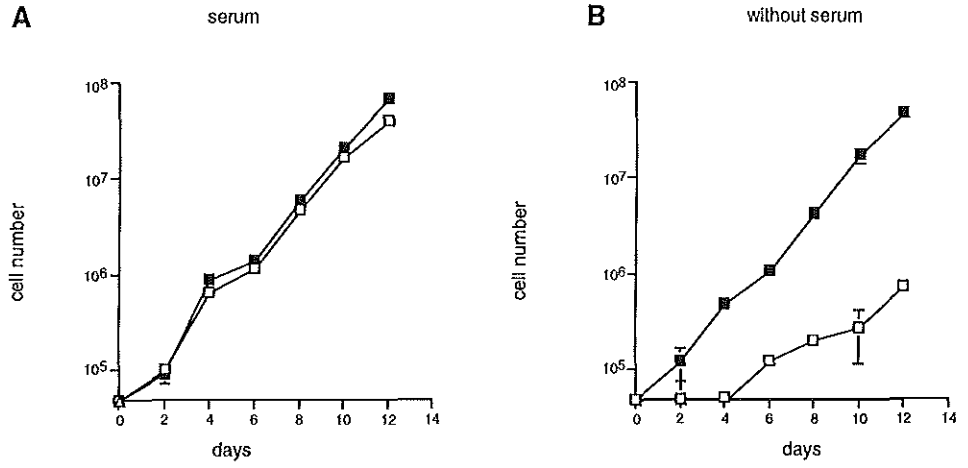

Figure 3: The effect of anandamide on the proliferation of the myeloid cell line 32Dcl3. Growth curves of 32Dcl3 cells cultured in the presence of fetal calf serum (A) or serum-free (B). Cells were cultured with no stimulus (-O-), with 10 μM anandamide alone (-Δ-), with 10 ng/ml IL-3 alone (-□-), or with IL-3 plus anandamide (-■-). Mean cell numbers (±1xSD) of triplicate experiments are plotted against number of days in culture. The doubling time in serum-free culture without anandamide was 75 hours and with anandamide 29 hours. ^{3}H-TdR incorporation data (cpm ±1xSD) of 32Dcl3 cells cultured in serum containing medium (C) or in serum-free medium (SFM) (D).

Anandamide enhances colony growth of normal bone marrow progenitors induced with IL-3 - Normal mouse bone marrow colony cultures were performed to investigate whether anandamide enhances IL-3-stimulated colony growth. In two independent experiments, a twofold elevation of colony formation was observed when the cells were cultured with IL-3 plus anandamide as compared to IL-3 alone (Table 2). Anandamide not only increased colony numbers, but also showed an effect on the size of the colonies (Figure 5). More colonies containing 250 cells or more

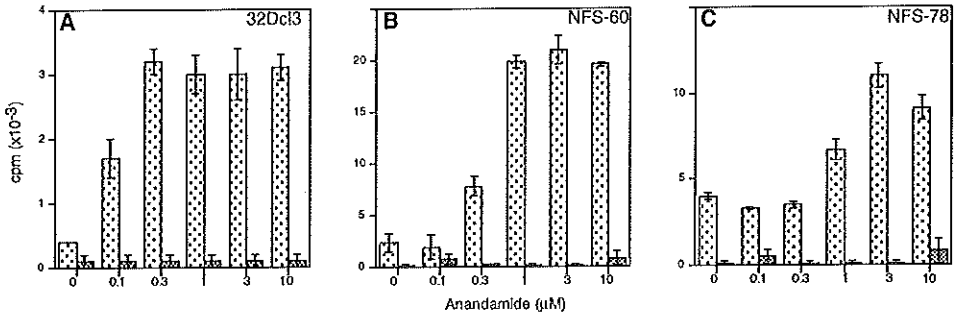

Figure 4: The effects of different concentrations of anandamide on IL-3-induced ^{3}H-TdR incorporation of three murine myeloid cell lines.
Cells of 32Dcl3 (A), NFS-60 (B), and NFS-78 (C) were cultured with titrated concentrations of anandamide (0-10μM) in the presence (10 ng/ml, □) or absence of IL-3 (■). The mean values ±1xSD (cpm x10^{-3}) of triplicate experiments are shown.

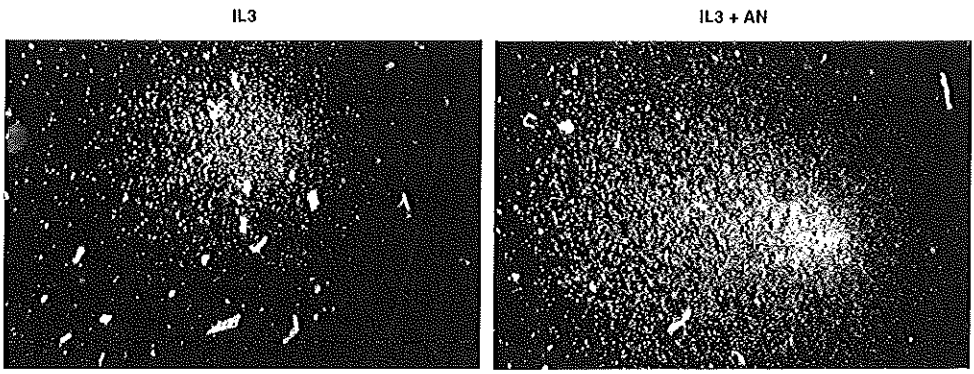

Figure 5: Effect of anandamide on the size of IL-3-induced normal bone marrow colonies.
Examples of representative IL-3-induced normal bone marrow colonies after 14 days of culture with (IL-3+AN) or without anandamide (IL-3).

were found in cultures with IL-3 plus anandamide. Mega-size colonies of 1,000 cells or more were found in IL-3 plus anandamide cultures, but none in colony cultures with IL-3 alone.

Stimulus	CFU-C per 10^5 cells			
	Exp. 1		Exp.2	
	>50 cells	>250 cells	>50 cells	>250 cells
No	0	0	0	0
AN	0	0	0	0
IL-3	20	6	37 ±8	11 ±4
IL-3 + AN	37	17	47 ±7	23 ±5

Table 2: Effect of anandamide on IL-3-stimulated colony formation of normal murine bone marrow CFU-C (day 14). In experiment 1 mean colony numbers of duplicate experiments and in experiment 2 the mean and SD of quaduplicate CFU-C counts are shown. Abbreviations: No: No stimulus; AN: 10 µM anandamide; IL-3: 10 ng/ml IL-3).

Effects of different cannabinoid ligands on IL-3-induced proliferation of myeloid cells- To investigate whether various synthetic molecules all capable of binding cannabinoid receptors would be capable of enhancing the proliferative effects of IL-3, 32Dcl3 cells were cultured with IL-3 plus the cannabinoid agonists CP55,940, WIN55212-2, Δ^8-THC, cannabinol and cannabidiol. While DNA synthesis of 32Dcl3 cells was augmented significantly when costimulated with IL-3 and anandamide, no enhancement of thymidine uptake was apparent when 32Dcl3 cells were stimulated with IL-3 plus any of the other cannabinoid ligands (Figure 6).

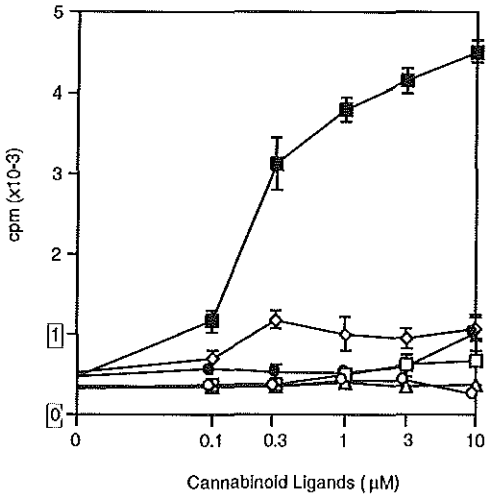

Figure 6: Dose effects of anandamide and other cannabinoid ligands on IL-3-induced ^{3}H-TdR incorporation of 32Dcl3 cells.
Cells were cultured serum-free with IL-3 (10 ng/ml) and titrated concentrations (0 to 10 µM) of anandamide (-■-), WIN55212-2 (-O-), Δ^8-THC (-□-), cannabinol (-●-), cannabidiol (-Δ-), and CP55,940 (-◊-).

Anandamide enhances DNA synthesis of hematopoietic cell lines in synergy with GM-CSF, Epo and G-CSF- ^{3}H-TdR incorporation experiments were carried out with three selected GM-CSF-responsive (NFS-36), Epo-responsive (32D-Epo) and G-CSF-responsive (BAF-G) cell lines to investigate whether anandamide would potentiate proliferation in synergy with hematopoietic growth factors other than IL-3. NFS-36 cells showed a weak response to GM-CSF alone or anandamide alone, but a significant increase of thymidine incorporation was evident when both ligands were added (Figure 7A). 32D cells cultured with Epo alone, i.e., in the absence of anandamide, did not stimulate DNA synthesis at all. 32D-Epo cells became - responsive to Epo in the presence of anandamide (Figure 7B). Finally, while G-CSF stimulated some DNA synthesis of BAF-G cells, anandamide supplemented to the culture medium augmented the G-CSF effect by twofold (Figure 7C). These experiments indicate that anandamide may enhance the stimulative activity of various HGFs.

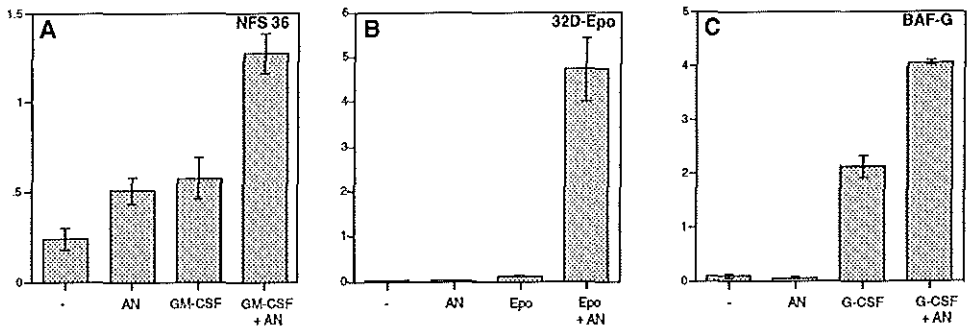

Figure 7: Synergistic activity of anandamide on GM-CSF-, Epo- or G-CSF-stimulated thymidine incorporation.
Cells were cultured with optimal concentrations of GM-CSF (50 ng/ml; **A.** NFS-36); Epo (2 IU/ml; **B.** 32D-Epo) or G-CSF (100 ng/ml; **C.** BAF-G) in the presence of 10 µM anandamide (AN). The mean values ±1xSD (cpm x10^{-3}) of triplicate experiments are shown.

Effects of anandamide and other cannabinoid ligands on *Cb2* overexpressing myeloid cells - To verify whether the stimulatory effect of anandamide is mediated through activation of the peripheral cannabinoid receptor, we overexpressed *Cb2* cDNA in 32D cells which express the G-CSF receptor (G-CSF-R), but do not respond to G-CSF (data not shown). *Cb2* transfected cells show high tritiated thymidine incorporation when cultured with G-CSF plus anandamide (Figure 8A). In comparison, anandamide alone or G-CSF alone did not induce DNA synthesis. Furthermore, anandamide plus G-CSF did not induce proliferation in control vector-

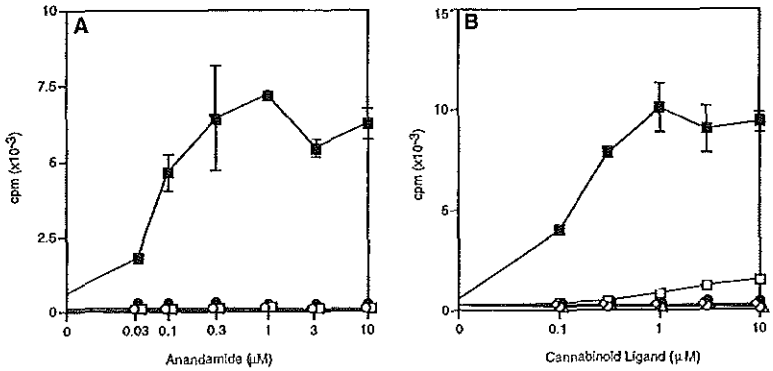

Figure 8: Effects of anandamide and other cannabinoid ligands on G-CSF-induced thymidine incorporation of *Cb2* transfected 32D/G-CSF-R cells.
A. 32D/G-CSF-R was transfected with *Cb2* cDNA (32D/G-CSF-R/*Cb2*) or with pBabe control vector (32D/G-CSF-R/pB). Cells were cultured without G-CSF with different concentrations anandamide (-O-, 32D/G-CSF-R/pB); (-●-, 32D/G-CSF-R/*Cb2*), or with G-CSF plus anandamide (-□-, 32D/G-CSF-R/pB); (-■-, 32D/G-CSF-R/*Cb2*).
B. 32D/G-CSF-R-*Cb2* cells were cultured with G-CSF plus different concentrations of the distinct cannabinoid ligands, anandamide (-■-), WIN55212-2 (-O-), Δ^8-THC (-□-), cannabinol (-●-), cannabidiol (-Δ-), and CP55,940 (-◊-).

transfected 32D(G-CSF-R) cells. These data indicate that anandamide stimulates DNA synthesis after the specific activation of *Cb2*. In addition, ^{3}H-TdR incorporation experiments using various concentrations of the other cannabinoid ligands showed that DNA synthesis of 32D(G-CSF-R/*Cb2*) cells was not influenced by any of the other ligands (Figure 8B). Anandamide is apparently selectively capable of stimulating hematopoietic cells through activation of the peripheral cannabinoid receptor among several cannabinoid ligands.

Discussion

In this study we demonstrate that the gene encoding the peripheral cannabinoid receptor is expressed in hematopoietic cells and appears important for the efficiency of stimulation of growth by a variety of HGFs.
Several studies had previously demonstrated the presence of cannabinoid binding sites on hematopoietic cells (43, 154, 190), but these studies had not distinguished between the central and the peripheral cannabinoid receptor. *Cb2* expression was demonstrated in spleen and in thymus. The *Cb2* mRNA expression in heart tissue might be the result of residual blood that was not eliminated before extraction. Others

demonstrated *Cb2* mRNA expression in spleen, in the myeloid cell line HL60 and in mast cell lines (94, 222). We show here that *Cb2* may be expressed in myeloid, erythroid, B-lymphoid, T-lymphoid, macrophage, and mast cells. This indicates that *Cb2* encodes a hematopoietic receptor that may have a function in a broad scala of hematopoietic lineages. By applying RT-PCR several groups demonstrated *Cb1* transcripts in hematopoietic cells (43, 65, 154, 272). RNase protection studies presented here show that *Cb1* could be detected in brain and testis but not in spleen and thymus. Futhermore, *Cb1* could be detected in 1 out of 51 cell lines only. These data suggest that *Cb1* may occasionally be expressed in hematopoietic cells, whereas *Cb2* is commonly expressed. These results enforce the notion that *Cb2* rather than *Cb1* encodes a hematopoietic cannabinoid receptor.

In vitro studies with murine hematopoietic cell lines and normal bone marrow precursors demonstrated that the peripheral cannabinoid receptor has a function in the regulation of proliferation by HGFs. Stimulatory effects of anandamide on hematopoietic cell proliferation had not been reported. Anandamide enhanced the cellular proliferation induced with IL-3, GM-CSF, G-CSF and Epo when the cells were cultured in serum-free medium. Whether anandamide synergizes with other cytokines remains open to future investigation. Most of the cell lines analysed for *Cb2* mRNA expression in this study are HGF independent and therefore did not allow for an extended analysis of the stimulative effects of anandamide with other HGFs. Interestingly, however, when a panel of HGF independent cell lines were cultured in a serum-free medium, i.e., DA-2 (T-Lymphoid), DA-25 (B-Lymphoid), RED-5 (Erythroid) and, J774 cells (Macrophage), anandamide was required to induce proliferation *in vitro* (data not shown). This indicates that the *Cb2* may have a role in stimulation of growth of several, if not all, hematopoietic lineages. An important modification of the culture conditions used in this study is the elimination of FCS and the use of a serum-free culture system. The effects of anandamide are not evident when cells are cultured with FCS and therefore other investigators may have missed the effects of anandamide stimulation. The results of this study would suggest that anandamide or another ligand for the cannabinoid receptor is present in FCS. In fact, four other fatty acids have recently been identified to bind and activate cannabinoid receptors (14, 94, 179). The role and presence of anandamide or any of these fatty acids may explain at least in part the serum dependence of various hematopoietic cell lines and primary hematopoietic cells. The *in vitro* experiments show that among a selected number of cannabinoid ligands studied, only anandamide was capable of stimulating the proliferation of hematopoietic cells synergistically with HGFs. This is remarkable, since according to other investigators, WIN55212-2, CP55,940, and THC bind and activate the peripheral cannabinoid receptors more efficiently than anandamide (222, 284, 294). Our findings thus suggest strongly that in hematopoietic cells anandamide acts as the most potent agonist through the latter receptors. Up to 1 to 10 µM Anandamide was needed for optimal activation of proliferation, which is within the concentration range required for optimal binding (65, 94, 190, 222, 272). The

transfection studies of *Cb2* (Figure 8) confirm that anandamide specifically activates proliferation of 32D(G-CSF-R/*Cb2*) cells through activation of the peripheral cannabinoid receptor. In contrast, the other cannabinoid ligands fail to stimulate these *Cb2* transfected cells. In fact, when cultured with serum, the other cannabinoid receptor ligands inhibit proliferation (data not shown). Because the cannabinoid agonists CP55,940 and THC have been shown to stimulate an additional nonreceptor-mediated signal transduction pathway (100), it is perhaps possible that the alternative nonreceptor mediated signals suppress proliferation. In any case, the current available data would suggest that only anandamide is capable of stimulating proliferation synergistically with HGFs. Whether the other fatty acids are capable of stimulating proliferation will be investigated.

We have recently identified the *Cb2* gene in a common virus integration site (*Evi11*) (315) and *Cb2* was suggested to be a proto-oncogene. Transfection of *Cb2* in 32D(G-CSF-R) cells generated G-CSF-dependent cell lines that could be maintained serum-free when cultured with anandamide. The studies presented here show that activation of the *Cb2* receptor has a profound effect on the proliferation of cells. This adds further support to the notion that this receptor, when aberrantly expressed, may alter the proliferative response of hematopoietic cells and contributes to the development of leukemia. *Cb2* transgenic animals are currently being studied to investigate whether abnormal *Cb2* expression might contribute to the development of leukemia *in vivo*.

Cb2 receptor-mediated signal transduction by anandamide has been observed by others (284). How activated cannabinoid receptors may stimulate proliferation synergistically with HGFs is unresolved. The costimulatory effects may occur at different levels of HGF receptor signaling. Stimulation of the peripheral cannabinoid receptor may have the following effects: (1) transactivation of the HGF receptors, (2) potentiation of HGF receptor-mediated signal transduction, e.g., JAK/STAT or the $p21^{ras}$/MAP kinase pathways (17, 233, 308), and (3) activation of signalling pathways that, in parallel with the HGF receptor signaling routes, enhance cell cycling. In fact, examples in support of each of those possibilities exist for other seven transmembrane receptors (40-42, 67, 155, 193, 284, 319, 331). Whether these alternative mechanisms are activated by *Cb2* requires verification in future studies.

The results presented in Table 2 and Figure 5 show that the synergism between IL-3 and anandamide is also evident in normal bone marrow colony formation. A greater number of IL-3-dependent colonies were formed in the presence of anandamide. These results indicate that in the presence of anandamide, IL-3 stimulates the - outgrowth of additional populations of precursor cells. IL-3 plus anandamide also stimulated colonies of greater size, which would indicate that the combination of the two factors augments the production of progeny from individual precursor cells as well. Whether anandamide synergizes with other HGFs in the stimulation of normal marrow precursor cells, is currently under investigation.

CHAPTER 7

ENHANCEMENT OF PROLIFERATION OF EPO-STIMULATED CELLS BY ANANDAMIDE CORRELATES WITH INCREASED ACTIVATION OF THE MITOGEN-ACTIVATED PROTEIN KINASES ERK1 AND ERK2.

Peter J.M. Valk, Sandra Verbakel, Marieke von Lindern, Bob Löwenberg and Ruud Delwel.

Submitted

Abstract

Recently we demonstrated that anandamide, an endogenous ligand for the cannabinoid receptors Cb1 and Cb2, is able to synergistically stimulate proliferation of hematopoietic growth factor (HGF)-dependent blood cells in serum-free culture. To further elucidate the mechanisms by which anandamide enhances the proliferative responses of hematopoietic cells we investigated the anandamide-mediated effects on proliferation, cell cycling, apoptosis and intracellular signaling of eryhropoietin (Epo)-stimulated 32D/Epo cells. Simultaneous addition of Epo and anandamide enhanced DNA-synthesis and increased cell numbers of 32D/Epo cells in serum-free culture. Interestingly, anandamide did not only alter the G1/S transition of the cell cycle, but it accelerated each of the successive cell cycle phases of Epo-stimulated 32D/Epo cells. Apoptosis analysis showed that the percentages of apoptotic 32D/Epo cells were equally low in Epo- or Epo and anandamide-stimulated cultures. The enhanced activation of the mitogen-activated protein kinases (MAPKs), ERK1 and ERK2, as well as the MAPK-target gene protein c-Fos, fully correlated with the synergistic stimulation of proliferation of 32D/Epo cells by anandamide. Anandamide had no effect on Epo-induced STAT-5 activation of 32D/Epo cells. Experiments with the Cb2 receptor-specific antagonist SR144528 demonstrated that the synergistic stimulation of proliferation by anandamide was partially Cb2 receptor-mediated. Together, these data suggest that the positive effects of anandamide on the Epo-induced proliferation of 32D/Epo cells are mediated by receptor-dependent as well as receptor-independent mechanisms, both involving activation of the MAPKs, ERK1 and ERK2.

Introduction

Proliferation and differentiation of hematopoietic progenitor cells is stimulated by hematopoietic growth factors (HGFs). HGFs stimulate blood cells following binding and activation of specific HGF receptors on the surface-membrane of the cells. Many HGFs are able to stimulate proliferation *in vitro* when added as single factors, e.g., interleukin-3 (IL-3), granulocyte-macrophage colony-stimulating factor (GM-CSF) or erythropoietin (Epo). However, other regulators are not capable of stimulating proliferation independently. These peptides, like e.g. SCF, enhance the proliferative effects induced by other HGFs. For instance, Epo is capable of stimulating proliferation and maturation of Epo-receptor expressing cells (165). However, a marked synergistic proliferation is apparent when the cells are exposed to a combination of Epo and stem cell factor (SCF) (303). Recently, we (314) and others (76) demonstrated that the fatty acid anandamide, acts similarly as a synergistic growth factor for hematopoietic cells. The growth rate of multiple HGF-dependent cell lines or IL-3-dependent primary bone marrow precursors is significantly

increased by anandamide (314). Anandamide is an endogenous ligand for the peripheral cannabinoid receptor Cb2, a $G\alpha_{i/o}$ protein-coupled receptor (GPCR), which is primarily expressed on hematopoietic cells (314). The stimulation of proliferation by anandamide of hematopoietic cells expressing the Cb2 receptor would suggest that anandamide is an important regulator of hematopoietic proliferation.
To further investigate the mechanism of synergistic proliferation of Epo and anandamide, we used the murine Epo-dependent cell line 32D/Epo (206). Since HGFs stimulate cell proliferation early in the G1 phase of the cell cycle, we first investigated whether anandamide is required for Epo-induced G0/G1 progression and entry into the S-phase of the cell cycle. We present evidence to suggest that anandamide accelerates Epo-induced cell cycling of 32D/Epo cells by shortening all phases of the cell cycle.
After stimulation by Epo, the Epo receptor is tyrosine phosphorylated which leads to activation of several intracellular signaling pathways, e.g., the STAT5 (111) and the Ras/MAPK pathways (210). We demonstrate that addition of anandamide to serum-free cultures of Epo-dependent 32D/Epo cells synergistically stimulates the MAPKs, ERK1 and 2 (ERK1/2), resulting in an increased expression of the ERK1/2 target gene c-*Fos* (107).
Recently, Derocq *et al.* (76) confirmed the enhanced stimulation of proliferation of HGF-dependent cell lines by anandamide. However, the Cb2-specific antagonist SR144528 (261) and the $G\alpha_{i/o}$-inhibitor pertussis toxin did not interfere with the anandamide-mediated effect in the lymphoid B9 cell line (76). These data suggested that anandamide did not act through the Cb2 receptor, but that non-receptor-mediated mechanisms were responsible for the synergistic activity of anandamide on proliferation of the IL-6-dependent B9 cell line. Using the same Cb2-specific antagonist we show here that anandamide stimulates Epo-induced proliferation of 32D/Epo cells through Cb2 receptor-dependent as well as receptor-independent mechanisms.

Materials and methods.

In vitro culture of 32D/Epo cells - 32D/Epo cells (206) were maintained at 37^0C in RPMI 1640 culture medium supplemented with penicillin (100 IU/ml), streptomycin (100 ng/ml), 10% fetal calf serum (FCS) and Epo (1 IU/mL; generous gift from Jansen-Cilag). A serum-free culture system, as described previously (314), was used to study responses of 32D/Epo cells to Epo and cannabinoid ligands. DNA-synthesis was measured by tritiated thymidine (^{3}H-TdR) incorporation exactly as reported previously (314). The effects of Epo and anandamide on the expression and activation of specific proteins was carried out following a starvation procedure. This procedure included an 18-hour (overnight) incubation in serum-free medium with Epo. The cells were washed two times in Hanks balanced salt solution (Gibco-BRL, Breda, The

Netherlands), followed by a four-hour incubation in serum-free medium without any growth factor.

Ligands, antagonists and inhibitors – The cannabinoid receptor ligand anandamide was obtained from Sigma (Zwijndrecht, The Netherlands) and CP 55,940 from Pfizer (Groton, CT). The Cb1- and Cb2-specific antagonists, SR141716 (260) and SR144528 (261), were kindly donated by Dr. Casellas (Sanofi Recherche, Montpellier, France). The MEK-1-specific inhibitor PD98059 was purchased from New England Biolabs, Inc., Beverly, MA.

Northern blot analysis - The polyA$^+$ RNA Northern blot was kindly donated by Dr. J.N. Cleveland at the St. Jude Children's Research Hospital in Memphis, TN. PolyA$^+$ RNA from the cell lines 32D/Epo, BXH2-4S, DA22, DA24 and DA34 was performed as described previously (12). The RNA blots were hybridized with an [^{32}P]dATP-labeled 1.2 kb *Eco*RI-*Bam*HI murine genomic *Cb2* DNA fragment and an α-L-fucosidase cDNA probe (315). Probe labeling, hybridization and washing procedures were identical to those described previously (315).

Western blot analysis and monoclonal antibodies - Following starvation, 10^6 cells/ml were stimulated with ligands at 37 ^{0}C. At different time points the reactions were terminated with ice-cold phosphate buffered saline (PBS) containing 1mM Na_3VO_4. Cells were lysed by incubation at 4^{0}C for 30 minutes in lysis buffer (50mM Tris-HCl pH 8.0, 100mM NaCl, 1% Triton X-100, 0.1mM Na_3VO_4, 1mM DTT and 1% Pefabloc SC, 50µg/ml aprotinin, 50µg/ml leupeptin, 50µg/ml bacitracin, 50µg/ml iodoacetamide as protease inhibitors). Insoluble materials were removed by centrifugaton for 30 minutes at 10.000g at 4^{0}C. Following SDS-polyacrylamide electrophoresis (SDS-PAGE) proteins were electroblotted onto nitrocellulose (0.2µm; Schleiger & Schuell, Dassel, Germany). Filters were blocked by incubation in blocking buffer (Tris-buffered saline (10 mM Tris-HCL pH 7.4, 150 mM NaCl) containing 0.05% Tween-20 (TBST), 0.6% bovine serum albumin (BSA) and 1 mM EDTA) for 1 hour at 37^{0}C, washed in TBST and incubated with antibodies diluted in blocking buffer. The filters were incubated with rabbit polyclonal antibodies. Antibodies directed to phospho-specific ERK1/2 (1:1000 dilution), phospho-specific p38 MAPK (1:500), phospho-specific Jun N-terminal kinase (JNK; 1:1000), and antibodies directed to phosphorylation-state-independent ERK1/2 (1:200), p38 MAPK (1:1000) and JNK (1:1000) were obtained from New England biolabs, Inc, Beverly, UK. Rabbit-anti-mouse c-Fos (dilution 1:200) was purchased from Santa Cruz Biotechnology, Inc, CA. After washing with TBST, immune complexes were detected with horseradish peroxidase (HRP)-conjugated goat-anti-rabbit IgG-specific antiserum (DAKOPATS, Copenhagen, Denmark) in TBS containing 1% milk-powder, followed by enhanced chemiluminescence reaction (DuPont, Boston, MA).

Immunohistochemistry - Immunohistochemistry was carried out on cytocentrifuged 32D/Epo cells. Paraformaldehyde (3.7% in PBS) treated (16 minutes at room temperature) and triton-X-100 (0.5 %) exposed cells (2 minutes at 4^0C) on glass-slides were incubated in PBS (pH7.8) supplemented with 0.05% (v/v) Tween (PBS-Tw) for 15 minutes on ice. Cells were incubated for 30 minutes with rabbit-anti-mouse c-Fos polyclonal antibodies (dilution 1:200; Santa Cruz) at room temperature. During incubations the slides were kept in a moist chamber to prevent air-drying. Following rinsing with PBS-Tw the slides were incubated for 30 minutes at room temperature with HRP-conjugated goat-anti-rabbit antiserum (DAKOPATS), diluted in PBS plus 2% mouse serum. Slides were rinsed in PBS-Tw and binding of the conjugate was visualized by incubation with a diaminobenzidine (DAB; Sigma, St. Louis, USA) solution (1 mg DAB/ml PBS) supplemented with 20µl 1% (v/v) H_2O_2. The cells were embedded in Entallan mounting medium (Merck, FRG) after dehydration and coverslipped.

Apoptosis analysis - Early stages of apoptosis in 32D/Epo cells, were studied by Annexin-V-Fluos (Boehringer Mannheim, Germany) and propidium iodide double-labeling. Following washing in PBS by centrifugation (5 minutes, 200 x g), 10^6 cells were incubated with 20 µl Annexin-V-Fluos labeling solution and 20 µl propidium iodide (50 µg/ml H_2O, in 100 µl HEPES buffer (10 mM Hepes/NaOH pH 7.4, 140 mM NaCl, 5 mM $CaCl_2$). The percentage of early apoptotic cells, i.e., Annexin-V-Fluos$^+$/PI$^-$ cells, was determined by FACSCAN (Becton Dickinson, Mountain View, CA) analysis.

Cell cycle analysis - For flowcytometric analysis of DNA content, cells were collected by centrifugation and resuspended in 0.1% sodium citrate containing 50 µg/ml of propidium iodide. The fluorescence of stained cells was measured using a FACSCAN (Beckton Dickinson). The Cell Fit program was used to determine the percentages of cells in the different phases of the cell cycle.

Electrophoretic mobility shift assay (EMSA) - Nuclei of 2 x 10^6 cells were obtained by lysis in a hypotonic buffer (22 mM HEPES pH 7.8, 20 mM NaF, 1 mM Na_3VO_4, 1mM $Na_4P_2O_7$, 1mM DTT, 1mM EDTA, 1 mM EGTA, 0.2 % Nonidet P40, 0.125 µM okadic acid and the cocktail of protease inhibitors). After cell lysis, nuclei were precipitated by centrifugation at 15.000 g for 30 seconds. Nuclear extracts were prepared using a high-salt buffer (hypotonic buffer with 420 mM NaCl and 20% glycerol). Insoluble materials were removed by centrifugation for 20 minutes at 20.000g at 4 °C. The extracts were incubated at room temperature for 20 minutes with 0.2 ng of ^{32}P-labeled double-stranded STAT-5-binding β-casein (5'-AGATTTC-TAGGAATTCAATCC-3') oligonucleotide and 2 µg of poly(dIdC) in binding buffer (13mM HEPES pH7.8, 80mM NaCl, 3 mM NaF, 3 mM $NaMoO_4$, 1 mM DTT, 0.15 mM EDTA, 0.15 mM EGTA and 8% glycerol). DNA-protein complexes were

separated on 5% non-denaturating polyacrylamide gels in 0.25x TBE and visualized by autoradiography.

Results

Cb2 mRNA expression in 32D/Epo cells – We performed Northern blot analysis to compare the expression levels of *Cb2* mRNA in 32D/Epo cells with other hematopietic cell lines (Figure 1). High level *Cb2* mRNA was demonstrated in polyA$^+$ mRNA samples from 32D/Epo cells, while expression was low or undetectable in other hematopoietic cell lines. α-L-fucosidase mRNA messages were demonstrated in all hematopoietic cell lines. In previous studies we have shown by RNase protection analysis that the 32D/Epo cells do not express *Cb1* mRNA (314).

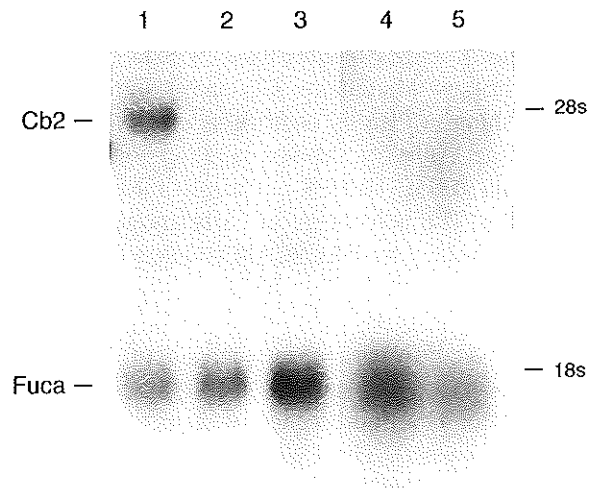

Figure 1: Northern blot analysis of 32D/Epo and other hematopoietic cell lines.
PolyA$^+$ RNA Northern blot analysis of 32D/Epo (1), BXH2-4S (2), DA34 (3), DA24 (4) and DA22 (5). Hybridization signals of the genes encoding the Cb2 receptor (*Cb2*) and α-L-fucosidase (*Fuca*) and the sizes of the 18S and 28S rRNAs are indicated.

Anandamide enhances Epo-induced proliferation of 32D/Epo cells – The *in vitro* studies on the Epo-dependent cell line 32D/Epo were performed in serum-free culture, as the anandamide-mediated stimulatory effect on cell proliferation may be masked in the presence of serum (314). A dose dependent synergistic stimulatory effect of anandamide on Epo-induced DNA-synthesis was observed (Figure 2A). Anandamide at 300 nM added to Epo-containing cultures, was sufficient to enhance

DNA-synthesis. Anandamide as a single stimulus did not induce ^{3}H-TdR uptake. Anandamide also increased 32D/Epo cell numbers *in vitro* during culture with Epo (Figure 2B).

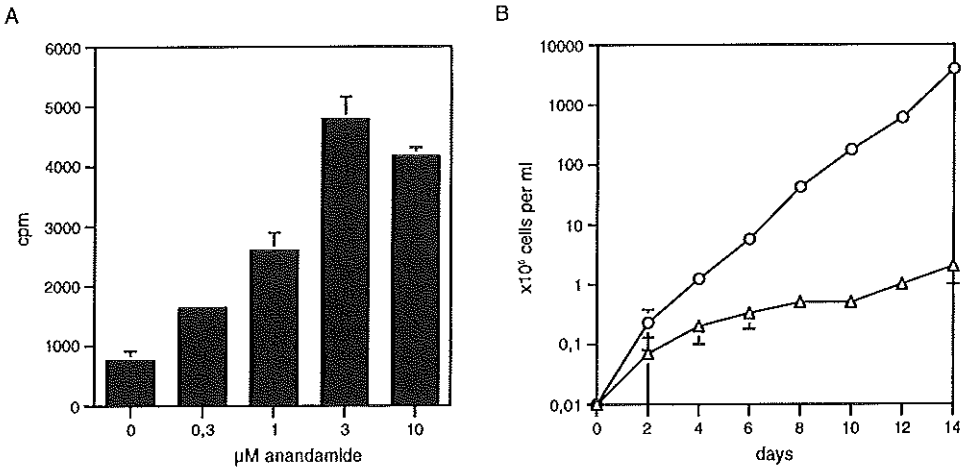

Figure 2: Dose effects of anandamide on ^{3}H-TdR incorporation and increase in cell numbers of the 32D/Epo cell line by anandamide in serum-free culture.
A. Incorporation of ^{3}H-TdR in 32D/Epo cells cultured serum-free with Epo (1 IU/ml) and dose-titrated concentrations of anandamide (0 to 10 μM).
B. The effect of anandamide on cell numbers of the 32D/Epo cell line. Cells were cultured with Epo alone (1 IU/ml) (-Δ-) or with Epo plus anandamide (3 μM) (-O-). 32D/Epo cultures with no factor or anandamide alone extinguished within 24 hours.

Anandamide increases the Epo-induced cell cycle rate of 32D/Epo cells - Since cells arrest in G0/G1 in the absence of mitogenic signaling, we investigated whether 32D/Epo cells were arrested in G0/G1 in the presence of Epo alone and whether anandamide enhanced Epo-induced G1 progression and entry into S-phase. FACSCAN analysis of propidium iodide stained 32D/Epo cells exposed to either Epo or Epo/anandamide after starvation, revealed comparable distributions of cells in G0/G1-, S- or G2/M-phases of the cell cycle in time (Figure 3 and Table 1). Interestingly, however, when after 4 days of culture identical cell numbers were harvested from each fraction and pulse-labeled with ^{3}H-TdR, significantly more radiolabeled thymidine per 10^{4} 32D/Epo cells was incorporated in Epo/anandamide- (5110±415 cpm) versus Epo- (1157±106 cpm) stimulated cultures.
Although cell cycle analysis experiments using propidium iodide did not indicate the presence of high percentages of dead cells in Epo-exposed 32D/Epo cell fractions,

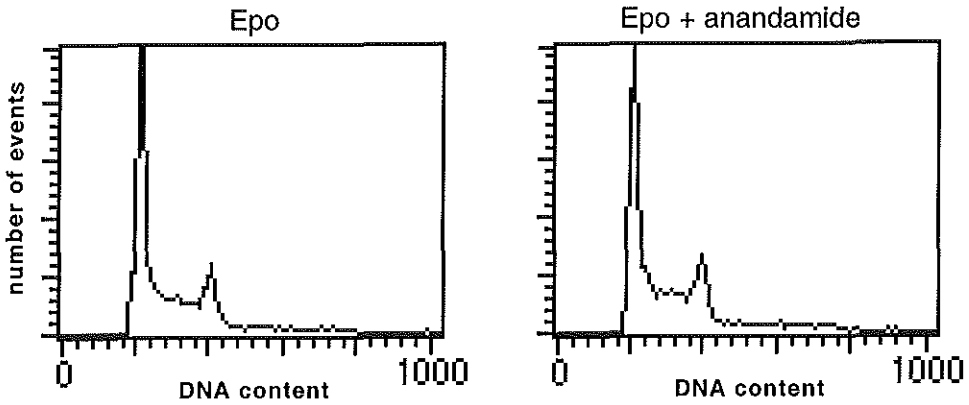

Figure 3: Effects of anandamide on the cell cycle of 32D/Epo cells.
Representative cell cycle profiles (t=124 hours) of 32D/Epo cells cultured serum-free with Epo (1 IU/ml) in the absence (left) or presence (right) of anandamide (3 µM). Percentages of the cells in G0/G1-, S- and G2/M-phases of the cell cycle in time are shown in Table 1.

apoptosis analysis was carried out using Anexin-V-Fluos/propidium iodide double staining and FACS analysis. No significant differences in the percentages of early apoptotic (Annexin-V-Fluos (positve)/propidium-iodide (negative)) cells were apparent at different time points after stimulation (up to 7 days) between Epo- (4.9±2.7%) or Epo/anandamide- (2.5±1.6%) stimulated 32D/Epo cells.

Time (hours)	Epo (%) G0/1	S	G2/M	Epo/anandamide (%) G0/1	S	G2/M
4	34	48	18	34	49	17
18	33	51	16	30	52	18
22	27	54	19	30	56	14
26	30	57	13	27	61	12
42	50	44	6	41	48	11
100	34	58	7	39	50	11

Table 1: Distribution of 32D/Epo cells in G0/1, S and G2/M in the presence of Epo or Epo and anandamide

Epo and anandamide synergistically activate MAPKs ERK1/2 in 32D/Epo cells – The MAPKs ERK1/2 are important transducers of mitogenic signals (274). To investigate the importance of ERK1/2 in the proliferative response of 32D/Epo cells, we examined the effect of the MEK1/2 inhibitor PD98059 on Epo- and Epo/anandamide-stimulated DNA-synthesis. PD98059 dose-dependently inhibited

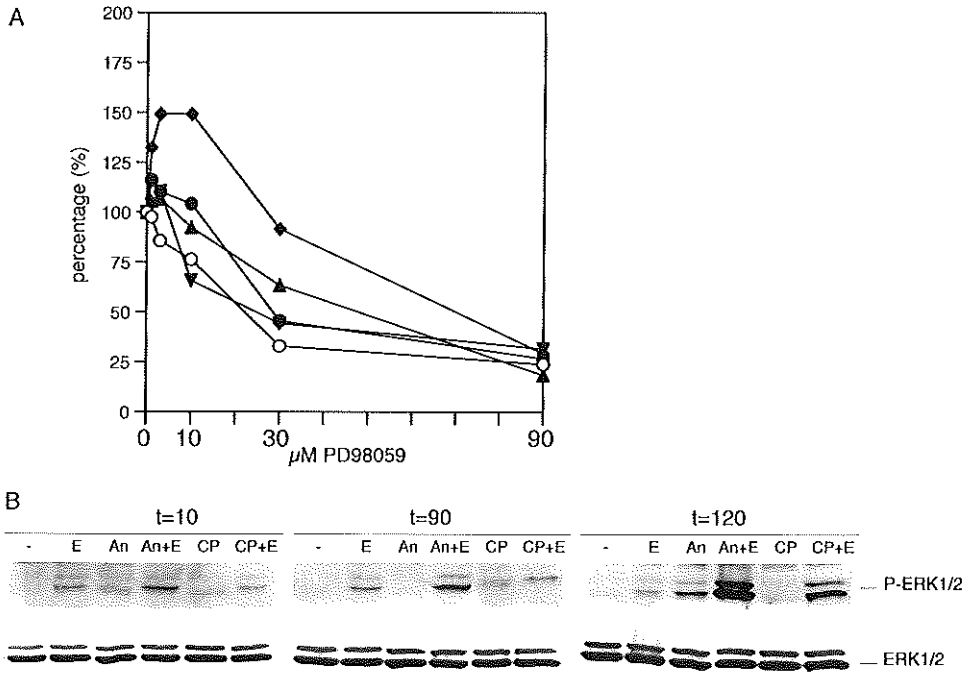

Figure 4: Activation of the MAPKs ERK1/2 in 32D/Epo cells.
A. Incorporation percentages (cpm with PD/cpm without PD)x100% of ^{3}H-TdR in 32D/Epo cells cultured serum-free with Epo (1 IU/ml) or Epo and titrated concentrations of anandamide (0 μM (-O-), 0.3 μM (-▼-), 1μM (-◆-), 3 μM (-▲-), 10μM (-●-)) in the presence of different concentrations MEK1/2 inhibitor PD98059 (0 – 90 μM).
B. Western blot analysis at different time points (t=10, 90 and 120 min) with phospho-specific (upper panel) or phosphorylation-status-independent ERK1/2 antibodies (lower panel) of 32D/Epo cells cultured serum-free without stimulus (-), with Epo (E) (1 IU/ml), with anandamide (An) (10 μM), with Epo and anandamide, with CP55,940 (CP) (100nM) or Epo and CP55,940. Phosphorylation-status-independent ERK1/2 antibodies demonstrated equal levels of ERK1/2 protein in each lane.

DNA-synthesis of Epo- as well as Epo/anandamide-stimulated cells (Figure 4A). In fact, 90 μM PD98059 inhibited 75% of thymidine uptake in cultures with Epo alone or with Epo plus various concentrations of anandamide. Since these data are suggestive for a role of ERK1/2 in synergistic stimulation of proliferation by Epo and anandamide, we analyzed whether anandamide acts synergistically in the activation of ERK1/2. Western blot analysis, using phospho-specific ERK1/2 antibodies, demonstrated synergistic activation of ERK1/2 in 32D/Epo cells when stimulated by Epo and anandamide in time (Figure 4B). Weak synergistic activity of ERK1/2 was observed after 10 minutes of stimulation, but a progressively increased activation was

evident after 120 minutes in Epo/anandamide-stimulated cells as compared to stimulation with Epo alone. Anandamide alone had only limited effect on ERK1/2 phosphorylation. Synergistic ERK1/2 activation was also observed between Epo and the synthetic cannabinoid CP55,940, although the synergism between Epo/anandamide was stronger. Western blot experiments using phospho-specific antibodies directed to p38 MAPK or JNK did not reveal any activation of these kinases following stimulation of 32D/Epo cells with Epo or Epo/anandamide (data not shown).

Epo and anandamide synergistically stimulate c-Fos protein expression in 32D/Epo cells - The c-*Fos* gene has been shown to be a downstream target of MAPKs ERK1/2 (107). To investigate the effects of sustained MAPK1/2 activation on c-Fos protein expression immuno-histochemistry using c-Fos-specific antibodies was carried out at day 1, 2 and 3 following stimulation. The percentages of c-Fos-positive cells in culture were significantly elevated following Epo/anandamide-stimulation (Figure 5 and Table 2).

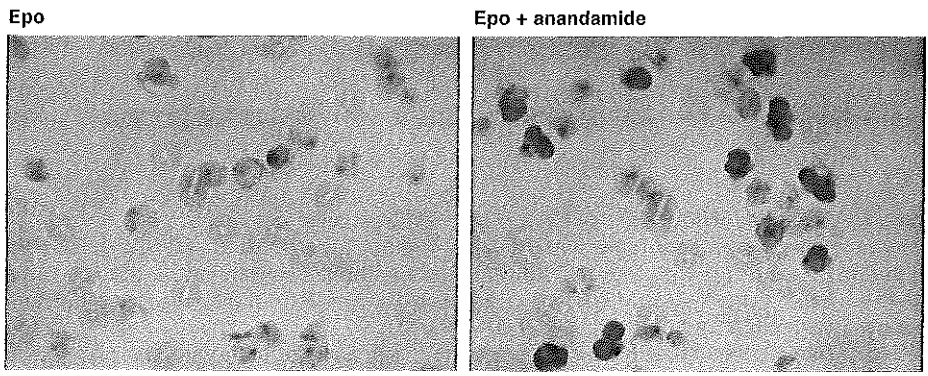

Figure 5: Stimulation of c-Fos protein in 32D/Epo cells.
Immunohistochemistry with c-Fos-specific antibodies of 32D/Epo cells cultured 2 days serum-free with Epo (1 IU/ml) (left) or Epo and anandamide (10 µM) (right).

	Percentages of c-Fos-positive 32D/Epo cells	
Day	Epo	Epo + anandamide
1	26%	38%
2	24%	48%
3	15%	34%

Table 2: Immunohistochemistry with c-Fos antibodies of 32D/Epo cells cultured serum-free in the presence of Epo or Epo and anandamide

Anandamide has no effect on Epo-induced STAT-5 activation in 32D/Epo cells – Since anandamide cooperates with Epo in the activation of ERK1/2, we examined whether anandamide also synergizes with Epo in the activation of other pathways recruited by the Epo receptor-Jak2 (339) complex, like STAT-5 (111). Electro mobility shift assays with a β-casein probe showed equal levels of activated STAT-5 in 32D/Epo cells stimulated with Epo- or Epo/anandamide in time (Figure 6).

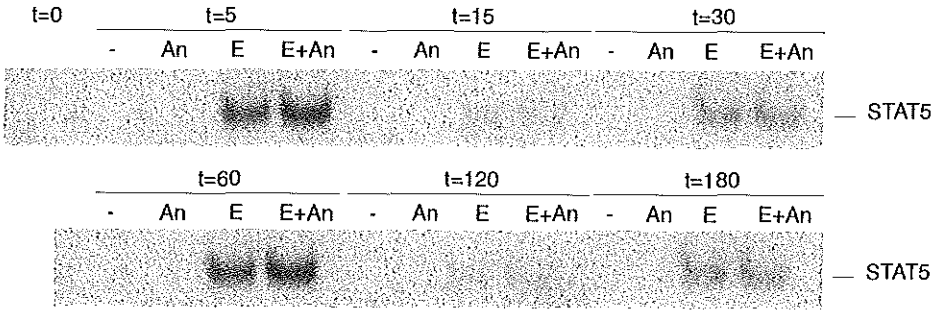

Figure 6: STAT-5 activation in 32D/Epo cells.
EMSA results at different time points (0, 5, 15, 30, 60, 90 and 120 minutes) of 32D/Epo cells cultured serum-free without factors (-), with anandamide (An) (50 μM), Epo (E) (10 IU/ml) or Epo and anandamide.

The Cb2 receptor-specific antagonist SR144528 inhibits anandamide/Epo-induced DNA-synthesis of 32D/Epo cells – Although, anandamide activates the peripheral cannabinoid receptor Cb2 (97), non-receptor-mediated activation by anandamide has also been demonstrated (76). Therefore we analyzed whether the specific Cb2 antagonist SR144528 blocked the stimulation of proliferation by anandamide. Addition of 1μM SR144528 resulted in a 50% reduction of Epo/anandamide-stimulated DNA-synthesis in 32D/Epo cells and 300 nM SR144528 already caused inhibition of DNA-synthesis (Figure 7). SR144528 (1μM) also reduced ^{3}H-TdR incorporation of Epo-stimulated 32D/Epo cells. The Cb1 receptor-specific antagonist SR141716 at identical concentrations did not inhibit Epo/anandamide-stimulated DNA-synthesis (Figure 7).

Discussion

Anandamide is an endogenous ligand for the peripheral cannabinoid $G\alpha_{i/o}$ protein-coupled receptor Cb2. Strong synergy between anandamide and HGFs has been shown in two independent studies (76, 314). Among the different HGF-dependent cell lines that we have studied previously, 32D/Epo cells showed the greatest response to

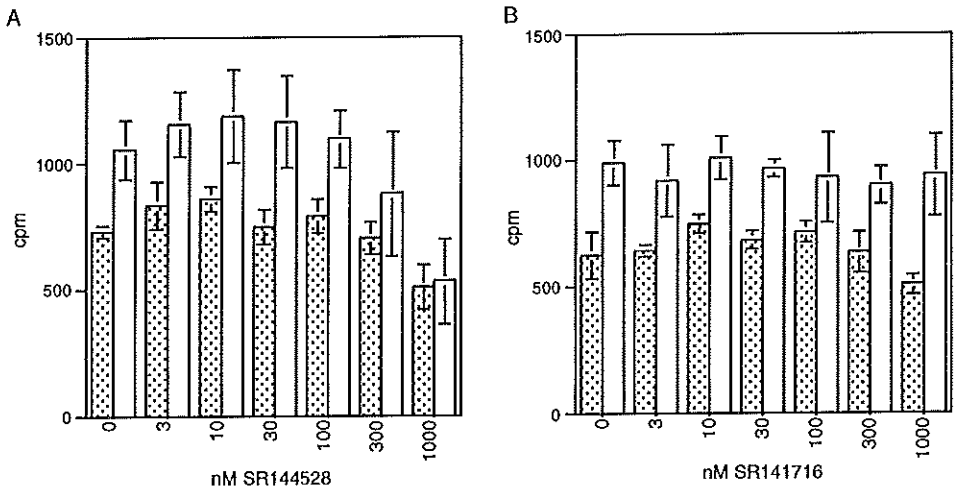

Figure 7: Effects of Cb1- and Cb2 receptor-specific antagonists on anandamide-stimulated DNA-synthesis of 32D/Epo cells.
Incorporation of ^{3}H-TdR in 32D/Epo cells cultured serum-free with Epo (1 IU/ml) (dotted bars) and Epo and anandamide (1 μM) (blanc bars) in the presence of different concentrations (0-1000nM) SR144528 (Cb2 antagonist; left) or SR141716 (Cb1 antagonist; right). Background levels of tritiated thymidine incorporation in 32D/Epo cells were measured without the addition of any factor or in cultures with anandamide alone (14-68cpm).

anandamide (314). In this study we demonstrate that in 32D/Epo cells the MAPKs ERK1/2 and c-Fos are targets of the synergistic action of Epo and anandamide.
The MAPKs ERK1/2, rather than JNK or p38, have been shown to be important mitogenic signaling intermediates of $G\alpha_{i/o}$ GPCRs (320). Here we show sustained activation of MAP kinase ERK1/2, but not JNK or p38, by anandamide in combination with Epo in 32D/Epo cells. Sustained rather then early transient activation of MAPK ERK1/2 has been demonstrated to determine biological responses, e.g., proliferation or differentiation (194). In fact, experiments with the MAPKs MEK1/2 inhibitor PD98059 showed that activation of the MAPKs ERK1/2 is required for proliferation of the 32D/Epo cells. Furthermore, the prolonged stimulating effect of anandamide on ERK1/2 resulted in increased expression of c-Fos and accelerated cell cycling of the 32D/Epo cells. These data underscore the key role of the MAPKs ERK1/2 in stimulation of hematopoietic cell proliferation.
Similar to the results from previous studies with Epo and SCF in primary erythroid bone marrow precursors (303), we demonstrate here that Epo/anandamide sustain the

activation of MAPK ERK1/2 in 32D/Epo cells. The fact that neither anandamide nor SCF (303) affect Epo-induced STAT-5 activation, suggests that the cooperative effects between Epo/anandamide or Epo/SCF can not be explained by increased activation of the Epo-receptor or the Jak2 kinase (339). Other pathways involving distinct tyrosine-kinases, as for instance focal adhesion kinase (FAK), might be activated. FAK has recently been shown to be activated by anandamide in rat hippocampus via CB1 (75). Interestingly, FAK has been implicated in GPCR as well as integrin signaling (347). Integrins collaborate with growth factors in MAPK activation (212), which suggests that FAK-like kinases may be involved in anandamide-mediated synergistic MAPK activation in hematopoietic cells as well.

Western blot analyses suggested that activation of ERK1/2 in HGF-dependent hematopoietic cells by anandamide only occurs when the cells are costimulated with the proper HGFs. In previous studies the MAPKs ERK1/2 could be activated when cells were stimulated by cannabinoids as single factors (42, 76, 331). Those studies were carried out in growth factor-independent cell lines, which require the addition of serum to proliferate *in vitro*. We assume that in these factor-independent cells anandamide cooperates with signaling pathways stimulating cell cycle progression that are constitutively activated as the result of genetic alterations. We recently demonstrated that HGF-independent hematopoietic cell lines also require anandamide to proliferate optimally in serum-free culture (316). In those cell lines the MAPKs ERK1/2 may be activated by anandamide when added as a single stimulus and synergize with the constitutively activated pathways.

Several pieces of evidence suggest that the Cb2 receptor mediates the enhanced proliferation of the Epo-dependent 32D/Epo cells in response to anandamide. Firstly, we demonstrate high levels of *Cb2* mRNA in the 32D/Epo cells. Secondly, both anandamide and CP55,940 synergistically activate the MAPKs ERK1/2. The MAPK activation by CP55,940 demonstrates that 32D/Epo cells contain functional Cb2 receptors since CP55,940-mediated signaling is entirely receptor-dependent (76). Thirdly, the Cb2 receptor-specific antagonist SR144528 inhibited Epo/anandamide-stimulated 32D/Epo cell proliferation, whereas the Cb1 receptor-specific antagonist SR141716 did not. Addition of 1 μM SR144528 to Epo/anandamide-stimulated cultures suppressed tritiated thymidine uptake to levels equal to cultures stimulated with Epo alone. This concentration of SR144528 has shown to be inhibitory to MAPK activation (261) and proliferation of human B-cells (49) induced by CP55,940. The data obtained with SR144528 suggest that anandamide-mediated enhanced proliferation of 32D/Epo cells is at least partially Cb2 receptor-dependent.

CP55,940, in contrast to anandamide, did not stimulate proliferation of 32D/Epo cells in synergy with Epo (data not shown). However, both CP55,940 and anandamide enhance ERK1/2 activation. This may indicate that the Epo/anandamide-stimulated 32D/Epo cell proliferation also requires a receptor-independent activation mechanism. In fact, Epo/anandamide induces higher ERK1/2 phosphorylation than Epo/CP55,940, suggesting that anandamide may activate ERK1/2 activation through

Cb2 receptor-dependent and receptor-independent mechanisms, which are both required for enhanced proliferation of 32D/Epo cells. Derocq *et al.* (76) demonstrated that in B9 cells anandamide could be replaced by the growth stimulator (112, 238) arachidonic acid (AA). Anandamide is degraded into AA and also stimulates release of AA (97, 331). In addition, stimulation of proliferation of B9 cells by IL-6 and anandamide was not blocked by the Cb2 specific antagonist SR144528 (76). These series of experimental data indicated that an anandamide-mediated Cb2 receptor-independent mechanism was responsible for the enhancement of proliferation by anandamide in B9 cells. In contrast, Wartmann *et al.* (331) demonstrated that MAPK activation as well as AA release in WI-38 fibroblasts was entirely receptor-mediated, most probably via the CB2 receptor (128). Together, these data indicate that the Cb2 receptor-dependent mechanisms of anandamide-mediated signal transduction critically depend on the cellular background. Although, additional analyses in Cb2 non-expressing hematopoietic cells are required to further clarify this issue, in 32D/Epo cells anandamide most probably activates proliferation in synergy with Epo through Cb2 receptor-dependent as well as an receptor-independent mechanisms, which is in agreement with studies carried out in CB2-transfected CHO-cells (76).

Cell cycle analysis studies of 32D/Epo cells confirm that anandamide acts differently from classical HGFs, which signal solely via their cognate receptors. As a matter of fact, anandamide is not required for G1-progression and entry into the S-phase. Cell cycle analysis as a function of time following Epo/anandamide stimulation showed constant proportions of cells in G0/G1-, S- or G2/M-phases, while the proliferation (thymidine uptake) increased. These results suggest that anandamide accelerates cell cycling of Epo-induced 32D/Epo by shortening all cell cycle phases non-selectively. Therefore, anandamide may be considered as a proliferation-acceleration factor.

Anandamide, synergistically stimulates proliferation of different hematopoietic cell lines with multiple HGFs, e.g., IL-3, GM-CSF or Epo (76, 314). The effects of anandamide have only been observed in serum-free culture (76, 314) or when cells were cultured at low serum conditions (76). This would suggest that anandamide represents one of the crucial serum components required for optimal *in vitro* proliferation of eukaryotic cells in general. This idea is strengthened by the finding that anandamide synergistically enhances the expression of c-Fos protein. The expression of the immediate early c-*Fos* gene is regulated by a combination of transcription factors (311). The serum response factor binds to the serum response element present in the c-*Fos* promoter and the ternary complex factor activates c-*Fos* transcription (311). The MAPKs ERK1/2 have been shown to be critical intermediates in the transcriptional activation of c-*Fos* (107). In this study, we demonstrate increased long-term expression of c-Fos protein by Epo and anandamide in the context of synergistic activation of the MAPKs ERK1/2. Whether anandamide is a critical stimulus *in vitro* for non-hematopoietic cell lines remains an interesting question to be addressed.

CHAPTER 8

GENERAL DISCUSSION

Part of this general discussion has been published in:

Valk PJM and Delwel R
The peripheral cannabinoid receptor, Cb2, in leukemic transformation and hematopoiesis
Leukemia and Lymphoma 32(1-2), 29-44, 1998

General discussion

8.1 *The peripheral cannabinoid receptor in leukemogenesis*

8.1.1 *The common virus integration site, Evi11, is located within the gene encoding the peripheral cannabinoid receptor*

By retroviral insertional mutagenesis, a novel common VIS was isolated from Cas-Br-M MuLV-induced leukemias and designated ecotropic virus integration site 11 (*Evi11*), consistent with previously identified common VISs (*Evi1-Evi10*). *Evi11* was initially identified by Southern blot analysis of genomic DNA from two Cas-Br-M MuLV-induced IL-3 dependent myeloid cell lines, NFS78 and NFS107 (Chapter 2).
To determine the frequency of proviral insertion in *Evi11*, a novel panel of Cas-Br-M MuLV-induced leukemias in NIH/Swiss mice was established. Immunophenotyping of these Cas-Br-M MuLV-induced primary CSL (Cas-Br-M MuLV Swiss Leukemias) leukemias revealed that the majority of the leukemias were of myeloid origin, and the remaining tumors displayed a T-cell or mixed myeloid/T-cell phenotype (Chapter 5). This newly established well-characterized panel of Cas-Br-M MuLV-induced leukemias in NIH/Swiss mice (Chapter 5) and the novel rapid RT-PCR-based method to isolate VIS flanking cDNA fragments (Chapter 3) carry enormous potential for the isolation of new VISs and identification of novel proto-oncogenes in myeloid and T-cell leukemias.
Additional proviral integrations in *Evi11* were demonstrated in the newly established Cas-Br-M MuLV-induced primary CSL leukemias (Chapters 2, 4 and 5). In fact, proviruses within the *Evi11* locus were shown in 11 out of 84 Cas-Br-M MuLV-induced primary CSL leukemias and tumor cell lines (13%). Compared to all known (common) VISs in myeloid leukemias (Chapter 1 and Table 1), the occurrence of proviral integration within *Evi11* is relatively frequent. Immunophenotyping of the Cas-Br-M MuLV-induced CSL leukemias demonstrated that proviral insertion in *Evi11* appeared not to be restricted to the myeloid lineage (Chapter 5), which may suggest that mutation of *Evi11* in Cas-Br-M MuLV-induced leukemogenesis occurs in a pluripotent progenitor cell.
To detect mRNA coding sequences in *Evi11*, a novel exon trapping system was established, and coding sequences representing the genes encoding α-L-fucosidase, *Fuca1*, and the peripheral cannabinoid receptor 2, *Cb2*, were isolated (Chapter 2). Retroviral insertions occurred either in intron sequences (NFS leukemic cell lines) or in the 3' untranslated region (UTR) of *Cb2* (CSL primary leukemias), indicating that *Cb2* rather than *Fuca1* is the target gene in *Evi11* (Figure 1).
Cb2 is a seven-transmembrane receptor, which belongs to the super family of receptors that couple to guanine-nucleotide-binding proteins (G protein-coupled receptors (GPCRs)). The Cb2 receptor is one of two distinct receptors, i.e., Cb1 and Cb2, which both specifically interact with cannabinoids, including Δ^9-tetrahydro-

Common VIS	Number	Percentage	Reference
Evi1[#]	9/9 (myeloid)	100%	(219)
	13/140 (all tumors)	9.3%	(219)
	11/60	18%	(29)
Evi2	11/69	15%	(46)
Evi6		2.9%	(228)
Evi7		7.2%	(228)
Evi8		4.8%	(228)
Evi9		1.0%	(228)
Evi11*[#]	**11/84**	**13%**	**this thesis**
Evi12*[#]	**16/84**	**19%**	**this thesis**
Fli1[#]	16/24	67%	(31)
	36/51	70%	(30)
	43/60	72%	(29)
Myb		3%	(218)
His1[#]	3/52	5.8%	(6)
His2[#]	2/52	3.8%	(6)
p53[#]	14/60	23%	(29)
Meis1	8/87	9.2%	(218)
Fim2	14/68	20%	(109)
Mml1	10/77	13%	(160)

Table 1: Frequencies of common VISs in myeloid leukemias
[*]Evi11 and *Evi12* leukemias induced by Cas-Br-M MuLV in NFS or HIH/Swiss mice
[#]Common VISs identified in Cas-Br MuLV induced leukemias

cannabinol (Δ^9-THC), the major active ingredient of marijuana. Cb2 is also referred to as the peripheral cannabinoid receptor since the *Cb2* gene is primarily expressed in peripheral tissues (222). Although the peripheral cannabinoid receptor is generally abbreviated by *Cb2* (241), the official mouse genome locus is *Cnr2* (240).

8.1.2 *The peripheral cannabinoid receptor gene: genomic structure, tissue-specific expression, and abnormal expression in Cas-Br-M MuLV-induced NFS cell lines and CSL primary leukemias*

Human *CB2* was isolated by Munro and co-workers (222) in 1993, whereas murine *Cb2* was cloned only recently (Chapter 2) (284). Murine *Cb2* was initially cloned in our lab as a single exon gene encoding the full-length Cb2 protein (Chapter 2). The protein-coding region of GPCR genes, including *Cb1* (285), are frequently located in one exon. Interestingly, however, in many instances those protein-coding exons of GPCR genes are preceded by single small 5' exons, many of which are non-coding (316). The presence of those small non-coding exons upstream of the protein coding exon in many GPCR genes is remarkable and may suggest a role in pre- or post-transcriptional regulation. Indeed, 5' RACE analysis of the murine *Cb2* gene

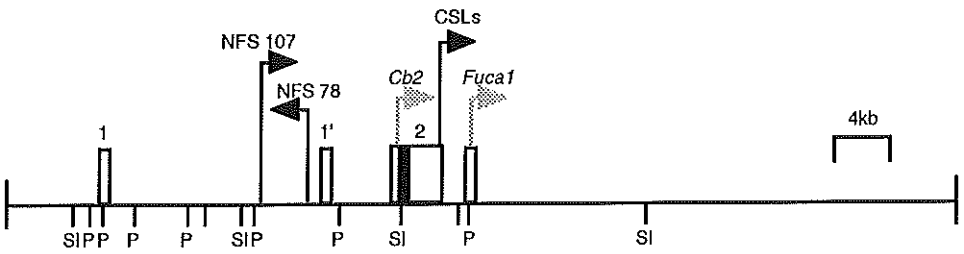

Legend to Figure 1:
Genomic structure of *Evi11*.
Partial restriction map of the *Evi11* locus (SI: *Sal*I and P: *Pst*I). The boxes represent 5' upstream exons 1 and 1', the protein coding exon 2 of the peripheral cannabinoid receptor gene (*Cb2*), and the most 5' exon of the α-L-fucosidase gene (*Fuca1*). The black box indicates the *Cb2*-coding region, while the black arrows indicate the insertion sites and orientations of the proviruses in the leukemic cell lines (NFS) and primary tumors (CSL).

demonstrated the presence of two non-protein-coding 5' exons, exon 1 and exon 1' (Chapter 2 and Figure 1).
Interestingly, different *Cb2* mRNAs are expressed in normal mouse tissues (data not shown). *Cb2* exon 1 fused to exon 2 is expressed in thymus, spleen, bone marrow and many hematopoietic cell lines (Chapter 6), whereas an alternative *Cb2* exon 1' fused to exon 2 is expressed exclusively in spleen (data not shown). In fact, tissue-specific expression has also been proposed for the *CB1* receptor gene at different sites of the brain (196, 197). The distinct expression of the non-coding *Cb2* exons may suggest that these exons have an important role in normal lineage-specific expression of the Cb2 receptor in hematopoietic progenitors.
High cannabinoid receptor levels, most probably representing Cb2, have been demonstrated by radioligand studies in spleen in regions enriched for B-lymphocytes (190). By RT-PCR, *Cb2* mRNA was shown in spleen and tonsils (105). Furthermore, in hematopoietic cells the highest levels of *Cb2* mRNA (105) and protein (49) were demonstrated in B-cells. These results taken together suggest that translation of exon 1' fused to 2 *Cb2* mRNA, which is expressed exclusively in spleen, results in high level Cb2 protein expression. This is also consistent with recent *in vitro* binding studies with radiolabeled synthetic Cb2 ligand [^{3}H] CP55,940 which demonstrated a high number of Cb2 receptors on the IL-3 dependent myeloid cell line NFS78, expressing *Cb2* exon 1' plus 2 mRNA (Chapter 2 and data not shown). Other cell lines expressing Cb2 exon 1 plus 2 mRNA contained a low number of Cb2 receptors.
The expression of the alternative exon 1', instead of exon 1, might affect protein expression of *Cb2*, since there is a change in upstream reading frames within the

5'UTR of *Cb2*. It has been established that upstream cistrons may influence the efficiency of reinitiation by eukaryotic ribosomes, thereby affecting protein synthesis (164). Modulation of protein synthesis by insertion of alternative 5' sequences has also been suggested for the angiotensin II type 1 GPCR (62) and the *lck* (195) and c-*cis* proto-oncogenes (257).
In two leukemic cell lines, NFS78 and NFS107, retroviral insertion occurred in the intron that separates exon 1 from protein coding exon 2 (Figure 1). In NFS78 and NFS107 retroviral insertion causes aberrant expression of exon 1. In NFS107 truncated mRNA transcripts representing exon 1 alone are expressed, while in NFS78 exon 1 is replaced by exon 1' (Chapter 2). Although high levels of Cb2 receptor were demonstrated by *in vitro* binding studies on NFS78 cells as compared to other NFS cell lines without Cas-Br-M MuLV inserted in *Evi1* (data not shown), the mechanism of proviral activation of *Cb2* in NFS107 is at present unclear.
Additional retroviral integrations were demonstrated in multiple novel Cas-Br-M MuLV-induced primary CSL leukemias (Chapter 4). In these cases provirus inserted within the 3'UTR of *Cb2* in the same orientation compared to *Cb2* transcription (Figure 1). These insertions clearly resemble classical integrations, which result in overexpression of the target proto-oncogene by enhancer sequences on the LTR (Chapter 1) (148, 340). This might indicate that the insertions in the 3'UTR of *Cb2* result in increased expression of the G protein-coupled peripheral cannabinoid receptor. The analyses of putative aberrant expression of *Cb2* mRNA and Cb2 protein in the primary CSL leukemias is hampered by the low numbers of leukemic cells in these samples and the high levels of endogenous expression of the *Cb2* mRNAs and Cb2 protein in spleen and thymus. In order to address this issue, cell lines should be made from these primary Cas-Br-M MuLV-induced leukemias, to study Cb2 receptor expression.
Interestingly, *MAS,* another gene that encodes a GPCR, has been shown to be oncogenic (141, 346). The *MAS* oncogene and *CB2* receptors appear to belong to the same structural subclass of GPCRs since both lack several conserved cystein residues specific for most GPCRs, which appear to stabilize the tertiary structure of the receptor (269). The transforming ability of *MAS* was shown by transfection of DNA from a human ovarian carcinoma into NIH3T3 fibroblasts (346) or the monoblastic cell line CTV-2 (141). In each case where this gene showed transforming ability, deletions upstream of the protein coding exon were demonstrated. By 5'RACE, a small non-coding exon upstream of the protein coding exon of the *Mas* proto-oncogene has been isolated (273). Actually, the 5'RACE product of the *Mas* oncogene represents multiple upstream non-coding exons of *Mas* (personal communication D. Barlow). The presence of these upstream exons suggests crucial roles for these small non-coding exons in MAS protein expression. Most likely, absence of the 5' non-coding exons in the *MAS* mRNA causes aberrant protein expression resulting in oncogenic transformation. Thus, transformation by the *MAS*

oncogene shows similarities with that of the retroviral integrations in the *Cb2* gene in the myeloid Cas-Br-M MuLV-induced cell lines (Figure 2).

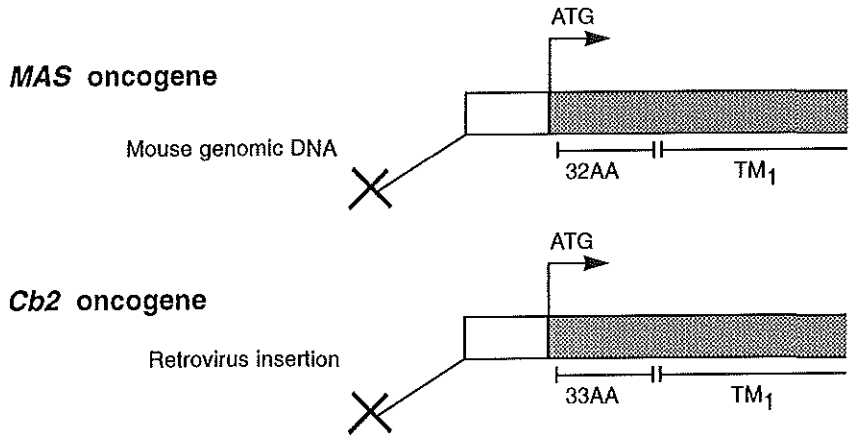

Legend to Figure 2:
Comparison of *Cb2* and *Mas* proto-oncogene transformation.
Schematic repesentation of the genomic organisation of the *Cb2* proto-oncogene and the *Mas* proto-oncogene. In both situations transcription of the upstream region of the GPCR proto-oncogene is interfered by either mouse genomic DNA (*Mas*) or by retroviral insertion (*Cb2*). AA: Amino Acids; TM_1: first transmembrane region.

8.1.3 *Cb2 in AML and other human malignancies*

By fluorescence *in situ* hybridization (FISH) with cosmid clones representing the entire *Evi11* locus, the location of *Evi11* was identified on mouse chromosome 4 (316). Interspecific backcross analysis confirmed that *Evi11* is indeed present on mouse chromosome 4 (Chapter 2). This region shares homology with the human chromosomal region 1p36. The human chromosomal localisation of *EVI11* was confirmed by exon trapping sequences representing α-L-fucosidase, since this gene had already been mapped to human 1p36 (103). This chromosomal region is relatively frequently involved in chromosomal rearrangements and deletions in blood cell disorders, like AML (37, 325), Fanconi's anaemia (104), non-Hodgkin lymphoma (334), primary macroglobulinemia (144), and T-cell lymphoma (305), as well as other non-hematopoietic malignancies, such as melanoma (306), ovarian carcinoma (307), and neuroblastoma (33, 55). Although this could be an indication that *CB2* might be involved in human chromosomal abnormalities as well, no extensive studies have been carried out so far to demonstrate involvement of *CB2* in tumorigenesis in man. Obviously, the importance of CB2 in leukemic transformation would improve enormously when large-scale screening of human hematopoietic malignancies, by

Southern blot analysis or FISH, would prove the involvement of CB2 in chromosomal abnormalities of 1p36.

8.1.4 *Other G protein-coupled receptors in tumorigenesis*

The peripheral cannabinoid receptor belongs to the superfamily of GPCRs, which have been shown a number of times to be involved in cell growth and oncogenesis (80). Frequently, the transforming potential of GPCRs is caused by mutations in one of the cytoplasmic loops, causing constitutive activation of the receptors, leading to increased cell proliferation and to tumorigenicity. Examples of constitutively activated transforming GPCRs are the α1B-adrenergic receptor (4) and the thyroid-stimulating hormone receptor (302). Multiple constitutive active Gα proteins have also been implicated in tumorigenesis (79, 80). Examples of non-mutated GPCR genes that are transforming following overexpression, are the genes encoding thrombin (335), α1B-adrenergic (4), muscarinic acetylcholine (118), serotonin 1c (150) receptors or *MAS*-oncogene (section 8.1.2) (324, 346), which induce a transformed phenotype of NIH/3T3 cells. Furthermore, paracrine and autocrine stimulation of GPCRs, by secretion of particularly neuropeptides, have been implicated in a number of human neoplasias (117).
The *Cb2* gene in NFS78 and NFS107 does not contain mutations in its protein-coding, region and overexpression of Cb2 cDNA does not transform NIH/3T3 cells (Chapter 2 and unpublished observation). Thus, although we have clear evidence that *Cb2* is involved in tumorigenesis in certain cases of leukemia, the mechanism of transformation is probably different from that of other GPCR oncoproteins. *In vivo* evidence demonstrating that *Cb2* is transforming may come from *Cb2* transgenic mice that have been generated.

8.1.5 *Cb2-transgenic mice*

Several lines of transgenic mice (FVB inbred) were made to determine the oncogenic potential of *Cb2* (unpublished data). In these transgenic mice *Cb2* expression is controlled by the promoter (207) of the early-hematopoietic stem cell marker gene *Sca1* (293). Transgenic mice of both types of *Cb2* mRNA, exon 1 plus 2 and 1' plus 2 (Figure 1), were generated. Differential expression corresponding to *Sca1*-promoter-driven expression (207) of the *Cb2* transgenes in the different organs was shown by RNase protection analysis (data not shown).
Macroscopic analyses did not reveal any abnormality in the anatomy of up to one-year-old transgenic mice. Furthermore, cell counting experiments as well as colony forming assays (CFU and BFU) of peripheral blood and bone marrow did not show any imbalance of hematopoiesis in transgenic animals. The introduction of the *Cb2*

transgene resulted in only several-fold elevation of *Cb2* mRNA as compared to endogenous *Cb2*. It might therefore be possible that the elevated levels of *Cb2* expression in these transgenic mice are insufficient for inducing leukemia. Since the *ScaI*-promoter is γ-interferon responsive (292), it would be of interest to investigate the transforming abilities of *Cb2* by increasing *Cb2* mRNA levels in the transgenic mice following administration of γ-interferon.
It has generally been accepted that leukemia is the resultant of sequential activation of proto-oncogenes or disruption of tumor suppressor genes (1, 129). Thus, the lack of transforming ability of *Cb2* in transgenic mice might also be explained by this phenomenon. Retroviral infections of *Cb2*-transgenic mice to introduce secondary genetic abnormalities are in progress and should address the question whether *Cb2*-transgenic mice are indeed predisposed to develop leukemia. Preliminary results indicate that *Cb2* transgenic mice indeed show an increased susceptibility for developing leukemia in the context of additional oncogenic events. At this stage of our investigations, 32% (exon 1+2) and 58% (exon 1'+2) of the *Cb2*-transgenic mice versus 8% (3/39) of control FVB littermates developed leukemia after Cas-Br-M MuLV infection.

8.1.6 *Retroviral insertions in the gene encoding the peripheral cannabinoid receptor Cb2 frequently coincide with insertions in a novel common VIS Evi12*

We designed a novel RT-PCR based method to rapidly identify common VISs from murine leukemias (Chapter 3). This new method is easy applicable to different tumor tissues. The identification of proviral insertions in *Evi1*, *Erg* and *Evi12* confirmed the power of this new technique to rapidly determine unknown VIS-flanking sequences.
In order to identify *Cb2*-cooperating proto-oncogenes, the same method was applied to RNA of the IL-3-dependent myeloid cell line NFS107 for isolating provirus flanking DNA fragments, and several cDNA fragments were isolated (Chapter 5). Subsequently, an unknown common VIS, designated *Evi12*, was isolated. *Evi12* rearrangements were found in 16 out of 84 Cas-Br-M MuLV-induced cell lines and primary CSL leukemias (19%). This value is in the same order as the frequency of *Evi11* proviral insertions (Table 1). Proviral insertions in *Evi12* were demonstrated in myeloid as well as T-cell tumors, alike the insertions in *Evi11*. The notable similarities of *Evi11* and *Evi12* insertions in myeloid and T-cell tumors might indicate that mutations in both *Evi11* and *Evi12* occur early in Cas-Br-M MuLV-induced leukemogenesis. Further, the high coincidence of proviral insertions in *Evi11* and *Evi12* in Cas-Br-M MuLV-induced leukemias (Chapters 4 and 5) may suggest a cooperative role between *Cb2* and an *Evi12* proto-oncogene in leukemogenesis in NIH/Swiss mice. Cas-Br-MuLV infections of *Cb2*-transgenic mice (section 8.1.5) are in progress to verify whether *Cb2* collaborates with an *Evi12* proto-oncogene in

hematopoietic transformation.
Although Cas-Br-M MuLV insertions were clustered upstream of the gene encoding the molecular chaperone Tra1/Grp94 (Chapter 4), the experimental data exclude *Tra1/Grp94* as the target proto-oncogene in *Evi12*. Additional studies will be needed to reveal the identity of an *Evi12* proto-oncogene.
By interspecific backcross analysis it was shown that *Evi12* is located on mouse chromosome 10 in a region that shares homology with human chromosome 12q22-24. The chromosomal localisation of *Evi12* in mice and man was confirmed by the demonstration that proviral insertions in *Evi12* were clustered upstream of the *Tra1/Grp94* gene (191, 258, 300). No putative proto-oncogene has been described in the mouse *Evi12* locus by others. A possible candidate, located on human chromosome 12q22, may be the *BTG1* gene, which was originally identified as a translocation partner in t(8;12)(q24;q22) in B-cell CLL (259). However, no relation between the tumor suppressor gene *BTG1* and *Evi12* has been demonstrated. Translocations of 12q22-24 have been found in AML, CLL and B-cell non-Hodgkin lymphoma (151, 343, 348). Thus, further studies to examine whether *EVI12* is involved in translocations in human hematopoietic malignancies appear appropriate.

8.2 *The peripheral cannabinoid receptor in normal hematopoiesis*

8.2.1 *The peripheral cannabinoid receptor gene: expression pattern*

The presence of cannabinoid receptors on membranes of hematopoietic cells and tissues was first shown by using radiolabeled cannabinoids. *In vitro* radioligand binding studies with [^{3}H] CP55,940 demonstrated specific binding sites on the surface membrane of spleen cells (154). Furthermore, by using radiolabeled [^{3}H] CP55,940 for autoradiography, Lynn and Herkenham (190) showed cannabinoid receptors in the marginal zone of the spleen, in the cortex of the lymph nodes and in the nodular corona of Peyer's patches, areas enriched for B-lymphocytes. Cannabinoid binding sites were also found on the surface of myeloid cell lines, e.g., U937 (43).
In the early nineties, the rat and human genes encoding the central cannabinoid receptor, *CB1*, were cloned and mRNA expression was predominantly demonstrated in brain tissue (106, 198). RT-PCR analysis demonstrated very low numbers of *CB1* mRNA transcripts in different peripheral human organs, various hematopoietic cell lines and in peripheral blood lymphocytes and neutrophils (43, 105, 243), suggesting that binding of cannabinoids to hematopoietic cells was through central cannabinoid receptors. In 1993, however, Munro *et al.* (222) cloned a human and a rat homologue of *CB1*, and designated this gene *CB2*. Human *CB2* was isolated from the promyelocytic cell line HL60, and *CB2* transcripts rather than *CB1* mRNAs were identified in this cell line by Northern blot analysis. Northern blot analysis on various rat tissues probed with rat *Cb2* cDNA showed high expression in spleen, but not in

brain, whereas *Cb1* transcripts could only be identified in brain tissue (222). RT-PCR analysis, by Galiègue *et al.* demonstrated *CB2* mRNA in human spleen, tonsils and peripheral blood mononuclear cells. High levels of *CB2* transcripts were found in B cells and NK cells (105). In fact, the rank order of *CB2* mRNA in hematopoietic cells demonstrated by Galiègue *et al.* was B cells > NK cells >> monocytes > neutrophils > T8 cells > T4 cells (105). This rank order was recently confirmed by using polyclonal antibodies directed against the N-terminus of the CB2 receptor (49). In addition, *CB2* mRNA as well as CB2 receptor expression has also been demonstrated on mast cells (94). From these results, showing *CB2* mRNA and protein expression in human blood cells, it was concluded that the *CB2* gene encodes the hematopoietic cannabinoid receptor.
The murine *Cb2* gene has been cloned recently (Chapter 2) (284). In our laboratory *Cb1* and *Cb2* mRNA expression was investigated by RNase protection analysis in murine tissues and in a large panel of murine hematopoietic cell lines (Chapter 6). By using RNA probes covering both exons of the *Cb2* gene false positivity caused by genomic DNA contamination was excluded. *Cb2* mRNA expression was demonstrated in bone marrow, spleen, thymus and in 45 of the 51 cell lines studied, i.e., in myeloid, erythroid, macrophage, T- and B lymphoid and mast cell lines (Chapter 6). These studies in mice confirm that *Cb2* encodes the hematopoietic cannabinoid receptor. *Cb2* appeared, in contrast to human studies, to be frequently expressed in murine thymocytes and T cells. Expression of *Cb2* in murine thymus has recently been confirmed by others (270). In fact, tissue-specific expression of different Cb2 mRNAs in murine spleen and thymus was demonstrated (see 8.1.2).
Interestingly, Carayon *et al.* (49) recently demonstrated that *CB2* mRNA and CB2 protein expression are modified during B-cell differentiation. If regulation of *Cb2* expression also occurs in myeloid and T-cell differentiation, these data may imply that aberrant expression of the peripheral cannabinoid receptor caused by Cas-Br-M MuLV insertion may indeed interfere with normal hematopoietic development.

8.2.2 *Cannabinoid receptor agonists and hematopoiesis: stimulation of proliferation by anandamide*

A number of (i) natural cannabinoids, e.g., Δ^9-THC and cannabinol, (ii) synthetic cannabinoid agonists, e.g., WIN55212-2 or CP55,940, and (iii) putative endogenous ligands of cannabinoid receptors, e.g., anandamide and palmitoylethanolamide, have been described (241). The putative endogenous ligand of cannabinoid receptors, anandamide or arachidonylethanolamide, was isolated in 1992 from porcine brain (78) and demonstrated many of the biological effects associated with cannabinoids (97, 241). In human, anandamide has been detected in brain, spleen and heart, and in rats also in skin tissue (99). The experiments in Chapters 6 and 7 demonstrate that

anandamide synergistically stimulates proliferation of several HGF-dependent cell lines in serum-free culture.

Effects of cannabinoids on hematopoietic cell proliferation in human were observed long before the cannabinoid receptors were identified. *In vivo* administration of cannabinoids resulted in inhibition of cell proliferation or showed no effect (159, 176, 225, 242). Likewise, administration of cannabinoids to *in vitro* cultures of human (224) and mouse (50, 156, 159, 251) B- and T-cells generally caused inhibition of proliferation. These inhibitory effects on B- and T-cell proliferation as well as many other effects on immune function (reviewed by (158)) established a role for cannabinoids in immune homeostasis. In addition, it was shown that stimulation of the myeloid cell lines ML-2 and HL60 with cannabinoids caused incomplete maturation (223, 264), suggesting a possible function for cannabinoids during hematopoietic differentiation as well.

Cultures of hematopoietic cell lines or peripheral blood leukocytes demonstrated that cannabinoids inhibit proliferation at concentrations much higher (>1μM) (Chapter 6) (156, 223, 224, 264, 272) than those required in binding experiments (nanomolar concentrations) (222). In contrast, Derocq *et al.* (77) demonstrated that human B-cell growth is stimulated synergistically by crosslinking of immunoglobulins (Ig) and addition of cannabinoids, i.e., Δ^9-THC, WIN55212-2 or CP55,940 at nanomolar concentrations. These data raise the issue of non-receptor-mediated (inhibition at micromolar concentrations) versus receptor mediated mechanisms (stimulation at nanomolar concentrations) (100).

The synergistic stimulation of B-cell proliferation was the first result suggesting a stimulatory role for natural and synthetic cannabinoids in proliferation. The experiments in Chapters 6 and 7 show that the endogenous Cb2 ligand anandamide synergistically stimulates proliferation of several HGF-dependent cell lines in serum-free culture. The stimulatory effects of anandamide were demonstrated at relatively high concentrations (±1 μM) anandamide. This is consistent with the affinity of anandamide for the Cb2 receptor which is lower than that of the natural or synthetic cannabinoids (222). In contrast, anandamide-mediated inhibition of lymphocyte proliferation and induction of apoptosis was shown at 10-100 μM (272). These inhibitory effects are most probably non-receptor mediated toxic effects, since these concentrations are 10-100 fold above the concentrations required for complete saturation of the receptors. Interestingly, Derocq *et al.* (76) confirmed recently that anandamide (±1 μM) indeed acts as a synergistic growth factor for hematopoietic cell lines in the presence of low concentrations of serum. These investigators concluded that the stimulation of proliferation by anandamide was mediated by receptor-independent mechanisms (76). The studies in Chapter 7 suggest that both receptor-independent as well as receptor-dependent mechanisms may be involved in synergistic stimulation of proliferation by anandamide.

No stimulatory effects of anandamide have been observed when hematopoietic cells were cultured in the presence of serum (Chapter 6). Derocq *et al.* (77) demonstrated

stimulatory effects of cannabinoids at low serum concentrations, whereas no effects were observed at high serum concentrations. According to the authors of this study, these differences may be explained by loss of activity by the lipophilic cannabinoid ligands because of non-specific interactions with serum components (77). An alternative explanation could be that anandamide or another component with similar activities is present in serum, and masks the activity of exogenously administered anandamide.
Anandamide also enhances the numbers and sizes of IL-3 induced myeloid colonies from mouse bone marrow. Although the effects were significant, some IL-3 induced myeloid colonies appeared without the addition of anandamide in serum free culture. Recent studies demonstrated the production of anandamide as well as palmytoylethanolamide by macrophages and neutrophils (34). Therefore, it is possible that the effects of anandamide on normal marrow colony formation are partly masked by the production of endogenous cannabinoid ligands in the cultures. Experiments with purified stem cells may give further insight in the dependence of hematopoietic cells on CB2 ligands in culture, and reveal how distinct precursor cells in the marrow depend on CB2 agonists for optimal proliferation.

8.2.3 *Signal transduction pathways of the Cb2 receptor activated by anandamide*

Heterotrimeric G proteins consist of three heterologous subunits, i.e., the α-, β- and γ-subunits, that are associated in the inactive GDP bound state. Upon activation of the GPCR by agonist, the GDP is exchanged for GTP and the G protein trimer dissociates into a Gα subunit and a Gβγ dimer, which are both capable of activating intracellular signalling pathways. Cb2 belongs to the family of GPCRs that couple to $G\alpha_{i/o}\beta\gamma$ proteins. The pertussis toxin (Ptx) sensitive $G\alpha_{i/o}$ subunits decrease cAMP levels by inhibition of adenylyl cyclase, whereas the Gβγ dimers have been shown to mediate p21Ras-dependent mitogen-activated protein kinase (MAPK) activation (117, 320). No direct correlation has been observed between DNA synthesis and decreased cAMP levels caused by GPCRs (117), and mitogenic responses mediated by $G\alpha_{i/o}\beta\gamma$-linked GPCRs appear to be strictly dependent on Gβγ-mediated MAPK activation (320).
The intracellular signals that are initiated by cannabinoid receptors upon activation by anandamide and other cannabinoids are currently subject of active investigation. Cannabinoid receptors agonists decrease cAMP levels following exposure to forskolin of cells endogenously expressing Cb2 receptors as well as Chinese hamster ovary (CHO)-cells transfected with this receptor (153). Although this property is shared by most cannabinoids, anandamide did not inhibit (20, 294), or appeared to be the least effective ligand for CB2-mediated inhibition of forskolin-induced cAMP production (98, 179, 284). These results are most probably caused by the lower affinity of anandamide for the CB2 receptor (222). Since the demonstrated inhibitory

effects of anandamide on forskolin-induced cAMP by CB2 have been inconsistent and no positive effects of decreased intracellular cAMP levels on cell proliferation have been documented before (117), a pathway other than the cAMP signaling pathway is most probably responsible for Cb2-induced synergistic proliferation.
An obvious pathway responsible for Cb2-induced synergistic proliferation is the p21Ras/MAPK pathway, since mitogenic responses mediated by $G\alpha_{i/o}\beta\gamma$-linked GPCRs are strictly dependent on $G\beta\gamma$-mediated MAPK activation (320). It has recently been demonstrated that stimulation of CB2 by the synthetic cannabinoid CP55,940 indeed caused activation of the MAPKs, ERK1 and ERK2 (42). This MAPK activation via CB2 is apparently $G\beta\gamma$-mediated since it depends on $G\alpha_{i/o}\beta\gamma$ protein (Ptx-sensitive), but is independent of the cAMP pathway (42). Derocq *et al.* (76) showed CB2-dependent MAPK activation by anandamide in CB2-transfected CHO-cells; however, they claimed that the enhanced proliferation of hematopoietic cell lines by anandamide is receptor-independent. Experiments in Chapter 7 show synergistic activation of MAPKs and enhanced proliferation following stimulation of erythropoietin (Epo)-dependent cells with Epo and anandamide. Furthermore, by using the Cb2 antagonist SR144528 it was shown that the synergistic stimulation of proliferation was at least partially receptor-mediated (Chapter 7). These data (Chapter 7 and (76)) are in agreement with the notion that the anandamide-mediated synergistic MAPK activation and enhanced proliferation are mediated by both receptor-dependent and non-receptor-dependent pathways (Chapter 7 and (76)).

8.3 *Concluding remarks and future prospects*

The experiments described in this thesis demonstrate that the common VIS *Evi11* is located within the murine peripheral cannabinoid receptor *Cb2* gene. *Cb2* is therefore indicated as a proto-oncogene involved in Cas-Br-M MuLV-induced leukemogenesis in NIH/Swiss mice. In addition, a second common VIS *Evi12* has been identified, and the currently unknown *Evi12* proto-oncogene is suggested to cooperate with *Cb2* in tumor induction by Cas-Br-M MuLV in NIH/Swiss mice. Furthermore, the normal role of the GPCR Cb2 has been studied, demonstrating that *Cb2* encodes a hematopoietic cannabinoid receptor and that anandamide, an endogenous ligand for the Cb2 receptor, is able to enhance proliferation of HGF-dependent cell lines in serum free culture.
The mechanism by which Cas-Br-M MuLV activates *Cb2* by insertion in *Evi11* is currently unknown, although preliminary results show that the Cb2 receptor is overexpressed in NFS78 (data not shown). The effect of proviral insertion in the 3'UTR of *Cb2* on *Cb2* mRNA expression in the Cas-Br-M MuLV-induced primary CSL leukemias may confirm the exact mechanism of transformation by *Cb2*. Generation of cell lines from these Cas-Br-M MuLV-induced leukemias may be

informative for understanding the role of *Cb2* mRNA and Cb2 protein expression in these primary leukemias.

The ultimate proof that *Cb2* encodes a proto-oncogene involved in leukemogenesis should come from the Cas-Br-M MuLV-infected *Cb2*-transgenic mice. These experiments may simultaneously demonstrate whether the *Evi12* target proto-oncogene indeed cooperates with mutant *Cb2* in tumor induction.

The target proto-oncogene in *Evi12* will have to be identified by isolation of mRNA coding sequences by using, e.g., exon trapping, Northern analysis, sequence analysis, and database searches. *Evi12* proto-oncogene bearing transgenic mice will then be generated and crossed with *Cb2*-transgenic animals to examine cooperation between these two proto-oncogenes in leukemogenesis.

The demonstration that *Evi11/Cb2* and *Evi12* are also involved in human hematopoietic diseases would enormously increase the clinical importance of the experimental work described in this thesis. Therefore, efforts will be made in the near future to investigate whether *EVI11/CB2* and *EVI12* are involved in chromosomal abnormalities of 1p36 and 12q22-24, respectively, in human leukemias. Additionally, large-scale screening of human leukemias to demonstrate aberrant *CB2* mRNA or CB2 protein expression by using RNase protection analysis or antibodies raised against CB2, respectively, may reveal a potential role for CB2 in human leukemogenesis as well.

The CB2-ligand anandamide has been implicated in stimulation of hematopoietic cell proliferation. Further studies are required to unravel the normal Cb2 receptor-dependent signal transduction pathways involved in hematopoietic cell proliferation.

REFERENCES

References

1. **Adams, J. M., and S. Cory.** 1992. Oncogene co-operation in leukaemogenesis. Cancer Surv. **15:**119-41.
2. **Aihara, Y., H. J. Buhring, M. Aihara, and J. Klein.** 1986. An attempt to produce "pre-T" cell hybridomas and to identify their antigens. Eur J Immunol. **16:**1391-9.
3. **Algate, P. A., and J. A. McCubrey.** 1993. Autocrine transformation of hemopoietic cells resulting from cytokine message stabilization after intracisternal A particle transposition. Oncogene. **8:**1221-32.
4. **Allen, L. F., R. J. Lefkowitz, M. G. Caron, and S. Cotecchia.** 1991. G-protein-coupled receptor genes as protooncogenes: constitutively activating mutation of the alpha 1B-adrenergic receptor enhances mitogenesis and tumorigenicity. Proc Natl Acad Sci U S A. **88:**11354-8.
5. **Amati, B., and H. Land.** 1994. Myc-Max-Mad: a transcription factor network controlling cell cycle progression, differentiation and death. Curr Opin Genet Dev. **4:**102-8.
6. **Askew, D. S., C. Bartholomew, A. M. Buchberg, M. B. Valentine, N. A. Jenkins, N. G. Copeland, and J. N. Ihle.** 1991. His-1 and His-2: identification and chromosomal mapping of two commonly rearranged sites of viral integration in a myeloid leukemia. Oncogene. **6:**2041-7.
7. **Askew, D. S., C. Bartholomew, and J. N. Ihle.** 1993. Insertional mutagenesis and the transformation of hematopoietic stem cells. Hematol Pathol. **7:**1-22.
8. **Askew, D. S., J. Li, and J. N. Ihle.** 1994. Retroviral insertions in the murine His-1 locus activate the expression of a novel RNA that lacks an extensive open reading frame. Mol Cell Biol. **14:**1743-51.
9. **Auch, D., and M. Reth.** 1990. Exon trap cloning: using PCR to rapidly detect and clone exons from genomic DNA fragments. Nucleic Acids Res. **18:**6743-4.
10. **Austyn, J. M., and S. Gordon.** 1981. F4/80, a monoclonal antibody directed specifically against the mouse macrophage. Eur J Immunol. **11:**805-15.
11. **Azumi, J. I., and L. Sachs.** 1977. Chromosome mapping of the genes that control differentiation and malignancy in myeloid leukemic cells. Proc Natl Acad Sci U S A. **74:**253-7.
12. **Badley, J. E., G. A. Bishop, T. St. John, and J. A. Frelinger.** 1988. A simple, rapid method for the purification of poly A+ RNA. Biotechniques. **6:**114-6.
13. **Ballester, R., D. Marchuk, M. Boguski, A. Saulino, R. Letcher, M. Wigler, and F. Collins.** 1990. The NF1 locus encodes a protein functionally related to mammalian GAP and yeast IRA proteins. Cell. **63:**851-9.
14. **Barg, J., E. Fride, L. Hanus, R. Levy, N. Matus-Leibovitch, E. Heldman, M. Bayewitch, R. Mechoulam, and Z. Vogel.** 1995. Cannabinomimetic behavioral effects of and adenylate cyclase inhibition by two new endogenous anandamides. Eur J Pharmacol. **287:**145-52.
15. **Bartholomew, C., and J. N. Ihle.** 1991. Retroviral insertions 90 kilobases proximal to the Evi-1 myeloid transforming gene activate transcription from the normal promoter. Mol Cell Biol. **11:**1820-8.
16. **Bartholomew, C., K. Morishita, D. Askew, A. Buchberg, N. A. Jenkins, N. G. Copeland, and J. N. Ihle.** 1989. Retroviral insertions in the CB-1/Fim-3 common site of integration activate expression of the Evi-1 gene. Oncogene. **4:**529-34.
17. **Bashey, A., L. Healy, and C. J. Marshall.** 1994. Proliferative but not nonproliferative responses to granulocyte colony-stimulating factor are associated with rapid activation of the p21ras/MAP kinase signalling pathway. Blood. **83:**949-57.

18. **Baumbach, W. R., E. M. Colston, and M. D. Cole.** 1988. Integration of the BALB/c ecotropic provirus into the colony- stimulating factor-1 growth factor locus in a myc retrovirus-induced murine monocyte tumor. J Virol. **62**:3151-5.
19. **Baumbach, W. R., E. J. Keath, and M. D. Cole.** 1986. A mouse c-myc retrovirus transforms established fibroblast lines in vitro and induces monocyte-macrophage tumors in vivo. J Virol. **59**:276-83.
20. **Bayewitch, M., T. Avidor-Reiss, R. Levy, J. Barg, R. Mechoulam, and Z. Vogel.** 1995. The peripheral cannabinoid receptor: adenylate cyclase inhibition and G protein coupling. FEBS Lett. **375**:143-7.
21. **Bazan, J. F.** 1990. Structural design and molecular evolution of a cytokine receptor superfamily. Proc Natl Acad Sci U S A. **87**:6934-8.
22. **Bedigian, H. G., D. A. Johnson, N. A. Jenkins, N. G. Copeland, and R. Evans.** 1984. Spontaneous and induced leukemias of myeloid origin in recombinant inbred BXH mice. J Virol. **51**:586-94.
23. **Bedigian, H. G., B. A. Taylor, and H. Meier.** 1981. Expression of murine leukemia viruses in the highly lymphomatous BXH-2 recombinant inbred mouse strain. J Virol. **39**:632-40.
24. **Ben-David, Y., E. B. Giddens, and A. Bernstein.** 1990. Identification and mapping of a common proviral integration site Fli-1 in erythroleukemia cells induced by Friend murine leukemia virus. Proc Natl Acad Sci U S A. **87**:1332-6.
25. **Ben-David, Y., E. B. Giddens, K. Letwin, and A. Bernstein.** 1991. Erythroleukemia induction by Friend murine leukemia virus: insertional activation of a new member of the ets gene family, Fli-1, closely linked to c-ets-1. Genes Dev. **5**:908-18.
26. **Bennett, J. M., D. Catovsky, M. T. Daniel, G. Flandrin, D. A. Galton, H. R. Gralnick, and C. Sultan.** 1976. Proposals for the classification of the acute leukaemias. French- American-British (FAB) co-operative group. Br J Haematol. **33**:451-8.
27. **Bennett, J. M., D. Catovsky, M. T. Daniel, G. Flandrin, D. A. Galton, H. R. Gralnick, and C. Sultan.** 1985. Proposed revised criteria for the classification of acute myeloid leukemia. A report of the French-American-British Cooperative Group. Ann Intern Med. **103**:620-5.
28. **Berger, R., L. Theodor, J. Shoham, E. Gokkel, F. Brok-Simoni, K. B. Avraham, N. G. Copeland, N. A. Jenkins, G. Rechavi, and A. J. Simon.** 1996. The characterization and localization of the mouse thymopoietin/lamina- associated polypeptide 2 gene and its alternatively spliced products. Genome Res. **6**:361-70.
29. **Bergeron, D., J. Houde, L. Poliquin, B. Barbeau, and E. Rassart.** 1993. Expression and DNA rearrangement of proto-oncogenes in Cas-Br-E-induced non-T-, non-B-cell leukemias. Leukemia. **7**:954-62.
30. **Bergeron, D., L. Poliquin, J. Houde, B. Barbeau, and E. Rassart.** 1992. Analysis of proviruses integrated in Fli-1 and Evi-1 regions in Cas-Br-E MuLV-induced non-T-, non-B-cell leukemias. Virology. **191**:661-9.
31. **Bergeron, D., L. Poliquin, C. A. Kozak, and E. Rassart.** 1991. Identification of a common viral integration region in Cas-Br-E murine leukemia virus-induced non-T-, non-B-cell lymphomas. J Virol. **65**:7-15.
32. **Berns, A.** 1991. Tumorigenesis in transgenic mice: identification and characterization of synergizing oncogenes. J Cell Biochem. **47**:130-5.
33. **Biegel, J. A., P. S. White, H. N. Marshall, M. Fujimori, E. H. Zackai, C. D. Scher, G. M. Brodeur, and B. S. Emanuel.** 1993. Constitutional 1p36 deletion in a child with neuroblastoma. Am J Hum Genet. **52**:176-82.
34. **Bisogno, T., S. Maurelli, D. Melck, L. De Petrocellis, and V. Di Marzo.** 1997. Biosynthesis, uptake, and degradation of anandamide and palmitoylethanolamide in leukocytes. J Biol Chem. **272**:3315-23.

35. **Blatt, C., D. Aberdam, R. Schwartz, and L. Sachs.** 1988. DNA rearrangement of a homeobox gene in myeloid leukaemic cells. Embo J. **7**:4283-90.
36. **Blenis, J.** 1993. Signal transduction via the MAP kinases: proceed at your own RSK. Proc Natl Acad Sci U S A. **90**:5889-92.
37. **Bloomfield, C. D., O. M. Garson, L. Volin, S. Knuutila, and A. de la Chapelle.** 1985. t(1;3)(p36;q21) in acute nonlymphocytic leukemia: a new cytogenetic-clinicopathologic association. Blood. **66**:1409-13.
38. **Borrow, J., A. M. Shearman, V. P. Stanton, Jr., R. Becher, T. Collins, A. J. Williams, I. Dube, F. Katz, Y. L. Kwong, C. Morris, K. Ohyashiki, K. Toyama, J. Rowley, and D. E. Housman.** 1996. The t(7;11)(p15;p15) translocation in acute myeloid leukaemia fuses the genes for nucleoporin NUP98 and class I homeoprotein HOXA9. Nat Genet. **12**:159-67.
39. **Bos, J. L.** 1989. ras oncogenes in human cancer: a review. Cancer Res. **49**:4682-9.
40. **Bouaboula, M., B. Bourrie, M. Rinaldi-Carmona, D. Shire, G. Le Fur, and P. Casellas.** 1995. Stimulation of cannabinoid receptor CB1 induces krox-24 expression in human astrocytoma cells. J Biol Chem. **270**:13973-80.
41. **Bouaboula, M., C. Poinot-Chazel, B. Bourrie, X. Canat, B. Calandra, M. Rinaldi-Carmona, G. Le Fur, and P. Casellas.** 1995. Activation of mitogen-activated protein kinases by stimulation of the central cannabinoid receptor CB1. Biochem J. **312**:637-41.
42. **Bouaboula, M., C. Poinot-Chazel, J. Marchand, X. Canat, B. Bourrie, M. Rinaldi-Carmona, B. Calandra, G. Le Fur, and P. Casellas.** 1996. Signaling pathway associated with stimulation of CB2 peripheral cannabinoid receptor. Involvement of both mitogen-activated protein kinase and induction of Krox-24 expression. Eur J Biochem. **237**:704-11.
43. **Bouaboula, M., M. Rinaldi, P. Carayon, C. Carillon, B. Delpech, D. Shire, G. Le Fur, and P. Casellas.** 1993. Cannabinoid-receptor expression in human leukocytes. Eur J Biochem. **214**:173-80.
44. **Breuer, M. L., H. T. Cuypers, and A. Berns.** 1989. Evidence for the involvement of pim-2, a new common proviral insertion site, in progression of lymphomas. Embo J. **8**:743-8.
45. **Brewer, J. W., J. L. Cleveland, and L. M. Hendershot.** 1997. A pathway distinct from the mammalian unfolded protein response regulates expression of endoplasmic reticulum chaperones in non-stressed cells. Embo J. **16**:7207-16.
46. **Buchberg, A. M., H. G. Bedigian, N. A. Jenkins, and N. G. Copeland.** 1990. Evi-2, a common integration site involved in murine myeloid leukemogenesis. Mol Cell Biol. **10**:4658-66.
47. **Buckler, A. J., D. D. Chang, S. L. Graw, J. D. Brook, D. A. Haber, P. A. Sharp, and D. E. Housman.** 1991. Exon amplification: a strategy to isolate mammalian genes based on RNA splicing. Proc Natl Acad Sci U S A. **88**:4005-9.
48. **Campbell, S. L., R. Khosravi-Far, K. L. Rossman, G. J. Clark, and C. J. Der.** 1998. Increasing complexity of Ras signaling. Oncogene. **17**:1395-413.
49. **Carayon, P., J. Marchand, D. Dussossoy, J. M. Derocq, O. Jbilo, A. Bord, M. Bouaboula, S. Galiegue, P. Mondiere, G. Penarier, G. L. Fur, T. Defrance, and P. Casellas.** 1998. Modulation and functional involvement of CB2 peripheral cannabinoid receptors during B-cell differentiation. Blood. **92**:3605-15.
50. **Carchman, R. A., L. S. Harris, and A. E. Munson.** 1976. The inhibition of DNA synthesis by cannabinoids. Cancer Res. **36**:95-100.
51. **Ceci, J. D., L. D. Siracusa, N. A. Jenkins, and N. G. Copeland.** 1989. A molecular genetic linkage map of mouse chromosome 4 including the localization of several proto-oncogenes. Genomics. **5**:699-709.

52. **Chang, C. P., W. F. Shen, S. Rozenfeld, H. J. Lawrence, C. Largman, and M. L. Cleary.** 1995. Pbx proteins display hexapeptide-dependent cooperative DNA binding with a subset of Hox proteins. Genes Dev. **9**:663-74.
53. **Chang, S. C., A. E. Erwin, and A. S. Lee.** 1989. Glucose-regulated protein (GRP94 and GRP78) genes share common regulatory domains and are coordinately regulated by common trans-acting factors. Mol Cell Biol. **9**:2153-62.
54. **Chattopadhyay, S. K., B. M. Baroudy, K. L. Holmes, T. N. Fredrickson, M. R. Lander, H. C. d. Morse, and J. W. Hartley.** 1989. Biologic and molecular genetic characteristics of a unique MCF virus that is highly leukemogenic in ecotropic virus-negative mice. Virology. **168**:90-100.
55. **Cheng, N. C., N. Van Roy, A. Chan, M. Beitsma, A. Westerveld, F. Speleman, and R. Versteeg.** 1995. Deletion mapping in neuroblastoma cell lines suggests two distinct tumor suppressor genes in the 1p35-36 region, only one of which is associated with N-myc amplification. Oncogene. **10**:291-7.
56. **Church, D. M., L. T. Banks, A. C. Rogers, S. L. Graw, D. E. Housman, J. F. Gusella, and A. J. Buckler.** 1993. Identification of human chromosome 9 specific genes using exon amplification. Hum Mol Genet. **2**:1915-20.
57. **Clark, S. C., and R. Kamen.** 1987. The human hematopoietic colony-stimulating factors. Science. **236**:1229-37.
58. **Coffman, R. L.** 1982. Surface antigen expression and immunoglobulin gene rearrangement during mouse pre-B cell development. Immunol Rev. **69**:5-23.
59. **Copeland, N. G., and N. A. Jenkins.** 1991. Development and applications of a molecular genetic linkage map of the mouse genome. Trends Genet. **7**:113-8.
60. **Copeland, N. G., and N. A. Jenkins.** Unpublished results. .
61. **Cosman, D.** 1993. The hematopoietin receptor superfamily. Cytokine. **5**:95-106.
62. **Curnow, K. M., L. Pascoe, and P. C. White.** 1992. Genetic analysis of the human type-1 angiotensin II receptor. Mol Endocrinol. **6**:1113-8.
63. **Cuypers, H. T., G. Selten, W. Quint, M. Zijlstra, E. R. Maandag, W. Boelens, P. van Wezenbeek, C. Melief, and A. Berns.** 1984. Murine leukemia virus-induced T-cell lymphomagenesis: integration of proviruses in a distinct chromosomal region. Cell. **37**:141-50.
64. **Cuypers, H. T., G. C. Selten, M. Zijlstra, R. E. de Goede, C. J. Melief, and A. J. Berns.** 1986. Tumor progression in murine leukemia virus-induced T-cell lymphomas: monitoring clonal selections with viral and cellular probes. J Virol. **60**:230-41.
65. **Daaka, Y., T. W. Klein, and H. Friedman.** 1995. Expression of cannabinoid receptor mRNA in murine and human leukocytes. Adv Exp Med Biol. **373**:91-6.
66. **Darnell, J. E., Jr.** 1997. STATs and gene regulation. Science. **277**:1630-5.
67. **Daub, H., F. U. Weiss, C. Wallasch, and A. Ullrich.** 1996. Role of transactivation of the EGF receptor in signalling by G-protein-coupled receptors. Nature. **379**:557-60.
68. **Davis, R. W., M. Thomas, J. Cameron, T. P. St. John, S. Scherer, and R. A. Padgett.** 1980. Rapid DNA isolations for enzymatic and hybridization analysis. Methods Enzymol. **65**:404-11.
69. **de Boer, C. J., J. H. van Krieken, E. Schuuring, and P. M. Kluin.** 1997. Bcl-1/cyclin D1 in malignant lymphoma. Ann Oncol. **8**:109-17.
70. **de Both, N. J., A. Hagemeijer, E. H. Rhijnsburger, M. Vermey, E. van't Hull, and E. M. Smit.** 1981. DMSO-induced terminal differentiation and trisomy 15 in myeloid cell line transformed by the Rauscher murine leukemia virus. Cell Differ. **10**:13-21.
71. **Dechert, U., M. Weber, M. Weber-Schaeuffelen, and E. Wollny.** 1989. Isolation and partial characterization of an 80,000-dalton protein kinase from the microvessels of the porcine brain. J Neurochem. **53**:1268-75.

72. **Dechert, U., P. Weber, B. Konig, C. Ortwein, I. Nilson, W. Linxweiler, E. Wollny, and H. G. Gassen.** 1994. A protein kinase isolated from porcine brain microvessels is similar to a class of heat-shock proteins. Eur J Biochem. **225**:805-9.
73. **Decleve, A., M. Lieberman, J. N. Ihle, P. N. Rosenthal, M. L. Lung, and H. S. Kaplan.** 1978. Physicochemical, biological and serological properties of a leukemogenic virus isolated from cultured RadLV-induced lymphomas of C57BL/Ka mice. Virology. **90**:23-35.
74. **Delwel, R., T. Funabiki, B. L. Kreider, K. Morishita, and J. N. Ihle.** 1993. Four of the seven zinc fingers of the Evi-1 myeloid-transforming gene are required for sequence-specific binding to GA(C/T)AAGA(T/C)AAGATAA. Mol Cell Biol. **13**:4291-300.
75. **Derkinderen, P., M. Toutant, F. Burgaya, M. Le Bert, J. C. Siciliano, V. de Franciscis, M. Gelman, and J. A. Girault.** 1996. Regulation of a neuronal form of focal adhesion kinase by anandamide. Science. **273**:1719-22.
76. **Derocq, J. M., M. Bouaboula, J. Marchand, M. Rinaldi-Carmona, M. Segui, and P. Casellas.** 1998. The endogenous cannabinoid anandamide is a lipid messenger activating cell growth via a cannabinoid receptor-independent pathway in hematopoietic cell lines. FEBS Lett. **425**:419-25.
77. **Derocq, J. M., M. Segui, J. Marchand, G. Le Fur, and P. Casellas.** 1995. Cannabinoids enhance human B-cell growth at low nanomolar concentrations. FEBS Lett. **369**:177-82.
78. **Devane, W. A., L. Hanus, A. Breuer, R. G. Pertwee, L. A. Stevenson, G. Griffin, D. Gibson, A. Mandelbaum, A. Etinger, and R. Mechoulam.** 1992. Isolation and structure of a brain constituent that binds to the cannabinoid receptor. Science. **258**:1946-9.
79. **Dhanasekaran, N., L. E. Heasley, and G. L. Johnson.** 1995. G protein-coupled receptor systems involved in cell growth and oncogenesis. Endocr Rev. **16**:259-70.
80. **Dhanasekaran, N., S. T. Tsim, J. M. Dermott, and D. Onesime.** 1998. Regulation of cell proliferation by G proteins. Oncogene. **17**:1383-94.
81. **Di Majo, V., M. Coppola, S. Rebessi, A. Saran, S. Pazzaglia, L. Pariset, and V. Covelli.** 1996. The influence of sex on life shortening and tumor induction in CBA/Cne mice exposed to X rays or fission neutrons. Radiat Res. **146**:81-7.
82. **Dobner, T., I. Wolf, T. Emrich, and M. Lipp.** 1992. Differentiation-specific expression of a novel G protein-coupled receptor from Burkitt's lymphoma. Eur J Immunol. **22**:2795-9.
83. **Dong, F., C. van Buitenen, K. Pouwels, L. H. Hoefsloot, B. Löwenberg, and I. P. Touw.** 1993. Distinct cytoplasmic regions of the human granulocyte colony-stimulating factor receptor involved in induction of proliferation and maturation. Mol Cell Biol. **13**:7774-81.
84. **Drexler, H. G.** 1998. Review of alterations of the cyclin-dependent kinase inhibitor INK4 family genes p15, p16, p18 and p19 in human leukemia-lymphoma cells. Leukemia. **12**:845-59.
85. **Dreyfus, F., D. Bouscary, J. Melle, V. Ribrag, M. Guesnu, and B. Varet.** 1995. Expression of the Evi-1 gene in myelodysplastic syndromes. Leukemia. **9**:203-5.
86. **Dreyfus, F., B. Sola, S. Fichelson, P. Varlet, M. Charon, P. Tambourin, F. Wendling, and S. Gisselbrecht.** 1990. Rearrangements of the Pim-1, c-myc, and p53 genes in Friend helper virus-induced mouse erythroleukemias. Leukemia. **4**:590-4.
87. **Duby, A. D., K. A. Klein, C. Murre, and J. G. Seidman.** 1985. A novel mechanism of somatic rearrangement predicted by a human T-cell antigen receptor beta-chain complementary DNA. Science. **228**:1204-6.
88. **Dudek, H., and E. P. Reddy.** 1989. Murine myeloid leukemias with aberrant myb loci show heterogeneous expression of novel myb proteins. Oncogene. **4**:1489-95.

89. **Duhrsen, U., J. Stahl, and N. M. Gough.** 1990. In vivo transformation of factor-dependent hemopoietic cells: role of intracisternal A-particle transposition for growth factor gene activation. Embo J. **9**:1087-96.
90. **Duterque-Coquillaud, M., C. Niel, S. Plaza, and D. Stehelin.** 1993. New human erg isoforms generated by alternative splicing are transcriptional activators. Oncogene. **8**:1865-73.
91. **Duyk, G. M., S. W. Kim, R. M. Myers, and D. R. Cox.** 1990. Exon trapping: a genetic screen to identify candidate transcribed sequences in cloned mammalian genomic DNA. Proc Natl Acad Sci U S A. **87**:8995-9.
92. **Dzierzak, E., A. Medvinsky, and M. de Bruijn.** 1998. Qualitative and quantitative aspects of haematopoietic cell development in the mammalian embryo. Immunol Today. **19**:228-36.
93. **Engelman, A.** 1994. Most of the avian genome appears available for retroviral DNA integration. Bioessays. **16**:797-9.
94. **Facci, L., R. Dal Toso, S. Romanello, A. Buriani, S. D. Skaper, and A. Leon.** 1995. Mast cells express a peripheral cannabinoid receptor with differential sensitivity to anandamide and palmitoylethanolamide. Proc Natl Acad Sci U S A. **92**:3376-80.
95. **Fearon, E. R.** 1997. Human cancer syndromes: clues to the origin and nature of cancer. Science. **278**:1043-50.
96. **Feinberg, A. P., and B. Vogelstein.** 1983. A technique for radiolabeling DNA restriction endonuclease fragments to high specific activity. Anal Biochem. **132**:6-13.
97. **Felder, C. C., E. M. Briley, J. Axelrod, J. T. Simpson, K. Mackie, and W. A. Devane.** 1993. Anandamide, an endogenous cannabimimetic eicosanoid, binds to the cloned human cannabinoid receptor and stimulates receptor-mediated signal transduction. Proc Natl Acad Sci U S A. **90**:7656-60.
98. **Felder, C. C., K. E. Joyce, E. M. Briley, J. Mansouri, K. Mackie, O. Blond, Y. Lai, A. L. Ma, and R. L. Mitchell.** 1995. Comparison of the pharmacology and signal transduction of the human cannabinoid CB1 and CB2 receptors. Mol Pharmacol. **48**:443-50.
99. **Felder, C. C., A. Nielsen, E. M. Briley, M. Palkovits, J. Priller, J. Axelrod, D. N. Nguyen, J. M. Richardson, R. M. Riggin, G. A. Koppel, S. M. Paul, and G. W. Becker.** 1996. Isolation and measurement of the endogenous cannabinoid receptor agonist, anandamide, in brain and peripheral tissues of human and rat. FEBS Lett. **393**:231-5.
100. **Felder, C. C., J. S. Veluz, H. L. Williams, E. M. Briley, and L. A. Matsuda.** 1992. Cannabinoid agonists stimulate both receptor- and non-receptor-mediated signal transduction pathways in cells transfected with and expressing cannabinoid receptor clones. Mol Pharmacol. **42**:838-45.
101. **Ferreira, O. C., Jr., V. Planelles, and J. D. Rosenblatt.** 1997. Human T-cell leukemia viruses: epidemiology, biology, and pathogenesis. Blood Rev. **11**:91-104.
102. **Fichelson, S., B. Sola, F. Dreyfus, D. Bordereaux, S. Gisselbrecht, and P. Tambourin.** 1988. Early involvement of the fim-2 and fim-3 regions in mouse myeloblastic leukemogenesis. Leukemia. **2**:143S-150S.
103. **Fowler, M. L., H. Nakai, M. G. Byers, H. Fukushima, R. L. Eddy, W. M. Henry, L. L. Haley, O. B. JS, and T. B. Shows.** 1986. Chromosome 1 localization of the human alpha-L-fucosidase structural gene with a homologous site on chromosome 2. Cytogenet Cell Genet. **43**:103-8.
104. **Fundia, A., N. Gorla, and I. Larripa.** 1994. Spontaneous chromosome aberrations in Fanconi's anemia patients are located at fragile sites and acute myeloid leukemia breakpoints. Hereditas. **120**:47-50.
105. **Galiegue, S., S. Mary, J. Marchand, D. Dussossoy, D. Carriere, P. Carayon, M. Bouaboula, D. Shire, G. Le Fur, and P. Casellas.** 1995. Expression of central and

peripheral cannabinoid receptors in human immune tissues and leukocyte subpopulations. Eur J Biochem. **232**:54-61.

106. **Gerard, C. M., C. Mollereau, G. Vassart, and M. Parmentier.** 1991. Molecular cloning of a human cannabinoid receptor which is also expressed in testis. Biochem J. **279**:129-34.
107. **Gille, H., M. Kortenjann, O. Thomae, C. Moomaw, C. Slaughter, M. H. Cobb, and P. E. Shaw.** 1995. ERK phosphorylation potentiates Elk-1-mediated ternary complex formation and transactivation. Embo J. **14**:951-62.
108. **Gillis, S., and K. A. Smith.** 1977. Long term culture of tumour-specific cytotoxic T cells. Nature. **268**:154-6.
109. **Gisselbrecht, S., S. Fichelson, B. Sola, D. Bordereaux, A. Hampe, C. Andre, F. Galibert, and P. Tambourin.** 1987. Frequent c-fms activation by proviral insertion in mouse myeloblastic leukaemias. Nature. **329**:259-61.
110. **Gottlieb, T. M., and M. Oren.** 1996. p53 in growth control and neoplasia. Biochim Biophys Acta. **1287**:77-102.
111. **Gouilleux, F., C. Pallard, I. Dusanter-Fourt, H. Wakao, L. A. Haldosen, G. Norstedt, D. Levy, and B. Groner.** 1995. Prolactin, growth hormone, erythropoietin and granulocyte-macrophage colony stimulating factor induce MGF-Stat5 DNA binding activity. Embo J. **14**:2005-13.
112. **Graber, M. N., A. Alfonso, and D. L. Gill.** 1996. Ca2+ pools and cell growth: arachidonic acid induces recovery of cells growth-arrested by Ca2+ pool depletion. J Biol Chem. **271**:883-8.
113. **Green, E. L.** 1981. Linkage, recombination and mapping. Oxford University Press, New York, N.Y.
114. **Greenberger, J. S., M. A. Sakakeeny, R. K. Humphries, C. J. Eaves, and R. J. Eckner.** 1983. Demonstration of permanent factor-dependent multipotential (erythroid/neutrophil/basophil) hematopoietic progenitor cell lines. Proc Natl Acad Sci U S A. **80**:2931-5.
115. **Groffen, J., J. R. Stephenson, N. Heisterkamp, A. de Klein, C. R. Bartram, and G. Grosveld.** 1984. Philadelphia chromosomal breakpoints are clustered within a limited region, bcr, on chromosome 22. Cell. **36**:93-9.
116. **Gudermann, T., B. Nurnberg, and G. Schultz.** 1995. Receptors and G proteins as primary components of transmembrane signal transduction. Part 1. G-protein-coupled receptors: structure and function. J Mol Med. **73**:51-63.
117. **Gutkind, J. S.** 1998. Cell growth control by G protein-coupled receptors: from signal transduction to signal integration. Oncogene. **17**:1331-42.
118. **Gutkind, J. S., E. A. Novotny, M. R. Brann, and K. C. Robbins.** 1991. Muscarinic acetylcholine receptor subtypes as agonist-dependent oncogenes. Proc Natl Acad Sci U S A. **88**:4703-7.
119. **Hagemeijer, A., E. M. Smit, F. Govers, and N. J. de Both.** 1982. Trisomy 15 and other nonrandom chromosome changes in Rauscher murine leukemia virus-induced leukemia cell lines. J Natl Cancer Inst. **69**:945-51.
120. **Hamaguchi, M., H. Sakamoto, H. Tsuruta, H. Sasaki, T. Muto, T. Sugimura, and M. Terada.** 1992. Establishment of a highly sensitive and specific exon-trapping system. Proc Natl Acad Sci U S A. **89**:9779-83.
121. **Harris, A. W., A. D. Bankhurst, S. Mason, and N. L. Warner.** 1973. Differentiated functions expressed by cultured mouse lymphoma cells. II. Theta antigen, surface immunoglobulin and a receptor for antibody on cells of a thymoma cell line. J Immunol. **110**:431-8.
122. **Hartley, J. W., and W. P. Rowe.** 1976. Naturally occurring murine leukemia viruses in wild mice: characterization of a new "amphotropic" class. J Virol. **19**:19-25.

123. **Hestdal, K., F. W. Ruscetti, J. N. Ihle, S. E. Jacobsen, C. M. Dubois, W. C. Kopp, D. L. Longo, and J. R. Keller.** 1991. Characterization and regulation of RB6-8C5 antigen expression on murine bone marrow cells. J Immunol. **147**:22-8.
124. **Hirvonen, H., V. Hukkanen, T. T. Salmi, T. T. Pelliniemi, and R. Alitalo.** 1993. L-myc and N-myc in hematopoietic malignancies. Leuk Lymphoma. **11**:197-205.
125. **Holmes, K. L., W. Y. Langdon, T. N. Fredrickson, R. L. Coffman, P. M. Hoffman, J. W. Hartley, and H. C. d. Morse.** 1986. Analysis of neoplasms induced by Cas-Br-M MuLV tumor extracts. J Immunol. **137**:679-88.
126. **Holmes, K. L., E. Palaszynski, T. N. Fredrickson, H. C. d. Morse, and J. N. Ihle.** 1985. Correlation of cell-surface phenotype with the establishment of interleukin 3-dependent cell lines from wild-mouse murine leukemia virus-induced neoplasms. Proc Natl Acad Sci U S A. **82**:6687-91.
127. **Honjo, T., S. Nakai, Y. Nishida, T. Kataoka, Y. Yamawaki-Kataoka, N. Takahashi, M. Obata, A. Shimizu, Y. Yaoita, T. Nikaido, and N. Ishida.** 1981. Rearrangements of immunoglobulin genes during differentiation and evolution. Immunol Rev. **59**:33-67.
128. **Hunter, S. A., and S. H. Burstein.** 1997. Receptor mediation in cannabinoid stimulated arachidonic acid mobilization and anandamide synthesis. Life Sci. **60**:1563-73.
129. **Hunter, T.** 1991. Cooperation between oncogenes. Cell. **64**:249-70.
130. **Hunter, T.** 1997. Oncoprotein networks. Cell. **88**:333-46.
131. **Ichikawa, Y.** 1969. Differentiation of a cell line of myeloid leukemia. J Cell Physiol. **74**:223-34.
132. **Ihle, J. N.** 1995. Cytokine receptor signalling. Nature. **377**:591-4.
133. **Ihle, J. N., and D. Askew.** 1989. Origins and properties of hematopoietic growth factor-dependent cell lines. Int J Cell Cloning. **7**:68-91.
134. **Ihle, J. N., J. Keller, S. Oroszlan, L. E. Henderson, T. D. Copeland, F. Fitch, M. B. Prystowsky, E. Goldwasser, J. W. Schrader, E. Palaszynski, M. Dy, and B. Lebel.** 1983. Biologic properties of homogeneous interleukin 3. I. Demonstration of WEHI-3 growth factor activity, mast cell growth factor activity, p cell-stimulating factor activity, colony-stimulating factor activity, and histamine-producing cell-stimulating factor activity. J Immunol. **131**:282-7.
135. **Ihle, J. N., K. Morishita, T. Matsugi, and C. Bartholomew.** 1990. Insertional mutagenesis and transformation of hematopoietic stem cells. Prog Clin Biol Res. **352**:329-37.
136. **Ihle, J. N., A. Rein, and R. Mural.** 1984. Immunological and virological mechanisms in retrovirus-induced murine leukemogenesis. Viral Oncol. **4**:95-137.
137. **Ikuta, K., T. Kina, I. MacNeil, N. Uchida, B. Peault, Y. H. Chien, and I. L. Weissman.** 1990. A developmental switch in thymic lymphocyte maturation potential occurs at the level of hematopoietic stem cells. Cell. **62**:863-74.
138. **Introna, M., M. Luchetti, M. Castellano, M. Arsura, and J. Golay.** 1994. The myb oncogene family of transcription factors: potent regulators of hematopoietic cell proliferation and differentiation. Semin Cancer Biol. **5**:113-24.
139. **Ishimi, Y., Y. Y. Huang, S. Ohta, F. Hamano, K. Nagai, and Y. Takagaki.** 1996. Promoter region of mouse Tcrg genes. Immunogenetics. **43**:68-71.
140. **Jacks, T., T. S. Shih, E. M. Schmitt, R. T. Bronson, A. Bernards, and R. A. Weinberg.** 1994. Tumour predisposition in mice heterozygous for a targeted mutation in Nf1. Nat Genet. **7**:353-61.
141. **Janssen, J. W., A. C. Steenvoorden, M. Schmidtberger, and C. R. Bartram.** 1988. Activation of the mas oncogene during transfection of monoblastic cell line DNA. Leukemia. **2**:318-20.

142. **Jenkins, J. R., P. Ayton, T. Jones, S. L. Davies, D. L. Simmons, A. L. Harris, D. Sheer, and I. D. Hickson.** 1992. Isolation of cDNA clones encoding the beta isozyme of human DNA topoisomerase II and localisation of the gene to chromosome 3p24. Nucleic Acids Res. **20**:5587-92.
143. **Jenkins, N. A., N. G. Copeland, B. A. Taylor, and B. K. Lee.** 1982. Organization, distribution, and stability of endogenous ecotropic murine leukemia virus DNA sequences in chromosomes of Mus musculus. J Virol. **43**:26-36.
144. **Johansson, B., J. Waldenstrom, S. Hasselblom, and F. Mitelman.** 1995. Waldenstrom's macroglobulinemia with the AML/MDS-associated t(1;3)(p36;q21). Leukemia. **9**:1136-8.
145. **Johnson, G. R.** 1988. Effects of excess granulocyte-macrophage colony stimulating factor (GM- CSF) in mice infected with a GM-CSF retrovirus. Dev Biol Stand. **69**:3-8.
146. **Jolicoeur, P., N. Nicolaiew, L. DesGroseillers, and E. Rassart.** 1983. Molecular cloning of infectious viral DNA from ecotropic neurotropic wild mouse retrovirus. J Virol. **45**:1159-63.
147. **Jones, D. H., and S. C. Winistorfer.** 1992. Sequence specific generation of a DNA panhandle permits PCR amplification of unknown flanking DNA. Nucleic Acids Res. **20**:595-600.
148. **Jonkers, J., and A. Berns.** 1996. Retroviral insertional mutagenesis as a strategy to identify cancer genes. Biochim Biophys Acta. **1287**:29-57.
149. **Jonkers, J., H. C. Korswagen, D. Acton, M. Breuer, and A. Berns.** 1997. Activation of a novel proto-oncogene, Fratl, contributes to progression of mouse T-cell lymphomas. Embo J. **16**:441-50.
150. **Julius, D., T. J. Livelli, T. M. Jessell, and R. Axel.** 1989. Ectopic expression of the serotonin 1c receptor and the triggering of malignant transformation. Science. **244**:1057-62.
151. **Juliusson, G., and M. Merup.** 1998. Cytogenetics in chronic lymphocytic leukemia. Semin Oncol. **25**:19-26.
152. **Justice, M. J., H. C. Morse, 3rd, N. A. Jenkins, and N. G. Copeland.** 1994. Identification of Evi-3, a novel common site of retroviral integration in mouse AKXD B-cell lymphomas. J Virol. **68**:1293-300.
153. **Kaminski, N. E.** 1998. Regulation of the cAMP cascade, gene expression and immune function by cannabinoid receptors. J Neuroimmunol. **83**:124-32.
154. **Kaminski, N. E., M. E. Abood, F. K. Kessler, B. R. Martin, and A. R. Schatz.** 1992. Identification of a functionally relevant cannabinoid receptor on mouse spleen cells that is involved in cannabinoid-mediated immune modulation. Mol Pharmacol. **42**:736-42.
155. **Kato, J. Y., M. Matsuoka, K. Polyak, J. Massague, and C. J. Sherr.** 1994. Cyclic AMP-induced G1 phase arrest mediated by an inhibitor (p27Kip1) of cyclin-dependent kinase 4 activation. Cell. **79**:487-96.
156. **Kawakami, Y., T. W. Klein, C. Newton, J. Y. Djeu, S. Specter, and H. Friedman.** 1988. Suppression by delta-9-tetrahydrocannabinol of interleukin 2-induced lymphocyte proliferation and lymphokine-activated killer cell activity. Int J Immunopharmacol. **10**:485-8.
157. **Kitamura, Y., Y. M. Lee, and J. M. Coffin.** 1992. Nonrandom integration of retroviral DNA in vitro: effect of CpG methylation. Proc Natl Acad Sci U S A. **89**:5532-6.
158. **Klein, T. W., C. Newton, and H. Friedman.** 1998. Cannabinoid receptors and immunity. Immunol Today. **19**:373-81.
159. **Klein, T. W., C. A. Newton, R. Widen, and H. Friedman.** 1985. The effect of delta-9-tetrahydrocannabinol and 11-hydroxy-delta-9- tetrahydrocannabinol on T-lymphocyte and B-lymphocyte mitogen responses. J Immunopharmacol. **7**:451-66.

160. **Koller, R., M. Krall, B. Mock, J. Bies, V. Nazarov, and L. Wolff.** 1996. Mml1, a new common integration site in murine leukemia virus-induced promonocytic leukemias maps to mouse chromosome 10. Virology. **224:**224-34.
161. **Kongsuwan, K., J. Allen, and J. M. Adams.** 1989. Expression of Hox-2.4 homeobox gene directed by proviral insertion in a myeloid leukemia. Nucleic Acids Res. **17:**1881-92.
162. **Konopka, J. B., S. M. Watanabe, and O. N. Witte.** 1984. An alteration of the human c-abl protein in K562 leukemia cells unmasks associated tyrosine kinase activity. Cell. **37:**1035-42.
163. **Koren, H. S., B. S. Handwerger, and J. R. Wunderlich.** 1975. Identification of macrophage-like characteristics in a cultured murine tumor line. J Immunol. **114:**894-7.
164. **Kozak, M.** 1987. Effects of intercistronic length on the efficiency of reinitiation by eucaryotic ribosomes. Mol Cell Biol. **7:**3438-45.
165. **Krantz, S. B.** 1991. Erythropoietin. Blood. **77:**419-34.
166. **Kreider, B. L., S. H. Orkin, and J. N. Ihle.** 1993. Loss of erythropoietin responsiveness in erythroid progenitors due to expression of the Evi-1 myeloid-transforming gene. Proc Natl Acad Sci U S A. **90:**6454-8.
167. **Kretz, K. A., D. Cripe, G. S. Carson, H. Fukushima, and O. B. JS.** 1992. Structure and sequence of the human alpha-L-fucosidase gene and pseudogene. Genomics. **12:**276-80.
168. **Kroon, E., J. Krosl, U. Thorsteinsdottir, S. Baban, A. M. Buchberg, and G. Sauvageau.** 1998. Hoxa9 transforms primary bone marrow cells through specific collaboration with Meis1a but not Pbx1b. Embo J. **17:**3714-25.
169. **Krumlauf, R.** 1994. Hox genes in vertebrate development. Cell. **78:**191-201.
170. **Kuff, E. L., and K. K. Lueders.** 1988. The intracisternal A-particle gene family: structure and functional aspects. Adv Cancer Res. **51:**183-276.
171. **Lammie, G. A., R. Smith, J. Silver, S. Brookes, C. Dickson, and G. Peters.** 1992. Proviral insertions near cyclin D1 in mouse lymphomas: a parallel for BCL1 translocations in human B-cell neoplasms. Oncogene. **7:**2381-7.
172. **Langdon, W. Y., P. M. Hoffman, J. E. Silver, C. E. Buckler, J. W. Hartley, S. K. Ruscetti, and H. C. d. Morse.** 1983. Identification of a spleen focus-forming virus in erythroleukemic mice infected with a wild-mouse ecotropic murine leukemia virus. J Virol. **46:**230-8.
173. **Lanier, L. L., and N. L. Warner.** 1981. Cell cycle related heterogeneity of Ia antigen expression on a murine B lymphoma cell line:analysis by flow cytometry. J Immunol. **126:**626-31.
174. **Largaespada, D. A., C. I. Brannan, N. A. Jenkins, and N. G. Copeland.** 1996. Nf1 deficiency causes Ras-mediated granulocyte/macrophage colony stimulating factor hypersensitivity and chronic myeloid leukaemia. Nat Genet. **12:**137-43.
175. **Largaespada, D. A., J. D. Shaughnessy, Jr., N. A. Jenkins, and N. G. Copeland.** 1995. Retroviral integration at the Evi-2 locus in BXH-2 myeloid leukemia cell lines disrupts Nf1 expression without changes in steady-state Ras- GTP levels. J Virol. **69:**5095-102.
176. **Lau, R. J., D. G. Tubergen, M. Barr, Jr., E. F. Domino, N. Benowitz, and R. T. Jones.** 1976. Phytohemagglutinin-induced lymphocyte transformation in humans receiving delta9-tetrahydrocannabinol. Science. **192:**805-7.
177. **Laureys, G., F. Speleman, G. Opdenakker, Y. Benoit, and J. Leroy.** 1990. Constitutional translocation t(1;17)(p36;q12-21) in a patient with neuroblastoma. Genes Chromosomes Cancer. **2:**252-4.
178. **Ledbetter, J. A., and L. A. Herzenberg.** 1979. Xenogeneic monoclonal antibodies to mouse lymphoid differentiation antigens. Immunol Rev. **47:**63-90.

179. **Lee, M., K. H. Yang, and N. E. Kaminski.** 1995. Effects of putative cannabinoid receptor ligands, anandamide and 2-arachidonyl-glycerol, on immune function in B6C3F1 mouse splenocytes. J Pharmacol Exp Ther. **275:**529-36.
180. **Leenen, P. J., A. M. Jansen, and W. van Ewijk.** 1986. Murine macrophage cell lines can be ordered in a linear differentiation sequence. Differentiation. **32:**157-64.
181. **Leenen, P. J., M. J. Kroos, M. Melis, W. A. Slieker, W. van Ewijk, and H. G. van Eijk.** 1990. Differential inhibition of macrophage proliferation by anti-transferrin receptor antibody ER-MP21: correlation to macrophage differentiation stage. Exp Cell Res. **189:**55-63.
182. **Leenen, P. J., M. Melis, W. A. Slieker, and W. Van Ewijk.** 1990. Murine macrophage precursor characterization. II. Monoclonal antibodies against macrophage precursor antigens. Eur J Immunol. **20:**27-34.
183. **Leslie, K. B., F. Lee, and J. W. Schrader.** 1991. Intracisternal A-type particle-mediated activations of cytokine genes in a murine myelomonocytic leukemia: generation of functional cytokine mRNAs by retroviral splicing events. Mol Cell Biol. **11:**5562-70.
184. **Li, L. J., X. Li, A. Ferrario, N. Rucker, E. S. Liu, S. Wong, C. J. Gomer, and A. S. Lee.** 1992. Establishment of a Chinese hamster ovary cell line that expresses grp78 antisense transcripts and suppresses A23187 induction of both GRP78 and GRP94. J Cell Physiol. **153:**575-82.
185. **Liao, X., A. M. Buchberg, N. A. Jenkins, and N. G. Copeland.** 1995. Evi-5, a common site of retroviral integration in AKXD T-cell lymphomas, maps near Gfi-1 on mouse chromosome 5. J Virol. **69:**7132-7.
186. **Little, E., and A. S. Lee.** 1995. Generation of a mammalian cell line deficient in glucose-regulated protein stress induction through targeted ribozyme driven by a stress-inducible promoter. J Biol Chem. **270:**9526-34.
187. **Loh, E. Y., J. F. Elliott, S. Cwirla, L. L. Lanier, and M. M. Davis.** 1989. Polymerase chain reaction with single-sided specificity: analysis of T cell receptor delta chain. Science. **243:**217-20.
188. **Look, T. A.** 1997. Oncogenic transcription factors in the human acute leukemias. Science. **278:**1059-1064.
189. **Löwenberg, B., and I. P. Touw.** 1993. Hematopoietic growth factors and their receptors in acute leukemia. Blood. **81:**281-92.
190. **Lynn, A. B., and M. Herkenham.** 1994. Localization of cannabinoid receptors and nonsaturable high-density cannabinoid binding sites in peripheral tissues of the rat: implications for receptor-mediated immune modulation by cannabinoids. J Pharmacol Exp Ther. **268:**1612-23.
191. **Maki, R. G., R. L. Eddy, Jr., M. Byers, T. B. Shows, and P. K. Srivastava.** 1993. Mapping of the genes for human endoplasmic reticular heat shock protein gp96/grp94. Somat Cell Mol Genet. **19:**73-81.
192. **Maki, R. G., L. J. Old, and P. K. Srivastava.** 1990. Human homologue of murine tumor rejection antigen gp96: 5'-regulatory and coding regions and relationship to stress-induced proteins. Proc Natl Acad Sci U S A. **87:**5658-62.
193. **Marrero, M. B., B. Schieffer, W. G. Paxton, L. Heerdt, B. C. Berk, P. Delafontaine, and K. E. Bernstein.** 1995. Direct stimulation of Jak/STAT pathway by the angiotensin II AT1 receptor. Nature. **375:**247-50.
194. **Marshall, C. J.** 1995. Specificity of receptor tyrosine kinase signaling: transient versus sustained extracellular signal-regulated kinase activation. Cell. **80:**179-85.
195. **Marth, J. D., R. W. Overell, K. E. Meier, E. G. Krebs, and R. M. Perlmutter.** 1988. Translational activation of the lck proto-oncogene. Nature. **332:**171-3.
196. **Matsuda, L. A.** 1997. Molecular aspects of cannabinoid receptors. Crit Rev Neurobiol. **11:**143-66.

197. **Matsuda, L. A., and T. I. Bonner.** 1995. Molecular biology of the cannabinoid receptor. Academic Press, San Diego, CA.
198. **Matsuda, L. A., S. J. Lolait, M. J. Brownstein, A. C. Young, and T. I. Bonner.** 1990. Structure of a cannabinoid receptor and functional expression of the cloned cDNA. Nature. **346**:561-4.
199. **Matsugi, T., B. L. Kreider, R. Delwel, J. L. Cleveland, D. S. Askew, and J. N. Ihle.** 1995. The Evi-1 zinc finger myeloid transforming protein binds to genomic fragments containing (GATA)n sequences. Oncogene. **11**:191-8.
200. **Mayo, M. W., X. Y. Wang, P. A. Algate, G. F. Arana, P. E. Hoyle, L. S. Steelman, and J. A. McCubrey.** 1995. Synergy between AUUUA motif disruption and enhancer insertion results in autocrine transformation of interleukin-3-dependent hematopoietic cells. Blood. **86**:3139-50.
201. **Mazzarella, R. A., and M. Green.** 1987. ERp99, an abundant, conserved glycoprotein of the endoplasmic reticulum, is homologous to the 90-kDa heat shock protein (hsp90) and the 94-kDa glucose regulated protein (GRP94). J Biol Chem. **262**:8875-83.
202. **McCormick, T. S., K. S. McColl, and C. W. Distelhorst.** 1997. Mouse lymphoma cells destined to undergo apoptosis in response to thapsigargin treatment fail to generate a calcium-mediated grp78/grp94 stress response. J Biol Chem. **272**:6087-92.
203. **Melo, J. V.** 1996. The molecular biology of chronic myeloid leukaemia. Leukemia. **10**:751-6.
204. **Menoret, A., K. Meflah, and J. Le Pendu.** 1994. Expression of the 100-kda glucose-regulated protein (GRP100/endoplasmin) is associated with tumorigenicity in a model of rat colon adenocarcinoma. Int J Cancer. **56**:400-5.
205. **Metcalf, D.** 1989. The molecular control of cell division, differentiation commitment and maturation in haemopoietic cells. Nature. **339**:27-30.
206. **Migliaccio, G., A. R. Migliaccio, B. L. Kreider, G. Rovera, and J. W. Adamson.** 1989. Selection of lineage-restricted cell lines immortalized at different stages of hematopoietic differentiation from the murine cell line 32D. J Cell Biol. **109**:833-41.
207. **Miles, C., M. J. Sanchez, A. Sinclair, and E. Dzierzak.** 1997. Expression of the Ly-6E.1 (Sca-1) transgene in adult hematopoietic stem cells and the developing mouse embryo. Development. **124**:537-47.
208. **Milot, E., A. Belmaaza, E. Rassart, and P. Chartrand.** 1994. Association of a host DNA structure with retroviral integration sites in chromosomal DNA. Virology. **201**:408-12.
209. **Minami, M., K. Poussin, C. Brechot, and P. Paterlini.** 1995. A novel PCR technique using Alu-specific primers to identify unknown flanking sequences from the human genome. Genomics. **29**:403-8.
210. **Miura, Y., O. Miura, J. N. Ihle, and N. Aoki.** 1994. Activation of the mitogen-activated protein kinase pathway by the erythropoietin receptor. J Biol Chem. **269**:29962-9.
211. **Miyajima, A., T. Kitamura, N. Harada, T. Yokota, and K. Arai.** 1992. Cytokine receptors and signal transduction. Annu Rev Immunol. **10**:295-331.
212. **Miyamoto, S., H. Teramoto, J. S. Gutkind, and K. M. Yamada.** 1996. Integrins can collaborate with growth factors for phosphorylation of receptor tyrosine kinases and MAP kinase activation: roles of integrin aggregation and occupancy of receptors. J Cell Biol. **135**:1633-42.
213. **Moreau-Gachelin, F., A. Tavitian, and P. Tambourin.** 1988. Spi-1 is a putative oncogene in virally induced murine erythroleukaemias. Nature. **331**:277-80.
214. **Morishita, K., E. Parganas, C. Bartholomew, N. Sacchi, M. B. Valentine, S. C. Raimondi, M. M. Le Beau, and J. N. Ihle.** 1990. The human Evi-1 gene is located on chromosome 3q24-q28 but is not rearranged in three cases of acute nonlymphocytic leukemias containing t(3;5)(q25;q34) translocations. Oncogene Res. **5**:221-31.

215. **Morishita, K., E. Parganas, T. Matsugi, and J. N. Ihle.** 1992. Expression of the Evi-1 zinc finger gene in 32Dc13 myeloid cells blocks granulocytic differentiation in response to granulocyte colony-stimulating factor. Mol Cell Biol. **12**:183-9.
216. **Morishita, K., E. Parganas, C. L. William, M. H. Whittaker, H. Drabkin, J. Oval, R. Tactle, M. B. Valentine, and J. N. Ihle.** 1992. Activation of EVI1 gene expression in human acute myelogenous leukemias by translocations spanning 300-400 kilobases on chromosome band 3q26. Proc Natl Acad Sci U S A. **89**:3937-41.
217. **Morishita, K., D. S. Parker, M. L. Mucenski, N. A. Jenkins, N. G. Copeland, and J. N. Ihle.** 1988. Retroviral activation of a novel gene encoding a zinc finger protein in IL-3-dependent myeloid leukemia cell lines. Cell. **54**:831-40.
218. **Moskow, J. J., F. Bullrich, K. Huebner, I. O. Daar, and A. M. Buchberg.** 1995. Meis1, a PBX1-related homeobox gene involved in myeloid leukemia in BXH-2 mice. Mol Cell Biol. **15**:5434-43.
219. **Mucenski, M. L., B. A. Taylor, J. N. Ihle, J. W. Hartley, H. C. d. Morse, N. A. Jenkins, and N. G. Copeland.** 1988. Identification of a common ecotropic viral integration site, Evi-1, in the DNA of AKXD murine myeloid tumors. Mol Cell Biol. **8**:301-8.
220. **Muller, A. M., A. Medvinsky, J. Strouboulis, F. Grosveld, and E. Dzierzak.** 1994. Development of hematopoietic stem cell activity in the mouse embryo. Immunity. **1**:291-301.
221. **Muller, M. M., S. Ruppert, W. Schaffner, and P. Matthias.** 1988. A cloned octamer transcription factor stimulates transcription from lymphoid-specific promoters in non-B cells. Nature. **336**:544-51.
222. **Munro, S., K. L. Thomas, and M. Abu-Shaar.** 1993. Molecular characterization of a peripheral receptor for cannabinoids. Nature. **365**:61-5.
223. **Murison, G., C. B. Chubb, S. Maeda, M. A. Gemmell, and E. Huberman.** 1987. Cannabinoids induce incomplete maturation of cultured human leukemia cells. Proc Natl Acad Sci U S A. **84**:5414-8.
224. **Nahas, G. G., A. Morishima, and B. Desoize.** 1977. Effects of cannabinoids on macromolecular synthesis and replication of cultured lymphocytes. Fed Proc. **36**:1748-52.
225. **Nahas, G. G., N. Suciu-Foca, J. P. Armand, and A. Morishima.** 1974. Inhibition of cellular mediated immunity in marihuana smokers. Science. **183**:419-20.
226. **Nakai, A., T. Kawatani, S. Ohi, H. Kawasaki, T. Yoshimori, Y. Tashiro, Y. Miyata, I. Yahara, M. Satoh, and K. Nagata.** 1995. Expression and phosphorylation of BiP/GRP78, a molecular chaperone in the endoplasmic reticulum, during the differentiation of a mouse myeloblastic cell line. Cell Struct Funct. **20**:33-9.
227. **Nakamura, T., D. A. Largaespada, M. P. Lee, L. A. Johnson, K. Ohyashiki, K. Toyama, S. J. Chen, C. L. Willman, I. M. Chen, A. P. Feinberg, N. A. Jenkins, N. G. Copeland, and J. D. Shaughnessy, Jr.** 1996. Fusion of the nucleoporin gene NUP98 to HOXA9 by the chromosome translocation t(7;11)(p15;p15) in human myeloid leukaemia. Nat Genet. **12**:154-8.
228. **Nakamura, T., D. A. Largaespada, J. D. Shaughnessy, Jr., N. A. Jenkins, and N. G. Copeland.** 1996. Cooperative activation of Hoxa and Pbx1-related genes in murine myeloid leukaemias. Nat Genet. **12**:149-53.
229. **Nason-Burchenal, K., and L. Wolff.** 1993. Activation of c-myb is an early bone-marrow event in a murine model for acute promonocytic leukemia. Proc Natl Acad Sci U S A. **90**:1619-23.
230. **Nazarov, V., and L. Wolff.** 1995. Novel integration sites at the distal 3' end of the c-myb locus in retrovirus-induced promonocytic leukemias. J Virol. **69**:3885-8.

231. **Nicchitta, C. V.** 1998. Biochemical, cell biological and immunological issues surrounding the endoplasmic reticulum chaperone GRP94/gp96. Curr Opin Immunol. **10**:103-9.
232. **Nichols, J., and S. D. Nimer.** 1992. Transcription factors, translocations, and leukemia. Blood. **80**:2953-63.
233. **Nicholson, S. E., A. C. Oates, A. G. Harpur, A. Ziemiecki, A. F. Wilks, and J. E. Layton.** 1994. Tyrosine kinase JAK1 is associated with the granulocyte-colony-stimulating factor receptor and both become tyrosine-phosphorylated after receptor activation. Proc Natl Acad Sci U S A. **91**:2985-8.
234. **North, M. A., P. Sanseau, A. J. Buckler, D. Church, A. Jackson, K. Patel, J. Trowsdale, and H. Lehrach.** 1993. Efficiency and specificity of gene isolation by exon amplification. Mamm Genome. 4:466-74.
235. **Padua, R. A., B. A. Guinn, A. I. Al-Sabah, M. Smith, C. Taylor, T. Pettersson, S. Ridge, G. Carter, D. White, D. Oscier, S. Chevret, and R. West.** 1998. RAS, FMS and p53 mutations and poor clinical outcome in myelodysplasias: a 10-year follow-up. Leukemia. **12**:887-92.
236. **Palacios, R., and M. Steinmetz.** 1985. Il-3-dependent mouse clones that express B-220 surface antigen, contain Ig genes in germ-line configuration, and generate B lymphocytes in vivo. Cell. **41**:727-34.
237. **Parrish, J. E., and D. L. Nelson.** 1993. Methods for finding genes. A major rate-limiting step in positional cloning. Genet Anal Tech Appl. **10**:29-41.
238. **Peppelenbosch, M. P., R. G. Qiu, A. M. de Vries-Smits, L. G. Tertoolen, S. W. de Laat, F. McCormick, A. Hall, M. H. Symons, and J. L. Bos.** 1995. Rac mediates growth factor-induced arachidonic acid release. Cell. **81**:849-56.
239. **Perkins, A., K. Kongsuwan, J. Visvader, J. M. Adams, and S. Cory.** 1990. Homeobox gene expression plus autocrine growth factor production elicits myeloid leukemia. Proc Natl Acad Sci U S A. **87**:8398-402.
240. **Pertwee, R. G.** 1995. Cannabinoid receptors, 1 ed. Academic Press, London.
241. **Pertwee, R. G.** 1995. Pharmalogical, physiological and clinical implications of the discovery of cannabinoid receptors: an overview, p. 1-34. *In* R. Pertwee (ed.), Cannabinoid receptors. Academic press, London.
242. **Petersen, B. H., J. Graham, and L. Lemberger.** 1976. Marihuana, tetrahydrocannabinol and T-cell function. Life Sci. **19**:395-400.
243. **Pettit, D. A., D. L. Anders, M. P. Harrison, and G. A. Cabral.** 1996. Cannabinoid receptor expression in immune cells. Adv Exp Med Biol. **402**:119-29.
244. **Pevny, L., C. S. Lin, D. A. V, M. C. Simon, S. H. Orkin, and F. Costantini.** 1995. Development of hematopoietic cells lacking transcription factor GATA-1. Development. **121**:163-72.
245. **Pevny, L., M. C. Simon, E. Robertson, W. H. Klein, S. F. Tsai, D. A. V, S. H. Orkin, and F. Costantini.** 1991. Erythroid differentiation in chimaeric mice blocked by a targeted mutation in the gene for transcription factor GATA-1. Nature. **349**:257-60.
246. **Pierce, J. H., P. P. Di Fiore, S. A. Aaronson, M. Potter, J. Pumphrey, A. Scott, and J. N. Ihle.** 1985. Neoplastic transformation of mast cells by Abelson-MuLV: abrogation of IL-3 dependence by a nonautocrine mechanism. Cell. **41**:685-93.
247. **Ploemacher, R. E., P. L. van Soest, and A. Boudewijn.** 1993. Autocrine transforming growth factor beta 1 blocks colony formation and progenitor cell generation by hemopoietic stem cells stimulated with steel factor. Stem Cells. **11**:336-47.
248. **Ploemacher, R. E., P. L. van Soest, H. Voorwinden, and A. Boudewijn.** 1993. Interleukin-12 synergizes with interleukin-3 and steel factor to enhance recovery of murine hemopoietic stem cells in liquid culture. Leukemia. **7**:1381-8

249. **Poirier, Y., C. Kozak, and P. Jolicoeur.** 1988. Identification of a common helper provirus integration site in Abelson murine leukemia virus-induced lymphoma DNA. J Virol. **62**:3985-92.
250. **Porcher, C., W. Swat, K. Rockwell, Y. Fujiwara, F. W. Alt, and S. H. Orkin.** 1996. The T cell leukemia oncoprotein SCL/tal-1 is essential for development of all hematopoietic lineages. Cell. **86**:47-57.
251. **Pross, S. H., Y. Nakano, S. McHugh, R. Widen, T. W. Klein, and H. Friedman.** 1992. Contrasting effects of THC on adult murine lymph node and spleen cell populations stimulated with mitogen or anti-CD3 antibody. Immunopharmacol Immunotoxicol. **14**:675-87.
252. **Quint, W., W. Boelens, P. van Wezenbeek, T. Cuypers, E. R. Maandag, G. Selten, and A. Berns.** 1984. Generation of AKR mink cell focus-forming viruses: a conserved single- copy xenotrope-like provirus provides recombinant long terminal repeat sequences. J Virol. **50**:432-8.
253. **Rabbitts, T. H.** 1994. Chromosomal translocations in human cancer. Nature. **372**:143-9.
254. **Ralph, P., M. K. Ho, P. B. Litcofsky, and T. A. Springer.** 1983. Expression and induction in vitro of macrophage differentiation antigens on murine cell lines. J Immunol. **130**:108-14.
255. **Ralph, P., J. Prichard, and M. Cohn.** 1975. Reticulum cell sarcoma: an effector cell in antibody-dependent cell-mediated immunity. J Immunol. **114**:898-905.
256. **Raschke, W. C., S. Baird, P. Ralph, and I. Nakoinz.** 1978. Functional macrophage cell lines transformed by Abelson leukemia virus. Cell. **15**:261-7.
257. **Ratner, L., B. Thielan, and T. Collins.** 1987. Sequences of the 5' portion of the human c-sis gene: characterization of the transcriptional promoter and regulation of expression of the protein product by 5' untranslated mRNA sequences. Nucleic Acids Res. **15**:6017-36.
258. **Renault, B., J. Lieman, D. Ward, K. Krauter, and R. Kucherlapati.** 1995. Localization of the human achaete-scute homolog gene (ASCL1) distal to phenylalanine hydroxylase (PAH) and proximal to tumor rejection antigen (TRA1) on chromosome 12q22-q23. Genomics. **30**:81-3.
259. **Rimokh, R., J. P. Rouault, K. Wahbi, M. Gadoux, M. Lafage, E. Archimbaud, C. Charrin, O. Gentilhomme, D. Germain, J. Samarut, and et al.** 1991. A chromosome 12 coding region is juxtaposed to the MYC protooncogene locus in a t(8;12)(q24;q22) translocation in a case of B-cell chronic lymphocytic leukemia. Genes Chromosomes Cancer. **3**:24-36.
260. **Rinaldi-Carmona, M., F. Barth, M. Heaulme, D. Shire, B. Calandra, C. Congy, S. Martinez, J. Maruani, G. Neliat, D. Caput, and et al.** 1994. SR141716A, a potent and selective antagonist of the brain cannabinoid receptor. FEBS Lett. **350**:240-4.
261. **Rinaldi-Carmona, M., F. Barth, J. Millan, J. M. Derocq, P. Casellas, C. Congy, D. Oustric, M. Sarran, M. Bouaboula, B. Calandra, M. Portier, D. Shire, J. C. Breliere, and G. L. Le Fur.** 1998. SR 144528, the first potent and selective antagonist of the CB2 cannabinoid receptor. J Pharmacol Exp Ther. **284**:644-50.
262. **Rohdewohld, H., H. Weiher, W. Reik, R. Jaenisch, and M. Breindl.** 1987. Retrovirus integration and chromatin structure: Moloney murine leukemia proviral integration sites map near DNase I-hypersensitive sites. J Virol. **61**:336-43.
263. **Ross, P. C., R. A. Figler, M. H. Corjay, C. M. Barber, N. Adam, D. R. Harcus, and K. R. Lynch.** 1990. RTA, a candidate G protein-coupled receptor: cloning, sequencing, and tissue distribution. Proc Natl Acad Sci U S A. **87**:3052-6.
264. **Rowley, J. T., and P. T. Rowley.** 1990. Tetrahydrocannabinol inhibits adenyl cyclase in human leukemia cells. Life Sci. **46**:217-22.

265. **Ru, M., C. Shustik, and E. Rassart.** 1993. Graffi murine leukemia virus: molecular cloning and characterization of the myeloid leukemia-inducing agent. J Virol. **67**:4722-31.
266. **Salem, M., R. Delwel, I. Touw, L. Mahmoud, and B. Löwenberg.** 1988. Human AML colony growth in serum-free culture. Leuk Res. **12**:157-65.
267. **Sambrook, J., E. F. Fritsch, and T. Maniatis.** 1989. Molecular Cloning: a laboratory manual, 2 ed. Cold Spring Harbor Laboratory Press, Cold Spring Harbor, NY.
268. **Sanger, F., and A. R. Coulson.** 1975. A rapid method for determining sequences in DNA by primed synthesis with DNA polymerase. J Mol Biol. **94**:441-8.
269. **Savarese, T. M., and C. M. Fraser.** 1992. In vitro mutagenesis and the search for structure-function relationships among G protein-coupled receptors. Biochem J. **283**:1-19.
270. **Schatz, A. R., M. Lee, R. B. Condie, J. T. Pulaski, and N. E. Kaminski.** 1997. Cannabinoid receptors CB1 and CB2: a characterization of expression and adenylate cyclase modulation within the immune system. Toxicol Appl Pharmacol. **142**:278-87.
271. **Scherdin, U., K. Rhodes, and M. Breindl.** 1990. Transcriptionally active genome regions are preferred targets for retrovirus integration. J Virol. **64**:907-12.
272. **Schwarz, H., F. J. Blanco, and M. Lotz.** 1994. Anadamide, an endogenous cannabinoid receptor agonist inhibits lymphocyte proliferation and induces apoptosis. J Neuroimmunol. **55**:107-15.
273. **Schweifer, N., P. J. Valk, R. Delwel, R. Cox, F. Francis, S. Meier-Ewert, H. Lehrach, and D. P. Barlow.** 1997. Characterization of the C3 YAC contig from proximal mouse chromosome 17 and analysis of allelic expression of genes flanking the imprinted Igf2r gene. Genomics. **43**:285-97.
274. **Seger, R., and E. G. Krebs.** 1995. The MAPK signaling cascade. Faseb J. **9**:726-35.
275. **Setoguchi, M., Y. Higuchi, S. Yoshida, N. Nasu, Y. Miyazaki, S. Akizuki, and S. Yamamoto.** 1989. Insertional activation of N-myc by endogenous Moloney-like murine retrovirus sequences in macrophage cell lines derived from myeloma cell line-macrophage hybrids. Mol Cell Biol. **9**:4515-22.
276. **Severne, Y., S. Wieland, W. Schaffner, and S. Rusconi.** 1988. Metal binding 'finger' structures in the glucocorticoid receptor defined by site-directed mutagenesis. Embo J. **7**:2503-8.
277. **Shannon, K. M., O. C. P, G. A. Martin, D. Paderanga, K. Olson, P. Dinndorf, and F. McCormick.** 1994. Loss of the normal NF1 allele from the bone marrow of children with type 1 neurofibromatosis and malignant myeloid disorders. N Engl J Med. **330**:597-601.
278. **Shen-Ong, G. L., H. C. d. Morse, M. Potter, and J. F. Mushinski.** 1986. Two modes of c-myb activation in virus-induced mouse myeloid tumors. Mol Cell Biol. **6**:380-92.
279. **Shen-Ong, G. L., and L. Wolff.** 1987. Moloney murine leukemia virus-induced myeloid tumors in adult BALB/c mice: requirement of c-myb activation but lack of v-abl involvement. J Virol. **61**:3721-5.
280. **Sherr, C. J.** 1990. Colony-stimulating factor-1 receptor. Blood. **75**:1-12.
281. **Shevach, E. M., J. D. Stobo, and I. Green.** 1972. Immunoglobulin and theta-bearing murine leukemias and lymphomas. J Immunol. **108**:1146-51.
282. **Shih, C. C., J. P. Stoye, and J. M. Coffin.** 1988. Highly preferred targets for retrovirus integration. Cell. **53**:531-7.
283. **Shimizu, K., H. Ichikawa, A. Tojo, Y. Kaneko, N. Maseki, Y. Hayashi, M. Ohira, S. Asano, and M. Ohki.** 1993. An ets-related gene, ERG, is rearranged in human myeloid leukemia with t(16;21) chromosomal translocation. Proc Natl Acad Sci U S A. **90**:10280-4.
284. **Shire, D., B. Calandra, M. Rinaldi-Carmona, D. Oustric, B. Pessegue, O. Bonnin-Cabanne, G. Le Fur, D. Caput, and P. Ferrara.** 1996. Molecular cloning, expression

and function of the murine CB2 peripheral cannabinoid receptor. Biochim Biophys Acta. **1307**:132-6.

285. **Shire, D., C. Carillon, M. Kaghad, B. Calandra, M. Rinaldi-Carmona, G. Le Fur, D. Caput, and P. Ferrara.** 1995. An amino-terminal variant of the central cannabinoid receptor resulting from alternative splicing. J Biol Chem. **270**:3726-31.
286. **Shivdasani, R. A., E. L. Mayer, and S. H. Orkin.** 1995. Absence of blood formation in mice lacking the T-cell leukaemia oncoprotein tal-1/SCL. Nature. **373**:432-4.
287. **Shivdasani, R. A., and S. H. Orkin.** 1996. The transcriptional control of hematopoiesis. Blood. **87**:4025-39.
288. **Side, L. E., P. D. Emanuel, B. Taylor, J. Franklin, P. Thompson, R. P. Castleberry, and K. M. Shannon.** 1998. Mutations of the NF1 gene in children with juvenile myelomonocytic leukemia without clinical evidence of neurofibromatosis, type 1. Blood. **92**:267-72.
289. **Siglin, J. C., C. M. Weghorst, D. E. Rodwell, and J. E. Klaunig.** 1995. Gender-dependent differences in hepatic tumor promotion in diethylnitrosamine initiated infant B6C3F1 mice by alpha- hexachlorocyclohexane. J Toxicol Environ Health. **44**:235-45.
290. **Silver, J., and C. E. Buckler.** 1986. A preferred region for integration of Friend murine leukemia virus in hematopoietic neoplasms is closely linked to the Int-2 oncogene. J Virol. **60**:1156-8.
291. **Silver, J., and V. Keerikatte.** 1989. Novel use of polymerase chain reaction to amplify cellular DNA adjacent to an integrated provirus. J Virol. **63**:1924-8.
292. **Sinclair, A., B. Daly, and E. Dzierzak.** 1996. The Ly-6E.1 (Sca-1) gene requires a 3' chromatin-dependent region for high-level gamma-interferon-induced hematopoietic cell expression. Blood. **87**:2750-61.
293. **Sinclair, A. M., and E. A. Dzierzak.** 1993. Cloning of the complete Ly-6E.1 gene and identification of DNase I hypersensitive sites corresponding to expression in hematopoietic cells. Blood. **82**:3052-62.
294. **Slipetz, D. M., O. N. GP, L. Favreau, C. Dufresne, M. Gallant, Y. Gareau, D. Guay, M. Labelle, and K. M. Metters.** 1995. Activation of the human peripheral cannabinoid receptor results in inhibition of adenylyl cyclase. Mol Pharmacol. **48**:352-61.
295. **Sola, B., S. Fichelson, D. Bordereaux, P. E. Tambourin, and S. Gisselbrecht.** 1986. fim-1 and fim-2: two new integration regions of Friend murine leukemia virus in myeloblastic leukemias. J Virol. **60**:718-25.
296. **Sorensen, A. B., M. Duch, H. W. Amtoft, P. Jorgensen, and F. S. Pedersen.** 1996. Sequence tags of provirus integration sites in DNAs of tumors induced by the murine retrovirus SL3-3. J Virol. **70**:4063-70.
297. **Sorensen, A. B., M. Duch, P. Jorgensen, and F. S. Pedersen.** 1993. Amplification and sequence analysis of DNA flanking integrated proviruses by a simple two-step polymerase chain reaction method. J Virol. **67**:7118-24.
298. **Springer, T., G. Galfre, D. S. Secher, and C. Milstein.** 1979. Mac-1: a macrophage differentiation antigen identified by monoclonal antibody. Eur J Immunol. **9**:301-6.
299. **Srivastava, P. K., Y. T. Chen, and L. J. Old.** 1987. 5'-structural analysis of genes encoding polymorphic antigens of chemically induced tumors. Proc Natl Acad Sci U S A. **84**:3807-11.
300. **Srivastava, P. K., C. A. Kozak, and L. J. Old.** 1988. Chromosomal assignment of the gene encoding the mouse tumor rejection antigen gp96. Immunogenetics. **28**:205-7.
301. **Storch, T. G., and T. M. Chused.** 1984. Sex and H-2 haplotype control the resistance of CBA-BALB hybrids to the induction of T cell lymphoma by Moloney leukemia virus. J Immunol. **133**:2797-800.

302. **Suarez, H. G., D. Russo, R. Wicker, J. A. Du Villard, S. Filetti, B. Caillou, and M. Schlumberger.** 1995. Role of somatic genetic alterations of the cAMP pathway in thyroid hyperfunctioning tumorigenesis. J. Cell. Biochem. Suppl. **19A**:44.
303. **Sui, X., S. B. Krantz, M. You, and Z. Zhao.** 1998. Synergistic activation of MAP kinase (ERK1/2) by erythropoietin and stem cell factor is essential for expanded erythropoiesis. Blood. **92**:1142-9.
304. **Tanigawa, T., L. Robb, A. R. Green, and C. G. Begley.** 1994. Constitutive expression of the putative transcription factor SCL associated with proviral insertion in the myeloid leukemic cell line WEHI-3BD-. Cell Growth Differ. **5**:557-61.
305. **Thangavelu, M., W. G. Finn, K. K. Yelavarthi, H. H. Roenigk, Jr., E. Samuelson, L. Peterson, T. M. Kuzel, and S. T. Rosen.** 1997. Recurring structural chromosome abnormalities in peripheral blood lymphocytes of patients with mycosis fungoides/Sezary syndrome. Blood. **89**:3371-7.
306. **Thompson, F. H., J. Emerson, S. Olson, R. Weinstein, S. A. Leavitt, S. P. Leong, S. Emerson, J. M. Trent, M. A. Nelson, S. E. Salmon, and et al.** 1995. Cytogenetics of 158 patients with regional or disseminated melanoma. Subset analysis of near-diploid and simple karyotypes. Cancer Genet Cytogenet. **83**:93-104.
307. **Thompson, F. H., R. Taetle, J. M. Trent, Y. Liu, K. Massey-Brown, K. M. Scott, R. S. Weinstein, J. C. Emerson, D. S. Alberts, and M. A. Nelson.** 1997. Band 1p36 abnormalities and t(1;17) in ovarian carcinoma. Cancer Genet Cytogenet. **96**:106-10.
308. **Tian, S. S., P. Lamb, H. M. Seidel, R. B. Stein, and J. Rosen.** 1994. Rapid activation of the STAT3 transcription factor by granulocyte colony-stimulating factor. Blood. **84**:1760-4.
309. **Tomonari, K.** 1988. A rat antibody against a structure functionally related to the mouse T- cell receptor/T3 complex. Immunogenetics. **28**:455-8.
310. **Trakhtenbrot, L., R. Krauthgamer, P. Resnitzky, and N. Haran-Ghera.** 1988. Deletion of chromosome 2 is an early event in the development of radiation-induced myeloid leukemia in SJL/J mice. Leukemia. **2**:545-50.
311. **Treisman, R.** 1995. Journey to the surface of the cell: Fos regulation and the SRE. Embo J. **14**:4905-13.
312. **Triglia, T., M. G. Peterson, and D. J. Kemp.** 1988. A procedure for in vitro amplification of DNA segments that lie outside the boundaries of known sequences. Nucleic Acids Res. **16**:8186.
313. **Tsichlis, P. N., P. G. Strauss, and M. A. Lohse.** 1985. Concerted DNA rearrangements in Moloney murine leukemia virus-induced thymomas: a potential synergistic relationship in oncogenesis. J Virol. **56**:258-67.
314. **Valk, P., S. Verbakel, Y. Vankan, S. Hol, S. Mancham, R. Ploemacher, A. Mayen, B. Löwenberg, and R. Delwel.** 1997. Anandamide, a natural ligand for the peripheral cannabinoid receptor is a novel synergistic growth factor for hematopoietic cells. Blood. **90**:1448-57.
315. **Valk, P. J., S. Hol, Y. Vankan, J. N. Ihle, D. Askew, N. A. Jenkins, D. J. Gilbert, N. G. Copeland, N. J. de Both, B. Löwenberg, and R. Delwel.** 1997. The genes encoding the peripheral cannabinoid receptor and alpha-L-fucosidase are located near a newly identified common virus integration site, Evi11. J Virol. **71**:6796-804.
316. **Valk, P. J. M., and R. Delwel.** 1998. The peripheral cannabinoid receptor, Cb2, in retrovirally-induced leukemic transformation and normal hematopoiesis. Leuk Lymph. **32**:29-44.
317. **Valk, P. J. M., M. Joosten, Y. Vankan, B. Löwenberg, and R. Delwel.** 1997. A rapid RT-PCR based method to isolate complementary DNA fragments flanking retrovirus integration sites. Nucl. Acids Res. **25**:4419-4421.
318. **Valk, P. J. M., Y. Vankan, M. Joosten, N. A. Jenkins, N. G. Copeland, B. Löwenberg, and R. Delwel.** 1999. Retroviral insertions in a novel common virus

integration site *Evi12* upstream of *Tra1/Grp94* frequently coincide with insertions in the gene encoding the peripheral cannabinoid receptor. J Virol. *in press*.

319. **van Biesen, T., B. E. Hawes, D. K. Luttrell, K. M. Krueger, K. Touhara, E. Porfiri, M. Sakaue, L. M. Luttrell, and R. J. Lefkowitz.** 1995. Receptor-tyrosine-kinase- and G beta gamma-mediated MAP kinase activation by a common signalling pathway. Nature. **376**:781-4.
320. **van Biesen, T., L. M. Luttrell, B. E. Hawes, and R. J. Lefkowitz.** 1996. Mitogenic signaling via G protein-coupled receptors. Endocr Rev. **17**:698-714.
321. **van Lohuizen, M., and A. Berns.** 1990. Tumorigenesis by slow-transforming retroviruses--an update. Biochim Biophys Acta. **1032**:213-35.
322. **van Lohuizen, M., S. Verbeek, P. Krimpenfort, J. Domen, C. Saris, T. Radaszkiewicz, and A. Berns.** 1989. Predisposition to lymphomagenesis in pim-1 transgenic mice: cooperation with c-myc and N-myc in murine leukemia virus-induced tumors. Cell. **56**:673-82.
323. **van Lohuizen, M., S. Verbeek, B. Scheijen, E. Wientjens, H. van der Gulden, and A. Berns.** 1991. Identification of cooperating oncogenes in E mu-myc transgenic mice by provirus tagging. Cell. **65**:737-52.
324. **van 't Veer, L. J., L. A. van den Berg-Bakker, R. P. Hermens, R. L. Deprez, and P. I. Schrier.** 1988. High frequency of mas oncogene activation detected in the NIH3T3 tumorigenicity assay. Oncogene Res. **3**:247-54.
325. **Viguie, F., J. P. Marie, F. Poler, and A. Bernadou.** 1986. Three cases of preleukemic myelodysplastic disorders with the same translocation t(1;3). Cancer Genet Cytogenet. **19**:213-8.
326. **Vijaya, S., D. L. Steffen, and H. L. Robinson.** 1986. Acceptor sites for retroviral integrations map near DNase I-hypersensitive sites in chromatin. J Virol. **60**:683-92.
327. **Vogelstein, B., and K. W. Kinzler.** 1993. The multistep nature of cancer. Trends Genet. **9**:138-41.
328. **Walker, L. C., T. S. Ganesan, S. Dhut, B. Gibbons, T. A. Lister, J. Rothbard, and B. D. Young.** 1987. Novel chimaeric protein expressed in Philadelphia positive acute lymphoblastic leukaemia. Nature. **329**:851-3.
329. **Warner, N. L., M. J. Daley, J. Richey, and C. Spellman.** 1979. Flow cytometry analysis of murine B cell lymphoma differentiation. Immunol Rev. **48**:197-243.
330. **Warner, N. L., M. A. Moore, and D. Metcalf.** 1969. A transplantable myelomonocytic leukemia in BALB-c mice: cytology, karyotype, and muramidase content. J Natl Cancer Inst. **43**:963-82.
331. **Wartmann, M., D. Campbell, A. Subramanian, S. H. Burstein, and R. J. Davis.** 1995. The MAP kinase signal transduction pathway is activated by the endogenous cannabinoid anandamide. FEBS Lett. **359**:133-6.
332. **Weber-Nordt, R. M., R. Mertelsmann, and J. Finke.** 1998. The JAK-STAT pathway: signal transduction involved in proliferation, differentiation and transformation. Leuk Lymphoma. **28**:459-67.
333. **Weinberg, R.** 1993. Tumor suppressor genes. Neuron. **11**:191-6.
334. **Whang-Peng, J., T. Knutsen, E. S. Jaffe, S. M. Steinberg, M. Raffeld, W. P. Zhao, P. Duffey, K. Condron, T. Yano, and D. L. Longo.** 1995. Sequential analysis of 43 patients with non-Hodgkin's lymphoma: clinical correlations with cytogenetic, histologic, immunophenotyping, and molecular studies. Blood. **85**:203-16.
335. **Whitehead, I., H. Kirk, and R. Kay.** 1995. Expression cloning of oncogenes by retroviral transfer of cDNA libraries. Mol Cell Biol. **15**:704-10.
336. **Wilkie, T. M., D. J. Gilbert, A. S. Olsen, X. N. Chen, T. T. Amatruda, J. R. Korenberg, B. J. Trask, P. de Jong, R. R. Reed, M. I. Simon, and et al.** 1992. Evolution of the mammalian G protein alpha subunit multigene family. Nat Genet. **1**:85-91.

337. **Williamson, B. D., and C. L. Rutherford.** 1994. Enrichment-mediated PCR amplification of an unknown DNA fragment flanking a known sequence. Biotechniques. **17:**670, 672.
338. **Withers-Ward, E. S., Y. Kitamura, J. P. Barnes, and J. M. Coffin.** 1994. Distribution of targets for avian retrovirus DNA integration in vivo. Genes Dev. **8:**1473-87.
339. **Witthuhn, B. A., F. W. Quelle, O. Silvennoinen, T. Yi, B. Tang, O. Miura, and J. N. Ihle.** 1993. JAK2 associates with the erythropoietin receptor and is tyrosine phosphorylated and activated following stimulation with erythropoietin. Cell. **74:**227-36.
340. **Wolff, L.** 1997. Contribution of oncogenes and tumor suppressor genes to myeloid leukemia. Biochim Biophys Acta. **1332:**F67-104.
341. **Wong, P. M., S. W. Chung, C. E. Dunbar, D. M. Bodine, S. Ruscetti, and A. W. Nienhuis.** 1989. Retrovirus-mediated transfer and expression of the interleukin-3 gene in mouse hematopoietic cells result in a myeloproliferative disorder. Mol Cell Biol. **9:**798-808.
342. **Xu, G. F., O. C. P, D. Viskochil, R. Cawthon, M. Robertson, M. Culver, D. Dunn, J. Stevens, R. Gesteland, R. White, and et al.** 1990. The neurofibromatosis type 1 gene encodes a protein related to GAP. Cell. **62:**599-608.
343. **Yamagata, N., C. Shimazaki, T. Kikuta, H. Hirai, T. Sumikuma, Y. Sudo, E. Ashihara, H. Goto, T. Inaba, N. Fujita, and M. Nakagawa.** 1997. A translocation between 3q21 and 12q24 in a patient with minimally differentiated acute myeloid leukemia (AML-M0). Cancer Genet Cytogenet. **97:**90-3.
344. **Ymer, S., W. Q. Tucker, C. J. Sanderson, A. J. Hapel, H. D. Campbell, and I. G. Young.** 1985. Constitutive synthesis of interleukin-3 by leukaemia cell line WEHI-3B is due to retroviral insertion near the gene. Nature. **317:**255-8.
345. **Yoshida, K., K. Nemoto, M. Nishimura, and M. Seki.** 1993. Exacerbating factors of radiation-induced myeloid leukemogenesis. Leuk Res. **17:**437-40.
346. **Young, D., G. Waitches, C. Birchmeier, O. Fasano, and M. Wigler.** 1986. Isolation and characterization of a new cellular oncogene encoding a protein with multiple potential transmembrane domains. Cell. **45:**711-9.
347. **Zachary, I.** 1997. Focal adhesion kinase. Int J Biochem Cell Biol. **29:**929-34.
348. **Zani, V. J., N. Asou, D. Jadayel, J. M. Heward, J. Shipley, E. Nacheva, K. Takasuki, D. Catovsky, and M. J. Dyer.** 1996. Molecular cloning of complex chromosomal translocation t(8;14;12)(q24.1;q32.3;q24.1) in a Burkitt lymphoma cell line defines a new gene (BCL7A) with homology to caldesmon. Blood. **87:**3124-34.

SUMMARY

Summary

Leukemia is characterized by the accumulation of neoplastic cells in bone marrow, blood and other tissues. The overproduction of these non-functional blood cells interferes with normal blood cell formation or hematopoiesis. It has been generally accepted that leukemogenesis, like the development of other cancers, is a sequential activation of proto-oncogenes or inactivation of tumor suppressor genes. Mutant oncoproteins affect proliferation, differentiation, maturation, apoptosis, or survival of hematopoietic cells, by interference with the signaling pathways from hematopoietic growth factor receptor towards the nucleus, and by nuclear transcriptional regulation. Proto-oncogenes represent growth factors, growth factor receptors, signaling molecules, transcription factors, cell cycle regulators and molecules necessary for RNA and DNA synthesis. Inappropriate expression of these genes is caused by genetic abnormalities, including chromosomal translocations, viral infections, or point mutations. By cloning recurrent chromosomal translocations from human acute myeloid and acute lymphoid leukemias, many proto-oncogenes have been identified. Tumor suppressor genes are recognized on the basis of loss of heterozygosity in human hereditary cancer syndromes. Since these procedures used for the identification of proto-oncogenes and tumor suppressor genes are limited, other methods to analyze these genes are explored.

Retroviral insertional mutagenesis is an elegant and effective method to trace proto-oncogenes and tumor suppressor genes in mouse leukemias. Slow transforming murine leukemia viruses (MuLV), e.g., Cas-Br-M MuLV, are potent retroviruses to induce leukemia in susceptible mice. During their life cycle, the retroviruses integrate into the host blood cell genome and transform these hematopoietic cells by interference with normal gene expression. Recurrent retroviral insertion in an identical chromosomal locus on the host genome in independent leukemias is indicative for the location of proto-oncogenes or tumor suppressor genes. These loci are called common virus integration sites (VISs). Common VISs have been identified in genes encoding hematopoietic growth factors (HGFs), HGF receptors, signaling molecules, cyclins, and transcription factors. The main objectives of the research described in this thesis, is the identification of novel proto-oncogenes or tumor suppressor genes involved in myeloid leukemia development by using retroviral insertional mutagenesis (Chapters 2, 3, 4 and 5) and the characterization of these genes (Chapters 6 and 7).

Chapter 1 begins with a brief introduction about the current understanding of hematopoiesis and leukemogenesis. Thereafter, an overview is given about retroviral insertional mutagenesis, mainly focused on retrovirally-induced myeloid mouse leukemias.

Chapter 2 describes the identification of a novel common VIS, *Evi11*, in the Cas-Br-M MuLV-induced myeloid leukemia cell lines NFS78 and NFS107, and novel Cas-Br-M MuLV-induced primary leukemias (Chaptér 6). By interspecific backcross

analysis, it was shown that *Evi11* resides on mouse chromosome 4, in a region that shares homology with human chromosome 1p36. The genes encoding the peripheral cannabinoid receptor Cb2 and α-L-fucosidase were demonstrated to be located near *Evi11*, by using a novel exon trapping system. *Cb2* was suggested to be the target proto-oncogene for retroviral interference, since proviruses in *Evi11* were localized within the intron or the 3' untranslated region of *Cb2* (Chapter 4) and it was shown that provirus caused aberrant expression of the *Cb2* mRNA in the myeloid cell lines NFS107 and NFS78. Cb2 is a seven-transmembrane receptor, which belongs to the superfamily of G protein-coupled receptors. The Cb2 receptor is one of two distinct receptors, i.e., Cb1 and Cb2, which both specifically interact with cannabinoids, including Δ^9-tetrahydrocannabinol, the major active ingredient of marijuana. Cb2 is also referred to as the peripheral cannabinoid receptor, since its gene is primarily expressed in peripheral tissues.

Common VISs are visualized by Southern blot analysis with DNA probes flanking individual VISs. In **Chapter 3** the development of a novel method for the rapid isolation of VIS-flanking cDNA fragments from Cas-Br-M MuLV-induced leukemias or tumor cell lines is described. The power of this newly established method was confirmed by the isolation of cDNA fragments representing the known common VIS *Evi1*, the gene encoding the ets-transcription factor Erg, which is involved in the recurrent t(16;21) in human acute myeloid leukemia, and the novel common VIS *Evi12* (Chapters 4 and 5).

In **Chapter 4**, experiments are described concerning the isolation, cloning and sequencing of the exact sites of proviral integration in *Evi11* from multiple novel Cas-Br-M MuLV-induced primary leukemias. It is demonstrated that in these leukemias most of the proviruses inserted in the 3' untranslated region of the *Cb2* gene. These Cas-Br-M MuLV insertions resemble classical examples of common VISs resulting in proto-oncogene activation caused by proviral enhancement. This suggests that in the case of *Evi11* proviral enhancement results in overexpression of the Cb2 receptor.

Furthermore, in an attempt to isolate *Evi11/Cb2*-cooperating genes, by using the technique described in Chapter 3, a novel common VIS *Evi12* was identified. By interspecific backcross analysis it was shown that *Evi12* is located on mouse chromosome 10 in a region homologous to human chromosome 12q22-24. Nucleotide sequence analysis and database searches demonstrated that *Evi12* is located upstream of the gene encoding tumor rejection antigen *Tra1/Grp94*, which is a molecular chaperone involved in protein folding in the endoplasmic reticulum. However, *Tra1/Grp94* expression is not altered by proviral insertion in *Evi12*, indicating that not *Tra1/Grp94* but another gene is the target proto-oncogene in *Evi12*. Interestingly, the high coincidence of rearrangements as a result of Cas-Br-M MuLV insertion in *Evi11* and *Evi12* strongly suggests cooperation of *Cb2* and an *Evi12*-related proto-oncogene in retrovirally-induced leukemogenesis.

In **Chapter 5**, a new panel of 74 Cas-Br-M MuLV-induced leukemias initiated in NIH/Swiss mice is described. This new panel was established for analysis of known

and the isolation of new common VISs, and for identification of novel proto-oncogenes. The leukemias were characterized by gross pathology of the mice, and morphological analysis and immunophenotyping of the retrovirally-induced leukemias. In this panel most of the leukemias were myeloid; however, many T-cell leukemias were identified. The frequencies of known common VISs were determined. *Evi11* (12%) and *Evi12* (20%) (Chapter 4) proviral integrations were demonstrated in myeloid and T-cel leukemias. These data may indicate that mutations in *Evi11* and *Evi12* represent early events in leukemogenesis in multipotent progenitor cells. This well-characterized panel of new leukemias has been used successfully in experiments described in Chapters 2 and 4.

In **Chapter 6**, it is shown by RNase protection analysis that the *Cb2* gene encodes the hematopoietic cannabinoid receptor, since *Cb2* mRNA expression is restricted to hematopoietic tissues and cell lines representing multiple blood cell lineages. Furthermore, *in vitro* cell cultures show that anandamide, an endogenous ligand for the peripheral cannabinoid receptor, is a synergistic growth factor for hematopoietic cells in serum-free culture.

Experiments in **Chapter 7** demonstrate that synergistic stimulation of proliferation of erythropoietin (Epo)-dependent hematopoietic cells by Epo and anandamide results in enhanced mitogen-activated protein kinase (MAPK) activation and increased expression of the immediate-early MAPK-target gene c-*fos*. Experiments with Cb2-specific antagonist show that besides a Cb2 receptor-independent mechanism, anandamide may also stimulate proliferation of hematopoietic cell lines through Cb2 receptor-dependent mechanisms.

SAMENVATTING

Samenvatting

Leukemie of bloedkanker wordt gekenmerkt door een opeenhoping van abnormale neoplastische bloedcellen in het beenmerg, bloed en andere organen. Deze ophoping van niet-functionele cellen interfereert met de normale bloedcelvorming, de hematopoiese. Leukemie ontstaat door de activatie van proto-oncogenen of de inactivatie van tumor suppressor genen. Abnormale expressie van deze kankergenen stoort de normale processen van hematopoietische cellen, zoals bijvoorbeeld groei of proliferatie, differentiatie, apoptose of overleving van de bloedcellen. Proto-oncogenen en tumor suppressor genen coderen voor groeifactoren, groeifactor receptoren, signaal transductie moleculen, transcriptie factoren, celcyclus eiwitten en moleculen die betrokken zijn bij DNA en RNA synthese. De afwijkingen in het expressiepatroon van deze genen worden veroorzaakt door genetische abnormaliteiten, zoals bijvoorbeeld specifieke chromosomale translocaties, virale infecties en puntmutaties. Veel proto-oncogenen zijn geïdentificeerd in humane acute myeloide alsmede lymphoide leukemieën door klonering van chromosomale breekpunten. Tumorsuppressor genen worden herkend door het verlies van heterozygositeit in vormen van humane erfelijke kanker. Omdat deze procedures, die worden gebruikt voor de identificatie van proto-oncogenen en tumorsuppressor genen, gelimiteerd zijn, worden andere mogelijke methodes onderzocht.
Retrovirale insertionele mutagenese is een elegante en effectieve methode om oncogenen en tumor suppressor genen te traceren in muizenleukemieën. Langzaam transformerende muizenretrovirussen (MuLV), zoals bijvoorbeeld Cas-Br-M MuLV, zijn effectieve mutagenen om leukemie te induceren in tumorgevoelige muizen. Gedurende hun levenscyclus integreren de retrovirussen in het genoom van bloedcellen van de gastheer en transformeren deze hematopoietische cellen door interferentie met de normale specifieke genexpressie. Herhaalde retrovirale insertie in een identiek chromosomaal locus op het gastheer genoom in meerdere onafhankelijke leukemieën is indicatief voor de lokalisatie van een proto-oncogen of een tumor suppressor gen. Deze loci worden 'common virus integration sites (VISs)' genoemd. Common VISs zijn geïdentificeerd in genen die coderen voor hematopoietische groeifactoren (HGFn), HGF receptoren, signaal moleculen, moleculen betrokken bij de celcyclus en transcriptiefactoren. Het doel van het onderzoek beschreven in dit proefschrift is de identificatie van nieuwe proto-oncogenen of tumorsuppressor genen betrokken bij de ontwikkeling van myeloide leukemie (Hoofdstukken 2, 3, 4 en 5) en de karakterisering van deze nieuwe genen (Hoofdstukken 6 en 7).
Hoofdstuk 1 begint met een korte introductie over de huidige inzichten van hematopoiese en leukemogenese. Vervolgens wordt retrovirale insertionele mutagenese besproken met de nadruk op retroviraal geïnduceerde myeloide muizenleukemieën.
Hoofdstuk 2 beschrijft de identificatie van een nieuwe common VIS, *Evi11*, in de Cas-Br-M MuLV-geïnduceerde myeloide leukemie cellijnen NFS78 en NFS107, en

nieuwe Cas-Br-M MuLV-geïnduceerde primaire leukemieën (Hoofdstuk 6). Door middel van interspecifieke backcross analyse is het aangetoond dat *Evi11* gelokaliseerd is op muis chromosoom 4, in een regio die homoloog is met chromosoom 1p36 bij de mens. De genen die coderen voor de perifere cannabinoide receptor Cb2 en α-L-fucosidase werden geïdentificeerd nabij *Evi11* door gebruik te maken van een zogenaamde exon trap. De resultaten in dit hoofdstuk impliceerden dat *Cb2* het proto-oncogen in *Evi11*, is omdat provirussen in *Evi11* integreerden in het intron of in het 3' niet-getransleerde-deel van het *Cb2* gen en het geïntegreerde provirus abnormale expressie veroorzaakte van *Cb2* mRNA in de myeloide cellijnen NFS78 en NFS107. Cb2 is een zeven-transmembraan receptor die behoort tot de familie van G eiwit-gekoppelde receptoren. Cb2 is één van twee receptoren, namelijk Cb1 en Cb2, die beiden specifiek cannabinoiden binden, zoals bijvoorbeeld Δ^9-tetrahydrocannabinol, de voornaamste actieve component in marijuana. Cb2 wordt ook wel de perifere cannabinoide receptor genoemd, omdat het *Cb2* gen vooral in perifere organen tot expressie komt.

Common VISs worden aangetoond door middel van Southern blot analysis met DNA probes flankerend aan individuele VISs. In **Hoofdstuk 3** wordt de ontwikkeling van een nieuwe methode om snel VIS flankerende cDNA fragmenten te isoleren uit Cas-Br-M MuLV-geïnduceerde leukemieën of tumor cellijnen. De kracht van deze nieuwe methode werd bevestigd door het isoleren van cDNA fragmenten overeenkomend met de bekende common VIS *Evi1*, het gen coderend voor de ets-transcriptiefactor *Erg*, dat betrokken is bij de specifieke translocatie t(16;21) in humane acute myeloide leukemie en de nieuwe common VIS *Evi12* (Hoofstukken 4 en 5).

In **Hoofdstuk 4** staan experimenten beschreven betreffende de isolatie, de klonering en het sequencen van de exacte plaatsen van integratie van provirus in *Evi11* in meerdere nieuwe Cas-Br-M MuLV-geïnduceerde leukemieën. Hiermee wordt aangetoond dat de meeste provirussen integreerden in het 3' niet-getransleerde-deel van het *Cb2* gen. Deze Cas-Br-M MuLV integraties komen overeen met klassieke voorbeelden van common VISs die een verhoogde expressie van het proto-oncogen veroorzaken, wat suggereert dat in het geval van *Evi11* provirus insertie resulteert in overexpressie van Cb2 receptor.

In dit hoofdstuk staat verder de identificatie van een nieuwe common VIS, *Evi12*, beschreven, die werd geïsoleerd in een poging om *Evi11/Cb2* coöpererende genen te traceren. Hierbij werd gebruik gemaakt van de techniek beschreven in Hoofdstuk 3. Door middel van interspecifieke backcross analyse werd aangetoond dat *Evi12* gelokaliseerd is op muis chromosoom 10 in een regio die homoloog is met chromosoom 12q22-24 bij de mens. Nucleotide sequentie analyse en het raadplegen van verschillende databanken demonstreerden dat *Evi12* nabij het gen dat codeert voor *Tra1/Grp94* is gelokaliseerd. Het tumor rejection antigen Tra1/Grp94 is een moleculair chaperone eiwit dat betrokken is bij eiwitvouwing in het endoplasmatisch reticulum. De expressie van *Tra1/Grp94* is echter niet gestoord door integratie van provirus in *Evi12*. Dit wijst erop dat niet *Tra1/Grp94*, maar een ander gen, het proto-

oncogen in *Evi12* is. Echter, de hoge coincidentie van rearrangeringen veroorzaakt door Cas-Br-M MuLV integraties in *Evi11* en *Evi12* suggereert dat *Cb2* coöpereert met een *Evi12* gerelateerd proto-oncogen in Cas-Br-M MuLV-geïnduceerde leukemogenese.

Hoofdstuk 5 beschrijft de karakterisering van een nieuw panel van 74 Cas-Br-M MuLV-geïnduceerde leukemieën geïnitieerd in NIH/Swiss muizen. Dit panel van leukemieën werd gegenereerd met het doel meerdere myeloide leukemieën te verkrijgen voor de analyse van bekende en isolatie van nieuwe common VISs alsmede de identificatie van nieuwe proto-oncogenen. De door middel van retrovirus geïnduceerde leukemieën zijn gekarakteriseerd door middel van pathologie op de muizen, morfologische analyse en de bepaling van het immunophenotype van de leukemieën. In dit panel bleken de meeste leukemieën myeloid; echter, meerdere T-cell leukemieën werden eveneens aangetoond. De frequenties van bekende 'common VISs' werden bepaald in de nieuwe leukemieën. Retrovirale inserties in *Evi11* (12%) en *Evi12* (20%) (Hoofstuk 4) werden gevonden in zowel myeloide als T-cell leukemieën. Deze data suggereren dat mutaties in *Evi11* en *Evi12* vroeg plaatsvinden in leukemogenese in een pluripotente voorlopercel. Dit goed gekarakteriseerde panel van Cas-Br-M MuLV-geïnduceerde leukemieën is met succes gebruikt in de experimenten beschreven in Hoofdstukken 2 en 4.

In **Hoofdstuk 6** wordt door middel van RNase protectie analyse aangetoond dat het *Cb2* gen codeert voor de hematopoietische cannabinoide receptor, omdat *Cb2* mRNA alleen wordt aangetoond in hematopoietische organen en cellijnen die de verschillende bloed cellijnen representeren. Vervolgens werd in *in vitro* celkweek aangetoond dat anandamide, een endogeen ligand voor de perifere cannabinoide receptor, een synergistische groeifactor is voor hematopoietische cellen in serum-vrij medium.

Experimenten in **Hoofdstuk 7** tonen aan dat de synergistische stimulatie van de proliferatie van erythropoetine (Epo)-afhankelijke hematopoietische cellen door Epo en anandamide wordt gereflecteerd in een verhoogde mitogen-activated kinase (MAPK) activatie en een verhoogde expressie van het proto-oncogen c-*fos*, waarvan bekend is dat het gereguleerd wordt door MAPK. Experimenten met Cb2 receptor specifiek antagonist demonstreren dat anandamide de proliferatie van hematopoietische cellijnen kan stimuleren door middel van zowel receptor-afhankelijke als receptor-onafhankelijke mechanismen.

De studies beschreven in dit proefschrift kunnen leiden tot een beter inzicht in de tumorbiologie van bepaalde vormen van acute myeloide leukemie, waarin de perifere cannabinoide receptor Cb2 een rol speelt. De resultaten verkregen in het muizen-model zullen daarvoor verder moeten worden vertaald naar de patiënt. In vervolg studies zal daarom patientenmateriaal worden onderzocht op abnormale expressie van Cb2. De indentificatie van nieuwe proto-oncogenen, zoals *Cb2*, kunnen uiteindelijk in de kliniek gebruikt worden voor het stellen van betrouwbare diagnoses en prognoses en voor de juiste behandeling van de patiënt.

CURRICULUM VITAE

Curriculum vitae

Name	:	Peter J.M. Valk, born on October 26, 1966 in Delft
1979-84	:	St. Stanislas College, Delft, The Netherlands
1984-88	:	Hoge School Rotterdam eo, Delft, The Netherlands Hoger Laboratorium Onderwijs *Cum laude* Technician Molecular Genetics/Biotechnology Main subject: Hoofdgroep Maatschappelijke technologie TNO, Zeist, The Netherlands Title: Production of podophyllotoxins from plant cell cultures of *Podophyllum peltatum* and *Linum flavum*
1988-90	:	Military Service
1990-93	:	Leiden University, Leiden, The Netherlands *Cum laude* Msc Molecular Genetics Main subjects: -Institute of Molecular Plant Sciences, Leiden University, Leiden, The Netherlands. Title: Conjugative DNA transfer by *Agrobacterium tumefaciens*. -Department of Biological Sciences, Kent State University, Kent, OH, USA. Title: The effect of corticotropin and cAMP on the 3ßHSD-activity in cultured mouse adrenal glands. -Institute of Cell Biology and Genetics, Erasmus University Rotterdam, Rotterdam, The Netherlands. Title: The transcription factor Oct6.
1993-99	:	Institute of Hematology, Erasmus University Rotterdam, Rotterdam, The Netherlands PhD

Title: Identification of novel proto-oncogenes in murine myeloid leukemias by retroviral insertional mutagenesis - The peripheral cannabinoid receptor.

1999- : Dutch Cancer Society - Koningin Wilhelmina Fonds
Research fellowship

Children's Hospital, Boston, U.S.A.
Division of Hematology/Oncology (Prof. dr. S. Orkin)
Academic Hospital Utrecht
Department of Immunology (Prof. dr. H.C. Clevers)

LIST OF PUBLICATIONS

List of publications

Schweifer N, Valk PJM, Delwel R, Cox R, Francis F, Meier-Ewert S, Lehrach H, Barlow DP
Characterization of the C3 YAC contig from proximal mouse chromosome 17 and analysis of allelic expression of genes flanking the imprinted Igf2r gene.
Genomics 43, 285-297, 1997.

Valk PJM, Verbakel S, Vankan Y, Hol S, Mancham S, Ploemacher R, Mayen A, Löwenberg B, Delwel R
Anandamide, a natural ligand for the peripheral cannabinoid receptor is a novel synergistic growth factor for hematopoietic cells.
Blood 90, 1448-1457, 1997.

Valk PJM, Hol S, Vankan Y, Ihle JN, Askew D, Jenkins NA, Gilbert DJ, Copeland NG, de Both NJ, Löwenberg B, Delwel R
The genes encoding the peripheral cannabinoid receptor and alpha-L-fucosidase are located near a newly identified common virus integration site, *Evi11.*
Journal of Virology 71 (9), 6796-6804, 1997.

Valk, PJM, Joosten, M, Vankan, Y, Löwenberg B, Delwel R
A rapid RT-PCR based method to isolate complementary DNA fragments flanking retrovirus integration sites.
Nucleic Acids Research 25 (21), 4419-4421, 1997.

Valk PJM and Delwel R
The peripheral cannabinoid receptor, *Cb2*, in leukemic transformation and hematopoiesis. *Leukemia and Lymphoma* 32(1-2), 29-44, 1998.

Valk PJM, Vankan Y, Joosten M, Jenkins NA, Copeland NG, Löwenberg B, Delwel, R
Retroviral insertions in a novel common virus integration site *Evi12* upstream of *Tra1/Grp94* frequently coincide with insertions in the gene encoding the peripheral cannabinoid receptor *Cnr2.*
Journal of Virology 73(5), 1999: in press.

Joosten M, Valk PJM, Vankan Y, de Both N, Löwenberg B, Delwel R
Generation of a novel panel of Cas-Br-M MuLV-induced hematopoietic malignancies: Immunophenotypes of *Evi1*, *Evi11/Cb2*, and *Evi12* transformed leukemias.
Submitted for publication.

Valk PJM, Verbakel S, von Lindern M, Löwenberg B and Delwel R.
Enhancement of proliferation of Epo-stimulated cells by anandamide correlates with increased activation of the mitogen-activated protein kinases ERK1 and ERK2.
Submitted for publication.

DANKWOORD

Dankwoord

Langs deze weg wil ik iedereen die een bijdrage heeft geleverd aan mijn proefschrift hartelijk bedanken. Ik wil graag een aantal personen bij naam noemen.
Allereerst mijn co-promotor **Ruud Delwel**. Ruud, jouw bijdrage aan de het werk beschreven in dit proefschrift is van onschatbare waarde geweest. Je gedrevenheid en enthousiasme waren in de afgelopen jaren een enorme stimulans voor mij. Je wist me steeds weer op een prettige manier te motiveren, ook in moeilijke tijden. Niet alleen voor het werk, maar ook voor privé-zaken had je een luisterend oor. Ik zal het maf doen op het lab en het bomen over de resultaten (met een biertje) gaan missen. Ik heb het zeer gewaardeerd om met je samen te werken. Bedankt voor alles, we houden contact en succes met het vervolg van het onderzoek.
Mijn promotor **Bob Löwenberg** wil ik bedanken voor zijn steun en zijn opbouwende kritiek tijdens de werkbesprekingen op de zeer vroege vrijdagmorgen. Bob, bedankt voor het in het spoor houden van de Delwel-trein.
Prof. dr. A.J.M. Berns, Prof. dr. A.D.M.E. Osterhaus en Prof. dr. J.A. Grootegoed, als leden van de kleine commissie, wil ik bedanken voor het kritisch doorlezen van mijn proefschrift.
Dit proefschrift is mede tot stand gekomen door de tomeloze inzet en het grote enthousiasme van mijn paranimfe, **Yolanda Vankan**. Yolanda, we zijn samen op hoge toppen geweest, maar ook in diepe dalen. Ondanks het feit dat we nog wel eens een andere mening hadden over de inhoud van een experiment, heb ik het heel prettig gevonden om met je samen te werken. Hartelijk dank.
Dit proefschrift is het bewijs dat een stage lopen onder de bezielende leiding van mijn tweede paranimf en vriend **Ronald Zwart**, zeer waardevol kan zijn. Ronald, bedankt voor het aanleren van de grondbeginselen van de moleculaire biologie. We houden contact.
Veel van de celkweek en signaal transductie proeven zijn uitgevoerd door **Sandra Verbakel**. Sandra, bedankt voor je inzet en de vele experimenten die je hebt gedaan. Ik bewonder de nauwkeurigheid waarmee je werkt.
Marieke Joosten wil ik bedanken voor haar bijdrage aan het werk. Marieke, probeer het enthousiasme dat je uitstraalt tot aan het einde van jouw promotie vast te houden.
Samantha Hol heeft, samen met Yolanda, aan de basis gestaan van het werk aan Cb2. Samatha, bedankt voor al het werk dat je verzet hebt tijdens de eerste jaren van mijn promotieonderzoek.
R. Ploemacher, A. Mayen, S. Mancham, E.M.E. Smit, D. Meijer, K. van Lom, M. von Lindern en N. de Both wil ik bedanken voor hun bijdrage.
I also would like to thank N.G. Copeland, N.A. Jenkins, D.J. Gilbert, and H. Morse III (Frederick, MD), S. Munro (Cambridge, England), I.D. Hickson (Oxford, England), J. Cleveland and J.N. Ihle (Memphis, TN), D. Askew (Cincinnati, OH), J.W. Hartley and T.I. Bonner (Bethesda, MD), and P. Casellas (Montpellier, France) for their contributions.

Marion van de Broek wil ik bedanken voor de prettige sfeer in de groep Delwel en de helpende hand wanneer dat nodig was.
Derrick Louz bedank ik voor de mannenbabbels in het promohok, onder het genot van een heerlijk bakkie koffie.
Mijn zeer goede vriend en lotgenoot **John de Koning** wil ik bedanken voor alles. John, we hebben een hoop leuke maar ook moeilijke momenten samen gedeeld, ik zal je missen. Ik wil je nogmaals feliciteren met je promotie en wens je heel veel succes als fellow in San Francisco. We houden contact.
Ivo Touw wil ik bedanken voor zijn betrokkenheid bij ons werk. Ivo, bedankt voor alle steun die je me hebt gegeven de afgelopen jaren.
Karola van Rooyen bedank ik voor het maken van vele figuren en dia's. Karola, ondanks alle traumatische ervaringen, wist je van mijn kladjes prachtige figuren en kleurrijke dia's te maken. Succes met de wetensgrap.
Ik bedank de altijd goed gesoigneerde vloermanager **Jan van Kapel** voor alle hulp bij de experimenten, de heerlijke koffie en het aanleren van goed computermanagement.

Mijn **ouders** wil ik bedanken voor hun zorg en liefde. Zij hebben mij de mogelijkheden gegeven. Ma, ik mis je vreselijk. Pa, ik bewonder je, je bent een kanjer. Mijn zussen, **Esther** en **Annemiek**, bedank ik voor de steun en de liefde die ik van hun heb gekregen. **Mattie** en **Hans**, bedankt voor de zorg, de interesse en jullie prachtige dochter.

Barbara, bedankt voor alles. Je bent voor mij de ideale vrouw. Een zoen.

Menno, ik hou van je.

Peter.